



universität  
wien

# DISSERTATION

Titel der Dissertation

„Development of novel artificial ligands for antibody purification/enrichment based on affinity principles and cation exchangers combined with hydrophobic interaction motifs“

Verfasser

Mag. Stefan Hofer

angestrebter akademischer Grad

Doktor der Naturwissenschaften (Dr. rer. nat.)

Wien, 2011

Studienkennzahl lt. Studienblatt:

A 091 419

Dissertationsgebiet lt. Studienblatt:

Chemie

Betreuerin / Betreuer:

Prof. Wolfgang Lindner



## **Danksagung**

Diese vor Ihnen liegende Arbeit wurde während dem unglaublich langen Zeitraum vom März 2005 bis Mitte 2011 durchgeführt. Ich finde es selbst verblüffend, wie viel Geduld meine Umgebung für mich aufgebracht hat, und wie viel Verständnis für die Widrigkeiten, die Auftreten beim Schreiben einer derartigen Arbeit während des harten Arbeitsalltages da war.

Allen voran sei hier Professor Dr. Lindner erwähnt, welcher es immer wieder schaffte, mich mit aufmunternden Emails zu motivieren und damit meine Mühen in diese Arbeit nicht versiegen zu lassen. Weiters sollen die produktiven Diskussionen während des praktischen Abschnitts meiner Arbeit erwähnt sein, welche immer in neuen, kreativen Ideen endeten. Seine Aufopferungsbereitschaft für die Vernichtung unzähliger Flaschen „Flatlake“ selbst nach harten Arbeitstagen will ich in diesem Zusammenhang ganz besonders unterstreichen.

Weiters danke ich Dr. Jeannie Horak, welche in unzähligen Stunden mich bei meinen Publikationen tatkräftig unterstützte, und auch für ihre schier unerschöpfliche Hilfsbereitschaft.

Dr. Lämmerhofer danke ich besonders für die Unterstützung und Einführung in die Biochromatography zu Beginn meiner Arbeit.

Dank auch an die Arbeitsgruppe Lindner, welche immer ein ausgezeichnetes Arbeitsklima lieferte, und stets für soziale Events zu haben war.

Aber der größte Dank gebührt meinen Eltern, welche stets an mich glaubten und unglaubliche Geduld nicht nur während meiner Doktorarbeit, sondern während meines ganzen Studiums der Chemie bewiesen.



## **Table of content**

<b>0. Aim</b>	<b>1</b>
<b>1. Introduction</b>	<b>1</b>
<b>1.1. Antibody Purification</b>	<b>2</b>
<b>1.2. Methods for Antibody enrichment and purification</b>	<b>2</b>
<b>1.2.1. Chromatographic Methods</b>	<b>3</b>
<b>1.2.1.1. Affinity chromatography</b>	<b>3</b>
<b>1.2.1.1.1 Protein based affinity ligands</b>	<b>4</b>
<b>1.2.1.1.2. Biomimetic Ligands</b>	<b>7</b>
<b>1.2.1.1.2.1. Dye Ligands</b>	<b>7</b>
<b>1.2.1.1.2.2. Peptide based Protein A mimetics</b>	<b>9</b>
<b>1.2.1.2. Thiophilic Interaction Chromatography (TIC)</b>	<b>10</b>
<b>1.2.1.3. Hydrophobic Interaction Chromatography (HIC)</b>	<b>13</b>
<b>1.2.1.4. Ion exchanger Chromatography (IEX)</b>	<b>14</b>
<b>1.2.1.5. Mixed-mode ligands</b>	<b>16</b>
<b>1.2.2. Non chromatographic Methods</b>	<b>17</b>
<b>1.2.2.1. Precipitation/ Salting out/ Crystallization</b>	<b>18</b>
<b>1.2.2.2. Membrane Techniques</b>	<b>19</b>
<b>1.2.2.4. Aqueous two phase extraction</b>	<b>20</b>
<b>2. Objective</b>	<b>22</b>
<b>3. Results and discussion</b>	<b>22</b>
<b>3.1. Membranes with A2P/B14 ligands</b>	<b>22</b>
<b>3.2. Soft gels with A2P</b>	<b>25</b>
<b>3.3. Soft gels with B14</b>	<b>26</b>
<b>3.4. Soft gels with mixed modal ligands</b>	<b>27</b>
<b>4. Conclusions</b>	<b>30</b>
<b>5. References</b>	<b>31</b>
<b>6. Appendices</b>	<b>36</b>
<b>6.1 Publications</b>	<b>36</b>
<b>6.2. Additional experimental data</b>	
<b>7. Summary</b>	
<b>8. Zusammenfassung</b>	
<b>9. Curriculum Vitae</b>	



## **0. Aim**

Pharmaceutical industry is probably one of the fastest growing industry branches in the moment and right now the exploitation of monoclonal antibodies as drugs is in their main focus. The creation of even more economical production pathways is one of the main concerns and therefore a lot of investigation in this field is done. Especially the purification of crude and antibody containing cell culture supernatants is crucial to be improved and there are many ways to achieve this goal [1,2].

The aim of this thesis was the improvement of two possible purification methods: i) by affinity chromatography with artificial ligands and ii) via mixed mode ligands consisting of an ionic site in combination with a thiophilic increment and/or a hydrophilic molecule part. The focus was put on increasing the materials' binding capacities for IgG, but also on their tolerance against Pluronic F-68, an anti foaming agent, as well as on their selectivity for IgG out of cell culture supernatants.

In the first attempt biomimetic affinity ligands have been modified with different spacers to improve the materials' ability to capture antibodies. These ligands were further coupled onto different support materials and finally characterized with regard to their chemical as well as their functional properties. As support materials we investigated on the one hand typical chromatographic resins used for biochromatography but also membrane supports based on cellulose.

The first part of this thesis describes common methods for antibody purification without distinction whether it is used for industrial purification or on research scale. The major part summarizes the experimental results of this thesis including articles based on the investigations.

## **1. Introduction**

Mankind has always been enslaved by diseases and plagues, therefore medical science has always been playing an important role in human sciences. All the decades since then health of men have been of special importance so it is easily to believe that the pharmaceutical industry is the fastest growing branch besides the IT business. Not only the value of this area of business increased, also the

methods and especially the pharmaceuticals became more sophisticated. At the beginning of the 20<sup>th</sup> century simple compounds have been synthesized or have been extracted from plants or tissues of animals, but with time the production of drugs got more complex and ended in a new branch of industry for biopharmaceuticals.

A multitude of proteins are used for medical applications, e.g. blood factors (Factor VIII, Factor IX), Interferons ( $\alpha, \beta, \gamma$ ), blood clotting proteins and Insulin [3]. Besides those proteins also antibodies are becoming more and more important for the pharmaceutical industry [4], therefore easy and cheap manufacturing methods are looked for. IgGs are used for Alzheimers's syndrome, immunodeficiency and cancer [4-7]. But besides the costs of research and upstream processes [8], the costs of the downstream process should not be underestimated. The costs of the purification of the cell culture supernatant to receive a pure antibody can be up 60 to 80% of the production costs [1,2].

### **1.1. Antibody Purification**

The development of a monoclonal antibody needs several years, and until its final approval it can take up to ten years. Nevertheless this is not the key source of the high production costs. A thumb rule tells you that approximately 50-80% of the total manufacturing costs are caused by the purification and polishing steps [1]. Furthermore the growing production yields for monoclonal antibodies will probably reach 10 g/L during the next decade [9], and the challenge for the downstream process is to keep pace with this development. Therefore one of industries main focuses lies on the improvement of the downstream processing with special interest in economy. In the following sections some of the most common techniques are introduced, which can be used after a filtration and/or possibly a buffer adjusting step, depending on the subsequent capturing step.

### **1.2. Methods for Antibody enrichment and purification**

The following sections will be separated into a chapter dealing with chromatographic methods and a chapter enlightening non chromatographic techniques. Chromatographic methods are the far more popular and established



methods at the moment, because of the high capacities of beads. They will occupy the first part of this methods chapter. Nevertheless they suffer from certain drawbacks. Therefore alternatives to bead materials will be discussed in the subsequent chapter, giving a short introduction into these techniques.

### **1.2.1. Chromatographic Methods**

The range of applications for purification is legion, starting at precipitation and ending with aqueous two phase systems, but at industrial scale, chromatographic methods are still state of the art. Reasons are on the one hand the fear of novel technologies and especially their evaluation for governmental departments, e.g. FDA (in Europe: EMEA). Also for establishing of novel downstream processes for novel biopharmaceuticals chemical and biochemical engineers trust in proved and tested techniques. Other advantages of chromatographic systems are their high capacities and often higher purities compared to alternatives. The capture step is the most important one and a high binding capacity is demanded, therefore Protein A columns are very common. But also ion exchange chromatography (CEX and ALEX), hydrophobic interaction chromatography (HIC) and many more are used for the purification of antibodies [10].

#### **1.2.1.1. Affinity chromatography**

Affinity chromatography methods carry inherently certain advantages. Looking at their origin, nature itself, they can look back onto more than a billion years of developmental period which lead to unique binding properties. First of all, they work perfectly under isotonic conditions and inevitable bind IgG from the supernatant of cell cultures right after filtration without pH adjustment, diafiltration or dilution. What we are talking about are the IgG binding surface proteins of several bacteria such as Staphylococcal Aureus, group C and G Streptococcal bacteria and many more.

They offer very high affinity constants and are highly specific for the target compound. That makes them very effective ligands especially in complex matrices such as cell culture supernatants, where product and impurities compete for binding sites. But for several reasons, which are explained in the following

chapters the industry is looking for alternatives and that opened the market for the new research field of artificial affinity ligands. Two different approaches are commonly used right now: X-ray crystallography [11] and NMR data in combination with computational chemistry, and high through put screening methods [12]. The discussion which of these methods is the most successful is as old as the applications themselves, and I will lose some words about it at the end of the chapter "Biomimetic Ligands". No matter which path was chosen, both led to successful ligands and will be discussed later. At the moment 2 kind of artificial affinity ligands are of a certain importance namely dye ligands and peptide ligands although until now, none of them is in industrial use.

#### **1.2.1.1.1 Protein based affinity ligands**

At the moment a whole variety of antibody binding proteins coupled to solid beads are on the market, each of them equipped with different properties and different affinities for antibodies. For example, the typical ligand for IgA capturing is jacalin-agarose, a lectin from the jackfruit coupled onto the support material. Lectins show high affinity for the sugar side chains of antibodies and are especially interesting for IgA [13,14]. The binding occurs at neutral pH and the elution is achieved by adding sugar, mostly galactose, to the elution buffer. This latter aspect makes lectin ligands not attractive for large scale or industrial applications. Furthermore because of its high biological activity, namely being a strong B cell activator and a T cell mitogen, severe control of possible ligand leakage is required [14].

But IgA is of minor importance for the industry, and its focus lies mainly on IgG, for which several different affinity materials are available. As already mentioned, many proteins are known which are able to bind IgG. The most important one is a surface protein from *Staphylococcus aureus*. This bacterium uses that particular protein to bind the host's antibodies onto its surface, but not with the Fab part of the molecule, but with the Fc part, the one responsible for the subsequent immune answer of the host. By this means the intruder is able to evade the immune system and this makes bacteria of *S. aureus* very dangerous for human kind.

*Staphylococcal aureus* Protein A (SpA) was discovered in the year 1966 [15] and it is a 42 kDa protein composed of five almost homologous domains named E, D, A, B and C in order from the N-terminus. Whilst at the beginning Protein A was

harvested directly from *Staphylococcus aureus* by enzymatic digest, it is nowadays expressed by *E. coli* bacteria and since it is a recombinant protein, protein engineers improved its properties [16]. They exchanged for example Gly29 in the B domain which lead to a higher chemical stability toward hydroxylamine. This little change also eliminated the affinity of protein A for the Fab fragment of IgG. Furthermore the loop regions between the IgG binding helices have been elongated so the elution conditions became less harsh. Therefore the necessary pH for elution changed from pH 3.3 up to pH 4.5. Under these conditions dimerization of IgG is suppressed and the activity of the antibody is preserved. Also the stability against cleaning in place (CIP) conditions which demand a high alkaline environment could be improved by exchanging asparagines residues against alanine. An important fact for optimal binding capacities is the right adjusting of the linking to the support material so that every binding domain is accessible. Due to the 5 binding sites it is not difficult to get good capacities for Protein A materials, but nevertheless genetic engineering introduced a thiol for a single point anchoring onto an epoxy activated matrix for a defined orientation of the protein [16,17].

Another popular IgG binding protein is Protein G, which is also a surface protein. It originates from group C and G *Streptococcus* bacteria and has similar properties than protein A. They were discovered in the year 1984 by Reis et al. [18] and L. Björck and G. Kronvall, respectively [19] and is approximately 21.4 kD to 67 kD heavy (depends on the strain used as source). Protein G consists of 2 or 3 highly homologous binding domains (depends also on the source) [20,21], which bind to the same regions of the Fc part of antibodies as Protein A does. This is an interesting fact because the binding domains of these two proteins show no similarities. They exhibit different binding strengths for different IgG subclasses. Protein G has also been genetically modified and by this means the affinity for albumin and  $\alpha$ 2-macroglobulin was diminished [22]. Protein G columns and beads are also commercially available and have found their niche in laboratory applications but for industrial applications Protein A is the first choice for the following reasons: first of all, the binding affinity constants for Protein G are considerably higher and harsher elution conditions at pH around 2.5 - 3.0 are recommended. Secondly the lower stability of Protein G compared to Protein A inhibited its industrial implementation [16]. But it is recommended for laboratory

uses because of its higher applicableness for a greater range of Ig subclasses. Especially its affinity for hIgG<sub>3</sub> is of great importance.

The third and last commercially available IgG binding protein was discovered in the year 1985 and was called Protein L (PpL) and has its origins in the bacteria *Peptostreptococcus magnus*, has a molecular weight of 35.8 kDa and consists of 4 Ig binding domains. In contrast to Protein A and Protein G Protein L does not bind to the Fc part of antibodies. Its binding sites shows affinity towards the framework of the variable region of the  $\kappa$ -light chain, but only to  $\kappa_I$ ,  $\kappa_{III}$ ,  $\kappa_{IV}$ -light chain, not to  $\kappa_{II}$ -light chain. Because of the fact that two thirds of all antibodies consists of  $\kappa$ -light chains, and the deviation between  $\kappa_I$ ,  $\kappa_{III}$ ,  $\kappa_{IV}$ -light chains is 60, 28 and 2% respectively, almost 60% of all antibodies are covered by this protein [23]. Just like Protein A and Protein G Protein L is an elongated protein, which consists of 4 or 5 binding domains, depending on the strain chosen as the source [24].

As before mentioned, this protein binds to the framework of the variable regions but does not interfere with the antibody-antigen interaction, therefore the evolutionary purpose of Protein L is not fully understood yet.

Just like Protein G Protein L is not established in industrial processes yet and its mayor field of application is in laboratory scale because Protein L exhibits affinity towards antibodies which are out of the application range of Protein A and Protein G. Its elution conditions are also harsh: 0.1 M glycine/HCl buffer at pH 2.0

Besides Protein A, G and L are several other Ig binding bacterial surface proteins known, for example protein H and M1 protein. Both have similar structurally properties and belong to the same family, the so called M proteins. They originate from *Streptococcus pyogenes*. Interestingly they consist of a coiled coil dimer, although their amino acid sequence does not point to this fact. This is the reason why they are thermally very unstable and loose at 37°C their tertiary structure and therefore also loose their affinity for IgG. Therefore it is not possible to bind IgG properly at physiological conditions. Protein H possesses also affinity towards albumin and FNIII domains, whereas the M1 protein has additional affinities to albumin and fibrinogen. As it is also the case for Protein G the reason for their affinity for albumin is still a riddle [25].

The affinity constant of Protein H is approximately 10 times lower than of Protein A or Protein G but is still sufficient for affinity chromatography and milder elution conditions can be used.

For the sake of completeness the following proteins which are also able to bind antibodies should be mentioned.

There are Arp, Sir, FcRA76 and Mrp proteins, also from the M protein family and which IgG binding capability is therefore temperature dependent too. [380, p 13690] Protein P from *Clostridium perfringens* binds also to  $\kappa$ -light chains, protein D from *Branhamella catarrhalis* binds mainly IgD, but also small amounts of IgG and Protein P from Group A streptococci is an IgA binding protein, which also shows a weak affinity for IgG [26]. These materials are not commercially available and thus have no industrial relevance.

#### **1.2.1.1.2. Biomimetic Ligands**

The exploitation of dyes started with the discovery of the Cibacron Blue F3G-A for the capture of pyruvate kinase. It started a long series of biomimetic ligands based on cyanuric chloride, which exhibits 3 chlorine atoms with different reactivity [27]. This makes a selective introduction of substituents easily achievable. The advantages of biomimetic ligands are legion: The production costs are low, compared to their natural pendants, also the handling and stability are superior. The scale up potential is higher and because of their increased stability and the possibility to use harsher sanitation conditions the reusability is also improved [28]. Several examples for successful enzyme purifications are known, e.g. trypsin, urokinase, kallikrein, alkaline phosphatase, malate dehydrogenase, lactate dehydrogenase, oxaloacetate dehydrogenase, and formate dehydrogenase. These ligands are tools for protein purification for more than 30 years because of their stability, cheap production, flexibility and the potential to tailor them for certain applications [29].

A further approach for tailor made ligands is the screening of peptide libraries. The most prominent candidate is the protein A Mimetic (PAM) ligand developed by Fassina et al. [30,31].

##### **1.2.1.1.2.1. Dye Ligands**

The first attempts to capture IgG by dye ligands were based on the knowledge that the binding site of Protein A consists of 11 amino acids placed in helix 1 and helix 2 and the fact that the key amino acids are Phe132 and Tyr-133 [16,32].

This knowledge based on X-ray crystallography, computational chemistry and NMR spectroscopy lead to the first artificial Protein A (ApA) by Christopher R. Lowe [32,33], and resulted later in the 2 commercially available ligands A1P and A2P [34].

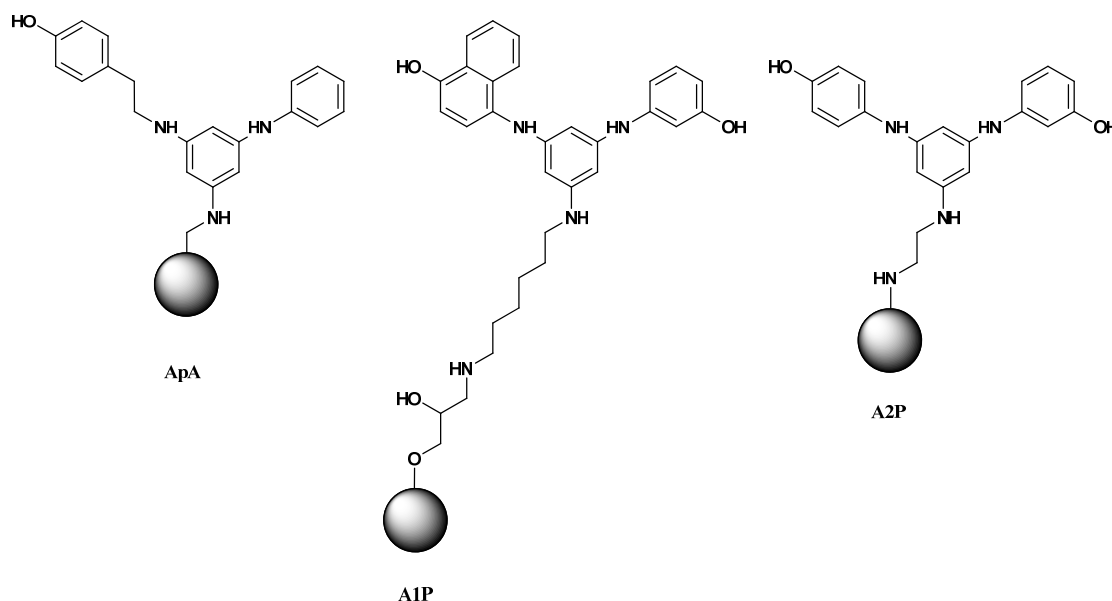
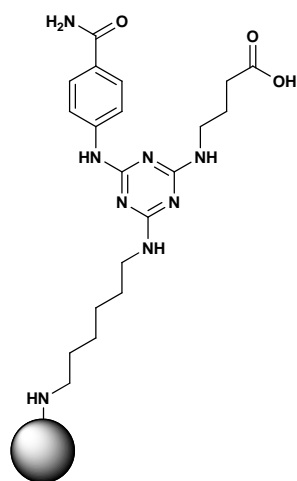


**Figure 1: ApA, A1P and A2P**

Ghose et al. [35] compared A1P and A2P with Protein A. The conclusion was that the mimetic materials exhibited high binding capacities for pure IgG, but they were not able to compete with protein in terms of selectivity and purity.

Another product of ProMetic's research is an artificial Protein L mimetic called ligand 8/7, with a  $K_a \sim 10^{-4} \text{ M}^{-1}$ . Ligand 8/7 binds to the Fab part of the IgG light chain, but contrary to Protein L it does not distinguish remarkably between  $\kappa$ - and  $\lambda$ - light chains. Such as all other biomimetic dyes this ligand draws advantages concerning sterilization in place (SIP) and cleaning in place (CIP) procedures. Ligand 8/7 consists of an aromatic and an aliphatic moiety, both comprising polar groups on them, namely 4-aminobenzamide and 4-amino butyric acid. The optimal spacer length consisted of 6 C atoms and was found in 1,6-diaminohexan. With this length best accessibility was granted on the one hand and on the other hand the tendency of the ligand to interact with the surface of the support material was minimized, avoiding loss of antibody binding capacity. Artificial Protein L gave comparable purities and the ligand is more versatile than the original protein [36].



Ligand 8/7

**Figure 2: Artificial Ligand 8/7**

#### 1.2.1.1.2.2. Peptide based Protein A mimetics

Protein A mimetic, also called PAM or Tg19318, is a tetrameric peptide with the molecular mass of 2141 Dalton and is based on the central amino acid coupled to Lysine. The two amino groups of this molecule are used to build a branching to which additional two Lysine amino acids are bound. To this scaffold 4 identical amino acid sequences Tyr-Thr-Arg are coupled. The main advantages are obvious: Like every synthetic ligand the production costs are lower than those for Protein A, even compared to the recombinant produced Protein A. Also the improved stability towards sanitation conditions and the negligible toxicity of PAM has to be mentioned. The affinity constant  $K_a$  of  $\sim 0.3 \mu\text{M}$  is even sufficient for purification and enrichment out of feedstock solutions with low antibody concentrations. The optimal binding conditions were at neutral pH and low buffer concentration, conditions common to feedstock solutions. Elution can be performed by several changes of conditions: A pH switch with acidic acid to pH 3 or with sodium bicarbonate buffer at pH 9, or by increasing the salt concentrations. Latter gave very sharp elution peaks and good recovery at 1 M NaCl concentrations. The specificity is broader than that of Protein A, because human, mouse, cow, horse, pig, rat, rabbit, goat and sheep IgG as well as IgM, IgA and IgE can be purified with this particular ligand. This goes hand in hand with lower purity compared to Protein A. Also a lower capacity was observed and therefore Tg19318 is no rival for the favourite purification method of biotechnologists [31,37].

### 1.2.1.2. Thiophilic Interaction Chromatography (TIC)

TIC was introduced to biotechnological purification techniques by Jerker Porath in the year 1985, when he tried to end cap a divinylsulfone activated agarose gel by mercaptoethanol, a common method for this purpose [38]. The surprise of Jerker Porath about the IgG binding abilities of this phase was good, and because of the lack of a better explanation he called this phenomenon “thiophilic adsorption”. Later explanation efforts resulted in a postulation of an “electron-donor-acceptor Interaction”, similar to that of hydrophobic interaction chromatography (HIC). In comparison to HIC TIC materials show a higher affinity to IgGs and a significant part of impurities of ascites or cell culture feed stocks can be removed. More intensive studies and detailed comparison to HIC materials, Phenylsepharose and Octylsepharose, showed differences among them, for example the fact, that lyotropic (structure forming) salts are of tremendous importance in the TIC. Without this salts no IgG binding could be observed whilst HIC binds IgG well at presence of salts of any kind. The reason, why lyotropic salts enhance the weak interaction of the ligand with the target compound has been commented by Porath. He postulated that structure forming salts increase the free energy,  $\Delta G$ , and in consequence proteins tend to expose as less of its surface to the solvent, resulting in the binding to the ligand. This of course does not explain the specificity of the material to antibodies [39]. The strength of lyotropic salts is described by the Hofmeister series:

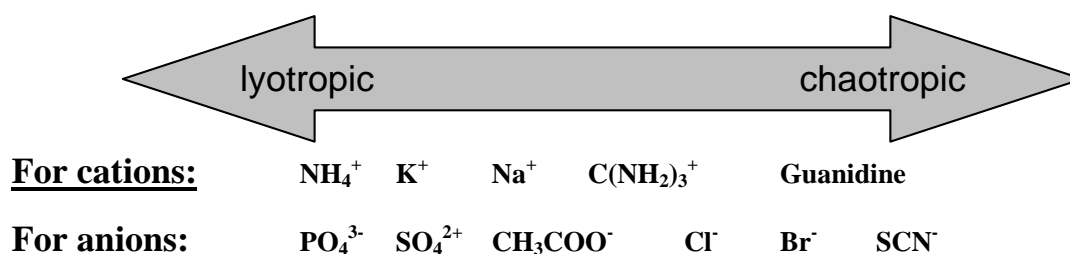
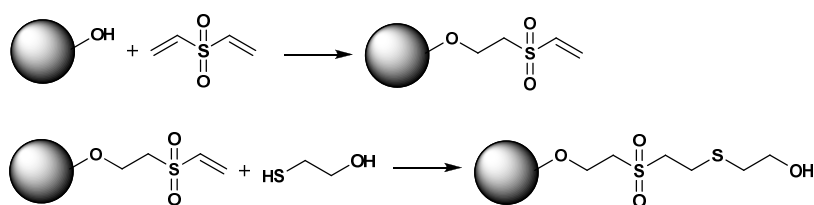


Figure 3: Hofmeister series

Poraths first approaches were quite simple: activation of the support material by divinylsulfone and subsequent binding of mercaptoethanol which yielded in the so called T-Gel (see Figure 4).





**Figure 4: Preparation of T-Gel**

Investigations showed that sulfid bridges are necessary for thiophilic adsorption, but the exchange of the sulfonyl group by sulfoxide or even sulfur did not affect the binding pattern. After the sulfone group was exchanged by Selenium the T-Gel has shown similar adsorption behaviour but with a noticeable decrease in binding capacity. The consequent step was the introduction of more sulphur atoms and the resulting ligands consisted of up to 6 sulphur atoms in both forms, as sulphide bridges and as sulfone groups. The measured  $K_d$  constants were increasing with growing numbers of sulphur atoms. But one problem occurred: also the binding constants towards other proteins increased and therefore these ligands lost their selectivity if more than 4 sulphur atoms are implemented. An interesting point of this work was the observation that oxidized ligands lost their affinity. This was another prove of the necessity of the sulphide bridge for antibody purification. Elution of bound antibodies is obtained by omitting the lyotropic salt. These mild elution conditions are beneficial for preserving the antibody functionality and also facilitate subsequent cleaning steps [40].

Further investigations led to 5- and 6-membered cyclic compounds, which contain at least one double bond, and consist usually of one or two heteroatoms, namely sulphur or nitrogen. The properties of these materials are very similar to the common TIC ligands, especially the selectivity and the need of structure forming salts as enhancer for the binding. In all cases a sulphide bridge was involved, but the base material was both, epoxy and divinyl sulfone activated [41-43].

All these ligands carry similar drawbacks: they show a high affinity to the commonly used indicator phenol red, a triphenylmethan dye, which competes with immunoglobulins for the binding sites. A tremendous decrease of the binding capacity is the consequence. This fact and the need of lyotropic salts for the enhancement of the binding capacity led scientists to the development of salt independent thiophilic gels. The first successful attempt was performed by Scholz

et al. in the year 1998 during screening of 2-mercaptopyridine (see Figure 5) and 2-mercaptopyrimidine [44]. Both materials were bound to divinyl sulfone activated materials and both of them comprised thiophilic adsorption properties in presence of lyotropic salts, but only the pyridine based ligand was able to capture antibodies also at low salt concentrations specifically. In the same year Scholz et al. presented 3-(2-mercaptoethyl)quinazoline-2,4(1H,3H)dione (MECH) [45] with common properties and similar increments as the 2-mercaptopyridine ligand. Again the ligand consists of an aromatic heterocyclic coupled per thioether linkage onto the divinyl sulfone activated agarose (see Figure 5).

The crown of these affords was the development of 4-mercapotethylpyridine ligand (see Figure 5), coupled onto the cellulose beads with a very hydrophobic spacer arm compared to the divinyl sulfone activated materials previously mentioned. Binding of antibodies occur at physiological conditions, but optimal adsorption is achieved with a 50 mM Tris-HCl buffer solution adjusted to pH 8, which is used for washing too, and desorption happens at mild conditions of pH 4.0 - 4.5. For improved purity of the antibody, additional washing steps can be added, for example washing with 25 mM sodium caprylate buffer for selective elution of albumin. It is commercially available at Pall Corporation, USA. This particular kind of separation is called Hydrophobic Charge Induction Chromatography (HCIC) although its roots lay in T-layer ligands. But differently to classic TIC materials is the total salt independence and that the adsorption and elution is rather controlled by pH switches than by changing the salt concentration.

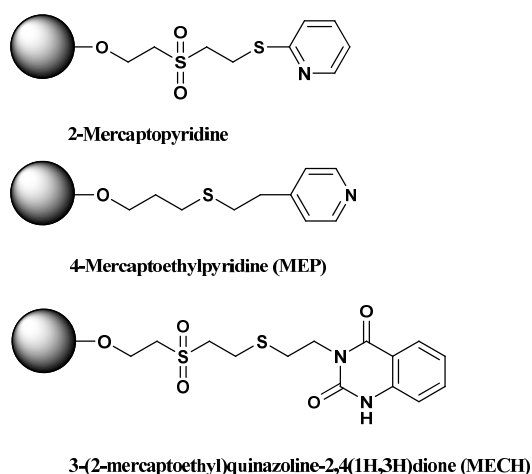


**Figure 5: Overview of HCIC materials**

### 1.2.1.3. Hydrophobic Interaction Chromatography (HIC)

HIC exploits the hydrophobicity of a protein and is therefore often used as an orthogonal purification step to ion exchange chromatography. The influence of hydrophobic amino acid residues onto the protein is well known from its folding behaviour, where hydrophobic sides tend to be bedded in the inside of the protein, whereas hydrophilic amino acids are usually placed on the outside of the molecule. The hydrophobicity is also known from the salting out effect, a technique named by Tiselius in the year 1948 [46]. By adding of structure forming salts (see Fig. 3) the proteins tend to minimize the surface area exhibited to the polar environment which means a minimization of the free energy and precipitation takes place. In the case of HIC materials the proteins bind to the hydrophobic ligands to minimize their free energy (see chapter. 1.2.2.1).

HIC materials consist of slightly hydrophobic materials such as short aliphatic groups (-methyl, -butyl) or aromatic groups as phenyl ligands. This is similar to reversed phase chromatography (RPC) but with some crucial differences. First of all the ligand density in HIC is in a range of 10-50  $\mu\text{mol/mL}$  gel vs. several 100  $\mu\text{mol/mL}$  in RPC, and secondly the ligands are typically less hydrophil and  $\text{C}_1 - \text{C}_8$  groups are typical for HIC. RP phases are typically equipped with ligands up to 18 carbon atoms [47] (see Fig.: 6). High ligand densities may lead to elution problems of the protein due to multi-point attachment between ligand and protein and elution under non-denaturing conditions, which means no addition of organic solvents, detergents or chaotropic agents, may be impossible [48]. Also the support material differs significantly: RPC uses usually silica gel, whereas HIC uses hydrophilic support materials such as agarose, polymethacrylate and other for biochromatography typical materials. RPC needs organic solvents for elution because of its high hydrophobicity. This may lead to denaturation, whereas HIC takes place in very polar environments. Porath et. al. investigated enforced adsorption of proteins in the presence of high concentrations of different salts such as sodium phosphate or sodium chloride and the impact on the interaction in dependency of the Hofmeister series [49], chapter 1.2.1.1. Most common in bioanalytical or preparative applications in downstream processing is ammonium sulfate [50]. General requirements for these neutral salts are high solubility to avoid salt precipitations, low viscosity, UV transparency and stability [51]. The

elution is enforced by decreasing salt gradient and by this means the bound biomolecules elute according to their hydrophobicity [52]. By applying a carefully selected gradient, high selectivity can be achieved. Furthermore the type of the stationary phase and pH contribute also to the selectivity of this method.

In preparative applications HIC is usually used as polishing step, after the primary capture step and an intermediate purification step, especially in antibody purification processes.

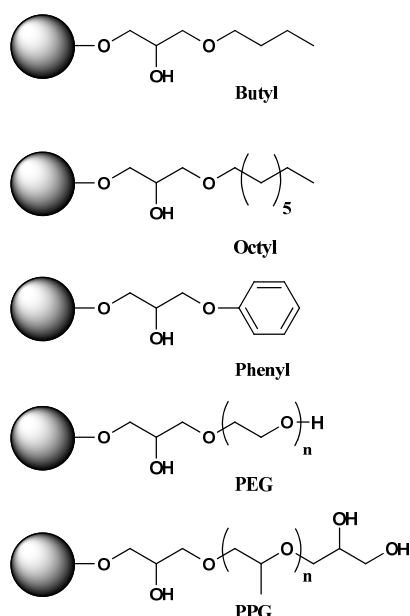


Figure 6: The schematic structure of some ligands for HIC

#### 1.2.1.4. Ion exchanger Chromatography (IEX)

In the year 1960 ion exchange chromatography started to play a mayor role in biotechnological applications. It is applicable for all charged biomolecules and thus makes it a universal separation technique. For that reason, the high capacities and good selectivity of IEX materials it is popular method in laboratory scale applications but also in the industry. Almost every industrial mAb purification process consists of an ion exchange step and at least one known commercial purification process starts with a cation exchanger (CEX) as first purification step (Humira<sup>®</sup> [26]). Usually a difference of one charged amino acid is sufficient for separation and this makes these materials a powerful tool in the purification of biomolecules.

Of course a distinction must be done between cation and anion exchangers as they are used in different modes for IgG capture. Whilst anion exchangers are

used in a flow through mode, where the target molecule passes the stationary phase without retention, the cation exchanger binds the antibody and the impurities are supposed to pass the column more or less non retarded.

CEX are more robust, cheaper and do not possess ligand leakage, compared to protein A resins. CEX are endowed with higher capacities than affinity materials but lack of a comparable selectivity for the target molecules [26]. Therefore a considerably higher amount of optimization has to be done to find the ideal pH and salt concentrations for the load, washing and elution buffer which is often time consuming although high throughput screening systems are commonly used. A rule of thumb says that the pH has to be at least one order below the pI of the target molecule. But because of possible intramolecular charge asymmetry of the protein significant deviations of above estimation can occur. As soon as the optimization is done, less basic impurities relative to the mAb can be removed during loading and washing, whilst more basic compounds can be separated from the target molecules during the elution step [53]. The fact that binding occurs at low salt concentrations and pH below isotonic conditions, time and buffer consuming production steps are often required.

CEX materials can be separated into strong and weak cation exchangers. First one typically comprise sulfonic acid groups coupled to the support materials by various spacers such as ethyl groups (Fractogel<sup>®</sup> EMD SE Hicap, Merck KGaA), isobutyl groups (Fractogel<sup>®</sup> EMD SO<sub>3</sub><sup>-</sup>, Merck KGaA) or isopropyl groups (SP Sepharose FF, GE Healthcare). A mixture of both, strong and weak acid groups is found in Heparin (see Fig. 7). Numerous studies have been published which compare the performances of different CEX materials in terms of their static and dynamic binding capacities, pressure drop, compressibility, efficiency, resolution, recovery and many more [54-63].

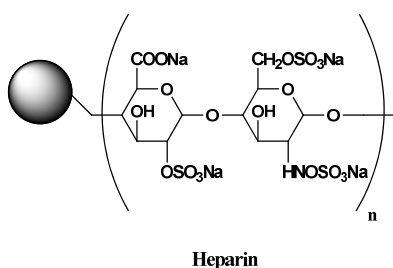


**Figure 7: Structure of Heparin**

In mAb purification processes anion exchanger (AEX) materials are used in the intermediate or the polishing steps. The effort for the optimizing the flow through conditions to bind a maximum of impurities without retention of the target molecule is comparable to those of CEX materials. Strong AEX materials consist of quaternary amines, e.g. trimethylammoniummethyl, whilst weak AEX exhibit tertiary amines as ligands, e.g. diethylaminoethyl or dimethylaminoethyl. Due to the fact, that AEX are used as a flow through technique in the downstream process of mAbs, this chapter will not go into detail but the interested reader is referred to the multitude of studies dealing with pore size distribution, capacities, titration curves, retention factors and many more [61,64-69].

#### **1.2.1.5. Mixed-modal ligands**

Although ion exchange plays an important role in protein purification, they suffer from a big drawback: the cell culture supernatant cannot be directly applied onto those gels as they need a dilution step and an adjustment of the pH. Therefore alternatives are demanded and mixed mode materials could be a solution. Mixed modal ligands can consist of any mixture of functional groups, e.g. thiophilic groups, hydrophobic groups, ionic groups, etc., but most commonly a combination of ionic and hydrophobic moieties is used. One of the main drawbacks of ion exchangers is the incompatibility with cell culture supernatants and therefore additional adjustments besides filtration have to be done. These adjustments should be avoided and cation exchangers working under more isotonic conditions were demanded by industries. Again mixed modal ligands carrying cationic and anionic groups are available. Several examples are given in Figure 8 and further ligands are summarized by Zhao et al. [70]. Although commercially available no industrial application of these materials for mAb purification is known to the author.

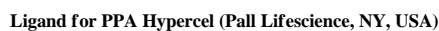
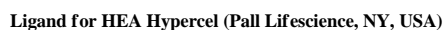


### Figure 8: Commercial available mixed-modal ligands

### 1.2.2. Non chromatographic Methods

The previously discussed techniques are commonly used in combination with gels but that does not mean they are limited to them. Several drawbacks are associated with beads, e.g. the resin compression is typical for bead based separation techniques. Inherent problems of beads are also the high pressure drops and hence resulting flow rate limitations. Therefore columns with diameters of about 2m are typical. But this again causes other problems, the so called hysteresis effect of columns and edge effects, which means that in worst cases because of the lower packing densities at the edges and the resulting higher flow rates can even lead to a collapse of the resin and subsequently also to cracks in the column bed [71]. Further problems of packed beads is column fouling. Because of the huge dimensions of the column the buffer consumption is enormous and also the floor space requirements for the columns, buffer preparation (we are talking of about ten thousands of litres) and its storage. An additional point to be considered is the fact that biomolecules with their high

molecular weight are hindered to invade the pores of the particles by their diffusion constants ( $K_{diff}$ ), which is a further reason for a limitation of the flow rate besides the high pressure drop. Antibody purification without chromatographic process will probably never be feasible, but a possible reduction of chromatography in downstream processes is still attractive and having alternatives in his sleeves is always a plus.

The search for more efficient and cost effective methods led to several alternatives to chromatographic separations, e.g. precipitation, crystallization and several others [9].

#### **1.2.2.1. Precipitation/ Salting out/ Crystallization**

##### **Precipitation**

Precipitation is not exactly considered as an alternative for chromatographic media, as it does not exhibit the necessary selectivity, but it can definitely facilitate subsequent purification steps. The amount of host cell proteins and host cell DNA should be diminished as good as possible prior the capture step to avoid reduced binding capacities. Typical materials used are calcium chloride in combination with potassium phosphate. After flocculation the target molecule can be centrifuged. Also polyethyleneimine, ammonium sulfate and caprylic acid were reported as reagent for precipitation [9,72]. A promising approach could be affinity precipitation due to an improved selectivity. Functionalized polymers such as Eudragit, poly-*N*-isopropylacrylamide or elastin-like polypeptides have been proposed for such applications [26,73-75]. After binding of the target molecule a change of pH and/or temperature makes the polymer insoluble and impurities can be removed. Afterwards non binding conditions are adjusted and the ligand gets free, whilst the still insoluble polymer can be removed [37].

##### **Crystallization**

Another powerful tool for protein purification is crystallization, which is able to purify, concentrate and stabilize the product. Under optimized solution conditions concerning such parameters as temperature, pH, salt concentration and others, a



protein can start to build crystal nuclei (nucleation), followed by the post nucleation step and the cessation of growth. This needs of course a lot of optimization work but if established, crystallization can be a cheap and effective method for purification. Therefore prior crystallization studies are done automated by robotic systems to determine the ideal crystallization conditions for the protein in nL volumes [76]. Due to the highly flexible Fab part of antibodies and the hinge regions, their crystallization turned out to be difficult and not many studies about the crystallization of antibodies are available [53]. Not unusual is the adding of certain substances to enhance crystallization such as PEG, small organic molecules and others [77].

### Salting out

Salting out is a technique known for more than 130 years [78] and is a simple method for protein enrichment. The adding of lyotropic salts to a protein solution leads to precipitation due to increased hydrophobicity. The ability of salts to precipitate protein is depicted by the Hofmeister series (Fig. 3). The most common salt for this purpose is ammonium sulfate, which is also frequently used for salting out of antibodies. The reason lies in the ability of ammonium sulphate to stabilize proteins at concentrations higher than 0.5 M. Furthermore ammonium sulfate is cheap and can easily be removed from the solution by dialysis or ion exchange chromatography [79]. Due to the unspecific nature of these salts, the purity of the target molecule is poor. Although the purity can be improved by fractional precipitation, which means a portion wise adding of the lyotropic salt, industrial applications of this technique to purify antibodies is not known to the author.

#### **1.2.2.2. Membrane Techniques**

The most promising alternative at the moment is membrane chromatography, which exhibit several advantages to classical packed bead chromatography. First of all membranes experience almost no pressure drop restrictions because of its superior flow properties. Additionally they do not suffer from diffusion controlled mass transfer limitations, because the biomolecules do not have to penetrate any pores of the particle, as it is illustrated by Boi et al. [80]. Because the target

molecule is brought to the binding sites by convection and not by diffusion, binding capacity is almost flow rate independent. Due to the high flow rates the cycle time is reduced and therefore also the possibility of column fouling. Furthermore reduced buffer consumption leads to reduced downstream costs. The easier assembling of a membrane cartridge compared to a packed column and therefore the easier scale up ability has also to be taken into account. Because membranes are handled as disposables and there is no need of validation of the cartridges.

For these reasons, membrane techniques are of increasing interest for industries, especially in combination with flow through techniques such as anion exchange membranes (i.e. polishing, virus removal) [81-85] or with on-off binding mechanisms such as affinity chromatography with Protein A [71]. IEX, affinity, hydrophobic interaction and reversed phase (RP) membrane were discussed in several studies, but most common are affinity and ion exchange materials [86-89]. Ion exchange materials are available as strong and weak cation and anion exchangers, while affinity membranes can be divided in 4 subclasses: Immunoaffinity, Protein A and G, low molecular mass ligands and others. For IgG purification of course Protein A materials are the most prominent [90].

Several geometries are possible, as there are the flat sheet design, hollow fibres and the radial flow design. Ready to use cartridges are already commercially available for the flat sheet and the radial flow design [81,86]. Typical materials for membranes are cellulose, cellulose acetate, polytetrafluoroethylene (PTFE), poly(ether sulfone) (PES) and others [87].

#### **1.2.2.4. Aqueous two phase extraction**

Aqueous two phase extraction is a technique, which exploits the affinity of proteins for additives in the aqueous phase. It is applicable to almost all sorts of separation problem and at optimum conditions there is no need of purification like filtration or adjustment of the broth necessary. One phase is usually doted with polyethyleneglycol (PEG) and the other phase consists of dextran as additive, but salts such as sulphates or phosphates are also possible. Other possible systems consist of PEG/Ficoll, PEG/citrate, PEG/levan, PEG/pullulan or dextran/polyvinylalcohol [91]. PEG is often modified by affinity increments to improve the partition coefficient and to increase the yield of the target molecule in

the upper phase, which is usually the PEG-phase. Best results are achieved when the target molecule does not interact with non PEG-moiety, which means in an aqueous two phase system without ligand the solute concentrates in the lower phase. This minimizes unspecific binding and increases selectivity of the system with introduced affinity ligands. Affinity ligands are not always available and then this method can lack of selectivity, which makes this method unattractive for industrial applications. Even the fact, that it is a very mild and conserving method, can not compensate that drawback.

The ultimate aim of Aqueous two phase systems is to cultivate the expression systems in the lower phase and bring the product into the upper phase, so there would be no need for filtration of the cell culture supernatant and only the upper phase have to be exchanged periodically. Recycling of the PEG phase is no problem because it withstands also harsh conditions and can be reused afterwards. Therefore establishment of aqueous two phase systems could result in a decrease of costs of the downstream process for the industries. But the introduction into a downstream process is the main bottleneck of this method: usually pH, salt and polymer concentration have to be chosen carefully, and of course on parameter influences another. That means that finding the optimal conditions for a maximal partition coefficient has to be investigated. But the parameters of the cell culture supernatant are not that flexible that separation of the desired protein is not always possible [92].

A recently published article about affinity partitioning showed promising results with a diglutamic acid functionalised PEG/dextran system. These ligands showed high affinity towards IgG and were able to increase the partition constant 60-fold compared to non functionalised systems, tested with cell culture supernatants. An interesting point is the fact, that polymers derivatised with triazine (dye) ligands (see chapter 1.2.1.1.2.1. dye ligands) were not able to bring IgG into the upper phase (A1P and the A2P). Also all PEG/salt systems failed presumably because of the high salt concentrations which suppressed electrostatic interactions between ligand and solute [93].

Right now the mayor drawback of this technique is the lack of appropriate large scale devices, and industrial applications for antibody purification are not known to the author.

## **2. Objective of this thesis**

The main topic of this thesis was the creation of novel materials for antibody capturing. This started with the synthesis of novel ligands, their immobilization onto different solid support materials and their chemical as well as functional characterization. The idea behind the thesis was the creation of economic alternatives to the state of the art capture media for IgG: Protein A resins.

Several approaches are thinkable and one of them is the creation of low molecular biomimetics. Those have been coupled onto soft gel support materials in the first place. Unfortunately soft gel supports also carry certain disadvantages with them and therefore biomimetics were coupled also onto membrane materials. For resins and for membranes static binding capacities (SBC) as well as dynamic binding capacities (DBC) have been determined using pure IgG feed solutions, mock feed solutions and cell culture supernatants.

Other potent alternatives tested were mixed modal ligands. Multi modal ligands consist of two or more functional groups or moieties whose properties should complement each other. In this study one of the functional group should be an acidic group, which should be made capable to bind h-IgG under isotonic conditions, which are typical for cell culture feed solutions. Therefore the ionic groups were combined with different moieties with focus on thiophilic and hydrophobic increments. Those ligands were coupled on tentacle grafted polymers (Fractogel) and afterwards tested via SBC using pure IgG solutions with different sodium chloride concentrations pH values. After this screening the most promising materials were tested via DBC measurements using pure IgG solutions and a dialysed cell culture supernatant. For further details please be referred to chapters 7 and 8, comprehending publications 1 - 5 and additional experimental results.

## **3. Results and discussion**

### **3.1. Membranes with A2P/B14 ligands**

Due to high material costs as well as several other economic and practical considerations alternatives to Protein A soft gel materials for IgG capturing are wanted by the pharmaceutical industry. One possibility to circumvent the

drawbacks of Protein A is using low molecular weight biomimetic ligands. Prometic Biosciences Ltd (UK) has specialized in creating such tailor made molecules and the latest inventions on the field of Protein A mimetics have been A2P and B14 (Fig. 1 and 9).

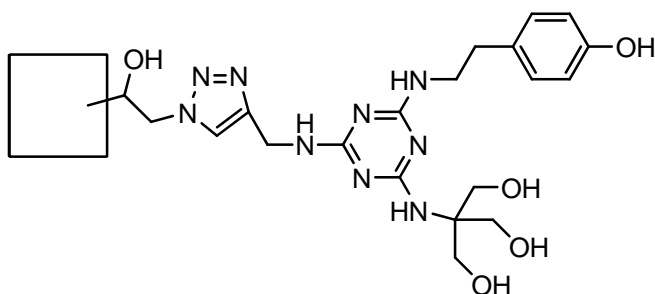


**Figure 9: B14 ligand with triazole (TRZ) spacer**

These ligands have not only been coupled, as described latter, on soft gel supports (see section 3.2. and 3.3), but also onto regenerated cellulose materials, provided by Sartorius Stedim GmbH (Goettingen, Germany). First experiments took place using Sartorius's epoxy activated standard membrane, which will later be referred to as Sartoepoxy membrane. During the study 3 additional membrane materials, exhibiting different sheet thicknesses, pore sizes have been tested for IgG capturing purposes (Epoxy 1, Epoxy 2 and Epoxy 3).

Starting point was A2P coupled via a two ether groups containing dithiol, 3,6-dioxa-1,8-octanedithiol, onto Sartoepoxy (A2P-DES-Sartoepoxy). Advantage of this spacer compared to the often used diamino spacer was the lack of basic groups, which would act as anion exchanger group. Anion exchangers are known to bind impurities such as DNA out of cell culture feed stock and would therefore contribute negatively to the binding capacities by blocking binding sites. Although A2P-DES-Sartoepoxy exhibited good binding capacities (4.42 mg/mL), it lacked from proper recoveries, which were at about 30%. As computational studies indicated, an unfavourable effect of the spacer seemed to be responsible for the low recovery. A more detailed description of the outcome of this study can be found in Appendix 3. This outcome demanded a different spacer, which was found in a 1,2,3-triazole (TRZ) group. This spacer was obtained by employing the so called Click Chemistry on the membrane materials. After azide activation of the support material and alkylation of the ligand, they could be coupled via a copper

(I) mediated Huisgen 1,3-dipolar cycloaddition. By the introduction of the TRZ spacer the recovery for A2P could be improved by 20%.

After successful introduction of the new spacer chemistry this ligand-spacer combination was also applied to Epoxy 1, 2 and 3 membranes. Capacities for Epoxy 1 membranes with A2P-TRZ spacer were determined in a preliminary test and resulted in a capacity of ~0.70 mg/mL and therefore no further experiments were conducted. This is most likely the result of the very low epoxy group density of this material. Epoxy 2 and Epoxy 3 membranes showed highly improved capacities compared to membranes Epoxy 1, namely 4.25 mg/mL and 1.99 mg/mL, respectively.

The very new ligand B14 by Prometic Biosciences Ltd (UK) was coupled to Sartoepony and Epoxy 2 membranes, as they were the most promising materials for IgG capturing. These materials showed during static binding tests good capacities with 2.61 mg/mL and 3.07 mg/mL, respectively. Though these values were below static capacities obtained with A2P-TRZ, these membranes exhibited recoveries of >90%. This fact makes those membranes more valuable for industrial applications as the elution capacities are higher and therefore the loss of IgG is lower.

The most promising membranes have been tested in terms of their dynamic binding properties. Due to the low IgG recovery of A2P based membranes those have been tested less severely. Main focus was on B14-TRZ-Sartoepony and B14-TRZ-Epoxy2 membranes, which showed 100% DBC for pure IgG solutions of 2.30 and 3.17 mg/mL, respectively. The recovery was >90%, which mirrored the results of the batch experiments.

Dynamic binding experiments were conducted also with cell culture supernatants, and these experiments were applied on A2P-TRZ-membranes as well as on B14-TRZ-membranes. The results are depicted in Table 1.

Membrane	DBC100% BT	Recovery
	[mg/mL]	[%]
A2P-TRZ-Sartoepony	0.49	7
A2P-TRZ-Epoxy 2	0.70	1
B14-TRZ-Sartoepony	0.74	35
B14-TRZ-Epoxy 2	1.41	92

**Table 1: Summary of DBC results, tested with cell culture supernatants**

This table shows that B14-TRZ-Epoxy 2 is not only the material providing the highest binding capacity, it also exhibits the highest recovery of IgG out of cell culture supernatant. More detailed information can be found in Appendix 1.

### **3.2. Soft gels with A2P**

Although soft gels carry certain drawbacks with them, they are still state of the art. Therefore the main focus of researchers still lies on bead materials. This part of the study deals with the coupling of the biomimetic ligand A2P (Fig. 1) onto soft, compressible gels and the chemical and functional characterisation. A series of support materials as well as 3 different kinds of spacer have been used for coupling. 3,6-dioxa-1,8-octandithiol (DES, see chapter 3.1), 1,3-propanedithiol (SS3) and the novel TRZ-spacer were used to couple A2P onto Fractogel, Fractoprep (non commercial material by Merck KGaA), and Purabead, a commercial material from Prometic Biosciences. All materials were evaluated in terms of their binding properties of IgG out of pure IgG solutions, mock feed stocks and cell culture supernatants. Special focus was put on Pluronic tolerance, due to its frequent use in antibody production as an antifoaming agent. A huge data set was built up and compared to the results of molecular dynamic (MD) simulations. The main outcome was the intolerance of the commercial A2P Mabsorbent by Prometic Biosciences. This material is carrying a diaminoethane group as a spacer which seems to either interact strong with Pluronic and is therefore not further able to interact with IgG. Or this spacer-ligand combination is not able to bring the A2P ligand far enough away from the surface of the support material, which is probably also interacting with Pluronic. If this would be the case, the ligand would not be in an ideal position to capture IgG. Further outcome was the fact that the TRZ spacer seems to be almost immune against the effects of Pluronic. The binding capacities for the AG-TRZ-A2P combination were even able to compete with commercial rmp-Protein A Sepharose FF, when tested with cell culture supernatant. As computational calculations predicted, the TRZ spacer showed on the one hand no tendency to interact strongly with Pluronic, and on the other hand this spacer turned out to be comparatively rigid and does not interact significantly with the surface of the support material. Latter fact is not self-evident

as shown in paper published by Busini et al. [94] and Zamolo et al. [95] for the DES spacer. A more detailed description of the outcome of this work can be found in Appendix 3 and the corresponding electronic supplementary material.

### 3.3. Soft gels with B14

Due to the successful implementation of the TRZ spacer for antibody absorbents described in chapters 3.1 and 3.2, the novel ligand B14 (Fig. 9) was also bound via TRZ spacer onto a series of different non commercial absorbents provided by Merck KGaA, namely FractoAIMs 1, 2 and 3. These epoxy activated polymethylmethacrylate tentacle materials differ from each other by differences in pore size as well as in epoxy group densities. For comparison reasons B14 was bound to PuraBead via 2LP (1,2-diaminoethane) spacer. A summary of the different support materials is depicted in Table 2.

Support media (abbreviation)	Epoxide Density <sup>a)</sup> [ $\mu\text{mol/g}$ ] (T)	Epoxide Density <sup>a)</sup> [ $\mu\text{mol/g}$ ] (EA)	Average PSD <sup>b)</sup> [nm] (Hg)	Max. of PSDV <sup>c)</sup> [nm] (ISEC)	Width of PSD <sup>c)</sup> [nm] (ISEC)	Pore volume [% of CV] (ISEC)	Surface area <sup>d)</sup> [ $\text{m}^2/\text{g}$ ] (N2)
PuraBead (AG)	200	n.a.	n.a.	n.a.	n.a.	n.a.	n.a.
Fractogel (FG)	750	931	n.a.	n.a.	n.a.	n.a.	n.a.
FractoAIMs-1 (FA1)	248	876	47	59	1	40	98
FractoAIMs-2 (FA2)	442	1426	47	59	1	40	98
FractoAIMs-3 (FA3)	454	1380	60	68	7	44	91

**Table 2:**

a) Epoxide group density determined by titration (T) as stated by the manufacturer and by elemental analysis (EA) after full coverage with azide groups

b) Pore size diameter (PSD) by mercury intrusion (Hg)

c) Pore size diameter with volume (v) based distribution and pore volume determined by inverse size-exclusion chromatography (ISEC)

d) Surface area determined by nitrogen adsorption (N2) using the BET method

b)-d) This information was provided by the manufacturer Merck KGaA (Darmstadt, Germany)

n.a. not available

All materials have been tested with cell culture supernatants and B14-TRZ ligands exhibited astonishing capacities, especially compared to B14-2LP ligands. Note that the azide group of B14-TRZ materials have been endcapped with 2-propargylalcohol resulting in a methyl alcohol coupled to the TRZ ring. It has to be mentioned, that, although Click Chemistry is known as a straight forward one pot reaction, several difficulties occurred when applying this kind of reaction to



Fractogel, FractoAIMs and other related materials (e.g. Sartobind Epoxy, etc.) in combination with A2P and B14 ligands and yields of the immobilization reactions never exceeded 43%. Also endcapping with 2-propargylalcohol proved to be more difficult as expected. The yield of this reaction can not be verified by elemental analysis, but by retaining of impurities during DBC runs, a non stoichiometric reaction was assumed. For latter reasons B14-TRZ-FA3 has been triple endcapped and tested again with cell culture feed solutions, providing elution fractions with lower impurity levels. In contrast B14-2LP-Purabead and B14-2LP-FA1 materials have been endcapped using ethanolamine, which is per se a weak anion exchanger, which is known to bind impurities out of feed solutions. These bound impurities, of course, block binding sites on the affinity materials and therefore reducing binding capacities. Fortunately a selective elution can be applied, resulting in a considerably pure IgG solution. More details can be found in Appendix 2.

The binding of impurities and IgG by non endcapped azide groups was investigated deeper in another study. A comparison of different endcapping strategies (ethanolamine, mercaptoethanol, acidic hydrolysis) was done and also the properties of adsorbents carrying azide groups only were investigated. During this study the immense importance of a correct endcapping strategy was underlined, and therefore also the in house established Click Chemistry protocol for our adsorbents was further improved. The results can be viewed in detail in Appendix 4.

### **3.4. Soft gels with mixed modal ligands**

Cation exchangers play a big role in protein purification and a big band width of commercial materials is available on the market. Cell cultures typically grow under isotonic conditions which imply about 150 mM NaCl and pH 7 and above. Common cation exchange materials exhibit only minor binding abilities under those conditions and adsorbent bearing ionic groups less prone to such environment is demanded. Several techniques are known to work sufficiently under isotonic condition, as there are for example HIC or TIC. The approach in this study was the combination of those with ionic groups. Thiophilic groups combined with sulfonic acids, based on immobilized, oxidized dithiols bound to commercial

available epoxy activated Fractogel<sup>®</sup> EMD showed rather low binding capacities compared to commercial cation exchangers (materials **B1**, **C** and **D**, Fig. 10) and could not exceed 36 mg/mL under 0 mM sodium chloride and pH 5. By comparison of elemental analysis and titration results cross linking was assumed to be responsible for this considerable low SBC results.

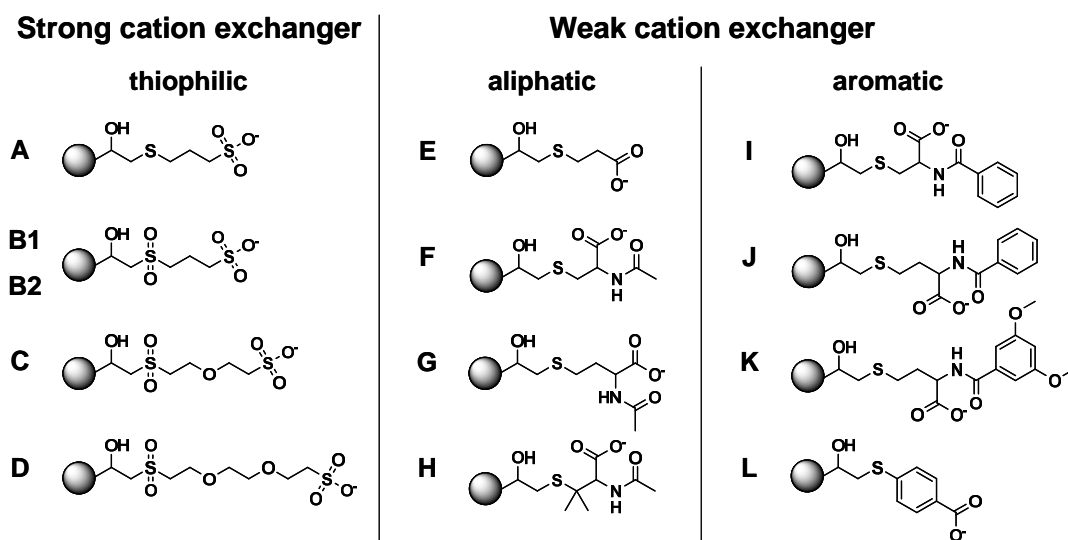


Figure 10: Summary of strong and weak mixed mode cation exchanger materials

With increasing pH and sodium chloride concentration the capacities dropped down to 2 mg/mL. A different approach to obtain comparable ligands without the use of dithiols was the coupling of 3-mercaptopropanesulfonic acid, resulting in material **A**. By this means no cross linking was able to occur during synthesis, which was proofed by better accordance of the results for elemental analysis and titration. Nevertheless the capacities of this ligand were again not able to compete with the benchmark material from Merck KGaA. This adsorbent captured 86 mg/mL out of a feed solution containing no salt and pH 5, lower compared to 118 mg/mL of Merck's strong cation exchanger. Furthermore binding properties for more isotonic solutions have not improved. A further test was conducted by oxidation of material **A**, resulting in a material similar to **B1**. The conversion of the sulfanyl group into a sulfonyl group was not able to improve capacities for higher sodium chloride concentrations and pH. Note that thiophilic increments are enhanced by adding structure forming salts, which was not done during this study and was not desired for an industrial application.

An improvement was achieved by coupling of a carboxylic acid, 3-mercaptopropionic acid (material **E**). At the first glance this material did not seem to possess much improved properties, as the bound IgG for pH 5 and no sodium chloride added was about 29 mg/mL. But after closer inspection the capacities under conditions more similar to isotonic solutions exceeded the benchmark material by Merck KGaA. Material **E** was able to capture 20 mg IgG/mL gel out of a feed solution containing 150 mM NaCl and pH 5.0, out of which Merck's SO<sub>3</sub> ion exchanger bound 9 mg/mL.

Further tests were conducted with N-acetyl-cysteine and a couple of highly related compounds. All of these 3 materials (material **F**, **G** and **H**) exhibited quite similar results and capacities and the binding habits for high sodium chloride concentrations and pH were not satisfactory.

An improvement was accomplished by the coupling of aromatic moieties to a cysteine or homocysteine backbone (material **I**, **J** and **K**). Until now the binding of substantial amounts of IgG were restricted to a maximum pH of 5.5 and 150 mM sodium chloride the investigated adsorbents. Latter materials were able to bind 15, 26 and 22 mg/mL at presence of 150 mM NaCl and pH 6.5, respectively. The conclusion was that carboxylic acids in the proximity of aromatic moieties performed well, and a further step was the coupling of a benzoic acid onto a solid support material. This was accomplished by immobilization of 4-mercaptopbenzoic acid onto Fractogel and the results were quite astonishing (material **L**). Although the material showed rather low capacities at very low pH, the capacities increased up to a pH of 6.0 to 7.0, beyond which they decreased again. E.g. the material captured 41 mg/mL out of a 150 mM sodium chloride solution and pH 6.5.

The most promising materials of this study were subject of more severe investigations, namely their performance under dynamic conditions. Materials **J**, **K** and **L** were used for these experiments. While material **J** and **K** were examined under 75 and 150 mM sodium chloride conditions with pH 5.5 and 6.5, material **L** was further investigated by using solutions with pH 6.5 (75 mM and 150 mM sodium chloride) and pH 7.4. Furthermore experiments were conducted to examine Pluronic tolerance of the material and also cell culture feed solution (75 mM NaCl and pH 6.5) was used to test the material against more realistic solutions. All DBC results stood in good accordance to the results obtained by prior SBC tests. Further details can be found in Appendix 5.

## 4. Conclusions

The following conclusions can be drawn from this study:

The importance of further developments in antibody purification can not be neglected and this work shows that a lot of potential is still there, although Protein A adsorbents are a tough benchmark to break.

Membranes are a possible alternative and the combination with affinity ligands was tested during this study. A2P showed good binding capacities for pure IgG, no matter if they were coupled with DES spacer or TRZ. TRZ spacer leads to slightly better recoveries, but when tested with cell culture supernatants, the binding capacities decreased, what led to the consumption that A2P-TRZ also binds impurities. B14-TRZ membranes exhibited lower binding capacities, but due much improved recoveries these membranes outperformed A2P-DES and A2P-TRZ-membranes. Several types of epoxy activated materials were tested, and the novel SartoAIMs Epoxy 2 membranes turned out to be superior in all cases.

Above mentioned spacer-ligand combinations were also immobilized onto beads, leading to similar conclusions in terms of selectivity, capacities and recoveries. Furthermore, also the influence of different support media was investigated. Again B14-TRZ turned out to be the one with best yields, purities and recoveries. Especially with novel FractoAIMs materials, with optimized pore size and decreased particle sizes astonishing results were obtained. During these experiments residual azide groups showed unexpected behavior as they were capable to bind IgG as well as impurities. This azide-IgG interaction was undesired as IgG seemed to be stuck to the azide groups on the one hand, and on the other hand it turned out that azide groups, especially bound to organic molecules, seemed to induce aggregation of IgG. This drawback was overcome by optimized azide densities and an improved endcapping strategy. By this means a B14-TRZ in combination with FractoAIMs 3 exhibited binding capacities in the region of commercial rmp Protein A Sepharose FF while applying high flow rates.

The investigations on the field of mixed modal ligands exhibited several interesting conclusions. Sulfonic acids in combination with thiophilic increments such as a sulfide bridge or sulfonyl group showed no signs of binding sufficient amounts of h-IgG under conditions containing 75 mM sodium chloride in combination with pH > 5.5. A simple weak cation exchanger, 3-mercaptopropionic acid, bound to the

support via sulfanyl group was able to bind IgG under more isotonic conditions than common cation exchangers, e.g. Fractogel EMD SO<sub>3</sub>. Furthermore N-acetylated cysteine and cysteine related substances did not exhibit improved binding capacities for desired conditions. But cysteine and cysteine related substances combined with aromatic moieties showed much improved properties, therefore aromatic systems were declared mandatory for binding IgG out of feed solutions containing salt concentrations of > 75 mM and pH above 5.5. The crown of these experiments was the introduction of 4-mercaptobenzoic acid as a ligand. This very simple adsorbent can be produced in a one pot reaction and was able to bind during DBC experiments 52 mg/mL h-IgG out of a pure IgG solution with 150 mM sodium chloride and pH 6.5.

## 5. References

- [1] S.S. Farid, Journal of Chromatography, B: Analytical Technologies in the Biomedical and Life Sciences 848 (2007) 8.
- [2] S. Sommerfeld, J. Strube, Chemical Engineering and Processing 44 (2005) 1123.
- [3] S.C. Gad, Editor, Handbook of Pharmaceutical Biotechnology, Wiley-Interscience, 2007.
- [4] J. Reichert, A. Pavlou, Nature Reviews Drug Discovery 3 (2004) 383.
- [5] E.O. Saphire, P.W.H. Parren, R. Pantophlet, M.B. Zwick, G.M. Morris, P.M. Rudd, R.A. Dwek, R.L. Stanfield, D.R. Burton, I.A. Wilson, Science 293 (2001) 1155.
- [6] Q. Zhang, G. Chen, X. Liu, Q. Qian, Cell Research 17 (2007) 89.
- [7] M. Trikha, L. Yan, M.T. Nakada, Current Opinion in Biotechnology 13 (2002) 609.
- [8] E. Jain, A. Kumar, Biotechnology Advances 26 (2008) 46.
- [9] J. Thoemmes, M. Etzel, Biotechnology Progress 23 (2007) 42.
- [10] N. Tugeu, D.J. Roush, K.E. Goklen, Biotechnology and Bioengineering 99 (2007) 599.
- [11] J. Deisenhofer, Biochemistry 20 (1981) 2361.
- [12] J.L. Coffman, J.F. Kramarczyk, B.D. Kelley, Biotechnology and Bioengineering 100 (2008) 605.

- [13] K. Huse, H.-J. Bohme, G.H. Scholz, *Journal of Biochemical and Biophysical Methods* 51 (2002) 217.
- [14] G. Fassina, G. Palombo, A. Verdoliva, M. Ruvo, in, 2002, p. 1013.
- [15] A. Forsgren, J. Sjoquist, *Journal of immunology* 97 (1966) 822.
- [16] S. Hober, K. Nord, M. Linhult, *Journal of Chromatography, B: Analytical Technologies in the Biomedical and Life Sciences* 848 (2007) 40.
- [17] G. Healthcare, *Antibody purification*, 2002.
- [18] K.J. Reis, M. Yarnall, E.M. Ayoub, M.D.P. Boyle, *Scandinavian Journal of Immunology* 20 (1984) 433.
- [19] L. Bjorck, G. Kronvall, *Journal of immunology (Baltimore, Md. : 1950)* 133 (1984) 969.
- [20] Thermo Fisher Scientific Inc.
- [21] B. Guss, M. Eliasson, A. Olsson, M. Uhlen, A.K. Frej, H. Joernvall, J.I. Flock, M. Lindberg, *EMBO Journal* 5 (1986) 1567.
- [22] S. Guelich, M. Linhult, S. Stahl, S. Hober, *Protein Eng.* 15 (2002) 835.
- [23] B.H.K. Nilson, A. Solomon, L. Bjoerck, B. Aakerstroem, *Journal of Biological Chemistry* 267 (1992) 2234.
- [24] N.G. Housden, S. Harrison, S.E. Roberts, J.A. Beckingham, M. Graille, E. Stura, M.G. Gore, *Biochemical Society Transactions* 31 (2003) 716.
- [25] B.H.K. Nilson, I.-M. Frick, P. Aakesson, S. Forsen, L. Bjoerck, B. Aakerstroem, M. Wikstroem, *Biochemistry* 34 (1995) 13688.
- [26] D. Low, R. O'Leary, N.S. Pujar, *Journal of Chromatography, B: Analytical Technologies in the Biomedical and Life Sciences* 848 (2007) 48.
- [27] C.R. Lowe, S.J. Burton, J.C. Pearson, Y.D. Clonis, V. Stead, *Journal of Chromatography* 376 (1986) 121.
- [28] C.R. Lowe, S.J. Burton, N.P. Burton, W.K. Alderton, J.M. Pitts, J.A. Thomas, *Trends in Biotechnology* 10 (1992) 442.
- [29] Y.D. Clonis, N.E. Labrou, V.P. Kotsira, C. Mazitsos, S. Melissis, G. Gogolas, *Journal of Chromatography, A* 891 (2000) 33.
- [30] G. Fassina, A. Verdoliva, G. Palombo, M. Ruvo, G. Cassani, *Journal of Molecular Recognition* 11 (1998) 128.
- [31] G. Fassina, *Methods in Molecular Biology (Totowa, New Jersey)* 147 (2000) 57.

- [32] R. Li, V. Dowd, D.J. Stewart, S.J. Burton, C.R. Lowe, *Nature Biotechnology* 16 (1998) 190.
- [33] C.R. Lowe, *Current Opinion in Chemical Biology* 5 (2001) 248.
- [34] Prometic BioSciences.
- [35] S. Ghose, B. Hubbard, S.M. Cramer, *Journal of Chromatography, A* 1122 (2006) 144.
- [36] A.C.A. Roque, M.A. Taipa, C.R. Lowe, *Journal of Chromatography, A* 1064 (2005) 157.
- [37] A.C.A. Roque, C.S.O. Silva, M.A. Taipa, *Journal of Chromatography, A* 1160 (2007) 44.
- [38] J. Porath, F. Maisano, M. Belew, *FEBS letters* 185 (1985) 306.
- [39] P.P. Berna, N. Berna, J. Porath, S. Oscarsson, *Journal of Chromatography, A* 800 (1998) 151.
- [40] A. Schwarz, F. Kohen, M. Wilchek, *Reactive Polymers* 22 (1994) 259.
- [41] A. Schwarz, F. Kohen, M. Wilchek, *Journal of Chromatography, B: Biomedical Applications* 664 (1995) 83.
- [42] K.L. Knudsen, M.B. Hansen, L.R. Henriksen, B.K. Andersen, A. Lihme, *Analytical Biochemistry* 201 (1992) 170.
- [43] A. Schwarz, *Journal of Molecular Recognition* 9 (1996) 672.
- [44] G.H. Scholz, P. Wippich, S. Leistner, K. Huse, *Journal of Chromatography, B: Biomedical Sciences and Applications* 709 (1998) 189.
- [45] G.H. Scholz, S. Vieweg, S. Leistner, J. Seissler, W.A. Scherbaum, K. Huse, *Journal of Immunological Methods* 219 (1998) 109.
- [46] A. Tiselius, *Arkiv. Kemi, Mineral. Geol.* 26B (1948) 5 pp.
- [47] J.L. Fausnaugh, L.A. Kennedy, F.E. Regnier, *Journal of Chromatography* 317 (1984) 141.
- [48] S. Hjerten, J. Rosengren, S. Pahlman, *Journal of Chromatography* 101 (1974) 281.
- [49] J. Porath, L. Sundberg, N. Fornstedt, I. Olsson, *Nature (London, United Kingdom)* 245 (1973) 465.
- [50] G. Sofer, L. Hagel, *Handbook of Process Chromatography: A Guide to Optimization, Scale Up, and Validation*, 1997.
- [51] L.O. Narhi, Y. Kita, T. Arakawa, *Analytical Biochemistry* 182 (1989) 266.
- [52] F.E. Regnier, *Science* 238 (1987) 319.

- [53] A.I. Jion, L.-T. Goh, S.K.W. Oh, *Biotechnology and Bioengineering* 95 (2006) 911.
- [54] A. Staby, M.-B. Sand, R.G. Hansen, J.H. Jacobsen, L.A. Andersen, M. Gerstenberg, U.K. Bruus, I.H. Jensen, *Journal of Chromatography, A* 1034 (2004) 85.
- [55] A. Staby, M.-B. Sand, G. Hansen Ronni, H. Jacobsen Jan, A. Andersen Line, M. Gerstenberg, K. Bruus Ulla, H. Jensen Inge, *Journal of chromatography. A* 1069 (2005) 65.
- [56] A. Staby, H. Jacobsen Jan, G. Hansen Ronni, K. Bruus Ulla, H. Jensen Inge, *Journal of Chromatography, A* 1118 (2006) 168.
- [57] P. DePhillips, A.M. Lenhoff, *Journal of Chromatography, A* 883 (2000) 39.
- [58] P.R. Levison, C. Mumford, M. Streater, A. Brandt-Nielsen, N.D. Pathirana, S.E. Badger, *J. Chromatogr., A* 760 (1997) 151.
- [59] P. DePhillips, A.M. Lenhoff, *Journal of chromatography. A* 933 (2001) 57.
- [60] D.C. Nash, H.A. Chase, *Journal of chromatography. A* 807 (1998) 185.
- [61] S. Yamamoto, T. Ishihara, *Journal of chromatography. A* 852 (1999) 31.
- [62] S. Yamamoto, E. Miyagawa, *Journal of chromatography. A* 852 (1999) 25.
- [63] R. Hahn, P.M. Schulz, C. Schaupp, A. Jungbauer, *Journal of Chromatography, A* 795 (1998) 277.
- [64] A. Staby, I.H. Jensen, *Journal of Chromatography, A* 908 (2001) 149.
- [65] A. Staby, I.H. Jensen, I. Mollerup, *Journal of Chromatography, A* 897 (2000) 99.
- [66] P.R. Levison, R.M.H. Jones, D.W. Toome, S.E. Badger, M. Streater, N.D. Pathirana, *Journal of Chromatography, A* 734 (1996) 137.
- [67] K. Miyabe, G. Guiochon, *Journal of Chromatography, A* 866 (2000) 147.
- [68] M. McCoy, K. Kalghatgi, F.E. Regnier, N. Afeyan, *Journal of Chromatography, A* 743 (1996) 221.
- [69] M.A. Fernandez, W.S. Laughinghouse, G. Carta, *Journal of Chromatography, A* 746 (1996) 185.
- [70] G. Zhao, X.-Y. Dong, Y. Sun, *Journal of Biotechnology* 144 (2009) 3.
- [71] U. Gottschalk, *Biotechnology Progress* 24 (2008) 496.
- [72] G.C. Howard, M.R. Kaser, Editors, *Making and Using Antibodies: A Practical Handbook*, 2007.



- [73] M.B. Dainiak, V.A. Izumrudov, V.I. Muronetz, I.Y. Galaev, B. Mattiasson, Bioseparation FIELD Full Journal Title:Bioseparation 7 (1998) 231.
- [74] M.A. Taipa, R. Kaul, B. Mattiasson, J.M. Cabral, Journal of molecular recognition : JMR 11 (1998) 240.
- [75] M.A. Taipa, R.-H. Kaul, B. Mattiasson, J.M.S. Cabral, Bioseparation 9 (2000) 291.
- [76] T.M. Przybycien, N.S. Pujar, L.M. Steele, Current Opinion in Biotechnology 15 (2004) 469.
- [77] S.D. Durbin, G. Feher, Annual Review of Physical Chemistry 47 (1996) 171.
- [78] F. Lottspeich, Bioanalytik, Spektrum, 1998.
- [79] A.C. Grodzki, E. Berenstein, Methods in Molecular Biology (Totowa, NJ, United States) 588 15.
- [80] C. Boi, Journal of Chromatography, B: Analytical Technologies in the Biomedical and Life Sciences 848 (2007) 19.
- [81] W. Demmer, D. Nussbaumer, Journal of Chromatography, A 852 (1999) 73.
- [82] H.L. Knudsen, R.L. Fahrner, Y. Xu, L.A. Norling, G.S. Blank, Journal of Chromatography, A 907 (2001) 145.
- [83] J.X. Zhou, T. Tressel, Biotechnology Progress 22 (2006) 341.
- [84] A. Brown, J. Bill, T. Tully, A. Radhamohan, C. Dowd, Biotechnology and Applied Biochemistry 56 (2010) 59.
- [85] W.T. Riordan, S.M. Heilmann, K. Brorson, K. Seshadri, M.R. Etzel, Biotechnology Progress 25 (2009) 1695.
- [86] R. Ghosh, Journal of Chromatography, A 952 (2002) 13.
- [87] X. Zeng, E. Ruckenstein, Biotechnology progress 15 (1999) 1003.
- [88] E. Klein, Journal of Membrane Science 179 (2000) 1.
- [89] C. Charcosset, J. Chem. Technol. Biotechnol. FIELD Full Journal Title:Journal of Chemical Technology & Biotechnology 71 (1998) 95.
- [90] C. Boi, S. Dimartino, G.C. Sarti, Biotechnology Progress 24 (2008) 640.
- [91] J. Sinha, P.K. Dey, T. Panda, Applied microbiology and biotechnology 54 (2000) 476.
- [92] G.M. Zijlstra, M.J.F. Michielsen, C.D. De Gooijer, L.A. Van Der Pol, J. Tramper, Bioseparation 7 (1998) 117.

- [93] P.A.J. Rosa, A.M. Azevedo, I.F. Ferreira, J. de Vries, R. Korporaal, H.J. Verhoef, T.J. Visser, M.R. Aires-Barros, *Journal of Chromatography, A* 1162 (2007) 103.
- [94] V. Busini, D. Moiani, D. Moscatelli, L. Zamolo, C. Cavallotti, *Journal of Physical Chemistry B* 110 (2006) 23564.
- [95] L. Zamolo, V. Busini, D. Moiani, D. Moscatelli, C. Cavallotti, *Biotechnology Progress* 24 (2008) 527.

## **6. Appedices**

### **6.1. Publications**

#### **Appendix 1: Publication 1**

Cristiana Boi, Simone Dimartino, Stefan Hofer, Jeannie Horak, Sharon Williams, Giulio C. Sarti, Wolfgang Lindner:

*Influence of different spacer arms on Mimetic Ligand A2P and B14 membranes for human IgG purification*

*Journal of Chromatography B* (2011), 879 (19), 1633 - 1640

#### **Appendix 2: Publication 2**

Jeannie Horak, Stefan Hofer, Chris Sadler, Sharon Williams, Wolfgang Lindner:

*Performance evaluation of Mimetic Ligand B14-triazole-FractoAIMs adsorbents for the capture of human monoclonal immunoglobulin G from cell culture feed*

*Analytical and Bioanalytical Chemistry* (2011), 400 (8), 2349 - 2359

#### **Appendix 3: Publication 3**

Laura Zamolo, Matteo Salvalaglio, Carlo Cavalotti, Benedict Galarza, Chris Sadler, Sharon Williams, Stefan Hofer, Jeanie Horak, Wolfgang Lindner:

*Experimental and Theoretical Investigation of Effect of Spacer Arm and Support Matrix of Synthetic Affinity Chromatographic Materials for the Purification of Monoclonal Antibodies*

*Journal of Physical Chemistry B* (2010), 114 (29), 9367 - 9380

#### **Appendix 4: Publication 4**

Jeannie Horak, Stefan Hofer, Wolfgang Lindner:

*Optimization of a ligand immobilization and azide group endcapping concept via Click-Chemistry for the preparation of adsorbents for antibody purification*

Journal of Chromatography B (2010), 878 (32), 3382 - 3394

#### **Appendix 5: Publication 5**

Stefan Hofer, Alexander Ronacher, Heiner Graalfs, Jeannie Horak, Wolfgang Lindner:

*Static and dynamic binding capacities of human immunoglobulin G on mixed-modal, thiophilic and hydrophobic poly(methacrylate) cation exchangers*

Journal of Chromatography A, article in press (DOI: 10.1016/j.chroma.2011.06.012)



## **Appendix 1**

### **Publication 1**





# Influence of different spacer arms on Mimetic Ligand<sup>TM</sup> A2P and B14 membranes for human IgG purification

Cristiana Boi<sup>a,\*</sup>, Simone Dimartino<sup>a</sup>, Stefan Hofer<sup>c</sup>, Jeannie Horak<sup>c,\*\*</sup>, Sharon Williams<sup>b</sup>, Giulio C. Sarti<sup>a</sup>, Wolfgang Lindner<sup>c</sup>

<sup>a</sup> DICMA, Alma Mater Studiorum Università di Bologna, via Terracini 28, 40131 Bologna, Italy

<sup>b</sup> ProMetic Biosciences Ltd., 211 Cambridge Science Park, Milton Road, Cambridge CB4 0WA, UK

<sup>c</sup> Department of Analytical Chemistry, University of Vienna, Waehringerstrasse 38, 1090 Vienna, Austria

## ARTICLE INFO

### Article history:

Received 15 February 2011

Accepted 31 March 2011

Available online 8 April 2011

### Keywords:

Antibody purification

A2P

B14

Click-Chemistry

Azide-functionalized membrane

Affinity membranes

## ABSTRACT

Microporous membranes are an attractive alternative to circumvent the typical drawbacks associated to bead-based chromatography. In particular, the present work intends to evaluate different affinity membranes for antibody capture, to be used as an alternative to Protein A resins. To this aim, two Mimetic Ligands<sup>TM</sup> A2P and B14, were coupled onto different epoxide and azide group activated membrane supports using different spacer arms and immobilization chemistries. The spacer chemistries investigated were 1,2-diaminoethane (2LP), 3,6-dioxo-1,8-octanedithiol (DES) and [1,2,3] triazole (TRZ). These new mimetic membrane materials were investigated by static and by dynamic binding capacity studies, using pure polyclonal human immunoglobulin G (IgG) solutions as well as a real cell culture supernatant containing monoclonal IgG<sub>1</sub>. The best results were obtained by combining the new B14 ligand with a TRZ-spacer and an improved Epoxy 2 membrane support material. The new B14-TRZ-Epoxy 2 membrane adsorbent provided binding capacities of approximately 3.1 mg/mL, besides (i) a good selectivity towards IgG, (ii) high IgG recoveries of above 90%, (iii) a high Pluronic-F68 tolerance and (iv) no B14-ligand leakage under harsh cleaning-in-place conditions (0.6 M sodium hydroxide). Furthermore, foreseeable improvements in binding capacity will promote the implementation of membrane adsorbents in antibody manufacturing.

© 2011 Elsevier B.V. All rights reserved.

## 1. Introduction

The demand and the importance of biopharmaceuticals is constantly growing and antibiotics such as penicillin and cephalosporin, hormones (insulin), blood factors (Factor VIII, Factor IX) and interferons ( $\alpha$ ,  $\beta$ ,  $\gamma$ ) [1,2] belong to the most important drugs on the pharmaceutical market. In recent years, monoclonal antibodies (MAb) gained much importance. The reasons for their increasing dominance are their applicability against a multitude of diseases such as Alzheimer's syndrome and cancer [3] combined with a high approval rate by governmental institutions [4]. Presently, more than 18 antibodies have already been approved in the United States, and more than 150 antibody-based therapeutics are under development or undergoing clinical trials [5,6].

In addition, the production yields of MAbs have significantly improved and it is reasonable to expect titers in the order of 10 g/L

in the near future [7]. Despite such improvements in upstream process development, the overall production costs are not reduced, since the real bottleneck in antibody manufacture lies in downstream processing, where purification costs may exceed 60% of the total production expenses [8]. The origin of that is directly related to stringent quality demands defined by purity, efficacy, stability, immunogenicity and several further aspects, which are clearly specified by regulatory agencies [9].

The most important step in downstream processing is the capture of MAbs from the cell culture supernatant, for which up to date Protein A-based resin adsorbents are the process platform of choice. Reason for their superior status is their high selectivity and high binding capacity for immunoglobulin G (IgG). Despite all benefits that Protein A adsorbents may offer, they also suffer from certain drawbacks such as high pressure drops, flow rate limitations and soft gel compression, which are typical for agarose-based separation techniques [10]. Furthermore, the rather high IgG molecular weight of 150 kDa entails additional restrictions due to the slow diffusion of the antibody molecules into the dead end pores of the adsorbent particles [11].

A promising alternative is represented by membrane adsorbents, which exhibit several advantages with respect to classical

\* Corresponding author. Tel.: +39 051 2090432; fax: +39 051 6347788.

\*\* Corresponding author. Tel.: +43 1 427752373; fax: +43 1 42779523.

E-mail addresses: [cristiana.boi@unibo.it](mailto:cristiana.boi@unibo.it) (C. Boi), [Jeannie.Horak@univie.ac.at](mailto:Jeannie.Horak@univie.ac.at) (J. Horak).

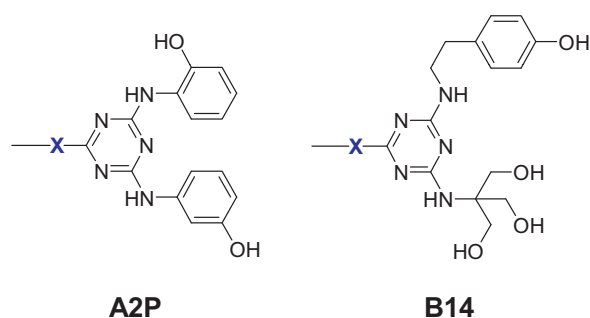


**Fig. 1.** Chemical structure of the Mimetic Ligands<sup>TM</sup> A2P and B14, which are linked with group X (X=NH or S) to the corresponding spacer chain.

packed-bed chromatography. Membranes have almost no pressure drop restrictions due to their superior flow properties and, in addition, diffusion mass transfer resistance is not important, since the main transport mechanism involved is convection [12].

For these reasons, membrane-based purification techniques are gaining increased interest in industrial applications. The use of anion exchange membranes in polishing steps of antibody manufacturing is well established, especially since they do not suffer from capacity limitations when operated in a flow through mode for trace impurity removal [13–15]. More recently, membrane adsorbers used in protein capture mode, such as cation exchange type membranes [16–18] and affinity based Protein-A membranes [10,19], were considered for IgG purification at production scale. Further improvements of membrane properties lead to a new Protein A based membrane from Sartorius Stedim Biotech, which possesses 12-times higher binding capacities for IgG compared to the former Sartobind Protein A affinity membrane [20].

However, Protein A is a large bacterial protein, which is rather sensitive towards harsh sanitation conditions and detached ligand has to be removed in additional polishing steps. Therefore, smaller and more stable ligands that can mimic the antibody binding region of Protein A represent an attractive alternative. Such synthetic ligands are inter alia the peptido-mimetic ligand D-PAM [21], the bio-mimetic triazine derived A2P ligand [22], and peptide sequences [23]. While D-PAM was created by screening of peptide libraries [24,25], A2P is the product of the combination of computational chemistry and a combinatorial ligand library approach, where the two phenolic substituents of the triazine core are designed to capture polyclonal IgG.

On the other hand, the newly developed B14-ligand from ProMetic BioSciences Ltd. was created to specifically capture human monoclonal IgG<sub>1</sub>. B14 was found through a diverse and rationally designed combinatorial library approach, and possesses the same triazine-core as A2P, but with a different set of substituents (Fig. 1). A recent study describes the IgG capture performance of B14-ligand bound via triazole linkage (TRZ) [26,27] to a new polymethacrylate based adsorbent (FractoAIMs-3). It was shown that B14 is suitable for IgG<sub>1</sub> capture at low bed heights and high flow-rates from cell culture feed [28], which can be considered being ideal properties for a corresponding membrane adsorber. Furthermore, molecular dynamic simulations performed

on different A2P-type affinity media showed that the bio-specific ligand is not the only factor which influences the antibody capture performance of affinity media [29,30]. It was found that spacer chain chemistry, immobilization chemistry and support chemistry may contribute in positive or negative ways. Therefore the present study includes a small variation of different ligand head groups (A2P and B14), spacer chains (2LP, DES and TRZ) and membrane supports, including two new cellulose-based membranes with improved pore structure and surface properties (Epoxy 2 and Epoxy 3). Membrane performance evaluation was performed with polyclonal IgG standard solutions as well as cell culture supernatant containing IgG<sub>1</sub>, employing in the first instance static binding experiments and dynamic binding tests for the most promising membrane adsorbents.

## 2. Experimental

### 2.1. Materials and methods

#### 2.1.1. Support media

Four different epoxide-activated regenerated cellulose membranes, namely Sartobind Epoxy<sup>TM</sup> and the new Epoxy 1, Epoxy 2 and Epoxy 3 membranes, were kindly provided by Sartorius Stedim Biotech GmbH (Goettingen, Germany). They differ in their physical and chemical parameters such as pore size, void volume, thickness and epoxide group density, as summarized in Table 1 and the latter in Table S1 of the electronic supplementary material. Sartobind Epoxy membranes are commercially available and have an average pore size of 0.45  $\mu\text{m}$  and an epoxide group density between 2.0 and 2.2  $\mu\text{mol}/\text{cm}^2$ , according to manufacturer's specifications. The Epoxy 1 and Epoxy 2 membranes have similar physical characteristics, but different epoxide group densities of 0.3–0.4  $\mu\text{mol}/\text{cm}^2$  for Epoxy 1 and ranging between 1.2 and 1.8  $\mu\text{mol}/\text{cm}^2$  for Epoxy 2 membranes. The Epoxy 3 material possesses not only the highest epoxide density, between 2.7 and 3.2  $\mu\text{mol}/\text{cm}^2$ , but also the greatest thickness. Its large average pore size of more than 3  $\mu\text{m}$  is mirrored by a very high permeability. For convenience, Sartobind Epoxy membranes will be denominated as Sartoeпоxy throughout this paper.

#### 2.1.2. Feed solutions

Polyclonal human immunoglobulin G, Gammanorm (165 mg/mL) from Octapharma (Stockholm, Sweden), was used as IgG source and diluted to the appropriate concentration with 0.1 M Phosphate Buffer Saline (PBS), pH 7.4. The cell culture supernatant employed in this study (ExcellGene, Monthey, Switzerland) contains monoclonal human IgG<sub>1</sub> at a concentration of about 0.11 mg/mL. 0.1 M PBS buffer (pH 7.4) was used as equilibration and washing buffer; 0.1 M glycine (pH 2.8), 0.05 M citric acid (pH 2.5) and 0.05 M acetic acid (pH 2.5) were used as elution buffers. Regeneration was accomplished using a 0.6 M NaOH solution.

#### 2.1.3. Protein quantification

IgG concentration in pure protein solutions was determined with a UV-spectrophotometer Shimadzu UV-1601 (Milano, Italy)

**Table 1**  
Summary of membrane properties.

Membrane	Thickness <sup>a</sup> [ $\mu\text{m}$ ]	Pore size <sup>b</sup> [ $\mu\text{m}$ ]	Porosity <sup>a</sup> [%]	Permeability <sup>b</sup> [ $\text{mL}/(\text{min bar cm}^2)$ ]	BET surface area <sup>a</sup> [ $\text{m}^2/\text{g}$ ]
Sartoeпоxy	230	0.45	72.7	50–60	2.25
Epoxy 1	192	<0.45	54.5	35–45	4.01
Epoxy 2	192	<0.45	58.5	30–35	4.78
Epoxy 3	237	>3	72.2	400–600	0.93

<sup>a</sup> Data provided by the Membrane Technology group at the University of Twente, The Netherlands.

<sup>b</sup> Data provided by Sartorius Stedim Biotech, Germany.



at a wavelength of 280 nm. For complex solutions, IgG concentration was measured with a HPLC system Alliance 2695 with a dual wavelength UV-detector 2487 from Waters (Milano, Italy) using a Protein A affinity cartridge PA ID from Applied Biosystems (Monza, MI, Italy) [20]. The purity of the eluted fractions was determined with SDS PAGE under denaturing conditions using coomassie blue for protein staining. Electrophoresis was performed using the Criterion system from Bio-Rad Laboratories (Segrate, MI, Italy) [20].

## 2.2. Preparation and characterization of affinity membranes

The synthetic Mimetic Ligands<sup>TM</sup> were provided as A2P-monochloride and B14-monochloride by ProMetic Biosciences Ltd. (Cambridge, UK). All other synthesis related chemicals were purchased from Sigma Aldrich (Vienna, Austria). The synthesis protocols for the below mentioned ligand-spacer combinations were published by Zamolo et al. [30]. The membrane preparation protocols as well as the determination of accessible epoxide groups on a membrane surface via titration with thiosulfate and via elemental analysis after immobilization of 2-ethanolamine and 2-mercaptoethanol were summarized in Table S1 in the electronic supplementary materials. The chemical structures of investigated membrane adsorbers can be found in Fig. S1 in the electronic supplementary materials. Table 2 provides an overview of the various ligands, spacers and support combinations together with the corresponding ligand densities.

A short schematic overview is reported below regarding the different membrane protocols for the immobilization of A2P and B14, onto the different porous membrane supports, namely Sartopoxy, Epoxy 1, Epoxy 2 and Epoxy 3:

- (i) Direct ligand immobilization via 1,2-diaminoethane linkage (2LP), with final epoxide group deactivation using 2-ethanolamine;
- (ii) Use of 3,6-dioxa-1,8-octanedithiol (DES) as spacer arm. The thiol-terminal A2P-DES ligand was linked via an epoxy-ring opening reaction onto the epoxy-activated membrane surface. The remaining epoxide groups were endcapped with 2-mercaptoethanol;
- (iii) Use of [1,2,3]-triazole ring (TRZ) as spacer arm. The introduction of an alkyne group on the biomimetic ligands was performed through nucleophilic substitution of the chlorine atom of A2P-Cl and B14-Cl with 3-propargylamine, obtaining A2P-propyne and B14-propyne moieties. Ligand immobilization was performed via Click-Chemistry [27], employing a copper (I) mediated Huisgen 1,3-dipolar cycloaddition reaction to connect the alkyne modified affinity ligand to an azide-functionalized membrane support. No endcapping was performed for these membranes.
- (iv) In order to evaluate possible non specific interactions between the target protein IgG and both spacer and surface, two additional test membranes were prepared, namely OH-(CH<sub>2</sub>)<sub>2</sub>-DES-Sartopoxy and OH-CH<sub>2</sub>-TRZ-Sartopoxy. In case of OH-(CH<sub>2</sub>)<sub>2</sub>-DES-Sartopoxy, 2-chloroethanol was attached to one of the two thiol-groups of 3,6-dioxa-1,8-octanedithiol prior to the immobilization of OH-(CH<sub>2</sub>)<sub>2</sub>-DES to Sartopoxy. The OH-CH<sub>2</sub>-TRZ-Sartopoxy was prepared by coupling 3-propargylalcohol to azide modified Sartopoxy membranes via Click-reaction with copper (I) as catalyst.

Note that in an earlier study Protein A Epoxy 1 showed good performance for IgG capture from cell culture supernatant [20]. Unfortunately, due to the low ligand densities of A2P and B14 ligands on Epoxy 1 membrane support, preliminary batch experiments showed rather low binding capacities for IgG. Nonetheless,

in order to provide a thorough description and comparison of membrane performance, Epoxy 1 membranes were included in our discussion, although no experimental data were explicitly shown.

## 2.3. Membrane performance evaluation and characterization

Batch adsorption experiments were performed by soaking the membrane discs in IgG solutions of known concentration and kept under gentle agitation until equilibrium was reached. The protein concentration in the supernatant was determined at the beginning and at the end of each experiment by measuring the absorbance of the solution at 280 nm [20]. This protocol was followed also in preliminary experiments performed during the preparation of affinity membranes to determine their optimal ligand density.

Dynamic binding experiments were performed using an ÄKTA purifier FPLC system from GE Healthcare (Milano, Italy). Layered stacks of membranes were housed in a membrane unit of 2.5 cm diameter. Pure IgG standard solutions were used to characterize the membranes and to obtain dynamic isotherms. The effect of different operating conditions, including flow rate and feed concentration, was investigated. Membrane selectivity was determined in further experiments using cell culture supernatant.

## 3. Results and discussion

### 3.1. Mimetic affinity membrane preparation

The underlying concept of the synthetic Mimetic Ligands<sup>TM</sup> A2P and B14 relates to their property to bind to the Fc-region of IgG and hence they are possible alternatives to Protein A as affinity ligand. Both synthetic ligands are stable in sanitation solutions containing up to 1 M sodium hydroxide without the risk of ligand leakage or denaturation, which may not be the case for Protein A.

The benchmarks for this study were the A2P ligand, the 2LP spacer chain and the Sartopoxy membrane supports [29,30]. The immobilization procedure was found to be strongly dependent on the chemical properties of the affinity ligand as well as the spacer chain and the support media. Therefore, it was necessary to perform extensive optimization experiments in order to achieve the desired ligand densities through the immobilization protocol. Naturally, an increase in ligand density would provide an increase in the IgG binding performance. However, since the mimetic ligand is much smaller than the target protein, IgG capacity will eventually reach a plateau with increasing A2P-TRZ densities, as shown for the A2P-TRZ-Sartopoxy membrane in Table S2 in the electronic supplementary material. In case of the Epoxy 1 support membranes, no increase in ligand density was achievable and the low number of attached ligand naturally led to unsatisfactory IgG capture performance (data not shown). Epoxy 1 was therefore not further investigated.

Concerning the choice of linkage chemistry, the coupling of thio-philic affinity ligands onto epoxy-activated supports (i.e. agarose) is a known and well-established technique in biochemistry [19]. Their immobilization onto cellulose membranes is, however, more sensitive due to the difference in handling membrane sheets compared to resin-like media. It was observed that specially Epoxy 2 membranes are highly sensitive to shear forces, therefore a mechanical stirrer, which is frequently used for spherical beads, cannot be used. Shear-force induced surface degradation makes the use of magnetic stirring devices, for temperature-controlled reactions, and horizontal shakers, for reactions at room temperature, essential. A careful adjustment of the agitation speed is required in order to gently mix the reaction solution, but leave the membrane sheets practically stationary and floating in solution.

**Table 2**  
Summary of investigated ligand-spacer-membrane combinations together with their ligand density.

Spacer <sup>a</sup>	Ligand	Membrane	Identification name	Ligand density [ $\mu\text{mol}/\text{cm}^2$ ]
2LP	A2P	Sartoepoxy	A2P-2LP-Sartoepoxy	0.25
	A2P	Epoxy 2	A2P-2LP-Epoxy 2	n/a
	A2P	Epoxy 3	A2P-2LP-Epoxy 3	n/a
	B14	Sartoepoxy	B14-2LP-Sartoepoxy	0.40
DES	A2P	Sartoepoxy	A2P-DES-Sartoepoxy	1.18
	OH-(CH <sub>2</sub> ) <sub>2</sub> -	Sartoepoxy	OH-(CH <sub>2</sub> ) <sub>2</sub> -DES-Sartoepoxy	n/a
	A2P	Sartoepoxy	A2P-TRZ-Sartoepoxy	0.73
TRZ	A2P	Epoxy 2	A2P-TRZ-Epoxy 2	0.22
	A2P	Epoxy 3	A2P-TRZ-Epoxy 3	0.48
	B14	Sartoepoxy	B14-TRZ-Sartoepoxy	0.70
	B14	Epoxy 2	B14-TRZ-Epoxy 2	0.26
	OH-CH <sub>2</sub> -	Sartoepoxy	OH-CH <sub>2</sub> -TRZ-Sartoepoxy	n/a

<sup>a</sup> spacer chain description: 1,2-diaminoethane (2LP), 3,6-dioxa-1,8-octanedithiol (DES) and [1,2,3] triazole (TRZ).

Employing this improved ligand immobilization procedure, an A2P-DES ligand density of  $1.18 \mu\text{mol}/\text{cm}^2$  could be obtained, which is double to triple higher than any ligand density for the other investigated membrane adsorbents. Although the static binding capacity of A2P-DES-Sartoepoxy materials was satisfactory, as shown in an earlier study [29], their elution recovery was rather low with the typical elution buffers used. Since this parameter indicates a loss of valuable IgG through irreversible binding, it was decided not to prepare nor investigate any B14-DES type membranes. Results for A2P-DES-Sartoepoxy are only shown in Table 2 and Fig. 2a strictly for comparison reasons.

In case of the B14-2LP ligand-spacer combination, an earlier study for polymethacrylate beads had provided evidence that the amino groups incorporated in the spacer chain and the surface endcapping had lead to reduced IgG binding capacities due to secondary binding of feed impurities [26]. Comparable adsorbents with B14-TRZ ligand spacer combination lacked this drawback and even showed an improved IgG capture performance compared to commercial Protein A media, when operated at low bead height and fast flow rates [28].

The incorporation of a TRZ linkage involves the so-called “Click Chemistry” [27]. Unfortunately the Click reaction was in the present case not as straightforward as described in the literature for cyclo-addition reactions of compounds in solution [31], therefore a modification of the reaction protocol was necessary. The usual amount of approximately 5 mol.% [32] of Cu(I) was not sufficient to catalyze the reaction to a satisfying extent and to obtain the desired ligand densities. Since copper (I) had to be added in large quantities (4 mol. equiv.) relative to the amount of available azide groups on the membrane surface, the overall problem that emerged was the final removal of copper (I) and (II) from the membrane surface. Another difficulty that arose was that copper (I) not only bound to the support surface but was also forming a complex with the amino and hydroxyl groups of the affinity-ligand. It is obvious that any remaining surface bound copper would reduce the IgG binding performance of the membrane adsorbent, since immobilized copper resembles a sterical hindrance for the target protein to reach the affinity ligand. A simple wash protocol using 50 mM citric acid and 0.5 M sodium hydroxide proved to be most effective for membrane adsorbents. An alternative approach employing a pre-activated copper (I)-acetylide complex was discussed elsewhere for anion exchange and B14-TRZ type adsorbents, but was not yet employed for membrane materials [27].

### 3.2. Batch characterization

The affinity membranes have been tested in batch experiments with pure polyclonal IgG solutions in order to investigate the effects that the ligand head group, the spacer arm and the immobilization chemistry, the membrane support and the number of active epoxy groups available for ligand coupling, may have on the overall material performance.

The experimental adsorption data were well described by the Langmuir model, which in equilibrium conditions can be expressed as:

$$q_{\text{eq}} = \frac{c_{\text{eq}} \cdot q_{\text{max}}}{c_{\text{eq}} + K_d}$$

where  $c_{\text{eq}}$  and  $q_{\text{eq}}$  are the equilibrium protein concentrations in the liquid and solid phase respectively,  $q_{\text{max}}$  represents the

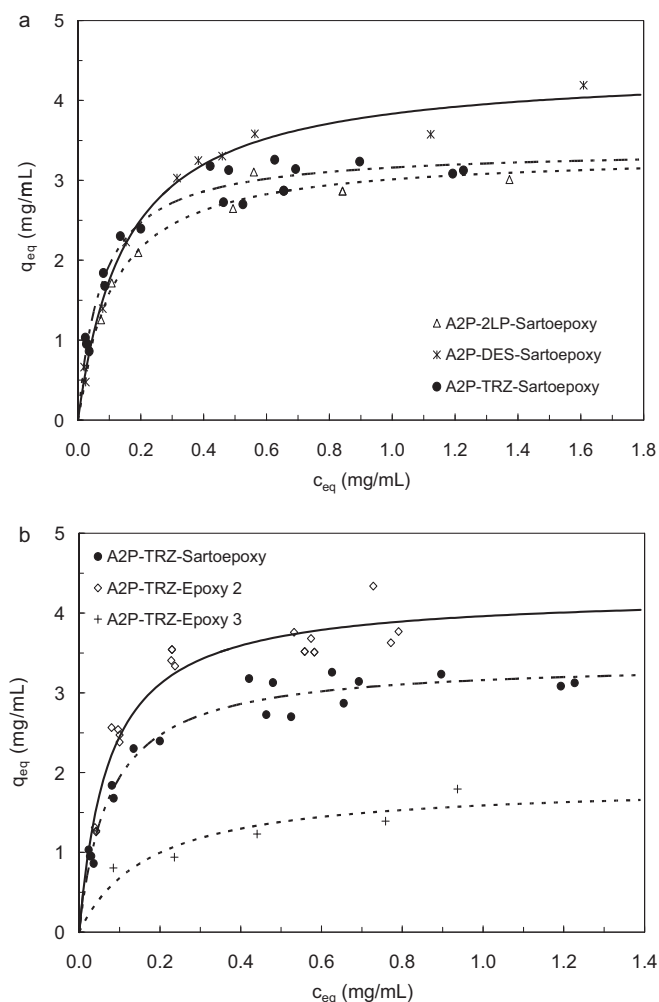


**Fig. 2.** Batch equilibrium adsorption isotherms using pure IgG solutions shows the effect of (a) spacer arm and (b) membrane support on the static binding capacity.

**Table 3**  
Langmuir equilibrium parameters and IgG recovery of the affinity membranes tested.

Membrane	$q_{\max}$ [mg/mL]	$K_d$ [mg/mL]	Recovery [%]
A2P-2LP-Sartoepoxy	3.34	0.109	62
A2P-DES-Sartoepoxy	4.42	0.152	31
A2P-TRZ-Sartoepoxy	3.40	0.0752	51
A2P-2LP-Epoxy 2	3.03	0.151	n/a
A2P-TRZ-Epoxy 2	4.25	0.0735	59
A2P-2LP-Epoxy 3	1.99	0.0897	n/a
A2P-TRZ-Epoxy 3	1.87	0.175	35
B14-2LP-Sartoepoxy	3.45	1.91	n/a
B14-TRZ-Sartoepoxy	2.61	0.0540	91
B14-TRZ-Epoxy 2	3.07	0.152	93

maximum binding capacity and  $K_d$  is the Langmuir equilibrium dissociation constant.

The thermodynamic equilibrium parameters, obtained by applying the Langmuir model, together with the average values of IgG recovery are reported in Table 3.

### 3.2.1. Spacer arm and immobilization chemistry

The effect of the different spacer arms on IgG adsorption is shown in Fig. 2a, where the equilibrium isotherms for the A2P affinity membranes prepared using the Sartoepoxy matrix are reported. It can be noticed that A2P-DES-Sartoepoxy membranes have the highest maximum static binding capacity, namely 4.4 mg/mL, while A2P-2LP-Sartoepoxy and A2P-TRZ-Sartoepoxy have a comparable capacity of about 3.4 mg/mL. However, if we consider the elution step it can be noticed that all A2P membranes have rather poor performance and, among those, A2P-DES-Sartoepoxy is the membrane with the lowest recovery, 31% compared to 51% for A2P-TRZ-Sartoepoxy and 62% for A2P-2LP-Sartoepoxy [33]. The synergic combination of the A2P ligand with the DES spacer chemistry causes an enhancement of the affinity bond, which improves the binding capacity for IgG, but at the same time provides much reduced elution yields, which resemble a major drawback [34]; thus DES spacer was not further investigated. The change in spacer chemistry, from DES to TRZ for A2P bound to Sartoepoxy membranes, increases the IgG recovery by 20%. Although the IgG recovery increases by 30% when changing from DES to 2LP, caution must be paid before a general conclusion is drawn since these tests were performed with pure IgG solutions. In case of a real cell culture feed, IgG would compete for the A2P-ligand binding sites with feed impurities such as host cell proteins and DNA, as well as the anion exchange type moieties of the amino-functional 2LP spacer chain and the ethanolamine surface endcapping. It was proven for resin-type mimetic ligands with 2LP spacer chain that they can capture a significant amount of feed impurities, while their IgG binding performance was at the same time much reduced [26]. For the other two spacer variations, control experiments with support-spacer combinations without affinity ligands, namely Sartoepoxy-DES-(CH<sub>2</sub>)<sub>2</sub>-OH and Sartoepoxy-TRZ-CH<sub>2</sub>-OH, were tested with pure IgG solution using static binding tests. They provided no significant evidence for non-specific binding of IgG towards either of the two spacer linkages. This result proves that the strong binding of IgG onto A2P-DES-Sartoepoxy was exhibited by a synergetic effect between the DES spacer and the A2P-ligand. It furthermore shows that the TRZ-spacer per se does not influence IgG binding. However, for Azido-Sartoepoxy membranes without ligand and without endcapping with propargyl alcohol a maximum static binding capacity for IgG of 1.13 mg/mL was observed. This result correlates with recently published results for azide group modified resin type adsorbents [26]. It is therefore noteworthy to mention that the spacer arm and the support surface modification can significantly

influence the IgG capture performance of an attached ligand-head group [26,28–30].

Overall, these results indicate that the Click-coupling procedure was the most promising approach compared to the other two alternatives. However, A2P-2LP-Epoxy 2, A2P-2LP-Epoxy 3 and B14-2LP-Sartoepoxy were prepared and investigated via static binding tests with pure IgG solution for the purpose of comparison.

### 3.2.2. Membrane support

From the results obtained in the previous section, only 2LP and TRZ affinity membranes were investigated with the improved Epoxy 2 and Epoxy 3 supports. The adsorption isotherms for the different A2P-TRZ affinity media employing pure IgG solutions under static binding condition are reported in Fig. 2b. A2P-TRZ-Epoxy 2 membranes have the highest binding capacity for IgG, followed by A2P-TRZ-Sartoepoxy and A2P-TRZ-Epoxy 3 membranes. It is apparent that Epoxy 3 membrane supports lead to a loss of separation performance. Interestingly, a similar trend is also observed for the 2LP modified membranes; however, the elution performance of these membranes was not reproducible and this problem became apparent for different production lots. A possible reason for this occurrence is the fact that epoxide groups can undergo an acid as well as base catalyzed ring-opening reactions in aqueous solution. A2P-2LP as well as ethanolamine are basic compounds. The number of residual epoxide groups after ligand attachment can vary from batch to batch and so does the number of the ethanolamine groups attached during epoxide group endcapping. As previously mentioned, these surface near amino groups are responsible for partial anion exchange type properties of adsorbents with 2LP spacer chain and ethanolamine endcapping. Their presence or absence may therefore have a very strong effect on material performance.

When considering the membrane structural parameters reported in Table 1, it is possible to derive more details on the separation performances of the different affinity membranes investigated. It is important to notice that the Epoxy 2 membrane support has the highest internal surface area per unit mass (4.78 m<sup>2</sup>/g), but with 1.2–1.8  $\mu\text{mol}/\text{cm}^2$  the second lowest epoxide group density (Table S1). This reveals on one hand a poor, yet sufficient, epoxide functionalization of the available specific surface area of the membrane matrix, but on the other hand the reactive epoxide or azide groups are highly isolated, leaving enough space for ligand-protein interaction. In comparison the Epoxy 1 support possesses only a slightly smaller surface area of 4.01 m<sup>2</sup>/g, but comes with a very low epoxide group density of 0.3–0.4  $\mu\text{mol}/\text{cm}^2$ . For large and spacious ligands exhibiting a very strong affinity for IgG capture such as it is the case for Protein A, the Epoxy 1 support was classified as being the ideal membrane support [20]. For smaller mimetic ligands, however, the attachable ligand densities on Epoxy 1 was simply too low to provide reasonable IgG binding capacities. This was discovered for A2P-DES-Epoxy 1 as well as for A2P-TRZ-Epoxy 1, for which a static binding capacity of only 0.70 mg/mL was detected with an IgG concentration in the feed of 1.0 mg/mL.

However, affinity membranes prepared with the Epoxy 2 membrane support provide comparable or higher binding capacities with respect to the corresponding membranes prepared with the Sartoepoxy support (i.e. A2P-TRZ-Epoxy 2 has a higher binding capacity than A2P-TRZ-Sartoepoxy). Sartoepoxy has the third highest surface area with 2.25 m<sup>2</sup>/g and the second highest epoxide group density with 2.0–2.2  $\mu\text{mol}/\text{cm}^2$ . Both membrane types, Sartoepoxy and Epoxy 2 come with an easily accessible and interconnected microporous structure, a feature that allows the target protein to readily interact with the affinity binding sites.

The Epoxy 3 membrane on the other hand, has a very small surface area of only 0.93 m<sup>2</sup>/g combined with the highest density of epoxide group, namely 2.7–3.2  $\mu\text{mol}/\text{g}$ . The ligand coupling reaction for A2P-TRZ onto Epoxy 2 and Epoxy 3 supports provides

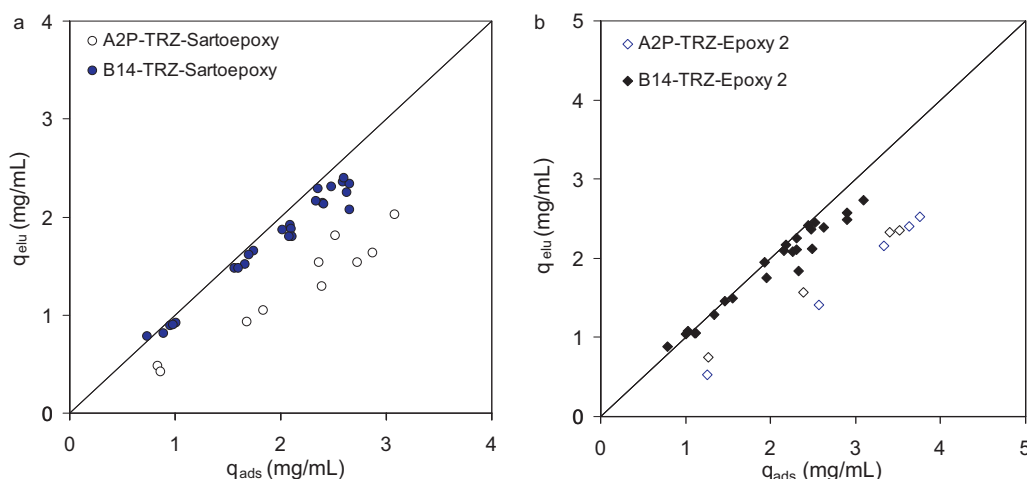


Fig. 3. Adsorption versus elution performance of A2P-TRZ and B14-TRZ affinity membranes in batch experiments using pure IgG solutions.

comparable low yield, which demonstrates that the more open membrane structure of Epoxy 2 facilitates IgG binding. Therefore it can be concluded that the Epoxy 2 matrix has a good potential for improvement. By increasing the epoxide group density, it may be possible to further increase the IgG binding capacity for Epoxy 2 type membrane adsorbents, making it competitive with chromatography beads at process scale.

### 3.2.3. Affinity ligand comparison

The new mimetic ligand B14 was immobilized only onto the two most promising membrane types, the standard Sartoepoxy and the Epoxy 2 membranes. Since A2P and B14 are designed with similar chemical and steric structure, it is reasonable to expect that the resulting interactions between the spacer arms investigated and the two ligands follow the same trend. Derived from preliminary tests, the Click reaction protocol can be considered the most promising coupling procedure, and will be hereafter applied for further experimentation and discussion.

When comparing affinity membranes that differ only by their immobilized ligand but not by the linking chemistry or the support, it was observed that A2P-TRZ-Epoxy 2 affinity membranes have a higher binding capacity for polyclonal IgG compared to the corresponding B14-TRZ Sartoepoxy membranes (Table 3). However, the recovery from A2P affinity membranes was consistently below 62% (Table 3), which is not satisfactory for industrial application purposes. On the other hand, IgG recovery from B14 affinity membranes was always greater than 90%, indicating that the membrane

matrix does not influence the elution performance of mimetic A2P or B14 affinity membranes. Therefore it must be the chemical structure of the mimetic ligand, which induces low or high IgG recoveries as it can be observed from the data reported in Fig. 3. It is worth to note that all investigated membranes with TRZ-spacer chain were not azide group endcapped, but possess approximately the same number of residual azide groups on the membrane surface, namely  $1.1 \mu\text{mol}/\text{m}^2$  for TRZ-Sartoepoxy and  $0.7 \mu\text{mol}/\text{m}^2$  for TRZ-Epoxy 2. Although residual azide groups can reduce IgG recovery, the fact that their numbers are comparable for these two membrane types, makes their presence not important for comparison purposes.

### 3.3. Dynamic characterization

The behaviour of affinity membranes has been analyzed in dynamic experiments with both pure IgG solutions and a cell culture supernatant containing human monoclonal IgG<sub>1</sub>, for an appropriate evaluation of their possible industrial application in the capture step of a monoclonal antibody production process. Due to the low recovery of A2P affinity membranes already observed in the batch experiments, a more extensive dynamic characterization was performed for B14 affinity membranes, for which the effects of flow rate and IgG concentration were also investigated. A2P-TRZ-Sartoepoxy membranes were tested only at one fixed value of IgG concentration, employing pure IgG solution at a constant flow rate of 2 mL/min.

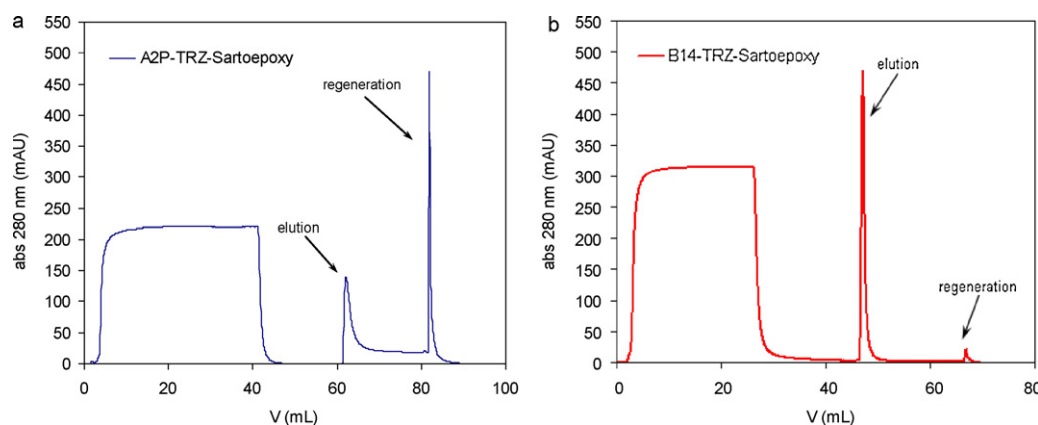


Fig. 4. Comparison between the IgG binding, elution and regeneration profiles for (a) A2P-TRZ-Sartoepoxy membranes, obtained with  $c_0 = 0.81 \text{ mg/mL}$  in the feed, and for (b) B14-TRZ-Sartoepoxy membranes at  $c_0 = 1.07 \text{ mg/mL}$ , for experiments performed at a constant flow rate of 2 mL/min in all chromatographic stages.



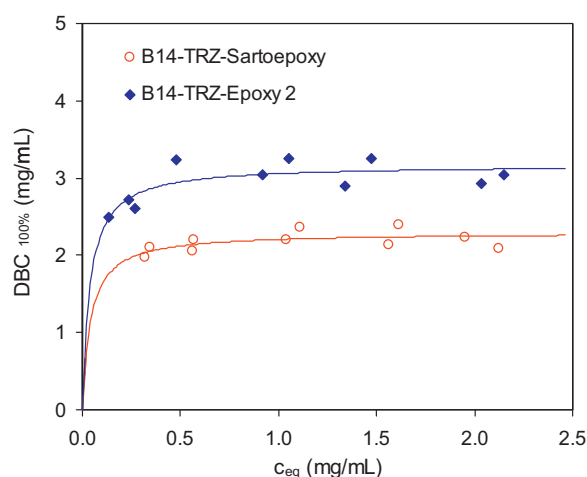


Fig. 5. Comparison between dynamic isotherms of B14-TRZ affinity membranes.

A comparison between A2P-TRZ-Sartoepoxy and B14-TRZ-Sartoepoxy membranes confirmed the results previously obtained in batch experiments, that is A2P-TRZ-Sartoepoxy membranes provide high dynamic binding capacities, but lower recoveries for IgG, as it is also evident from Fig. 4. The different area proportions of the elution and regeneration peaks can be seen as indicators of the binding strength towards IgG. In Fig. 4a, where a chromatographic cycle of A2P-TRZ-Sartoepoxy is presented, the regeneration peak has an area comparable with that of the elution peak. This indicates that after elution, a considerable amount of IgG still remains bound to the membrane adsorbent. A different behaviour was observed with the B14-TRZ-Sartoepoxy membrane, Fig. 4b, for which the regeneration peak is barely visible, indicating that almost all of the IgG adsorbed onto the affinity membranes is actually recovered in the elution step. Indeed, the average recovery for A2P-TRZ-Sartoepoxy membranes in dynamic experiments was 57%, while for B14-TRZ-Sartoepoxy membranes it was 92%, which correlates well with the batch experimental results.

All dynamic experiments were performed up to complete saturation in order to calculate the dynamic binding capacity at 100% breakthrough,  $DBC_{100\% BT}$ . The experimental values of  $DBC_{100\% BT}$ , obtained at different values of IgG concentration in the feed, were used to draw dynamic isotherms as it is shown in Fig. 5. The results were described using the Langmuir model, whose parameters are reported in Table 4. B14-TRZ-Epoxy 2 membranes are endowed with higher binding capacity for IgG than B14-TRZ-Sartoepoxy membranes, qualitatively confirming the results obtained in batch experiments.

Finally, the A2P-TRZ and B14-TRZ membranes were challenged with a cell culture supernatant possessing an IgG titer of 0.11 mg/mL. Fractions of 1 mL volume were collected and analyzed with HPLC using a Protein A HPLC column. An example of the UV profile for the cell culture supernatant and the concentration profile for IgG, obtained with Protein A HPLC analysis, are shown in Fig. 6. The dynamic binding capacities and the corresponding recoveries are reported in Table 5.

A2P membranes, which have higher binding capacity towards pure IgG compared to the corresponding B14 membranes (Table 3),

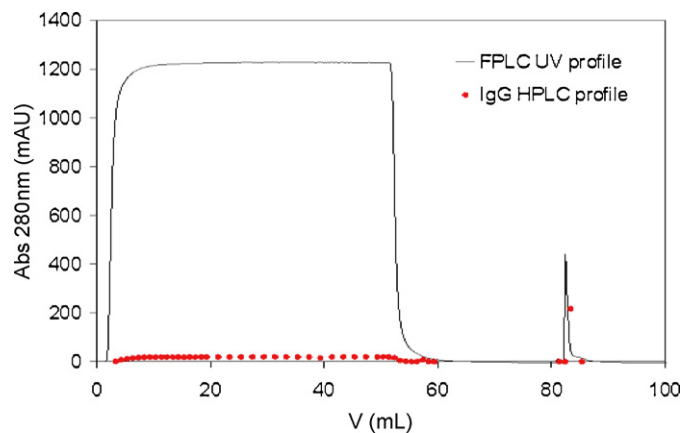


Fig. 6. Dynamic profiles obtained with the cell culture supernatant on B14-TRZ-Epoxy 2 membranes at a flow rate of 5 mL/min in all the chromatographic stages. FPLC UV signal (280 nm) overlays the IgG<sub>1</sub> concentration of the collected fractions (1 mL) determined by Protein A-HPLC analysis.

showed a lower binding capacity, when tested with cell culture supernatant (Table 5). It is also important to remark that little to no IgG was recovered from A2P membranes when tested with cell culture feed. This is also illustrated by the weak IgG bands in the elution fraction of A2P-TRZ-Epoxy 2 on SDS-PAGE gels compared to the corresponding B14-TRZ membranes as shown in Fig. S2 from the electronic supplementary material. B14 modified supports showed a clear superior performance. Especially, the B14-TRZ-Epoxy 2 provided the highest binding capacity of 1.41 mg/mL, combined with an IgG recovery of 92%.

The theoretical binding capacity, evaluated from the dynamic isotherm for pure IgG solutions at a concentration of 0.11 mg/mL (IgG<sub>1</sub> titer in the supernatant), is 2.49 mg/mL for A2P-TRZ-Sartoepoxy, 2.55 mg/mL for A2P-TRZ-Epoxy 2, 1.67 mg/mL for B14-TRZ-Sartoepoxy and 2.37 mg/mL for B14-TRZ-Epoxy 2. However, the binding capacities obtained with the cell culture supernatant are sensibly lower than expected on the basis of pure IgG solutions, as it can be noticed from the data reported in Table 5. The reason for the strong deviation between results from pure IgG solutions and cell culture feed may lay in the known sensitivity of A2P towards Pluronic F-68 [30], which is mostly added as an anti-foaming agent to cell culture media. On the contrary, membranes carrying the new ligand B14, which was designed to be Pluronic F-68 tolerant, are able to capture and release more IgG from cell culture feed. Furthermore, one has to take into account that the cell culture feed used for these experiments contained only a small amount of IgG<sub>1</sub>, while the feed related impurities are highly dominant (Fig. 6) and may compete with IgG for binding sites on the membrane adsorbent. Another possible explanation for that behaviour can be attributed to membrane fouling due to the complexity of the cell culture solution. This motivation is strengthened by the fact that the drop in binding capacity is less severe for the membranes prepared with the Epoxy 2 matrix, due to the more open structure than the Sartoepoxy membrane. The more probable solution, however, may lay in the lower number of residual azide groups on Epoxy 2 (0.7  $\mu\text{mol}/\text{cm}^2$ ) compared to Sartoepoxy

**Table 4**  
Langmuir parameters and recovery of B14-TRZ affinity membranes determined with pure IgG solutions.

Membrane	$DBC_{100\% \text{ max}}$ [mg/mL]	$K_d$ [mg/mL]	Recovery [%]
B14-TRZ-Sartoepoxy	2.30	0.0411	92
B14-TRZ-Epoxy 2	3.17	0.0374	96

**Table 5**  
 $DBC_{100\% BT}$  and recovery of A2P-TRZ and B14-TRZ affinity membranes determined with cell culture supernatant with an IgG<sub>1</sub> titer of 0.11 mg/mL.

Membrane	$DBC_{100\% BT}$ [mg/mL]	Recovery [%]
A2P-TRZ-Sartoepoxy	0.49	7
A2P-TRZ-Epoxy 2	0.70	1
B14-TRZ-Sartoepoxy	0.74	35
B14-TRZ-Epoxy 2	1.41	92

membranes ( $1.0 \mu\text{mol}/\text{cm}^2$ ). In a previous study, the influence of residual azide groups on the IgG capture and recovery performance of resin-type adsorbents was clearly shown [28]. It was discovered that organic azide groups are capable of disrupting the protein structure of IgG molecules, leading to an enhanced binding of IgG combined with a strongly reduced recovery from the adsorbent. The possibility of azide group endcapping after ligand attachment was not yet fully developed when this study was finalized, but resembles a possible next step in the performance optimization of B14-TRZ-Epoxy 2 membrane adsorbents.

#### 4. Conclusions

New biomimetic affinity membranes with different ligand head groups, A2P and B14, various spacer-arms and immobilization chemistries, 2LP, DES and TRZ, and different membrane supports have been prepared and tested with pure IgG solutions to obtain indications on the feasibility of their application in an industrial antibody manufacturing process. Early results obtained with simple batch experiments did not only help to optimize the coupling reactions for the Click Chemistry protocol, they also lead to optimized ligand densities for the capture of IgG.

High binding capacities for IgG have been obtained with A2P affinity membranes, but the strong binding of IgG to the A2P ligand leads to rather low recoveries. This general tendency was observed for all A2P affinity membranes and represents an important factor, when considering a possible industrial application of A2P affinity membranes. However, this behaviour was not observed with membranes prepared with the new B14 ligand, where elution recoveries greater than 90% were obtained in all cases.

From all the experiments the following conclusions can be drawn: (i) B14-ligands perform better than A2P-ligands both in terms of elution yields and of Pluronic F-68 tolerance; (ii) the TRZ-spacer is clearly superior to the earlier investigated 2LP and DES-spacer chains; (iii) the new Epoxy 2 membrane support exhibits a better performance than the commercial Sartoepony membrane.

In addition, it is worth noticing that there is space for further optimization of the B14-TRZ-Epoxy 2 affinity membrane. It seems realistic that an increase of the epoxide group density on the internal porous surface of the new Epoxy 2 matrix will provide an enhancement of its binding performance for IgG. Furthermore, the preparation of mimetic membrane adsorbents with TRZ-spacer chain should include an azide group deactivation protocol. A surface endcapping will not only increase the IgG recovery rate, but will also provide a higher dynamic binding for IgG, since the new surface modification is practically inert towards the non-specific binding of feed related impurities as well as IgG. The attainment of these goals could produce affinity membranes that are more competitive with conventional packed-beads, assessing the use of membrane adsorbents for protein capture in downstream processing.

#### Acknowledgements

The authors greatly acknowledge the contribution of Michela Giovannangelo for her help in the experiments, Zandrie Borneman

and the Membrane Technology Group at the University of Twente NL, for their data on membrane structural parameters, Rene Faber from Sartorius Stedim Biotech GmbH for the membrane support materials, Chris Sadler from ProMetic Biosciences Ltd. for his help with ligand preparation and immobilization. ProMetic BioSciences and Mimetic Ligands™ are trademarks of ProMetic BioSciences Ltd.

This work has been performed as part of the “Advanced Interactive Materials by Design” (AIMs) project, supported by the Sixth Research Framework Programme of the European Union (NMP3-CT-2004-500160).

#### Appendix A. Supplementary data

Supplementary data associated with this article can be found, in the online version, at doi:10.1016/j.jchromb.2011.03.059.

#### References

- [1] S.C. Gad, Handbook of Pharmaceutical Biotechnology, Wiley-Interscience, 2007.
- [2] H. Klefenz, Industrial Pharmaceutical Biotechnology, Wiley-VCH, 2002.
- [3] G. Walsh, Biopharmaceuticals: Biochemistry & Biotechnology, 2nd edition, 2003.
- [4] J.M. Reichert, C.J. Rosensweig, L.B. Faden, M.C. Dewitz, Nat. Biotechnol. 23 (2005) 1073.
- [5] P.J. Carter, Nat. Rev. Immunol. 6 (2006) 343.
- [6] J. Reichert, A. Pavlou, Nat. Rev. Drug Discov. 3 (2004) 383.
- [7] J. Thoenes, M. Etzel, Biotechnol. Prog. 23 (2007) 42.
- [8] S. Sommerfeld, J. Strube, Chem. Eng. Process 44 (2005) 1123.
- [9] C.R. Lowe, Curr. Opin. Chem. Biol. 5 (2001) 248.
- [10] U. Gottschalk, Biotechnol. Prog. 24 (2008) 496.
- [11] J. Curling, U. Gottschalk, Biopharm. Int. 20 (2007) 70.
- [12] C. Boi, J. Chromatogr. B 848 (2007) 19.
- [13] R. Faber, Y. Yang, U. Gottschalk, Biopharm. Int. (2009) 11.
- [14] J.A.C. Lim, A. Sinclair, D.S. Kim, U. Gottschalk, Bioprocess Int. 5 (2007) 48.
- [15] H. Yang, C. Viera, J. Fischer, M.R. Etzel, Ind. Eng. Chem. Res. 41 (2002) 1597.
- [16] L. Giovannoni, M. Ventani, U. Gottschalk, Biopharm. Int. 21 (2008) 48.
- [17] H.L. Knudsen, R.L. Fahrner, Y. Xu, L.A. Norling, G.S. Blank, J. Chromatogr. A 907 (2001) 145.
- [18] D. Yu, M.D. McLean, J.C. Hall, R. Ghosh, J. Chromatogr. A 1187 (2008) 128.
- [19] J.-C. Janson, L. Ryden, Protein Purification, Second Edition: Principles, High-Resolution Methods, and Applications, 1998.
- [20] C. Boi, S. Dimartino, G.C. Sarti, Biotechnol. Prog. 24 (2008) 640.
- [21] G. Fassina, Methods Biotechnol. 147 (2000) 57.
- [22] R. Li, V. Dowd, D.J. Stewart, S.J. Burton, C.R. Lowe, Nat. Biotechnol. 16 (1998) 190.
- [23] H. Yang, P.V. Gurgel, R.G. Carbonell, J. Pept. Res. 66 (Suppl. 1) (2005) 120.
- [24] G. Fassina, G. Palombo, A. Verdoliva, M. Ruvo, Affinity purification of immunoglobulins using Protein A mimetic (PAM), in: J. Walker (Ed.), The protein protocols handbook, 2nd ed., Humana Press, Totowa, NJ, 2002, pp. 1013–1024.
- [25] G. Fassina, A. Verdoliva, G. Palombo, M. Ruvo, G. Cassani, J. Mol. Recognit. 11 (1998) 128.
- [26] J. Horak, S. Hofer, W. Lindner, J. Chromatogr. B 878 (2010).
- [27] H.C. Kolb, M.G. Finn, K.B. Sharpless, Angew. Chem. Int. Ed. 40 (2001) 2004.
- [28] J. Horak, S. Hofer, C. Sadler, S. Williams, W. Lindner, Anal. Bioanal. Chem., in press, doi:10.1007/s00216-010-4571-1.
- [29] C. Boi, V. Busini, M. Salvalaglio, C. Cavallotti, G.C. Sarti, J. Chromatogr. A 1216 (2009) 8687.
- [30] L. Zamolo, M. Salvalaglio, S. Hofer, J. Horak, B. Galarza, C. Sandler, S. Williams, W. Lindner, C. Cavallotti, J. Phys. Chem. B 114 (2010) 9367.
- [31] V.V. Rostovtsev, L.G. Green, V.V. Fokin, K.B. Sharpless, Angew. Chem. Int. Ed. 41 (2002) 2596.
- [32] P. Wu, V.V. Fokin, Alrichchim. Acta 40 (2007) 7.
- [33] C. Boi, G.C. Sarti, Sep. Sci. Technol. 42 (2007) 2987.
- [34] V. Busini, D. Moiani, D. Moscatelli, L. Zamolo, C. Cavallotti, J. Phys. Chem. B 110 (2006) 23564.

## **Supporting Information**

### **Influence of different spacer arms on Mimetic Ligand<sup>TM</sup> A2P and B14 membranes for human IgG purification**

Cristiana Boi<sup>1\*</sup>, Simone Dimartino<sup>1</sup>, Stefan Hofer<sup>3</sup>, Jeannie Horak<sup>3\*</sup>, Sharon Williams<sup>2</sup>,

Giulio C. Sarti<sup>1</sup>, Wolfgang Lindner<sup>3</sup>

( \*Contact Email: [cristiana.boi@unibo.it](mailto:cristiana.boi@unibo.it) and [jeannie.horak@univie.ac.at](mailto:jeannie.horak@univie.ac.at) )

<sup>1</sup> *DICMA, Alma Mater Studiorum Università di Bologna,  
via Terracini 28, 40131 Bologna, Italy,*

<sup>2</sup> *ProMetic Biosciences Ltd.,  
211 Cambridge Science Park, Milton Road, Cambridge CB4 0ZA, UK*

<sup>3</sup> *Department of Analytical Chemistry, University of Vienna,  
Währingerstrasse 38, 1090 Vienna, Austria*

## 1. Determination of the epoxide group loading on membrane supports via elemental analysis

The number of accessible and reactive epoxide groups for the four investigated membranes was determined via elemental analysis (EA) after the addition of (i) 2-mercaptoethanol (10 mol-equiv. relative to the expected epoxide group amount provided by the manufacturer plus 10 mol-equiv. triethylamine) and (ii) 2-ethanolamine (10 mol-equiv.) to the corresponding membrane sheet. The immobilization reaction was performed in methanol under reflux condition, nitrogen atmosphere and gentle agitation for 18 h. After thorough washing with water and methanol, the epoxide group densities were determined via elemental analysis employing the sulphur and nitrogen content of the corresponding membranes for calculation. Note that elemental analysis results are calculated in  $\mu\text{mol/g}$  (dry) membrane, while epoxide densities provided by the manufacturer are listed in  $\mu\text{mol/cm}^2$ . Conversion factors for  $\mu\text{mol/g}$  to  $\mu\text{mol/cm}^2$  were determined by weighing 6 membrane sheets of 3 x 3 cm dimension ( $6 \times 9 \text{ cm}^2 = 54 \text{ cm}^2$ ) or membrane disc with a radius of  $r = 3.5 \text{ cm}$  ( $38.48 \text{ cm}^2$ ). Epoxide group densities as well as the conversion factors for all investigated membrane types are listed in Table S1.

**Table S1.** Determination of epoxide group densities on membrane supports

	<i>Manufacturer data</i>	<i>Experimental determination of epoxide group densities</i>		
		<i>Elemental Analysis</i>		
Membrane type	Epoxide density [ $\mu\text{mol/cm}^2$ ]	2-Mercaptoethanol [ $\mu\text{mol/cm}^2$ ]	2-Ethanolamine [ $\mu\text{mol/cm}^2$ ]	Area per unit mass [ $\text{cm}^2/\text{g}$ ]
Sartoepoxy	2.0 – 2.2	2.43	2.73	112.41
Epoxy 1	0.3 – 0.4	0.66	0.50	156.07
Epoxy 2	1.2 – 1.8	2.03	1.01	113.35
Epoxy 3	2.7 – 3.2	3.20	4.09	125.85



## 2. Preparation of Affinity Membranes

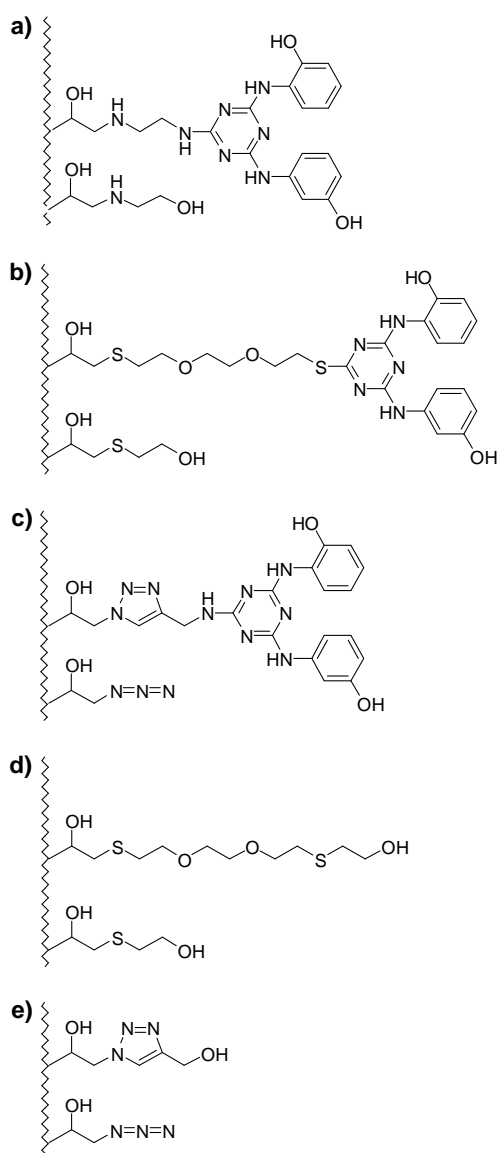


**Fig. S1.** Chemical structure of investigated ligand-spacer combinations including their support surface chemistries for the corresponding membrane supports  
a) A2P-2LP, b) A2P-DES, c) A2P-TRZ, d) OH-(CH<sub>2</sub>)<sub>2</sub>-DES and e) OH-(CH<sub>2</sub>)<sub>2</sub>-TRZ

Note, that for all mentioned ligand immobilization reactions, membrane sheets with a 3 x 3 cm sheet dimension (9 cm<sup>2</sup>) were used. Furthermore, if not otherwise stated, the amount of reactant is stated in mol-equivalents (mol-equiv.), relative to the mol-amount of reactive groups e.g. epoxide or azide groups available on the membrane surface. The abbreviation 2LP stands for 1,2-diaminoethane, DES stands for 3,6-dioxa-1,8-octanedithiol, TRZ stands for 1H-1,2,3-triazole and Sartoepony stands for Sartobind Epoxy.

### *Characterization of ligand synthesis*

Characterization of synthesis products was performed on a Bruker DRX 400 MHz spectrometer (Vienna, Austria). ESI-MS spectrometry was done on a PEsSciex API 365 triple quadrupole mass spectrometer from Applied Biosystems/MDS Sciex (Concord, Canada). The analysis of the elemental composition of modified membranes was performed with an EA 1108 CHNS-O from Carlo Erba (Rodano, Italy) and a 2400 Elemental Analyzer from Perkin Elmer (Vienna, Austria).

For column chromatography dichloromethane, petroleum ether, ethyl acetate and methanol of technical grade and silica gel 60 were used, purchased from Merck (Darmstadt, Germany).

#### ***2.1. Preparation of A2P-2LP-membranes and B14-2LP-membranes***

Epoxide activated membrane sheets were suspended in ethanol, before addition of the corresponding solutions containing 10 mol-equiv. A2P-2LP or B14-2LP in ethanol. The reaction mixtures were shaken overnight at 40°C. The membranes were then washed with ethanol and water. After re-equilibration of the membranes in ethanol, the residual epoxy groups were deactivated with 2-ethanolamine through gently stirring at 40°C for at least 12h in ethanol. The membranes were washed with ethanol and water, before storage in 20% aqueous ethanolic solution (Fig. S1a).

#### ***2.2. Preparation of membranes with DES-spacer***

##### ***2.2.1. Preparation of A2P-DES-Sartoepoxy***

The coupling of the A2P-DES ligand to the epoxide membrane sheets was performed in methanol, employing 5 mol-equiv. of ligand and 10 mol-equiv. of triethylamine, based on the epoxide group density on the corresponding membranes. The reaction solutions with membranes were refluxed under nitrogen atmosphere and gentle stirring for 18 h. After thorough washing with methanol, the remaining epoxide groups on the membrane surface were deactivated with 2-mercaptoethanol, employing 5 mol-equiv. 2-mercaptoethanol and 10 mol-equiv. triethylamine in methanol under reflux condition with nitrogen atmosphere overnight (Fig. S1b). Ligand densities were calculated using the sulfur content derived from the elemental analysis results.

#### **Elemental analysis:**

A2P-DES-coverage: 118  $\mu\text{mol/g}$ ; (C, 51.18%; H, 5.68%; N, 0.958%; S, 0.756%);

2-Mercaptoethanol coverage: 28  $\mu\text{mol/g}$ ; (C, 51.09%; H, 5.63%; N, 0.945%; S, 0.846%)

### **2.2.2. Preparation of DES-Sartoepoxy**

#### **2.2.2.1. Preparation of ligand 11-mercapto-3-thia-6,9-dioxa-1-undecanol (OH-(CH<sub>2</sub>)<sub>2</sub>-DES)**

To a solution of 4 mL 3,6-dioxa-1,8-octanedithiol (24 mmol) in 10 mL ethanol, an equimolar amount of 2-chloroethanol and 2.4 mL of a 10 M sodium hydroxide solution were added. The reaction solution was stirred under nitrogen at 60°C for 18h. Excess solvent was evaporated under vacuum. The oily residue was purified via column chromatography on silica gel 60 using petroleum ether and ethyl acetate at a ratio 25:20, yielding 19% of pure product.

<sup>1</sup>H NMR [400 MHz, CDCl<sub>3</sub>]: δ = 3.75 (t, 2H), 3.68 (t, 2H), 3.63 (t, 2H), 2.80-2.68 (m, 8H), 1.6 (t, 2H); MS [ESI, negative]: 224.9 [M-H<sup>+</sup>]<sup>-</sup>, 164.9 [M-C<sub>2</sub>H<sub>4</sub>S-H<sup>+</sup>]<sup>-</sup>.

#### **2.2.2.2. Immobilization of OH-(CH<sub>2</sub>)<sub>2</sub>-DES onto Sartoepoxy**

The immobilization reaction for the OH-(CH<sub>2</sub>)<sub>2</sub>-DES ligand as well as the endcapping of residual epoxide groups with 2-mercaptoethanol (2-ME) was performed as previously described for the A2P-DES ligand (Fig. S1d).

#### Elemental analysis:

OH-(CH<sub>2</sub>)<sub>2</sub>-DES-coverage: 216 μmol/g; (C, 51.72%; H, 5.96%; N, 0.054%; S, 1.38%).

2-Mercaptoethanol coverage: 22 μmol/g; (C, 51.68%; H, 6.01%; N, 0.067%; S, 1.45%).

### **2.3. Preparation of A2P-TRZ, B14-TRZ and OH-(CH<sub>2</sub>)-TRZ-membranes**

#### **2.3.1. Preparation of Azide group modified membrane supports**

The epoxide membrane sheets were soaked in water, before addition of 10 mol-equiv. of sodium azide. The reaction solution was gently agitated at room temperature for 3 days. After thorough washing with water, one sheet of each azide group modified membrane was dried prior to azide-group density determination employing the nitrogen values obtained by elemental analysis.

#### Elemental analysis:

Azido-Sartoepoxy: N<sub>3</sub>-coverage: 211 μmol/g (C, 52.03%; H, 5.53%; N, 0.897%);

Azido-Epoxy-2: N<sub>3</sub>-coverage: 132 μmol/g (C, 59.72%; H, 9.91%; N, 0.557%);

Azido-Epoxy-3: N<sub>3</sub>-coverage: 188 μmol/g (C, 53.16%; H, 5.33%; N, 0.788%)

### ***2.3.2. Immobilization of A2P-amino propyne, B14-amino propyne and 3-propargylalcohol onto azide modified membranes using Click Chemistry***

The synthesis protocol for triazine-type affinity ligands with an alkyne-terminal linking group was previously described by the authors in reference [1].

The azide activated membrane sheets (17  $\mu\text{mol}$  azido groups per sheet) were placed in a flat bottom flask with methanol, before addition of a solution containing 4 mol-equiv. of A2P-propyne (or B14-propyne) and 4 mol-equiv. of triethylamine in degassed methanol. The Click reaction was initialized by the addition of a ultrasonicated solution with 4 mol-equiv. Cu(I) in acetonitrile (0.1 g CuI per mL acetonitrile) and terminated after 48 h through removal of the supernatant. The modified membranes were washed successively with aqueous 50 mM citric acid, aqueous 0.5 M NaOH, water and methanol. This washing procedure was repeated until the membranes were white or near white in colour. The ligand densities were determined by elemental analysis using the nitrogen values (Fig. S1c).

#### Elemental analysis:

A2P-TRZ-Sartoepoxy: (A2P-coverage: 81  $\mu\text{mol/g}$ ; C, 52.97%; H, 5.76%; S, 1.48%);

A2P-TRZ-Epoxy-2: (A2P-coverage: 24  $\mu\text{mol/g}$ ; C, 62.01%; H, 10.38%; N, 0.772%);

A2P-TRZ-Epoxy-3 (A2P-coverage: 61  $\mu\text{mol/g}$ ; C, 53.09%; H, 5.16%; N, 1.297%);

B14-TRZ-Sartoepoxy: (B14-coverage: 75  $\mu\text{mol/g}$ ; C, 51.33%; H, 5.55%; N, 1.561%);

B14-TRZ-Epoxy-2 (B14-coverage: 31  $\mu\text{mol/g}$ ; C, 60.23%; H, 9.93%; N, 0.737%)

### ***2.3.3. Preparation of OH-(CH<sub>2</sub>)-TRZ membranes***

The coupling of 3-propargylalcohol to azide group activated membrane supports was performed in the same manner as earlier described for A2P-TRZ and B14-TRZ membranes. Note that the efficiency of this coupling reaction can not be determined via elemental analysis, since no traceable elements were introduced (Fig.S1e). However, the efficiency of different Click-reaction protocols for the immobilization of 3-propargylalcohol onto azide-activated polymeric beads was determined via material performance evaluation using cell culture feed, which will be discussed in more detail in another article [2].

### 3. Optimization of ligand density

**Table S2.** Static binding capacities at  $c_0=1$  mg/mL for pure IgG solution versus ligand densities per unit frontal membrane area for 3 different batches of A2P-TRZ-Sartoepoxy membranes

Ligand density [ $\mu\text{mol}/\text{cm}^2$ ]	Static binding capacity [mg/mL]
0.26	1.16
0.32	2.28
0.48	2.68

### 4. Purity determination for IgG capture from cell culture feed

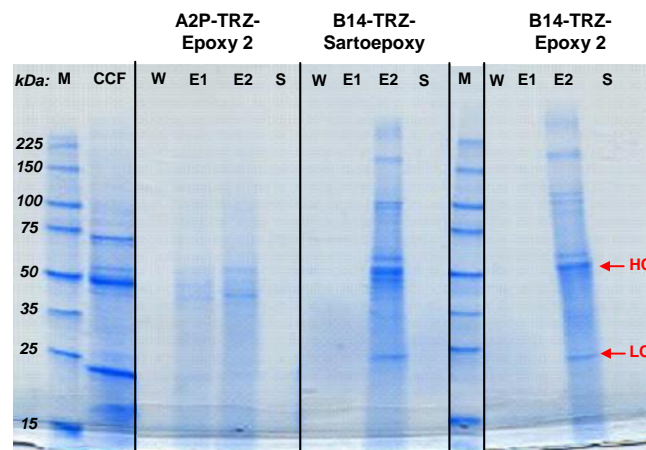


**Fig. S2.** SDS-Page slab gels (reduced and coomassie stained) of wash (W), elution (E1 and E2) and sanitation (S) solutions from A2P-TRZ-Epoxy 2, B14-TRZ-Sartoepoxy and B14-TRZ-Epoxy 2 investigated with dynamic binding tests employing cell culture feed (CCF). Lane M is the protein marker. Reduced IgG bands: HC is the heavy chain with 50 kDa and LC is the light chain with 25 kDa.

## References

- [1] L. Zamolo, M. Salvalaglio, C. Cavallotti, B. Galarza, C. Sandler, S. Williams, S. Hofer, J. Horak, W. Lindner, Experimental and Theoretical Investigation of Effect of Spacer Arm and Support Matrix of Synthetic Affinity Chromatographic Materials for the Purification of Monoclonal Antibodies. *J.Phys.Chem. B* 114 (2010) 9367–9380.
- [2] J. Horak, S. Hofer, W. Lindner, Optimization of a ligand immobilization and azide group endcapping concept via "Click-Chemistry" for the preparation of adsorbents for antibody purification. *J. Chromatogr. B* 878 (2010) 3382-3394.

## **Appendix 2**

### **Publication 2**





# Performance evaluation of Mimetic Ligand™ B14-triazole-FractoAIMs adsorbents for the capture of human monoclonal immunoglobulin G from cell culture feed

Jeannie Horak · Stefan Hofer · Chris Sadler ·  
Sharon Williams · Wolfgang Lindner

Received: 14 October 2010 / Revised: 25 November 2010 / Accepted: 29 November 2010  
© Springer-Verlag 2010

**Abstract** The new affinity-type Mimetic Ligand™ B14 was coupled with a 1,2-diaminoethane spacer (2LP) and a [1,2,3]-triazole spacer (TRZ) to three different support media. In addition to the agarose-based PuraBead and the polymethacrylate-type Fractogel, three new polymeric support media were introduced, the FractoAIMs 1, 2, and 3 (FA1, FA2, and FA3). These new FA supports differ in pore size as well as density of epoxide groups. The immobilization of the B14-ligand onto an azide-group-modified surface was performed with a copper (I)-mediated Click reaction. The IgG capture performance was tested for various ligand-spacer support combinations using cell culture feed containing human immunoglobulin G<sub>1</sub> (hIgG<sub>1</sub>). The most promising adsorbent, B14-TRZ-FA3, was further optimized by improving the surface chemistry through a triple endcapping concept employing an improved Click reaction protocol. This new technique enabled the most efficient deactivation of residual azide groups. In a direct comparison with a commercially available Protein A media, B14-TRZ-FA3 3× ec provided superior results at

fast flow-rates and low bed-height. Dynamic binding capacities of 11.4 g/L for 10% breakthrough of hIgG<sub>1</sub>, elution capacities of 16.0 g/L hIgG<sub>1</sub> and a recovery of 86% were achieved. The same results were obtained for a dialyzed and pre-purified feed solution, which is a clear indicator that triple-endcapped affinity support surfaces are practically inert to the non-specific binding of host cell proteins.

**Keywords** Click chemistry · Antibody purification · Affinity chromatography · Protein A · Size exclusion chromatography · Dynamic binding

## Introduction

In recent years, bioprocess engineers have increased the upstream yield in therapeutic protein production from antibody titers of originally 100 mg/L to 1 g/L, and very recently even up to 10 g/L, which resembles an overall increase in productivity of a factor of 100. The possibility to achieve such high antibody titers lies in much improved cell lines with higher expression numbers [1]. However, the major bottleneck which now arises is the still insufficient productivity and high cost of downstream processing, with column chromatography in the upfront line, followed by process optimization and process validation [2]. In downstream purification of therapeutic antibodies, Protein A is currently unsurpassed and unchallenged in both productivity and process robustness. However, the high adsorbent costs make the move towards newer, cheaper media and technologies more and more attractive. It is indisputable that the overall production costs could be reduced if new technologies can be found to replace the former more expensive ones [2, 3]. But, by how much must a new

Published in the special issue *Analytical Sciences in Austria* with Guest Editors G. Allmaier, W. Buchberger, and K. Francesconi.

**Electronic supplementary material** The online version of this article (doi:10.1007/s00216-010-4571-1) contains supplementary material, which is available to authorized users.

J. Horak (✉) · S. Hofer · W. Lindner  
Department of Analytical Chemistry, University of Vienna,  
Wahringenstrasse 38,  
1090 Vienna, Austria  
e-mail: Jeannie.Horak@univie.ac.at

C. Sadler · S. Williams  
ProMetic BioSciences Ltd.,  
211 Cambridge Science Park, Milton Road,  
Cambridge CB4 0WA, UK

technology such as simultaneous moving bed [4–6], multicolumn countercurrent solvent gradient purification process [7, 8], expanded bed adsorption [9, 10], aqueous two-phase extraction [11–13], an alternative HuMab capture media such as hydroxyapatite or fluoroapatite [14, 15], or protein precipitation [16] be more productive, for biopharm manufacturers to move away from well-established platform technologies. This question is difficult to answer and therefore worthwhile considering, for both researchers and industry alike.

Hence, it is not surprising that many new technologies are partially based on trusted and approved technologies such as Protein A and combine it with other new or improved support materials such as membranes [17, 18], monoliths [19], silica gel [20], zirconia beads [21] or magnetic cellulose microspheres [22]. Obviously, such an approach increases the overall chance that a promising new product achieves acceptance by manufacturers and get the opportunity to replace long existing platforms with less reservation.

One of the most promising of these is surely the combination of Protein A with an optimized membrane support from Sartorius-Stedim. This new Protein A membrane shows a 12-times higher binding capacity for IgG compared to Protein A-Sartobind [17] because the mass transport in membranes is based on convection, which enables protein capturing at much higher flow-rates. Membrane technology, in general, is gaining huge interest and certainly provides good candidates for process application [23–25], especially in the sector of disposable production media [26].

Besides the optimization of the support material, also the search for new improved affinity materials for antibody capturing is ongoing. Peptido-mimetic materials such as IRIS 97 [27], TG19318 [28], D-PAM [29], ZZ-Protein [30], or hexamer peptide HWRGWV [31] are interesting alternatives to Protein A, but the lower production costs and relatively easy manufacturing of smaller non-peptidyl mimetic ligands such as MAbsorbent A1P and A2P [32, 33] may be much more attractive. The possibility of a relatively easy combinatorial library approach to find new potential mimetic ligands, which mimic specific recognition and interaction motives of Protein A makes triazine-based chemistry ideal for affinity media development [34]. However, although the binding capacity for therapeutic antibodies can still be improved, the possibility to use these new mimetic affinity materials at much higher flow-rates with a reduction of required contact time and the mild binding and largely salt-free elution conditions for IgG at pH 3.5, make such new materials attractive for process applications.

The following article describes the improved IgG capture performance of a new triazine-based mimetic

affinity ligand B14, immobilized via Click Chemistry [35, 36] onto three new polymethacrylate-type support media with improved pore size and pore size distribution. Furthermore, the influence of different endcapping strategies will be discussed. Hence, the best performing B14-type adsorbent is tested with cell culture supernatant as well as two dialyzed (molecular weight cut-off (MWCO), 3–5 and 20 kDa) and with anion-exchange pre-purified feed solutions employing dynamic binding experiments. Their performance is compared to that of the Protein A media MabSelect employing a time-dependent binding study in batch mode. Sample fractions were analyzed with SDS-PAGE and with Protein A high-performance liquid chromatography (HPLC) as well as with an in-house-developed Protein A/size-exclusion HPLC method (PSEC-HPLC).

## Methods and materials

### Chemicals and samples

Diisopropylethylamine, ethylenediaminetetraacetic acid, 4-pentynoic acid, potassium dihydrogen phosphate, disodium hydrogen phosphate, 2-mercaptoethanol, sodium azide, sodium chloride (NaCl), citric acid (CA), and hydrochloric acid (HCl) were purchased from Sigma-Aldrich (Vienna, Austria).

Cell supernatant containing monoclonal human IgG1 (hIgG<sub>1</sub>) from CHO-expression systems were from Excell-Gene, (Monthey, Valais, Switzerland). Sample dialysis was performed with Spectra/Pore® CE Float-A-Lyzer® G2 with 10 mL volume size and a MWCO of 3–5 and 20 kDa. Bi-distilled water was filtered through a 0.22 µm cellulose acetate membrane filter from Sartorius-Stedim distributed by Wagner & Munz (Vienna, Austria) and ultrasonicated prior to use. Throughout this study, 10 mM phosphate buffer saline (PBS) solutions with increasing NaCl content of 0, 75, 150, and 300 mM will be denominated as PBS-O, PBS-75, PBS-150, and PBS-300.

### Bio-chromatography

For column chromatography an L-6200A Intelligent Pump with a D-6000A Interface from Merck-Hitachi (Darmstadt, Germany) and a single wavelength, UV-975 Intelligent UV–VIS detector from Jasco Biolab (Vienna, Austria) were used. The preparative column was connected over a manual 2-position/6-port switching valve from Rheodyne to the purge-outlet of the HPLC-pump. Feed application was performed with a Minipuls 3 peristaltic pump with a polyvinylchloride calibrated peristaltic tubing with 1.02 mm ID, both from Gilson (Villiers-le-Bel, France). For preparative chromatography, C10/10 columns with two AC10 flow

adapters and XK16/20 columns with 2 AK16 adapters from GE Healthcare (Vienna, Austria) were used in combination with Superformance Filter F with 10 mm and 16 mm ID from Götec-Labortechnik GmbH (Mühltal, Germany).

#### Sample analysis with high-performance liquid chromatography

All HPLC-analyses of collected sample fractions were performed on an Agilent 1100 series LC system equipped with a binary pump, a multi-wavelength detector and a two-position six-port switching valve from Agilent. For the isolation and quantification of IgG, a Protein A HPLC Cartridge PA ID Sensor Cartridge (particle size: 20 µm) from Applied Biosystems (Brunn am Gebirge, Austria) was used. The distribution of feed impurities was analyzed using a silica-based TSKgel G3000SWXL column (7.8 mm ID×30.0 cm length; particle size, 5 µm) with a TSK gel SWXL guard column (6.0 mm ID×4.0 cm length) from Tosoh Bioscience (Stuttgart, Germany). The Protein A cartridge was coupled in series with the SEC column using a six-port/two-position switching valve. Thereby, IgG was captured by the Protein A column and the non-bound feed impurities were then transferred to the SEC column and distributed by their molecular weight during the application step. Before the final elution of IgG from the Protein A cartridge, the switching valve connects the Protein A column back to the UV–VIS detector and bypasses the SEC column. After the complete elution of IgG and the reconditioning of the Protein A column with the application buffer, the switching valve is repositioned to the starting position for the next injection. The application buffer was a 10 mM PBS buffer with 150 mM sodium chloride (PBS-150), pH 7.20 and the elution buffer contained 12 mM HCl with 150 mM sodium chloride, pH 2–3. The visualization of material performance using cell culture feed was performed with PSEC diagrams [37]. Note that in this article both possible variations of the same instrumental set-up were employed, namely only using the Protein A column (Protein A-HPLC method) or using the Protein A column in combination with size exclusion (PSEC-HPLC method).

#### SDS-PAGE gel electrophoresis

All SDS-PAGE slab gels were hand-cast and prepared according to the general procedure for SDS-PAGE Laemmli buffer systems provided by Bio-Rad [38]. If not otherwise stated, 10%-Tris–HCl gels with 10 sample wells and 0.75 mm thickness were prepared. Since feed samples contain a low concentration of IgG in addition to a high feed impurity content, all samples were mixed in a 1:1 ratio with Laemmli buffer containing 10% 2-mercaptoethanol

before incubation at 90 °C for 5 min. In general, 15 µL samples and 3 µL molecular weight markers were applied. The Mini-PROTEAN® 3 Cell with a Mini-PROTEAN 3 Cell/PowerPac 300 System (220/240 V) and all required chemicals including a Precision Plus Protein Standard (unstained) were obtained from Bio-Rad Laboratories Inc. (Vienna, Austria). Protein staining was performed with the ProteoSilver™ Plus Silver Stain Kit (PROT-SIL2) from Sigma (Vienna, Austria) as earlier described [37].

#### Contact-time-dependent capture of IgG

For each adsorbent and each equilibration time investigated, aliquots of  $25.0 \pm 0.1$  mg were weighed into 1.5 mL reaction vessels, covered with 1 mL of cell culture feed and agitated at 25 °C and 1,400 rpm on a temperature controlled shaker from Eppendorf (Vienna, Austria). The investigated equilibration times for IgG capture by the adsorbents were 1, 2, 4, and 6 h as well as 5, 10, 20, and 30 min. All samples were centrifuged for 1 min and the supernatant was immediately removed. Note that for each investigated contact time all adsorbent samples were analyzed simultaneously using the Protein A-HPLC method.

#### Affinity materials

B14-monochloride, B14-2LP-AG and B14-2LP-FA1 were kindly provided by ProMetic BioSciences Ltd (Cambridge, UK). Note that AG stands for agarose and is ProMetic BioSciences in-house product PuraBead® P6HF (mean particle size, 90 µm). Fractogel® EMD Epoxy (FG; mean particle size, 40–90 µm) was purchased through VWR (Vienna, Austria). Epoxy FractoAIMs® 1, 2, and 3 (FA1, FA2, and FA3; mean particle size, 40 µm) are non-commercial products, kindly provided by Merck (Darmstadt, Germany). Manufacturer-provided and self-determined epoxide group densities as well as the average pore sizes of FG and FA supports are listed in Table S1 in the electronic supporting information.

3-Aminoquinuclidine-FractoAIMs-3 (AQ-FA3) was prepared and used as previously described [35]. MabSelect® was from GE Healthcare (Vienna, Austria). The synthesis of *N*-B14-*N*-(2-propynyl)-amine, the azidation of epoxide activated support media and the preparation of B14-triazole-adsorbents are described in detail in the electronic supporting information. Table 1 provides a list of all prepared and investigated B14-2LP-type and B14-TRZ-type adsorbents (Fig. 1). It also shows the amount of available azide groups, immobilized B14 ligands and the corresponding density of residual azide groups, which were endcapped.

**Table 1** List of azide group densities and B14-ligand densities of investigated adsorbents

Adsorbents	Azide group density [μmol/g]	B14-ligand density [μmol/g]	Residual azide groups [μmol/g]	Relative excess of azide groups <sup>a</sup>
B14-2LP-AG	—	200	—	—
B14-2LP-FA1	—	248	—	—
B14-TRZ-FG	783	343	440	1.28
B14-TRZ-FA1	395	138	257	1.86
B14-TRZ-FA1	696	157	539	3.43
B14-TRZ-FA2	1423	335	1088	3.25
B14-TRZ-FA3	1380	316	1064	3.37

<sup>a</sup> Excess azide groups relative to B14-ligand density = (residual azide groups) / (B14-ligand density). This factor should ideally be below 1 or even below 0.5

## Results and discussion

### Properties of the underlying support materials

The following study describes six IgG capture adsorbents, which all carry the same ligand head group B14, but combined with five different support media (AG, FG, FA1, FA2, and FA3) and two different spacer arms (2LP and TRZ). The PuraBead® P6HF support from ProMetic BioSciences contain 6% cross-linked agarose beads (AG) with a hydrophilic surface. It possesses excellent mechanical properties, which enables a high flow-rate of up to 750 cm/h at an operating pressure of 1 bar. The new FractoAIMs supports (FA1, FA2, and FA3) from Merck differ from the commercially available Fractogel (FG) by their smaller particle size of 40 μm as well as their tuned pore size and pore size distribution. These spherical beads show a low pressure drop combined with high efficiency. Furthermore, this hydrophilized surface is ideal for the preparation of affinity-type supports for hydrophilic target analytes in aqueous systems as it is required in chromatography. Both, Fractogel and FractoAIMs are polymethacrylate-based and have the tentacle grafting technology from Merck. These highly flexible tentacles increase the overall available surface area as they can be seen as a kind of extension to the spacer-chain of an immobilized affinity ligand (Fig. 1).

### B14-type adsorbent with 2LP and TRZ spacer on agarose and FractoAIMs

Dynamic binding capacity experiments were performed using the same batch of cell culture feed. The PSEC diagram in Fig. 2 summarizes the IgG breakthrough curves for the mimetic affinity adsorbents B14-2LP-AG, B14-2LP-FA1, B14-TRZ-FA1, and B14-TRZ-FA3 with single end-capping using cell culture feed. Those adsorbents with 1,2-diaminoethane spacer (2LP) were endcapped with 2-ethanolamine. B14-TRZ-type adsorbents having the [1,2,3]-triazole spacer incorporated were azide-group end-capped with 3-propargylalcohol using Click reaction protocol 1 [35]. To enable a better comparison of material

performance, only the flow-through curves for IgG were shown in the PSEC-Plots. In case of B14-2LP-FA1, the complete PSEC diagrams which include the breakthrough curves of the feed impurities can be found in an earlier published article [35].

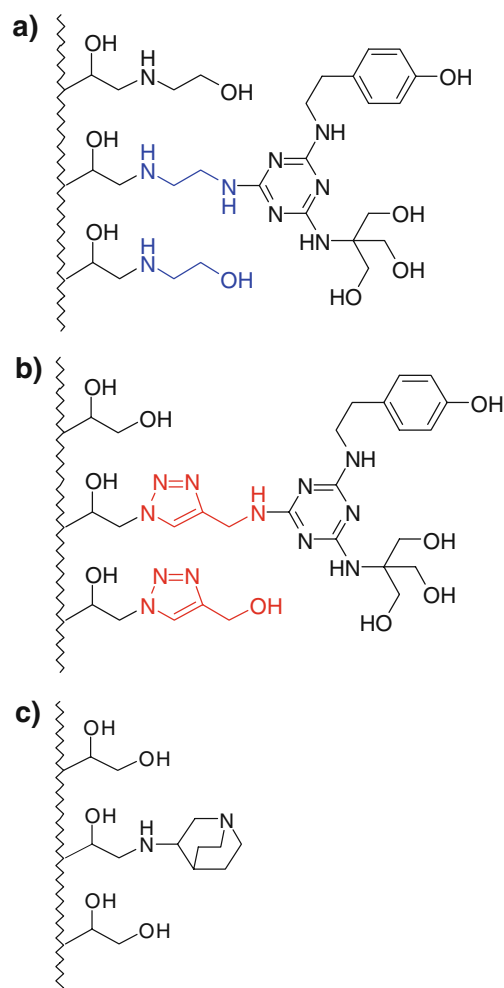


**Fig. 1** Chemical structure of investigated affinity ligand–spacer combinations: **a** B14-2LP with 1,2-diaminoethane spacer (2LP) and 2-ethanolamine endcapping; **b** B14-TRZ with [1,2,3]-triazole spacer (TRZ) and azide group endcapping using 3-propargyl alcohol; **c** AQ-FA3, an affinity-type weak anion-exchanger 3-aminoquiniclidine (AQ) on FractoAIMs-3 support (FA3)

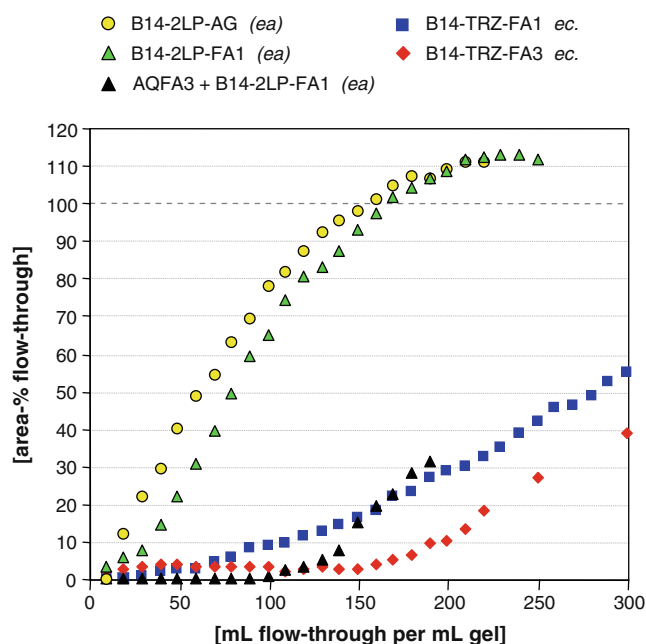


**Fig. 2** Dynamic breakthrough curves of B14-2LP-AG, B14-2LP-FA1, B14-TRZ-FA1 ec and B14-TRZ-FA3 ec using cell culture feed. B14-2LP-FA1 was additionally tested with a dialysed (MWCO, 3–5 kDa) and pre-purified ( $1\times$  AQ-FA3) cell culture feed

Comparing the breakthrough curves of the four investigated B14-type adsorbent, it seemed that the spacer and surface chemistry of a B14-type adsorbent had a stronger effect on material performance than the underlying support chemistry. Both B14-2LP-type adsorbents showed a rapid breakthrough of IgG, providing 10%-DBC values of 0.9 and 1.5 g/L for PuraBead (AG) and for FractoAIMs1 (FA1) with elution capacities of 0.7 and 3.2 g/L (Table 2). The two B14-TRZ adsorbents on FractoAIMs-type resins showed improved IgG binding properties, with 10%-DBC of 2.1 g/L and 7.2 g/L for B14-TRZ-FA1 ec and B14-TRZ-FA3 ec, with elution capacities of 7.7 and 11.1 g/L. Note that B14-TRZ-FA3 ec has double the number of B14-ligands

immobilized on its surface (Table 1) and has slightly larger pores compared to its FractoAIMs-1 counterpart (Table S1). Furthermore, the breakthrough curves for B14-2LP-AG and B14-2LP-FA1 exceeded 100% breakthrough, which may suggest that bound IgG was gradually replaced by feed impurities with progressing feed application. Accounting for the low recovery of 75% for B14-2LP-FA1 for the test run with pre-purified feed (A) compared to 93% when using cell culture media, it can be proposed that the IgG-portion which was replaced by feed impurities would otherwise not be eluted from the B14-2LP-type material. Nonetheless, the binding capacity of B14-2LP-FA1 for IgG could be increased from 1.5 to 4.1 g/L, when using the pre-purified feed. This effect can be directly correlated with the amino-groups, incorporated in the spacer and the surface endcapping of B14-2LP type adsorbents, which naturally exhibit weak anion-exchange characteristics. B14-2LP-AG and B14-2LP-FA1 are therefore mixed mode affinity materials, which can capture IgG and remove feed impurities in a single purification run [35]. The major drawback of B14-2LP type adsorbents lies in the low binding capacity for IgG due to a strong cross reactivity towards feed impurities. Hence, the main focus was set on the optimization of B14-TRZ-type adsorbents, which largely bind and release IgG with reduced negative attractions towards contaminants.

B14-TRZ-type adsorbent with improved surface chemistry

The reduced SDS-PAGE gels in Fig. 3 show that both adsorbents, B14-TRZ-FA1 ec and B14-TRZ-FA3 ec perform quite similar. A small amount of IgG had eluted with PBS-150 (lane 4). Note that IgG is represented by its light and heavy chain fragments at 25 and 50 kDa. The elution fractions (lane 5) from both B14-TRZ-type adsorbents showed the presence of IgG beside a significant amount of feed impurities. Both cleaning-in-place (CIP) fractions (lane 6), however, were less contaminated with feed

**Table 2** Summary of results obtained from the dynamic binding capacity studies

Adsorbents	Feed	10%-DBC [g/L]	30%-DBC [g/L]	Elution capacity <sup>a</sup> [g/L]	Recovery <sup>a</sup> [%]
B14-2LP-AG ec	Cell culture	0.9	1.5	0.7	21.8
B14-2LP-FA1 ec	Cell culture	1.5	2.3	3.2	93.4
B14-2LP-FA1 ec	Pre-purified (A) <sup>b</sup>	4.1	5.1	3.7 <sup>c</sup>	74.7 <sup>c</sup>
B14-TRZ-FA1 ec	Cell culture	2.1	6.4	7.7	69.3
B14-TRZ-FA3 ec	Cell culture	7.2	11.3	11.1	69.3
B14-TRZ-FA3 3 $\times$ ec	Cell culture	11.4	13.6	15.9	84.7
B14-TRZ-FA3 3 $\times$ ec	Pre-purified (B) <sup>b</sup>	11.3	13.5	16.0	86.5
MabSelect	Cell culture	1.7	8.8	20.4	80.5

<sup>a</sup> Elution capacity and recovery stated for 100% breakthrough of IgG

<sup>b</sup> (A) dialyzed (MWCO, 3–5 kDa) and purified with AQ-FA3 ( $1\times$ ); (B) dialyzed (MWCO, 3–5 kDa) and purified with AQ-FA3 ( $2\times$ )

<sup>c</sup> Elution capacity and recovery stated for 30% breakthrough of IgG



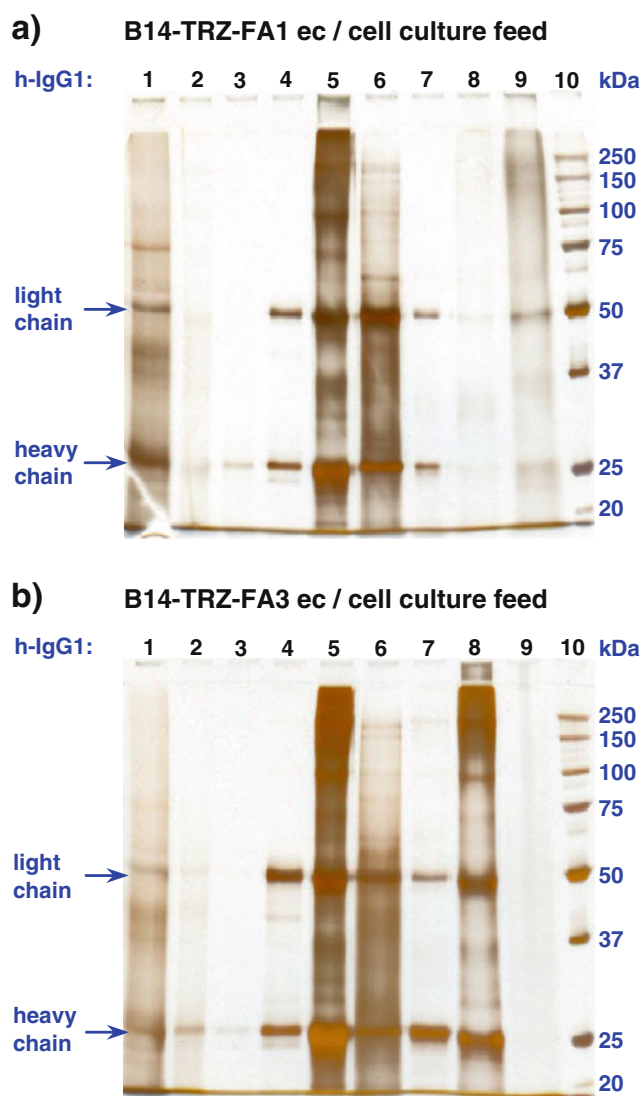


**Fig. 3** SDS-PAGE slab gels (10% Tris-HCl, silver stained) of collected fractions from DBC tests of **a** B14-TRZ-FA1 ec and **b** B14-TRZ-FA3 ec using cell culture feed. Elution fraction were dialysed (MWCO, 3–5 kDa) and purified with AQ-FA3. Lanes: (1) feed, (2) PBS-0, (3) PBS-75, (4) PBS-150, (5) elution with CA, (6) CIP, (7) AQ-FA3 flow-through, (8) AQ-FA3 elution with PBS-400, (9) AQ-FA3 CIP, (10) MW-marker

impurities compared to what was earlier observed for B14-2LP-FA1, but contained some IgG. These results would indicate that feed impurities bind weakly to the adsorbent, whilst IgG is bound more strongly. The elution fractions were pooled, dialyzed, and purified with the weak anion exchanger AQ-FA3. The feed impurity free flow-through fraction of AQ-FA3 (lane 7) proved the efficiency of the combination of B14-TRZ-type adsorbent with a final polishing step using AQ-FA3.

Since the FractoAIMs-3 support had performed best in combination with the B14-TRZ ligand, FractoAims-1 was excluded from further optimization studies. In an earlier

article, we had already described why residual azide groups on a support surface bind IgG and had shown strategies how to overcome this problem for the anion exchanger type media AdQ-TRZ-Fractogel [35]. The same strategy was applied here to improve the performance of the B14-TRZ-type adsorbent. The only difference was that the azide group density of the support surface of the B14-TRZ-type adsorbents was not optimized. The ideal ratio between residual azide groups and immobilized ligand ought to be below 1 or ideally even below 0.5, but was approximately 3.3 for all three B14-TRZ-FA materials (Table 1). Comparing the underlying azide group densities of 395 and 696  $\mu\text{mol/g}$  for B14-TRZ-FA1 with the obtainable B14-ligand densities of 138 and 157  $\mu\text{mol/g}$  in Table 1, it is apparent that a higher number of functional groups does not necessarily result in a higher ligand immobilization rate. For all shown experiments the B14-TRZ-FA1 adsorbent with the higher B14-ligand density was used. Note that the Click reaction protocol 2 can address remaining azide groups more efficiently than it would be possible with the conventional one-pot Click reaction. In the ideal case, a single endcapping with the modified Click reaction protocol 2 would have been sufficient to deactivate the few remaining azide groups as it was shown for AdQ-TRZ-FG [35]. However, in order to obtain the same results for a high azide density support, an aliquot of the same batch of single-endcapped B14-TRZ-FA3 adsorbent was further double endcapped using the improved Click reaction protocol. The now triple-endcapped adsorbent was tested with cell culture feed and with a pre-purified feed which was dialyzed (MWCO, 3–5 or 20 kDa) and double purified with AQFA3.

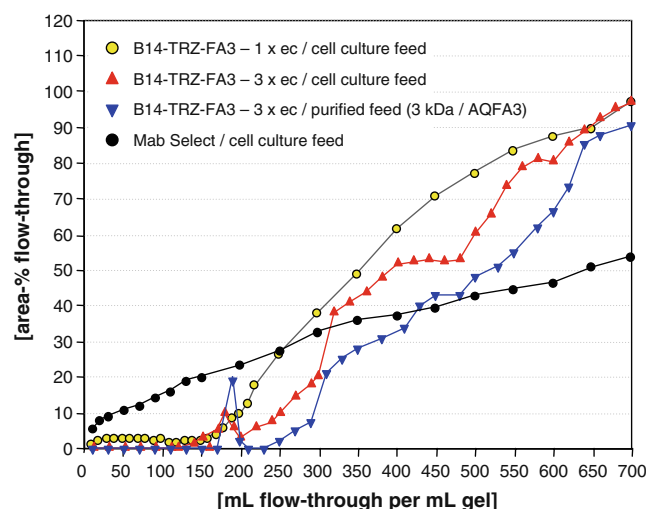


**Fig. 4** Dynamic breakthrough curves of B14-TRZ-FA3 ec, B14-TRZ-FA3 3 $\times$  ec and MabSelect using cell culture feed. B14-TRZ-FA3 3 $\times$  ec was additionally tested with a dialysed (MWCO, 3–5 kDa) and pre-purified (2 $\times$  AQ-FA3) cell culture feed

The IgG breakthrough diagram in Fig. 4 shows the improved IgG capture performance of B14-TRZ-FA3 3× ec compared to the original single-endcapped material and MabSelect, a Protein-A-based adsorbent.

The triple-endcapped B14-TRZ-FA3 3× ec provided a 10%-DBC of 11.4 g/L and an elution capacity of 16 g/L for hIgG<sub>1</sub>. Although B14-TRZ-FA3 3× ec appears to perform better with the pre-purified feed, the actual binding, elution and recovery figures as shown in Table 2 were practically identical to those obtained with cell culture feed. It was however surprising that B14-TRZ-FA3 outperformed MabSelect, which came with a rather low 10%-DBC of 1.7 g/L and a recovery of 81% for bound IgG. The elution capacity of 20.4 g/L hIgG<sub>1</sub> was only obtained after feed application in recycling mode until complete saturation was achieved.

A discussion of possible reasons for these results will be presented at a later point. There was also a different pattern of the breakthrough curves of the single- and the triple-endcapped adsorbent. The latter provided an IgG peak at 180 mL and four slopes at 310, 380, 480, and 620 mL flow-through per milliliter gel for the DBC test with cell culture feed. For the DBC run with the purified feed, the IgG peak was found at 190 mL and slightly less pronounced slopes at 300, 410, 480, and 620 mL flow-through per milliliter gel. The reasons for this phenomenon is yet unknown and require further investigations.

The PSEC diagrams in Fig. 5 provide additional information on the binding of feed impurities for adsorbents B14-TRZ-FA3 ec and B14-TRZ-FA3 3× ec investigated with cell culture feed and the latter also with pre-purified feed (MWCO, 3–5 kDa and 2× AQ-FA3). A comparison of Fig. 5a and b showed that the single-endcapped adsorbent had captured a significant amount of feed impurity fraction E (85%; <0.1 kDa plus adsorbed impurities) followed by impurities A and B (33%; 660–17 kDa) and impurities C and D (23%; 17–0.15 kDa) from the first 20 mL of application feed.

The triple-endcapped adsorbent in Fig. 5b bound less of the feed impurities E and B (15%), C and D (12%) and 28% A from the first 10 mL of application feed. Only feed impurity A was slightly captured from the first 50 mL of feed application, all other feed impurities flowed unretained through the column. Unfortunately, the size-exclusion column had decomposed during this measurement sequence. This is visible in the broken breakthrough curves for the feed impurities in Fig. 5b and may also be the reason why feed impurity E seemed to be attracted to the adsorbent in Fig. 5a and b. With progressing aging of the SEC column, the authors assume that the feed impurity E fraction, which also contained high molecular weight impurity was irreversibly bound to the exposed silanol groups on the silica particles. This may have resulted in the rapid degradation of the column.

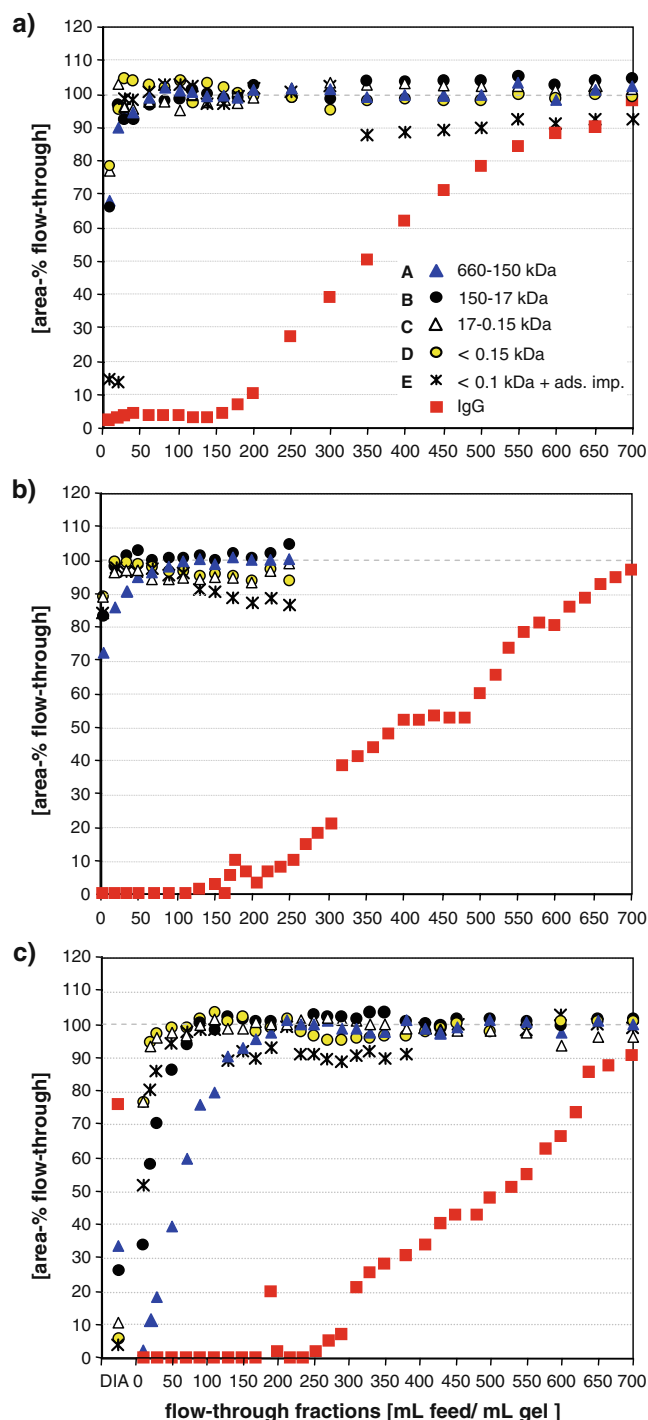


**Fig. 5** Performance evaluation via PSEC diagrams of affinity adsorbents **a** B14-TRZ-FA3 ec tested with cell culture feed and B14-TRZ-FA3 3× ec tested with **b** cell culture feed and with **c** dialysed feed (MWCO, 3–5 kDa)

The first column in the PSEC diagram of Fig. 5c summarizes the feed impurity composition of the dialysed feed using the cell culture feed composition as a reference point. For all other fractions, the composition of the dialysed feed was used as a reference. Due to the absence

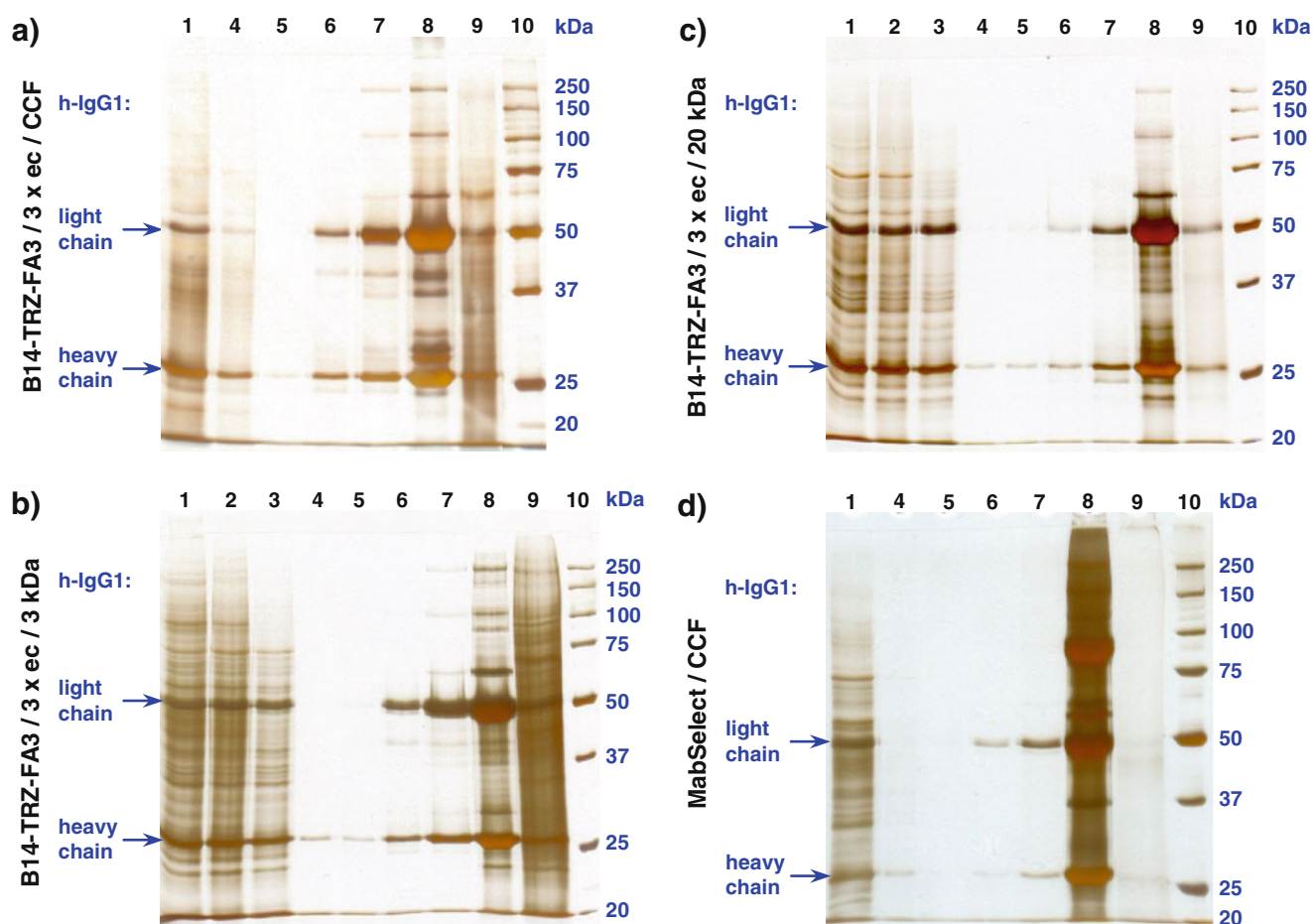


**Fig. 6** SDS-PAGE slab gels (10% Tris-HCl, silver stained) of collected fractions from DBC tests of B14-TRZ-FA3 3× ec using **a** cell culture feed (CCF), and **b** pre-purified feed dialyzed with MWCO, 3–5 kDa and purified 2× AQ-FA3 and **c** dialyzed with MWCO,

20 kDa and 2× AQ-FA3 compared to **d** MabSelect tested with cell culture feed. Lanes: (1) application feed, (2) after dialysis, (3) after 2× AQ-FA3, (4) PBS-0, (5) PBS-75, (6) PBS-150, (7) PBS-300, (8) elution with CA, (9) CIP, (10) MW-marker

of low molecular weight impurities in the dialyzed feed, binding sites that would otherwise be occupied by these low MW impurities were now vacant for high MW feed impurity A, followed by impurity B and E. The SDS-PAGE gels of the corresponding DBC-runs for B14-TRZ-FA3 3× ec tested with cell culture feed and dialyzed feed A (MWCO, 3–5 kDa) plus the results of a test run with dialyzed feed B (MWCO, 20 kDa) and MabSelect tested with cell culture feed were compiled in Fig. 6.

The only significant difference between the three slab gels for B14-TRZ-FA3 3× ec lies in the composition of the PBS-0 and PBS-150 wash fraction in lane 4 and lane 6 as well as the CIP fraction in lane 9. With decreasing amount of feed impurities present in the feed, the contaminant smear across lane 4 disappeared and less IgG was eluted into lane 6. Note that the SDS-PAGE gel in Fig. 6b was slightly over-stained. In case of the CIP lanes, the dialyzed feed A seemed to have promoted the highest capture of feed impurities, while feed B provided the cleanest CIP fraction.

The IgG elution fraction (lane 8, dialyzed feed A) in Fig. 6b showed slightly more bands from co-eluted impurities compared to the elution lanes of the other two B14-TRZ-FA3 3× ec DBC-runs. As expected, the elution fractions for the DBC run with dialyzed feed B showed less co-eluted impurities and the CIP lane 9 contained only a trace amount of bound IgG with a slight smear across the lane. A comparison to the performance of MabSelect under same test conditions using cell culture feed showed that more feed impurities were bound from the application feed and released into the elution fraction (lane 8) than earlier observed for B14-TRZ-FA3 3× ec. Furthermore the CIP lane 9 of MabSelect is practically free of impurities or IgG.

#### Comparison of investigated B14-type adsorbents

In order to reliably compare SDS-PAGE results of all investigated B14-2LP and B14-TRZ-type adsorbents with MabSelect, their elution fractions were diluted down to the



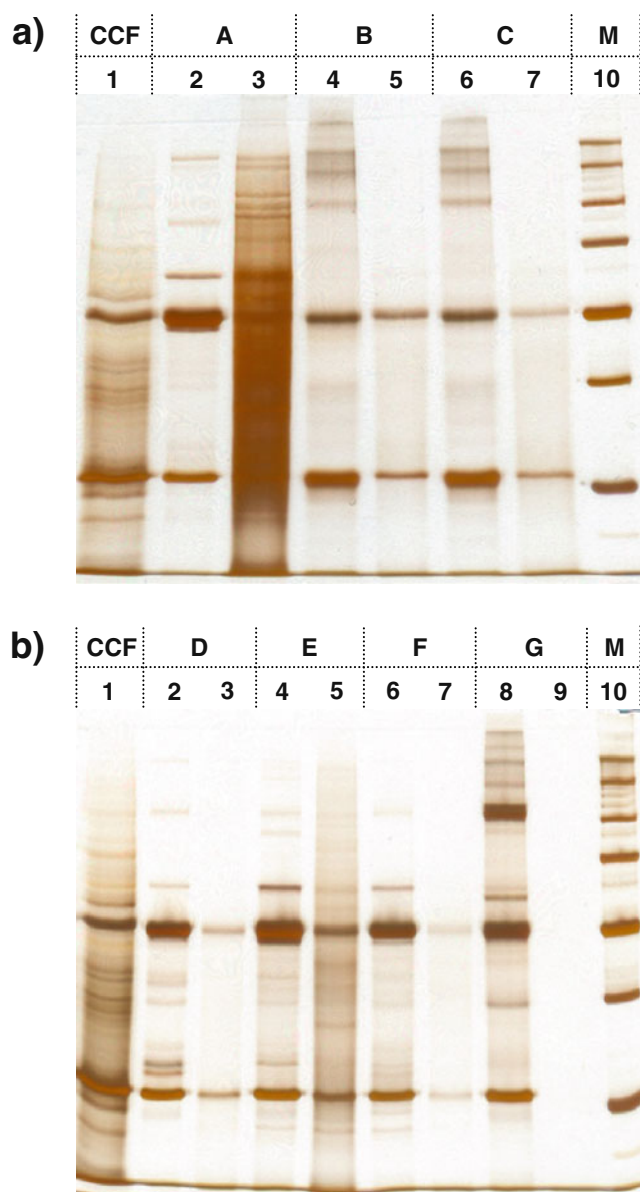


**Fig. 7** SDS-PAGE slab gels (10% Tris–HCl, silver stained) of feed, elution and CIP fractions of all investigated B14-type adsorbents normalized to approximately the same IgG concentration of the elution fractions. **A** B14-2LP-FA1, **B** B14-TRZ-FA1 ec, **C** B14-TRZ-FA3 ec and **G** MabSelect were tested with cell culture feed (CCF); B14-TRZ-FA3 3× ec was tested with **D** cell culture feed, with **E** pre-purified cell culture feed (MWCO 3–5 kDa and 2× AQ-FA3), with **F** pre-purified cell culture feed (MWCO 20 kDa and 2× AQ-FA3); lanes: (1) CCF, (2, 4, 6, 8) elution, (3, 5, 7, 9) CIP, and (10) MW-marker

IgG concentration of the adsorbent with the lowest IgG binding capacity. The same dilution factor was used for the corresponding CIP samples. All normalized samples were applied onto two SDS-PAGE gels (Fig. 7), which were stained simultaneously under identical conditions, allowing the most accurate comparison of test results.

The elution fraction with the highest purity for IgG was obtained with B14-TRZ-FA3 3× ec (dialyzed feed B), followed by B14-TRZ-FA3 3× ec (dialyzed feed A), B14-2LP-FA1 and B14-TRZ-FA3 3× ec (cell culture). The highest amount of feed impurities in the IgG elution fraction was found with increasing rate for the adsorbents B14-TRZ-FA3 ec, B14-TRZ-FA1 ec and MabSelect. For MabSelect, mainly high MW impurities above 100 kDa were present, besides distinct protein bands at 37, 60, and 65 kDa. The impurity at 65 kDa can also be found for B14-TRZ-FA3 3× ec (dialyzed feed A), B14-TRZ-FA3 3× ec (dialyzed feed B), and B14-2LP-FA1. The elution fraction for B14-TRZ-FA3 3× ec (cell culture) only shows two distinct impurities between 25 and 30 kDa. The two single-endcapped adsorbents B14-TRZ-FA1 ec and B14-TRZ-FA3 ec show three distinct impurity bands with a smear ranging from 100 to 250 kDa and an impurity band at about 24 kDa. Concerning the CIP fractions, the most contaminated lane was found for B14-2LP-FA1, followed by B14-TRZ-FA3 3× ec (dialyzed feed A). All other CIP fractions contained varying amount of IgG, with the most distinct lanes for B14-TRZ-FA1 ec (cell culture; B) followed by B14-TRZ-FA3 3× ec (dialyzed feed A; E) and B14-TRZ-FA3 3× ec (cell culture; D). The CIP fractions from B14-TRZ-FA3 3× ec (dialyzed feed B; F) and MabSelect were free of IgG. Note that the more distinct 25 kDa band in Fig. 7 lanes 4 and 6 was most probably caused by excess short chain IgG, due to a slight over-expression of the latter during antibody production.

The main reason for the deviating results for different endcapping strategies and different application feed composition may be the fact that the surface chemistry of an adsorbent can promote or repel the binding of feed impurities or the unspecific capture of IgG. Furthermore the same accounts for already bound feed impurities. These surface bound non-target compounds may also be able to promote the capture of other feed impurities or IgG. The same adsorbent can therefore perform quite differently with varying composition of the application feed. A reliable comparison of material performance can therefore only be conducted for the same production batch of cell culture feed, handled and pretreated under identical conditions.

#### Contact-time-dependent capture of IgG

The diagram of IgG breakthrough curves in Fig. 4 showed a fast and continuous breakthrough of IgG from the MabSelect column. The aim of this investigation was to determine the reason why B14-TRZ-type adsorbents perform, in this respect, better than the state-of-the-art Protein A affinity adsorbent. Note that all DBC tests were performed under identical condition, employing 1 mL resin, packed in a column with 1 cm column diameter at a bed-height of 1 cm

using a flow rate of 1 mL/min for feed application as well as for all wash, elution, and cleaning-in-place steps. Since the void volume of the investigated adsorbent was approximately 1 mL, the contact time between the target analyte IgG and the potential IgG binding site on the support surface was a maximum of 1 min.

Due to the limited available amount of B14-TRZ-type adsorbents, the time-dependent binding of IgG to the various types of adsorbent was conducted via static binding capacity experiments in batch mode. For each investigated contact time, the adsorbents were incubated with the same batch of cell culture feed at the same time under identical conditions (25 °C and 1400 rpm). Contact times investigated were 1 to 6 h in 1 h intervals (Fig. 8a) as well as 30, 20, 10, and 5 min (Fig. 8b). After incubation, all samples were immediately centrifuged. The supernatant were removed and analyzed via Protein A HPLC. The %-amount of unbound IgG was plotted for each adsorbent against the corresponding incubation time. The diagram (Fig. 8a) indicates that for a long-ranging incubation, the three triple-encapped B14-TRZ-type adsorbents on FractoAIMs-1, FractoAIMs-2, FractoAIMs-3 performed quite similar to MabSelect, leaving only 6–8% IgG unbound. For the other three investigated adsorbents, B14-TRZ-FG ec, B14-2LP-FA1 ec, and B14-2LP-AG ec, much higher incubation times were required. After 6 h of incubation, 11% IgG was found in the supernatant of B14-TRZ-FG ec, while for B14-2LP-FA1 18% and for B14-2LP-AG 20% of IgG remained unbound. With the reduction of the contact time to 1 h, the amount of residual IgG was only slightly increased for B14-2LP-FA1 and B14-2LP-AG to 20% and 22% of unbound IgG. B14-TRZ-FG ec captured 10% less IgG after 1 h of incubation. From Fig. 8b, the same trend was observed for the three B14-TRZ-type materials and MabSelect, but at a much shorter time frame of 30 to 5 min. While at 30-min incubation time all four adsorbents exhibited approximately the same non-binding rate of 6–8% for IgG, at 20 min MabSelect had already captured 5% less IgG compared to B14-TRZ-FA3 3× ec, and after 5 min MabSelect had bound approximately 12% less IgG. These results indicate that the fast dynamic breakthrough of IgG from MabSelect in Fig. 4 was caused by the slightly slower IgG capture kinetics of MabSelect compared to the B14-TRZ-type adsorbents.

## Conclusions

A new mimetic affinity ligand B14 bound via Click chemistry to the FractoAIMs-3 (FA3) support was introduced. It was shown that B14-TRZ-FA3 3× ec is an excellent IgG capture media tolerating fast flow-rates and low bed-heights. Although B14-TRZ-FA3 3× ec can only reach 75% of the elution capacities of MabSelect for complete IgG saturation of

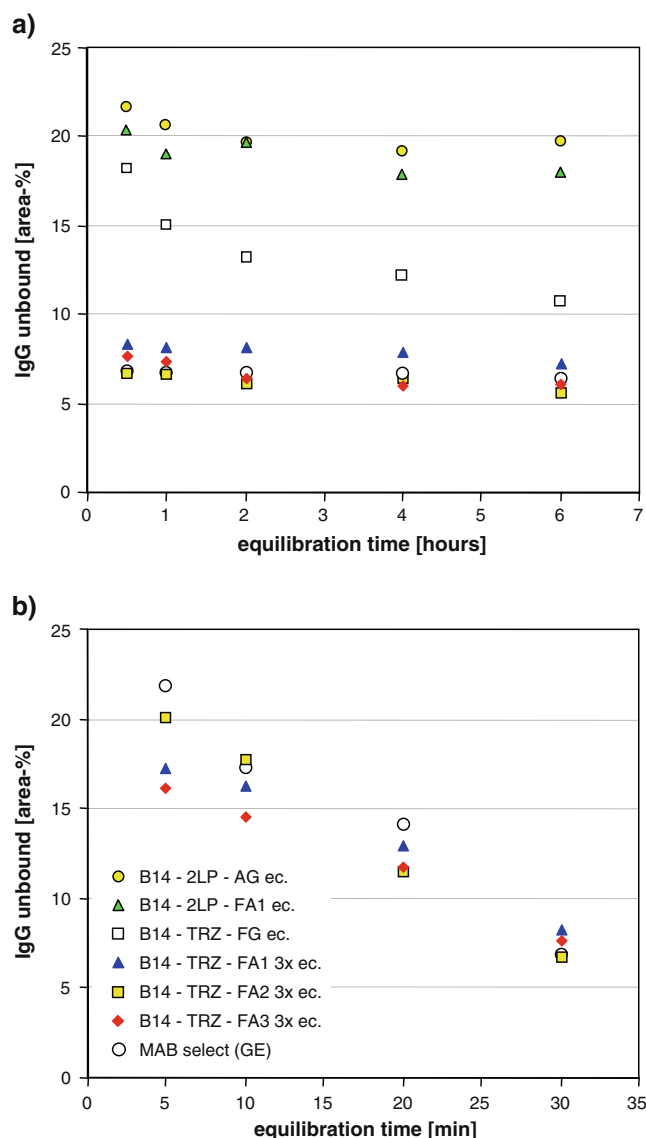


**Fig. 8** Equilibration kinetic diagrams for B14-2LP-AG ec, B14-2LP-FA1 ec, B14-TRZ-FG ec, B14-TRZ-FA1 3× ec, B14-TRZ-FA2 3× ec, B14-TRZ-FA3 3× ec and MabSelect, tested via static binding capacity experiments using aliquots of 25 mg ( $\pm 0.1$  mg) resin and 1 mL cell culture feed incubated at 25 °C and 1400 rpm for different time intervals ranging from 5 min to 6 h

the adsorbent, their 10%-DBC and 30%-DBC values are highly superior at high flow-rates. Taking the results of the IgG binding study into account, it can be assumed that B14-TRZ-FA3 3× ec would perform similarly to MabSelect if the contact time between resin and target analyte was increased by reduction of the flow-rate or an increase in column bed-height. Nonetheless this new mimetic media can capture IgG faster and with less cross-selectivity towards feed impurities than MabSelect. Furthermore, this study shows that co-eluted feed impurities can easily be removed from the elution fraction with an additional polishing step using an anion

exchanger as it was demonstrated with the affinity-based weak anion exchanger AQ-FA3.

**Acknowledgments** This study was performed within the EU-Project AIMs (Advanced Interactive Materials by Design; NMP3-CT-2004-500160), which is part of the 6<sup>th</sup> Framework Program of the European Union. The authors want to thank Merck KGaA for providing the Fractogel® and FractoAIMs® support media. Note that ProMetic BioSciences and Mimetic Ligands™ are trademarks of ProMetic BioSciences Ltd and that PuraBead® is registered with the U.S. Patent & Trademark Office.

## References

- Jagschies G, Groenberg A, Bjoerkman T, Lacki K, Johansson HJ (2006) *BioPharm Int* (June Suppl):10–19
- Langer ES (2008) *BioProcess Int* 6:72
- Kelley B (2007) *Biotechnol Prog* 23:995–1008
- Bisschops MAT, Ransohoff T (2008) Abstracts of Papers, 236th ACS National Meeting, Philadelphia, PA, United States (August 17–21):BIOT-251
- Imamoglu S (2002) *Adv Biochem Eng Biotechnol* 76:211–231
- Kessler LC, Gueorguieva L, Rinas U, Seidel-Morgenstern A (2007) *J Chromatogr A* 1176:69–78
- Muller-Spath T, Aumann L, Melter L, Strohlein G, Morbidelli M (2008) *Biotechnol Bioeng* 100:1166–1177
- Strohlein G, Aumann L, Muller-Spath T, Tarafder A, Morbidelli M (2007) *BioPharm Int* (Feb Suppl):42–48
- Fahrner RL, Blank GS, Zapata GA (1999) *J Biotechnol* 75:273–280
- Gonzalez Y, Ibarra N, Gomez H, Gonzalez M, Dorta L, Padilla S, Valdes R (2003) *J Chromatogr B* 784:183–187
- Azevedo AM, Rosa PAJ, Ferreira IF, Aires-Barros MR (2007) *J Biotechnol* 132:209–217
- Azevedo AM, Rosa PAJ, Ferreira IF, Aires-Barros MR (2008) *J Chromatogr A* 1213:154–161
- Azevedo AM, Rosa PAJ, Ferreira IF, Pisco AMMO, de Vries J, Korporaal R, Visser TJ, Aires-Barros MR (2009) *Sep Purif Technol* 65:31–39
- Gagnon P, Ng P, Zhen J, Aberin C, He J, Mekosh H, Cummings L, Zaidi S, Richieri R (2006) *BioProcess Int* 4:50–60
- Schubert S, Freitag R (2007) *J Chromatogr A* 1142:106–113
- McDonald P, Victa C, Carter-Franklin JN, Fahrner R (2009) *Biotechnol Bioeng* 102:1141–1151
- Boi C, Dimartino S, Sarti GC (2008) *Biotechnol Prog* 24:640–647
- Dancette OP, Taboureau JL, Tournier E, Charcosset C, Blond P (1999) *J Chromatogr B* 723:61–68
- Jungbauer A, Hahn R (2008) *J Chromatogr A* 1184:62–79
- Katoh S, Imada M, Takeda N, Katsuda T, Miyahara H, Inoue M, Nakamura S (2007) *J Chromatogr A* 1161:36–40
- Subramanian A, Martinez B, Holm J, Carr P, McNeff C (2006) *J Liq Chromatogr Relat Technol* 29:471–484
- Cao Y, Tian W, Gao S, Yu Y, Yang W, Bai G (2007) *Artif Cells Blood Substit Immobil Biotechnol* 35:467–480
- Arunakumari A, Wang J, Ferreira G (2007) *BioPharm Int* (Oct Suppl):6–10
- Giovannoni L, Ventani M, Gottschalk U (2008) *BioPharm Int* 21:48–52
- Knudsen HL, Fahrner RL, Xu Y, Norling LA, Blank GS (2001) *J Chromatogr A* 907:145–154
- Lim JAC, Sinclair A, Kim DS, Gottschalk U (2007) *BioProcess Int* 5:48–58
- Guerrier L, Flayoux I, Schwarz A, Fassina G, Boschetti E (1998) *J Mol Recognit* 11:107–109
- Fassina G, Verdoliva A, Palombo G, Ruvo M, Cassani G (1998) *J Mol Recognit* 11:128–133
- Fassina G (2000) *Methods Mol Biol* 147:57–68
- Chen C, Huang QL, Jiang SH, Pan X, Hua ZC (2006) *Biotechnol Appl Biochem* 45:87–92
- Yang H, Gurgel PV, Carbonell RG (2009) *J Chromatogr A* 1216:910–918
- Chhatre S, Titchener-Hooker NJ, Newcombe AR, Keshavarz-Moore E (2007) *Nat Protoc* 2:1763–1769
- Ghose S, Hubbard B, Cramer SM (2006) *J Chromatogr A* 1122:144–152
- Li R, Dowd V, Stewart DJ, Burton SJ, Lowe CR (1998) *Nat Biotechnol* 16:190–195
- Horak J, Hofer S, Lindner W (2010) *J Chromatogr B* 878:3382–3394
- Kolb HC, Finn MG, Sharpless KB (2001) *Angew Chem Int Ed* 40:2004–2021
- Horak J, Ronacher A, Lindner W (2010) *J Chromatogr A* 1217:5092–5102
- B.-R.L. Instruction Manual for Mini-PROTEAN® 3 Cell, Inc., <http://www.plant.uoguelph.ca/research/homepages/raizada/Equipment/RaizadaWeb%20Equipment%20PDFs/9B.%20miniprotean3%20cell%20manual.pdf>



## Performance evaluation of Mimetic Ligand™ B14-triazole-FractoAIMs adsorbents for the capture of human monoclonal immunoglobulin G from cell culture feed

Jeannie Horak, Stefan Hofer, Chris Sadler, Sharon Williams, Wolfgang Lindner

**Table S1** Characterisation of investigated support media

<b>Support media (abbreviation)</b>	<b>Epoxide Density <sup>a)</sup></b> [μmol/g] (T)	<b>Epoxide Density <sup>a)</sup></b> [μmol/g] (EA)	<b>Average PSD <sup>b)</sup></b> [nm] (Hg)	<b>Max. of PSD<sub>v</sub> <sup>c)</sup></b> [nm] (ISEC)	<b>Width of PSD <sup>c)</sup></b> [nm] (ISEC)	<b>Pore volume</b> [% of CV] (ISEC)	<b>Surface area <sup>d)</sup></b> [m <sup>2</sup> /g] (N <sub>2</sub> )
<b>PuraBead (AG)</b>	200	<i>n.a.</i>	<i>n.a.</i>	<i>n.a.</i>	<i>n.a.</i>	<i>n.a.</i>	<i>n.a.</i>
<b>Fractogel (FG)</b>	750	931	<i>n.a.</i>	<i>n.a.</i>	<i>n.a.</i>	<i>n.a.</i>	<i>n.a.</i>
<b>FractoAIMs-1 (FA1)</b>	248	876	47	59	1	40	98
<b>FractoAIMs-2 (FA2)</b>	442	1426	47	59	1	40	98
<b>FractoAIMs-3 (FA3)</b>	454	1380	60	68	7	44	91

a) epoxide group density determined by titration (T) as stated by the manufacturer and by elemental analysis (EA) after full coverage with azide groups

b) pore size diameter (PSD) by mercury intrusion (Hg)

c) pore size diameter with volume (v) based distribution and pore volume determined by inverse size-exclusion chromatography (ISEC)

d) surface area determined by nitrogen adsorption (N<sub>2</sub>) using the BET method

b)-d) this information was provided by the manufacturer Merck KGaA (Darmstadt, Germany)

*n.a.* not available

## **Preparation of B14-triazole-type adsorbents**

### ***Synthesis of N-B14-N-(2-propynyl)-amine***

To a solution of 1 g B14-monochloride (2.71 mmol) in 2-propanol, 0.460 mL diisopropylethylamine (DIPEA) and 0.346 mL (5.40 mmol) 3-propargylamine were added. The reaction solution was refluxed for 18 h. Excess solvent was removed under reduced pressure. The crude product was purified with column chromatography with silica gel 60 and a solvent mixture of methanol and dichloromethane. The reaction yield of the orange product was 694 mg (66%).

NMR [CD<sub>3</sub>OD]:  $\delta$  = 7.10 (d, 2H), 6.74 (d, 2H), 4.09 (s, 2H), 3.93-3.64 (m, 6H), 3.50 (s, 2H), 2.80 (t, 2H), 2.56 (t, 1H); MS (ESI, positive): 389 [M+H]<sup>+</sup>, 411 [M+Na]<sup>+</sup>, 777.6 [2M+H]<sup>+</sup>; MS (ESI, negative): 386.8 [M-H]<sup>-</sup>, 775.5 [2M-H]<sup>-</sup>

### ***Azidation of epoxide-activated support materials***

The azidation of support materials was performed as earlier described [1].

The binding of azide groups to epoxide functionalized support surfaces and its quantitative evaluation via elemental analysis was used to determine the epoxide group density of the supporting media. A summary of material properties is shown in **Table S1**. Note, that for the epoxide group densities a large divergence between titration and elemental analysis data was observed. Both methods are from a chemical view-point orthogonal to each other. An insufficient modification of epoxide groups to the titratable functionality might be the reason. The elemental analysis results are as followed:

FG-N3 coverage: 931  $\mu$ mol/g (C 51.23%; H 7.37%; N 5.16%); 876  $\mu$ mol/g (C 55.01%; H 7.36%; N 3.68%); 1426  $\mu$ mol/g (C 54.93%; H 6.98%; N 5.99%); 1380  $\mu$ mol/g (C 54.78%; H 6.91%; N 5.80%)

### ***Preparation of B14-triazole-Fractogel and B14-triazole-FractoAIMs***

To a slurry of 3 mL Azido-Fractogel or Azido-FractoAIMs in methanol, a solution containing 4 mol-equivalents (equiv) B14-propyne (22.5 mg/mL) and 3 mol-equiv. DIPEA in methanol were added. After addition of 5.7 mol-equiv. copper iodide in acetonitrile (20 mg/mL), the reaction slurry was covered with nitrogen and stirred for 3 days on an orbital shaker. The modified adsorbent was filtered and washed successively with 10 mM hydrochloric acid, 0.5 M sodium hydroxide, 0.1 M ethylenediaminetetraacetic acid (EDTA), methanol and in between with water until the original white colour of the adsorbent was obtained. All adsorbents were stored in 20% (v/v) methanol (HPLC-grade) prior to use. Note that all solvents and reaction solutions were degassed in order to remove traces of oxygen which would otherwise reduce the yield of the Click-reaction. The reaction yield was determined via elemental analysis employing the nitrogen content of the immobilized ligand.

In order to remove remaining azide groups on the surface of the activated support material, all adsorbents were single endcapped with 3-propargylalcohol using Click reaction protocol 1. The FractoAIMs based adsorbents were additionally twice endcapped with 3-propargyl alcohol using the improved Click reaction protocol 2, which involves the off-line pre-formation of the copper (I)-acetylide complex before addition to the adsorbent [1]. **Table 1** provides a summary of available azide groups, immobilized B14 ligands and the corresponding density of residual azide groups, which have to be endcapped.

**B14-TRZ-FG:** N3 coverage: 783  $\mu\text{mol/g}$  (C 51.55%; H 7.4%; N 3.29%); B14-density: 343  $\mu\text{mol/g}$  (C 52.25%; H 7.14%; N 6.17%); **B14-TRZ-FA1:** N3 coverage: 696  $\mu\text{mol/g}$  (C 54.48%; H 7.29%; N 2.93%); B14-density: 157  $\mu\text{mol/g}$  (C 53.98%; H 7.16%; N 4.25%); **B14-TRZ-FA2:** N3 coverage: 1426  $\mu\text{mol/g}$  (C 54.93%; H 6.98%; N 5.99%); B14-density: 335  $\mu\text{mol/g}$  (C 53.33%; H 6.97%; N 8.8%); **B14-TRZ-FA3:** FA3-N3 coverage: 1380  $\mu\text{mol/g}$  (C 54.78%; H 6.91%; N 5.80%); B14-density: 316  $\mu\text{mol/g}$  (C 52.76%; H 6.94%; N 8.45%).

### **Reference:**

[1] Horak J, Hofer S, Lindner W (2010) J Chromatogr B, doi:10.1016/j.jchromb.2010.10.025





## **Appendix 3**

### **Publication 3**



# Experimental and Theoretical Investigation of Effect of Spacer Arm and Support Matrix of Synthetic Affinity Chromatographic Materials for the Purification of Monoclonal Antibodies

Laura Zamolo,<sup>†</sup> Matteo Salvalaglio,<sup>†</sup> Carlo Cavallotti,<sup>\*,‡</sup> Benedict Galarza,<sup>‡</sup> Chris Sadler,<sup>‡</sup> Sharon Williams,<sup>\*,‡</sup> Stefan Hofer,<sup>§</sup> Jeannie Horak,<sup>\*,§</sup> and Wolfgang Lindner<sup>§</sup>

Department of Chemistry, Materials and Chemical Engineering “G. Natta”, Politecnico di Milano, Via Mancinelli 7, 20131 Milano, Italy, ProMetic BioSciences Ltd., 211 Cambridge Science Park, Milton Road, Cambridge CB4 0WA, United Kingdom, Department of Analytical Chemistry and Food Chemistry, University of Vienna, Waehringer Strasse 38, 1090 Vienna, Austria

Received: February 25, 2010; Revised Manuscript Received: May 31, 2010

The aim of this study was to elucidate the influence of each material component—the support, the spacer, and the surface chemistry—on the overall material performance of an affinity type purification media for the capture of immunoglobulin G (IgG). Material properties were investigated in terms of an experimental evaluation using affinity chromatography as well as computer modeling. The biomimetic triazine-based A2P affinity ligand was chosen as a fixed point, while spacer and support were varied. The investigated spacers were 1-2-diaminoethane (2LP), 1,3-propanedithiol (SS3), 3,6-dioxo-1,8-octanedithiol (DES), and a 1,4-substituted [1,2,3]-triazole spacer (TRZ). The support media considered were the agarose (AG) resins, PuraBead, the polyvinylether, Fractoprep, the polymethacrylate, Fractogel, and the porous silica, Fractosil. All materials were tested with pure IgG standard solution, with a mock feed solution as well as real cell culture supernatant. The interaction between IgG and A2P linked through the investigated spacers to AG was studied using molecular dynamics. The effect of a modification of the support chemical structure or of the protein–ligand binding site on the material performances was studied through target oriented simulations. Dynamic binding experiments (DBC) revealed that the performances of materials containing 2LP spacers were significantly decreased in the presence of Pluronic F68. The simulations indicated that this is probably determined by the establishment of intermolecular interactions between the 2LP charged amino group and the ether oxygen of Pluronic F68. The spacer giving the highest IgG dynamic binding capacity when Pluronic F68 was present in the feed was TRZ. The simulations showed that, among the investigated spacers, TRZ is the only one that prevents the adsorption of A2P on the support surface, thus suggesting that the mobility and lack of interaction of the ligand with the support is an important property for an affinity material. Both experiments and calculations agree that the chemistry of the support surface can have a significant impact on IgG binding, either affecting the IgG DBC, as found experimentally for materials having similar ligand densities and spacer arms but different supports, or competing with the affinity ligand when hydrophobic groups are added to the model surface, as was computationally predicted.

## 1. Introduction

The production and purification of monoclonal antibodies (Mabs) has been attracting considerable attention in recent years for their rising importance in diagnostic and therapeutic treatment of diseases such as immunodeficiency, Alzheimer's syndrome, and cancer.<sup>1–4</sup> The large scale manufacture of Mabs is an expensive process, characterized by high costs of both upstream and downstream processing.<sup>5,6</sup> To date the most commonly used purification process for Mab capture is affinity chromatography using protein A and protein G.<sup>7–9</sup> These protein-based ligands are highly selective for immunoglobulin G (IgG) showing high binding capacities of about 26–38 g/L at 10% break through for monoclonal antibodies from cell culture supernatant.<sup>10</sup> For pure antibody solutions of polyclonal

IgG, binding capacities of up to 36–50 g/L were found.<sup>11</sup> The major drawbacks of protein A and protein G type adsorbents are however their elevated cost for production, making their use for Mab isolation rather expensive. In addition, protein A adsorbents have a tendency to exhibit leakage of the immobilized protein A and a low stability during sterilization and sanitation with hydroxide.<sup>12,13</sup> Such problems are a strong motivation for researchers to use bioengineering to create a new modified protein A that shows increased stability and loading efficiency<sup>13</sup> as well as to develop new biomimetic or peptide-mimetic affinity materials, which might make cost-effective alternatives to protein A.<sup>14–23</sup>

In affinity chromatography it is the design of the ligand headgroup that is investigated most with respect to the capture and purification of a target protein. However, the design of a new affinity material should also consider the chemical and physical properties of all its constituents, that is the base support matrix, the ligand headgroup, and the spacer-arm by which they are connected. Nonetheless, in affinity material development, constraints have to be reduced. Therefore the main focus is being set on the optimization of support properties and the actual

\* Corresponding authors. (C.C.) Tel: +39-02-23993176. Fax: +39 02 23993176. E-mail: carlo.cavallotti@polimi.it. (J.H.) Tel: +43 1 4277 52373. Fax: +43 1 42779523. E-mail: Jeannie.Horak@univie.ac.at. (S.W.) Tel: +44 (0) 1223 433844. Fax: +44 1223 420270. E-mail: SWilliams@PrometicBioSciences.com.

<sup>†</sup> Politecnico di Milano.

<sup>‡</sup> ProMetic BioSciences Ltd.

<sup>§</sup> University of Vienna.

design of new ligand head groups for protein purification, mostly neglecting entirely the possible influence spacer chemistry or the surface chemistry of the support may have on the overall material performance, although their effect on the protein binding process is already known.<sup>7</sup> In a recent study, it was shown that ligands bound to a support with spacer arms of certain length and chemical composition can in actual fact interact with the support itself.<sup>24</sup> Such interactions are influenced by the physical and chemical properties of the spacer and can lead to a conformational change of the system in which the ligand, instead of being uniformly solvated by water, can be adsorbed on the support surface.<sup>25</sup>

The spacer contribution to the protein binding process has been the subject of several research works. Mateo and co-workers have compared different activations of agarose (AG)-type supports, finding that short spacer arms can fix the relative positions of the groups involved in the immobilization and thus increase the rigidity of the bound protein, which allowed the use of certain proteins as ligands in high performance liquid chromatography.<sup>26</sup> Fuentes and co-workers proposed a different interpretation of the role of the spacer-chain. They compared the efficacy of different AG matrices in the separation of a mixture of polyclonal anti-horseradish peroxidase (HRP) using HRP as a ligand. Several protocols of immobilization of HRP were compared with the performance of HRP immobilized onto AG through a long, flexible, and hydrophilic spacer arm (dextran). It was thus found that while glyoxyl-AG, monoaminoethyl-*N*-aminoethyl-AG (MANA-AG), glutaraldehyde-AG, and the commercial BrCN-AG were able to adsorb only up to 60–70% of a mixture of polyclonal anti-HRP antibodies,<sup>27,28</sup> HRP immobilized on dextran-AG was able to adsorb 100% of the polyclonal anti-HRP. On this basis Fuentes et al. concluded that the absence of steric hindrances plays a critical role in favoring the complete recognition of all classes of polyclonal antibodies and that a long, hydrophilic, and neutral spacer can prevent the undesirable interaction both with the target protein and the macromolecular ligand.<sup>29</sup>

In this context, the main goal of the here presented study is to investigate how the choice of a particular support and spacer can influence the ligands binding efficiency. Such information may be of importance for further studies in the field of material development for affinity-based capturing of Mabs. In order to investigate the possibility to actually predict material performance in advance, our study implies and compares both experimental as well as theoretical results.

At the experimental level, several new biomimetic affinity materials were prepared, which possessed the same ligand headgroup, namely the synthetic biomimetic affinity ligand A2P, also known as MAbsorbent, but differ in the composition of the base support and the connecting spacer arm (Figure 1).

Four different spacers were investigated. The first and also the shortest spacer arm was the benchmark, the simple diaminoethyl-spacer (2LP), followed by 1,3-propanedithiol (SS3), 3,6-dioxo-1,8-octanedithiol (DES), and a 1,4-substituted [1,2,3]-triazole spacer (TRZ), formed through a copper(I) mediated Huigen 1,3 dipolare azide-alkyne cycloaddition reaction (Figure 1).<sup>30–32</sup> These ligand-spacer combinations were coupled to four different support matrices, the cross-linked AG resins, PuraBead, from ProMetic BioSciences Ltd. (AG), the two tentacle-grafted polymeric beads, the polyacrylamide Fractoprep (FP) and polymethacrylate Fractogel (FG) from Merck KGaA, and Fractosil (FS), a porous form of silica, also from Merck KGaA. These new affinity-based materials were then tested for their

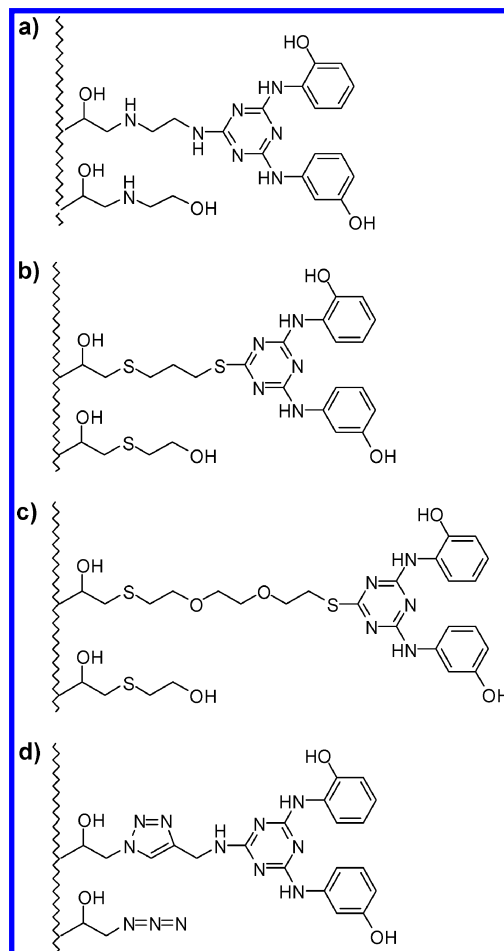


**Figure 1.** Chemical structures of A2P-type ligands with four different spacer arms and the end-capping strategy of the corresponding adsorbents (except of d): (a) A2P-2LP, (b) A2P-SS3, (c) A2P-DES, and (d) A2P-TRZ.

ability to capture IgG from a variety of mock feed solutions as well as real cell culture supernatant.

On the theoretical level, molecular dynamic (MD) and density functional theory (DFT) simulations were employed to determine the binding structure and energy of IgG with the spacer supported ligands, bound to an AG support. AG was chosen as a suitable support, since enough information is available from literature to build a reliable molecular model and it is a good model for at least one of the experimental supports, PuraBead.<sup>33,34</sup>

## 2. Experimental Section

**Affinity Materials.** The protocols for the synthesis of all investigated affinity ligands and their corresponding materials as well as details concerning support properties and protein quantification are described in the Supporting Information. A summary of epoxy, A2P and 2-mercaptoethanol densities of the investigated materials are listed in Table 1.

**Protein Standards.** Horse skeletal myoglobin (MYO), human serum albumin (HSA), and Pluronic F68 were obtained from Sigma (Poole, Dorset, U.K.). Bovine gamma globulin (BGG; 2 mg/mL) was from Pierce (Surrey, U.K.). Human polyclonal immunoglobulin G (IgG1), Sandoglobulin, was obtained from Sandoz (Hampshire, U.K.). *N*-Antiserum to human IgG and *N* protein standard PY reagent for nephelometric quantification of IgG were supplied by Siemens Healthcare (Surrey, U.K.). Cell culture supernatant containing human monoclonal antibody, h-IgG1 from CHO-cell expression system was obtained from

**TABLE 1: List of Investigated A2P-Type Materials and Their Epoxy, Azido, and A2P-Densities As Well As the Density of the Immobilized End-Capping Reagent and the Number of Residual Azido Groups**

adsorbents	epoxy density <sup>a</sup> [ $\mu\text{mol/g}$ (dry)]	azido density [ $\mu\text{mol/g}$ (dry)]	A2P density [ $\mu\text{mol/g}$ (dry)]	end-capping <sup>b</sup> [ $\mu\text{mol/g}$ (dry)]	residual azido groups [ $\mu\text{mol/g}$ (dry)]
AG-2LP-A2P	200		497	yes	
AG-SS3-A2P	200		231	0	
AG-TRZ-A2P	200	350	225	no	125
FG-2LP-A2P	1000		100/350	yes	
FG-SS3-A2P	1000		371	73	
FG-DES-A2P	1000		325	175	
FG-TRZ-A2P	1000	1126	335	no	790
FP-2LP-A2P	250		40/75/248	yes	
FP-SS3-A2P	250		330	237	
FP-DES-A2P	250		351	156	
FS-2LP-A2P	40		40	yes	

<sup>a</sup> Epoxy-densities for Fractogel (FG), Fractoprep (FP), and Fractosil (FS) are as stated by the manufacturer Merck; AG was calculated from  $\mu\text{mol/g}$  moist, suction dried gel (wet) using the corresponding correlation factors in Table S1 in the Supporting Information. <sup>b</sup> SS3-A2P and DES-A2P materials were end-capped with 2-mercaptoethanol and the end-capping efficiency determined via elemental analysis. 2LP-A2P materials were end-capped with 2-ethanolamine, but the efficiency was not determined. TRZ-A2P type materials are not azido-end-capped and the residual azido groups were determined through subtraction of the A2P-density from the originally determined azido group density on the support.

ExcellGene (Monthey, Valais Switzerland). The IgG titer of the feed was between 60 and 150 mg/L with a conductivity of 10–15 mS/cm and a pH between 6.5 and 7.5.

Three different antibody containing feed solutions were prepared and tested. The first feed solution (F1) is a mock feed of well-defined chemical composition that was designed to mimic a “real” Mab supernatant. It contains 1 g/L polyclonal IgG, 1 g/L horse skeletal myoglobin, and 5 g/L human serum albumin in PBS with pH 7.4. Alternatively 1 g/L of the antifoaming agent Pluronic F68 was added to F1. The second feed solution (F2) is a real CHO cell culture supernatant with human monoclonal IgG1. The third feed solution (F3) contains only 1 g/L of pure polyclonal IgG in PBS, pH 7.4. All feed solutions were filtered prior to use. Buffer solutions as well as cell culture feed solutions were filtered with reusable bottle top filters with 0.45  $\mu\text{m}$  nitrocellulose membranes from Fisher Scientific (Loughborough, U.K.).

The total protein concentration of the chromatography samples was determined using the Bradford Coomassie protein assay kit from Pierce, (Surrey, UK). The IgG concentration of F1 and F3 were determined using nephelometry and the IgG concentration of the cell culture supernatant F2 was determined via protein A HPLC (further details are available in the Supporting Information).

Note that all chromatographic experiments were performed in a temperature controlled environment (19–22 °C) and all buffer solutions were used at room temperature. The contribution of mass transfer effects can therefore be safely neglected, especially considering that the comparison between experiments and calculations were mostly of qualitative nature.

**Computer Modeling.** The procedure for the MD simulations used in this work is based on the experience developed in the study of similar systems and described in detail in our previous publications and in part in the Supporting Information.<sup>24,35</sup> Briefly, the molecular model of the chromatographic system here comprises four parts: the antibody, the affinity ligand, the spacer, and the support. These latter three components are covalently bound and form the stationary phase and can all interact with the protein through polar and apolar interactions.

The antibody was modeled as the full Fc domain of a human IgG. Its initial coordinates were obtained from the Protein Data Bank (PDB) entry 1HZH,<sup>2</sup> which reports the full structure of the antibody including the two Fab domains. However, the latter

were not considered in the MD simulations to reduce the size of the system. This approximation is justified by the fact that the ligand was designed to specifically interact with the Fc binding site of immunoglobulin G, which is that part of the molecule most directly involved in the adsorption process.

As mentioned, the ligand benchmark in this study is the synthetic affinity ligand A2P, while four different spacers (2LP, DES, SS3, and TRZ) were considered in the calculations.

AG, which is a good model for the PuraBead support matrix, was adopted as model of the support material. The basic structure of AG is well-defined: it consists of long fibres of alternated D-galactose and 3,6-anhydro-L-galactose units organized in double helixes, as can be noted from the crystallographic data (PDB entry 1AGA).<sup>36</sup> The AG crystal structure was used to build three molecular models of AG, which were successively used in the calculations. The first is the one reported in Figure S2a and was developed and adopted in our previous studies of the system.<sup>24</sup> To evaluate the effect that the density of hydrophobic groups on the support surface may have on the binding process, a second model was introduced. The AG surface was partially modified by substituting some of the D-galactose residues with 6-O-methyl-galactose residues, thus making it more hydrophobic with respect to AG. Only residues oriented toward the protein were substituted in order not to reduce the stability of the support by altering the structure of its helixes (Figure S2b). The third model of AG, sketched in Figure 2, consists of three sets of parallel double helixes and is thus three times larger than the model of Figure S2. It was used to test whether the calculations are converged with respect to the AG molecular model size.

The conformational evolution of the IgG-ligand-spacer-support system was investigated using molecular dynamics simulations. The force field adopted for the AG support was Glycam 04,<sup>37–40</sup> developed to study the interaction of carbohydrates with proteins, which was modified to include 3,6-anhydro-L-galactose and 6-O-methyl-D-galactose residues.<sup>24</sup> Spacers, ligands, and the protein were modeled with the Parm 94 force field,<sup>41</sup> supplied in the Amber suite.<sup>42,43</sup>

The input structures of the ligand-IgG complex were determined via docking, using AutoDock 3.0;<sup>44</sup> subsequently the complex was bound to the support and solvated using explicit TIP3P water molecules adding a solvent shell of 20 Å. The simulations were performed using periodic boundary conditions,



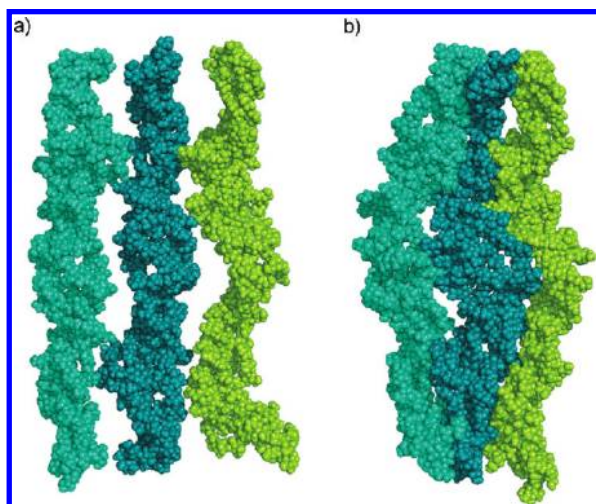


**Figure 2.** Structure of the molecular model consisting of three sets of intertwined double helices at the beginning of the simulations (a) and after relaxing the system for 10 ns in water (b).

according to which the system is divided in unit cells of equal size, calculating long-range electrostatic interactions using the particle mesh Ewald method.<sup>43</sup>

The computational protocol adopted for the MD simulations is described in detail in our previous papers<sup>24,35</sup> and in the Supporting Information.

The energetic analysis of the simulations was performed calculating the difference of the interactions developed by the ligand with its surrounding environment in its “bound” (i.e., the ligand in complex with the protein) and its “free” state (i.e., the ligand not bound to its receptor). Whereas in the here-examined system the surrounding environment of the bound ligand includes the solvent, antibody, and support matrix, in the free state, it consists of support and water molecules. Thus, two different MD simulations were performed for each system: the first for the support–spacer–ligand–Fc complex (15 ns) and the second for the supported ligand alone (support–spacer–ligand). In the latter case, the simulation protocol was analogous to the one used for the complex but a shorter time span (3 ns) was considered, as this was sufficient to stabilize the system. Interaction energies were determined with the Anal. program of the Amber 8 computational suite; their medium values for the bound state were averaged on a time span of 1 ns, whereas for the free state they were averaged on all the 3 ns of the simulation.

Finally, in order to investigate what determines the significant effect that Pluronic acid has on IgG adsorption, in particular when the spacer arm changes, some additional simulations were performed using simplified molecular models of Pluronic acid and ligand. Structures were determined with the integral equation formalism polarized continuum model (IEFPCM) at the B3LYP/6-31 g(d,p) level, while energies were calculated at the B3LYP/aug-cc-pVDZ level.

MD and *ab initio* simulations were performed using the Amber 8 computational suite<sup>42</sup> and Gaussian 03,<sup>45</sup> respectively; all structures reported in this work were produced using Molden 4.4,<sup>46</sup> VMD 1.8.2,<sup>47</sup> and Pymol.<sup>48</sup>

### 3. Results and Discussion

The synthetic biomimetic affinity ligand investigated in this study is a disubstituted aminophenol derivative of trichlorotriazine, named A2P. It was discovered by ProMetic BioSciences Ltd. (PBL) through a Chemical Combinatorial Library for

compounds active in the binding of polyclonal IgG. In combination with PBL’s own proprietary base matrix PuraBead, an AG-based support, A2P is also known as MAbsorbent A2P. A2P is a well characterized affinity ligand,<sup>22,49,50</sup> making it a suitable candidate for our elaborate biochromatographic and computer simulation studies. It was designed for human and humanized antibodies and mimics the dipeptide binding site of Phe 132 and Tyr 133 in the hydrophobic core structure of protein A,<sup>19</sup> which plays an important role in the formation of a binary complex between A2P and the Fc-domain of IgG. A2P possesses an affinity (dissociation constant) for human and humanized IgG of approximately  $1 \times 10^{-4}$  M and provides binding capacities of 15–25 g/L for polyclonal IgG from mammalian plasma with purities of >85 and 95% respectively.<sup>22</sup> In validation studies using monoclonal and polyclonal IgG sources, no A2P–ligand leakage has been detected after 300 process cycles and IgG product integrity was always maintained.

In this study, the influence of support chemistry and spacer chemistry on the overall performance of a number of different new affinity materials with A2P as the main ligand motive will be discussed. They all carry the same A2P ligand headgroup but possess different spacer arms. The benchmark has a simple amino linkage (2LP) with the formula  $\text{CH}_2\text{—CHOH—CH}_2\text{—NH—(CH}_2\text{)}_2\text{—NH—}$  (Figure 1a). To test the effect of spacer composition and flexibility, two thiophilic spacers differing in their chemical composition as well as length were investigated, the SS3 spacer,  $\text{CH}_2\text{—CHOH—CH}_2\text{—S—(CH}_2\text{)}_3\text{—S—}$  (Figure 1b), and the DES spacer,  $\text{CH}_2\text{—CHOH—CH}_2\text{—S—(CH}_2\text{)}_2\text{—O—(CH}_2\text{)}_2\text{—O—(CH}_2\text{)}_2\text{—S—}$  (Figure 1c). The fourth spacer arm contains a 1,4-substituted [1,2,3]-triazole ring,  $\text{CH}_2\text{—CHOH—CH}_2\text{—(C}_6\text{H}_3\text{N}_3\text{)—CH}_2\text{—NH—}$ , and will be referred to as TRZ (Figure 1d).

In the following sections, we will first discuss the outcome of the experimental affinity-chromatographic measurements, followed by a summary of material performance evaluation obtained by molecular dynamics simulations. In the final stage, we will then try to correlate the experimentally obtained results with the predictions obtained by computer simulation experiments.

**Experimental Results. Affinity-Chromatography.** Dynamic binding capacities (10%-DBC; BC) and elution recoveries (EC) for IgG on A2P bound by three different spacer arms to three different support matrixes were determined for the three different feed solutions: F1, F2, and F3. The performance of each combination of ligand, spacer arm, and support material was investigated chromatographically using the mock feed F1, which contains polyclonal IgG, myoglobin, and human serum albumin. Since Pluronic F68 is known to affect the separation process performance of certain affinity ligands due to an interaction with the ligand, additional measurements with 1 g/L of Pluronic F68 added to F1 were performed. In order to determine a possible cross-sensitivity of the investigated materials to proteins other than IgG, the concentration of HSA in the elution fractions was determined by nephelometry. The concentration of myoglobin, although also present in the feed F1, was not determined. Nonetheless, one has to consider that any additional binding of proteins other than IgG or any other compound present in the application feed will eventually reduce the overall binding capacity of the material for the target protein, IgG.

The results for the mock feed solution F1 and A2P-type materials in comparison to rmp protein A Sepharose FF are summarized in Table S2. It is clearly shown that, even for this simple mock feed solution (F1), all investigated A2P-type materials differ strongly in their performance. Binding as well as elution capacities vary depending not only on the ligand

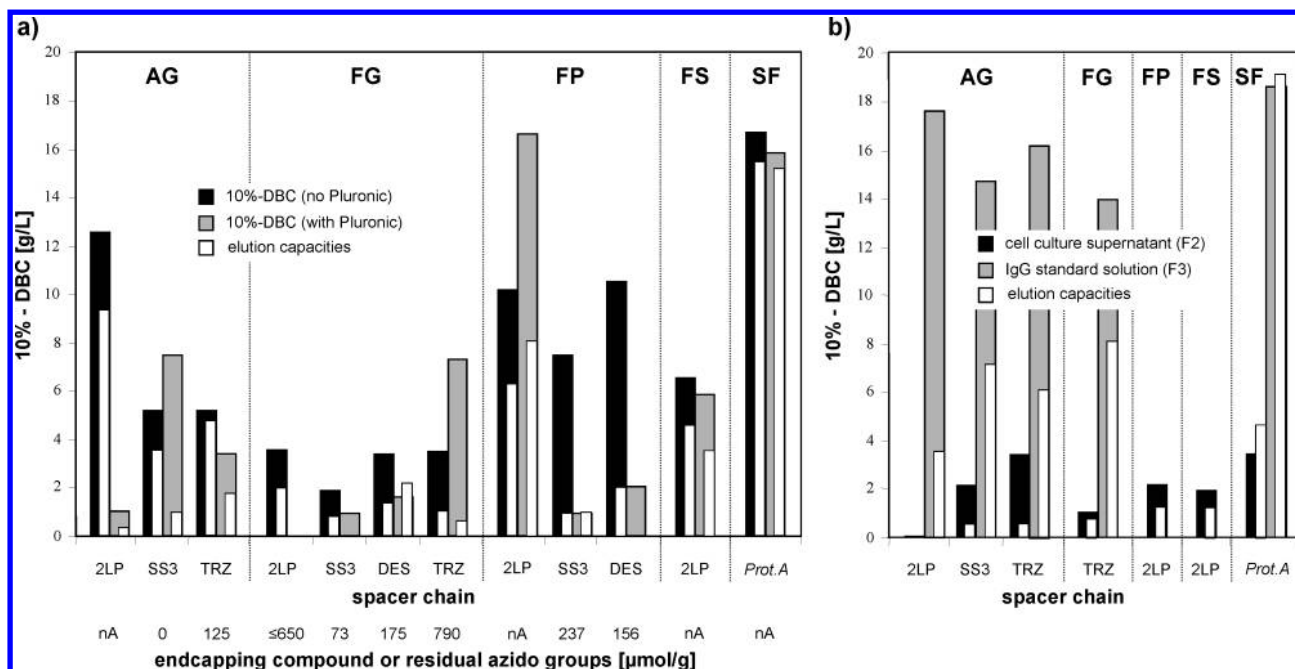


**Figure 3.** Material performance evaluation of A2P-type purification media investigated with (a) mock feed solution (F1) containing 1 g/L polyclonal human IgG, 1 g/L myoglobin, and 5 g/L human serum albumin with optional addition of Pluronic F68 and (b) cell culture supernatant (F2) containing 60–150 mg/L human monoclonal IgG1 plus 1 g/L sodium azide and approximately 1 g/L Pluronic F68 with a pH ranging from 6.5 to 7.5 (batch dependent) and a standard solution of polyclonal IgG in PBS buffer with pH 7.4 (F3). Support media are abbreviated as AG for AG, FG for Fractogel, FP for Fractoprep, FS for Fractosil, and SF for the rmp-protein A Sepharose FF.

density of A2P, where DBC values decrease with declining A2P-densities, but also strongly on the choice of spacer and support matrix. Surprisingly, the elution capacities are mostly lower than the corresponding binding capacities but are in some cases practically the same as it is the case for AG-TRZ-A2P using F1 without Pluronic acid, and FP3-2LP-A2P and FG-DES-A2P using F1 with Pluronic acid. Also the sensitivity of the materials toward the presence of Pluronic F68 in the test solution is differing with the change in spacer and support chemistry. Note that some materials such as FP1-2LP-A2P actually perform better in the presence of Pluronic F68. A2P-type materials with the least sensitivity toward Pluronic F68 addition are FP1-2LP-A2P with a binding capacity of 16.6 g/L, AG-SS3-A2P with 7.45 g/L, and FP3-2LP-A2P with 4.9 g/L, with only the latter providing practically same binding and elution recoveries for IgG.

Generally speaking, AG-2LP-A2P possesses the highest BC and EC values, with 12.6 and 9.4 g/L for F1 without Pluronic F68, whereas FP1-2LP-A2P performs best in the absence (BC 10.2 g/L and EC 6.4 g/L) as well as in the presence of Pluronic F68 (BC 16.6 g/L and EC 8.1 g/L).

The thiophilic A2P ligand SS3 shows a very low affinity for IgG in the presence of Pluronic F68. However in the absence of Pluronic F68, a change of support, from Fractogel to Fractoprep, provided an almost 4-fold increase in the DBC for A2P-SS3 from 1.9 g/L to 7.5 g/L. The same tendency was observed for A2P-DES and A2P-2LP, where a change of support from Fractogel to Fractoprep provided a 3-fold increase in DBC from 3.4 to 10.5 g/L and from 3.6 to 10.2 g/L, respectively.

The performance of the different A2P-type materials for the capture of IgG from feed solution F1, from a cell culture solution F2 and a standard solution of polyclonal IgG, is compared graphically in Figure 3. This plot shows clearly that material performance can not be deduced by the performance of the ligand headgroup per se but that a more or less strong fine-tuning of material performance can be achieved by introducing

another spacer-arm or another support. The Fractogel sector in Figure 3a shows that, on Fractogel-type supports, the binding capacity does not vary strongly in the absence of Pluronic F68.

However, as soon as Pluronic acid is present, binding capacities for IgG become highly spacer dependent and increase in the order of spacers used: 2LP, SS3, DES, and TRZ, with no binding for the 2LP spacer, which is surprising, since the corresponding Fractoprep material FP1-2LP-A2P performs best in the presence of Pluronic F68. For AG-based supports, the introduction of the spacer arms SS3 and TRZ reduces IgG binding in the absence of Pluronic F68, but on the contrary, increases IgG binding in the presence of Pluronic F68 for AG-SS3-A2P. Here the SS3-spacer performs best, followed by the TRZ-spacer. This result for AG suggests that the addition of a thiophilic spacer arm reduces the negative impact of Pluronic F68 on the AG adsorbent and the A2P ligand. The strongest Pluronic-dependency in terms of reduced BC values in the presence of Pluronic F68 was observed for AG-2LP-A2P, FG-2LP-A2P as well as FP-SS3-A2P and FP-DES-A2P, whereas FS-2LP-A2P was least influenced.

The best performing support-spacer combinations in terms of binding capacity for IgG and Pluronic F68 sensitivity are AG-2LP, FP1-2LP, FP1-DES, AG-SS3, AG-TRZ, FG-TRZ, and FS-2LP, which were selected for further testing with real cell supernatant (F2) as well as standard IgG solution without Pluronic F68 (F3) to determine their maximum achievable binding performance for IgG without competitive protein adsorption. The results for F2 and F3 are shown in Table S3.

Figure 3b (Table S3) demonstrates clearly the biggest difference in performance. While F3 is a typical standard protein solution of polyclonal IgG in PBS (pH 7.5) without any additives, F2 resembles a real cell culture solution of a CHO-cell expression system and, as expected, the mock feed F1 in Figure 3a (Table S2) provides BC and EC values that lie in all cases between those obtained for the feed solutions F2 and F3. Highest binding capacities for IgG using the feed F3 were

obtained for the following support-spacer combinations in declining order AG-2LP-A2P > AG-TRZ-A2P > AG-SS3-A2P > FG-TRZ-A2P, though BC values only vary slightly between 14 g/L and 17.7 g/L.

On the other hand, for the cell culture solution, the binding capacities for IgG were all rather low between 1.1 g/L and 3.5 g/L. The latter was obtained for AG-TRZ, followed by AG-SS3, FP1-2LP, FS-2LP, and FG-TRZ. The significant reduction of binding capacity of IgG from 10.2 to 2.1 g/L for FP1-2LP-A2P may be explainable by the fact that this support-spacer combination binds the most feed impurities from the cell culture feed. However the least difference in binding capacity for F1 as well as for F3, with and without Pluronic F68, was observed for affinity material AG-TRZ-A2P.

Generally speaking, the results in Figure 3b (Table S3) indicate that when using a short and charged spacer arm, such as 2LP, A2P on AG-based support does not bind IgG from the cell culture supernatant. However, when a spacer arm differing significantly in length and chemical composition is introduced, either DES or TRZ, the binding capacity increases significantly. The AG-TRZ-A2P adsorbent has a similar IgG binding performance as observed for the commercially available adsorbent Rmp protein A Sepharose FF. It is worth noting that the DBC values for all of the adsorbents investigated are rather low at below 4 g/L h-IgG1, which is most likely induced by the low IgG titer of below 100 mg/L in the cell culture solution plus the more or less strong binding of feed impurities, which definitely reduces the binding capacity of the materials for IgG. This effect is most pronounced for FP1-2LP-A2P, where BC was reduced from 10.2 g/L for F1 (no Pluronic acid) to 2.1 g/L IgG for F2 (with Pluronic acid) at a BC for the feed impurities of 3.5 g/L.

Note that all investigated materials with a 2LP-spacer were end-capped by reacting the remaining epoxy-groups with ethanolamine and all materials with SS3 and DES spacers were modified with 2-mercaptoethanol. In a separate study we have shown that a deactivation of residual, still reactive epoxy or azido groups on the support surface as well as the choice of end-capping reagent to deactivate them after ligand immobilization can have a tremendous impact on the overall material performance.<sup>51</sup> In actual fact the introduction of additional amino-groups by using ethanolamine may lead to mixed-mode type affinity materials, where the underlying support chemistry functions as a weak anion exchanger binding feed impurities and thereby reduces the BC of the material for IgG. In case of the affinity materials with a TRZ-spacer, the here-investigated materials are all nonazido end-capped, meaning that residual azido groups are present on the material surface, which are prone to capture IgG but provide low recoveries of the latter.<sup>51</sup>

Additionally it should be noted that different batches of cell culture supernatant were used to test the various affinity-materials, since they were prepared and tested over a period of 2–3 years. The variations in binding and elution capacities of these investigated materials can be explained through the variation in the feed impurity composition from the various production batches of the CHO cell expression system (Figure 4a, lane 1 and Figure 4b, lane 1). Taking all of this into account, one should consider that most material manufacturers frequently state the protein binding performance of their materials only for standard protein solutions, which as we have seen will most likely not correlate with the actual material performance for real sample solutions.

Another way to characterize materials is to simply distribute the proteins by their molecular weight on slab gels. The SDS-

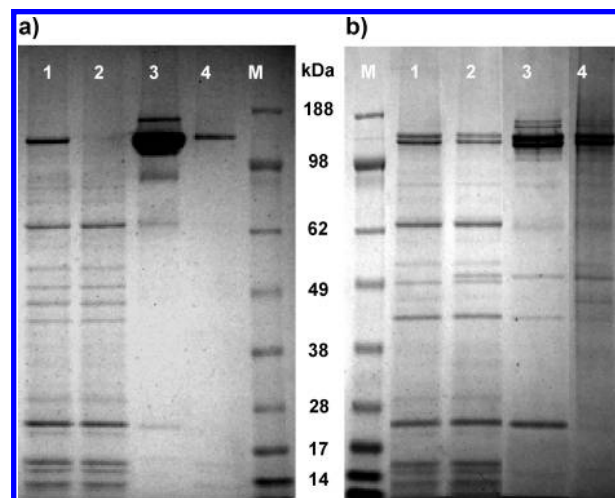


**Figure 4.** Nonreduced SDS-PAGE slab gels of affinity chromatographic fractions of (a) rmp-protein A Sepharose FF and (b) AG-TRZ-A2P tested with cell culture supernatant (F2), showing the feed loading (lane 1), feed flow-through (lane 2), IgG elution (lane 3), and the cleaning-in-place fraction (lane 4). Lane M shows the molecular weight marker.

PAGE gel in Figure 4b indicates that the presence of the TRZ spacer does improve the performance of the benchmark AG-2LP-A2P as there is significant capture and purification of IgG from the F2 feed solution. This confirms that the addition of a spacer arm increases the Pluronic F68 tolerance of the A2P ligand, as AG-2LP-A2P does not bind IgG from cell culture solution that contains Pluronic F68.

In addition to improving the binding capacity of AG-2LP-A2P with the addition of spacer chemistries, it is also important to consider the effect of the spacer arm on the purity of the eluted IgG. Figure 4a shows the SDS-PAGE gel for the commercial benchmark adsorbent rmp protein A Sepharose FF. If the purity of the elution fractions in lane 3 from Figure 4, panels a and b, are compared, a pronounced feed impurity band appears at ~25 kDa for the AG-TRZ-A2P, which is less distinct for rmp-protein A Sepharose FF. This band may be excess light chain, which is already present in the feed solution, but may just as well be an unidentified feed impurity. Overall, it can be stated that Protein A binds more of the high molecular weight (MW) impurities compared to AG-TRZ-A2P, which binds more of the low MW impurities. It is noteworthy that the elution conditions for AG-TRZ-A2P have not been optimized for this cell culture feed. Furthermore the ligand immobilization concept via “click reaction” was at this point of our study not yet fully optimized. Nonetheless, the experimental results show clearly that in terms of both binding capacity and purity the incorporation of the TRZ spacer instead of the benchmark 2LP has produced an affinity adsorbent with much improved IgG capture performance, although its elution performance still needs to be optimized.

**Influence of Pluronic F68 on Material Performance.** In order to investigate why and how Pluronic F68 is influencing the IgG binding performance of the A2P type materials, AG-2LP-A2P was tested with mock feed F3 under three different conditions, namely without addition of Pluronic F68 (A), with 1 g/L Pluronic F68 (B), and without Pluronic F68 in the feed, but with a pretreatment of the adsorbent with 1 g/L Pluronic F68 in PBS, pH 7.4 (C). Besides that, these experiments were performed in the same manner as previously described for the testing of A2P-type support materials. However, the new additional test conditions A, B, and C should verify which of



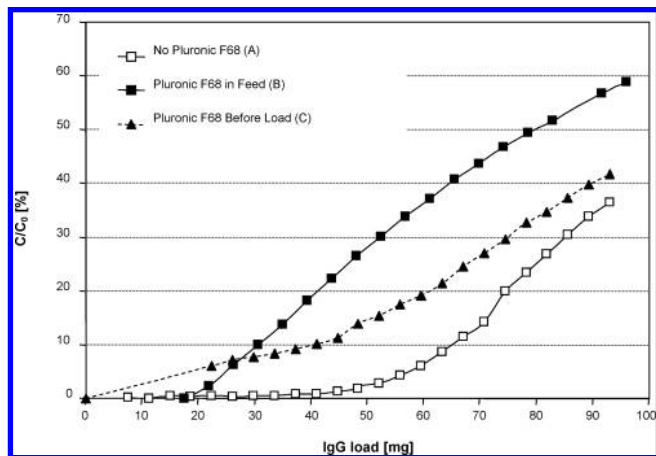


**Figure 5.** Break-through curve of IgG on AG-2LP-A2P tested under different conditions: (A) without addition of Pluronic F68 in the application feed, (B) with addition of 1 g/L Pluronic F68, and (C) with a material that was pre-equilibrated with PBS containing 1 g/L Pluronic F68 before addition of an application feed only containing 1 g/L IgG.

the three following hypotheses apply for AG-based A2P-type materials: first, if Pluronic F68 may interact with the IgG molecule and hinder thereby the binding to the surface bound A2P-ligand; second, if Pluronic F68 may interact with the A2P-ligand on the adsorbent surface; or third, if Pluronic F68 can actually form a complex with the AG-based matrix of the adsorbent and provide some kind of sterical hindrance preventing the IgG molecules binding to the A2P-ligand.

The breakthrough curves in Figure 5 show that for condition A a binding capacity, at 5%-DBC of 13 mg/mL adsorbent was obtained, which is more than 50% higher than for either of the two other conditions, where a 5%-DBC of 6 and 5 mg/mL were observed for conditions B and C, respectively. When Pluronic F-68 is loaded onto the material before the IgG containing feed was applied (condition C), a very early, almost immediate but shallow breakthrough of IgG was observed. It may be proposed that the binding of Pluronic F68 to AG is rather weak in nature and that due to the lack of Pluronic F68 in the application feed, some of the surface-attached Pluronic F68 molecules are being gradually washed off the surface, reducing thereby the concentration of Pluronic F68 on the material surface and increasing at the same time the binding capacity of the material for IgG. In case of condition (B), where both IgG as well as Pluronic F68 are present in the feed, the material binds first IgG and second Pluronic F68. It can be assumed that as more and more Pluronic F68 molecules attach to the surface, less IgG can bind to the A2P ligand.

The fact that Pluronic F68 affects the column both when loaded with IgG and when loaded prior to IgG clearly demonstrates that, rather than binding to the IgG molecule, Pluronic F68 is interacting with the adsorbent. Furthermore the results for A2P-2LP type ligands bound to different type of supports in Figure 3 show clearly that Pluronic-sensitivity of material performance is highly dependent on the chemistry of the support. It was observed that AG is being strongly influenced by the presence of Pluronic F68, followed by the polyacrylate-based Fractogel, the polyacrylamide-based Frac-toprep and the silica-based Fractosil, of which the latter provide the most consistent results for IgG capture and elution in the presence as well as absence of Pluronic F68.

In additional experiments (data not shown), it was verified that Pluronic F68 does not desorb or replace IgG once it is

securely bound to A2P. Furthermore it was found that an increase in spacer-length as well as an introduction of a specific surface-modification, through the change of chemical properties or by introduction of a physical barrier to prevent the attachment of Pluronic F68 to the support surface, can make A2P-type materials less sensitive to the presence of Pluronic F68 in the application feed.

**Molecular Dynamics Simulations. Determination of the Protein–Ligand Binding Structures: Docking.** The theoretical determination of the binding structure of a ligand with a large protein such as IgG is a complicated task. The problem is however slightly simplified if the favored binding sites of the protein of interest are already known. In the case of IgG, it is well-known that the Fc domain has a specific part of the surface that is usually directly involved in the formation of bonds with other proteins; this part is located at the hinge region between CH2 and CH3 domains and known as the “consensus binding site” (CBS). For these reasons the CBS has been the subject of many studies in the literature. Delano et al.<sup>25</sup> compared this site with several patches of the IgG surface similar in size, according to different criteria including hydrophobicity and accessible surface area, and observed that it presents a prevalent non polar nature, a high tendency to form H bonds and an elevated solvent accessibility. These features alone, however, cannot explain its predisposition for binding, since they are common to other patches and in particular to a larger region of the Fc domain comprising the consensus site. What discriminates the binding site is its high flexibility, distinctive of hinge regions, which provides the CBS with a significant conformational mobility and the possibility to adapt easily to different ligands.

The structure of the complex formed by IgG and A2P was determined through docking simulations focused on the CBS area. The adopted procedure was analogous to the one introduced for the system with the DES spacer<sup>35</sup> and is here briefly summarized. The protein surface was docked considering the ligand already bound to the spacer, to account for the steric hindrance of the AG chains that are to be bound to the spacer when the initial structure of the MD simulations is set up. However, a different flexibility was defined for two molecules: the sp<sup>3</sup> bonds of A2P were left free to rotate, while none of the bonds of the spacer were rotatable. The search box was centered on the CBS and large enough to allow the spacer–A2P pair to rotate freely; it consisted of a grid of 60 × 60 × 60 points with a spacing of 0.375 Å. Docking was carried out holding the Fc domain fixed and letting the ligand move over its surface; for each spacer–A2P pair about 50 poses were evaluated using a Lamarckian genetic algorithm.<sup>44</sup> The optimal pose is characterized by having the A2P–spacer pair located in the consensus binding site, the spacer turned toward the solvent, facing thereby the binding AG, and provided hence the minimum energy. Docking energies of the best 15 poses for each spacer–A2P pair are summarized in the Supporting Information. For the DES, SS3, and TRZ spacers, the first pose was chosen for the MD simulations, as it satisfied all of the requirements described above. For the 2LP spacer, instead, the 12th pose was considered since in the ones with higher interaction energy the spacer tended to align along the protein surface. The selected poses are very similar and indicate that the formation of the complex between A2P and IgG involves some specific residues of the antibody, which can be subdivided in three groups: HIS-310, GLN-311, and LEU 314 is the first, MET-428, ASN-434, and HIS-435 the second, and ILE-253 and SER-254 the third (Figure 6a). It can be noted that these are the same residues involved in the interaction of IgG with several natural and synthetic ligands.<sup>25</sup>

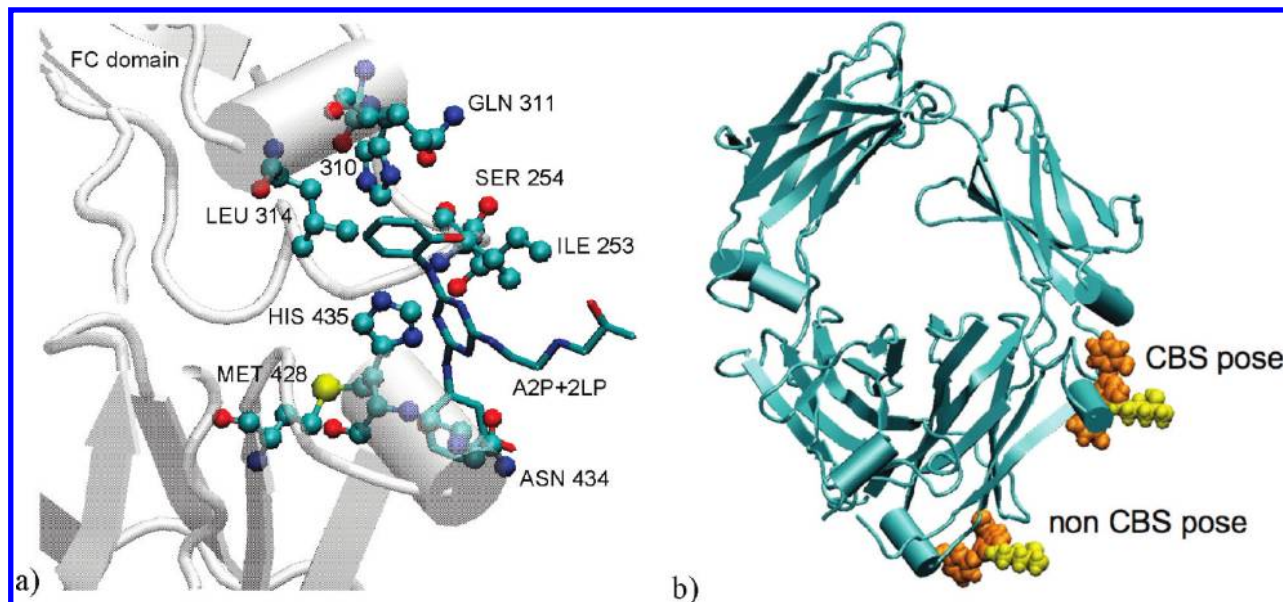


**Figure 6.** (a) Detail of the docking pose of the 2LP–A2P pair in the CBS; (b) comparison between the CBS and the non CBS pose.

This evidence is not surprising as A2P was specifically designed to mimic the interactions of the PHE 132–TYR 133 pair of protein A with IgG. It seems likely that also the spacer contributes to the interaction, as shown by the different docking energies of the A2P–spacer pairs.

To fully understand the properties of the consensus binding site, a system in which the initial pose of the ligand is not in the CBS was considered. For this investigation the 2LP spacer was chosen and also in this case the initial structure of the system was determined through docking. No significant differences in the docking energies of the CBS and non CBS complexes can be noted. In the chosen non CBS pose, sketched in Figure 6a, A2P is interacting with residues from SER-384 to GLU-389 and from ARG-417 to TRP-424 of one of the CH3 chains of the Fc domain.

**Analysis of the Interaction between IgG and A2P Supported on AG.** The conformational evolution of the complex consisting of full Fc domain, A2P, spacer, and AG was studied using 15 ns MD simulations. The A2P-DES complex was described in a previous publication, in which the effect of the interaction between ligand and support on the binding process was discussed.<sup>35</sup> In the present work, three new spacers (2LP, TRZ, and SS3) were introduced to investigate their influence on the conformational and energetic evolution of the complex.

The conformational analysis of the MD simulations shows that, as found for DES,<sup>35</sup> also when other spacers are used A2P has a certain mobility within the binding site. However in the investigated time span the ligand never leaves the CBS, thus confirming the stability of this binding structure. The simulated complexes exhibit a similar dynamic behavior in the investigated time span. The first nanoseconds of the simulation are characterized by the approach of the Fc domain to the support and the establishment of some interactions between the two macromolecules. The partial adsorption of the antibody on AG leads to a small reorganization of its structure, which is accompanied by a distortion of the spacer that abandons its initial elongated structure and partially folds on itself, probably to favor the establishment of an energetically preferred orientation between protein and AG. This is observed even in the case of 2LP, which is the shortest among the considered spacers. The initial and final structures assumed by the complexes are reported as Supporting Information.

The evolution of van der Waals and electrostatic interactions throughout the MD simulations is reported for all spacers in Figure 7. It can be noted that each system generally reaches an energetically stable configuration within the first 5 ns of simulation, after which only minor fluctuations are observed. An exception to this trend is given by A2P-2LP. In fact, though its average interaction energy, defined as sum of electrostatic and van der Waals terms, is constant between 5 and 12 ns, it oscillates significantly toward the end of the simulation. The analysis of the system structural evolution revealed that the energy oscillation can be attributed to a transient reorganization of A2P-2LP in the binding site, which leads to a temporary loss of electrostatic interactions of the spacer with the surrounding environment. Such oscillation, of statistical nature and determined by the high A2P-2LP mobility, leads to a slight decrease of the A2P interaction energy with IgG. It is not unlikely that the continuation of the simulations for a longer time span would smooth down this energy oscillation. The energy plots reported in Figure 7 give a first indication on the relative performances of the spacers, according to which TRZ has the highest interaction energy, followed by 2LP, DES, and SS3, which interaction energy is slightly positive.

To investigate in greater detail the influence of the spacer on the interaction of the ligand with both the support and the antibody, average interaction energies of the spacer-A2P pair with the surrounding environment in the free (i.e., when only the water surrounds the AG–spacer–A2P system) and bound state (i.e., when the ligand is in a complex with the antibody) were calculated and are reported in Table 2. For all systems the establishment of binding interactions between ligand and antibody is determined mostly by van der Waals forces, as expected for molecules designed to have a high affinity for a hydrophobic receptor. It is interesting to notice that the systems in which  $\Delta V_{\text{free} \rightarrow \text{bound}}^{\text{dw}}$  is the lowest (about  $-20$  kcal/mol) are those with the TRZ and SS3 spacers; however, the van der Waals interaction energy is mostly counterbalanced by the loss of electrostatic interactions. As previously observed for the system with the DES spacer,<sup>35</sup> it can be noted that for all spacers except TRZ, the formation of significant interactions between the ligand and the AG support leads to the most pronounced hindrance in the interaction of A2P with the antibody. The system with the TRZ spacer is the only one in which, in the

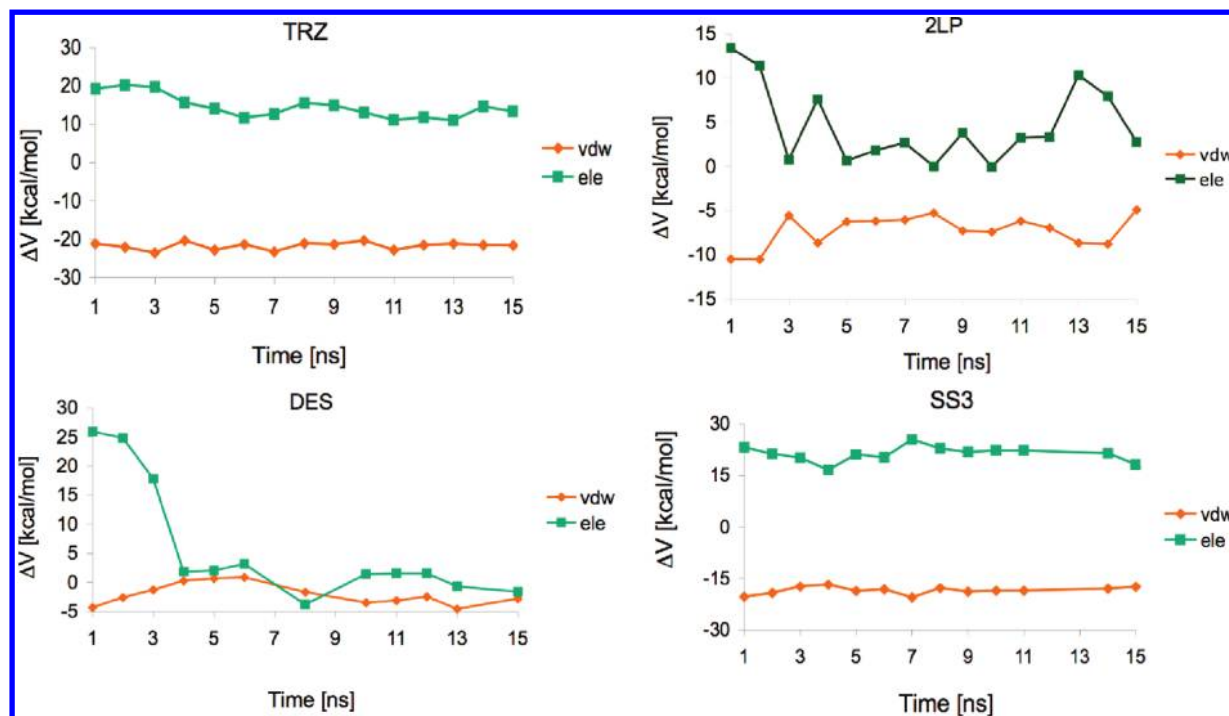


**Figure 7.** Electrostatic (ele) and van der Waals (vdw) interaction energies between immobilized A2P ligand and IgG evaluated as a function of simulations time and averaged on time spans of 1 ns.

**TABLE 2: Electrostatic (ele) and van der Waals (vdw) Average Interaction Energies Evaluated in the 5–15 ns Time Span for the Spacer–A2P Pair Supported on AG with the Initial Pose in the CBS**

		2LP	DES	TRZ	SS3
Free System (Support–Spacer–A2P)					
H <sub>2</sub> O <sup>a</sup>	vdw	−23.94	−27.76	−29.90	−28.20
	ele	−78.66	−87.96	−87.93	−75.74
support	vdw	−17.67	−29.93	−7.12	−12.07
	ele	−16.71	−16.51	1.98	−8.01
Bound System (Support–Spacer–A2P–Fc)					
H <sub>2</sub> O + FC	vdw	−46.29	−55.79	−50.44	−56.77
	ele	−85.82	−102.12	−72.21	−63.43
support	vdw	−2.06	−3.93	−8.47	−1.99
	ele	−6.30	−1.88	0.58	1.38
ΔV (Bound − Free)					
H <sub>2</sub> O + FC	vdw	−22.35	−28.03	−20.54	−28.57
	ele	−7.16	−14.15	15.72	12.32
support	vdw	15.61	26.00	−1.35	10.07
	ele	10.42	14.63	−1.40	9.39
Total ΔV					
H <sub>2</sub> O + FC + support	vdw	−6.70	−2.03	−21.89	−18.50
	ele	3.32	0.48	14.32	21.71

<sup>a</sup> The first column reports the contribution of the surrounding environment (H<sub>2</sub>O, Fc, and support) considered to evaluate the interaction of the spacer–A2P pair.

free state, the ligand does not strongly interact with AG. The simulations have in fact evidenced that it continuously shifts from the solvated to the adsorbed conformation. On the contrary, when the 2LP, SS3 and DES spacers were adopted it was found that A2P, when IgG is not present, is predominantly adsorbed on the support. This analysis leads to the conclusion that, from an energetic standpoint, the best performing spacers are either those with a relatively high length and flexibility (DES, TRZ) or those that possess some electrostatic groups that can contribute to increase the electrostatic interaction energy with the protein (2LP, TRZ). TRZ, the spacer that emerged from

the experiments as that with the best performances, is the only one that satisfies both requirements.

In order to test whether the size of the AG molecular model could affect the results of the simulations, additional calculations were performed adopting an enlarged AG molecular model developed following the procedure described in the method section. The molecular structure reached by the system after 10 ns of simulations is sketched in Figure 8. The structure so determined is qualitatively similar to that calculated employing the smaller AG molecular model, reported in Figure S2, thus giving a first confirmation of the reliability of the adopted computational procedure. A second, and more important confirmation comes from the calculation of the interaction energies between A2P and IgG, reported as Figure S5, which shows that the energy determined for the model implementing the large molecular surface is similar to the one calculated adopting the smaller, and computationally more tractable, AG molecular model.

**Analysis of the Interaction between IgG and A2P for a Non-CBS Binding Site.** The molecular systems described in the previous paragraph was adopted as initial structure for the MD simulation of a docking pose in which the A2P molecule is interacting with the main binding site of the Fc domain of IgG: the CBS. However other binding sites, different from the CBS, were identified in the docking analysis. The purpose of this section is therefore to study the interactions developed between IgG and A2P for a binding site different from the CBS. The ligand-spacer system chosen to perform this analysis is A2P-2LP, i.e. the experimental benchmark. The starting structure for the simulations was determined by docking and involves an interaction site located on one of the CH3 chains of the Fc domain of IgG.

The final conformation reached by the system after 15 ns of simulation is shown in Figure 9. From a macroscopic viewpoint, the structure of Figure 9 is similar to that reached in the simulations performed for the CBS binding site, in which the antibody partially interacts with AG through one of its CH



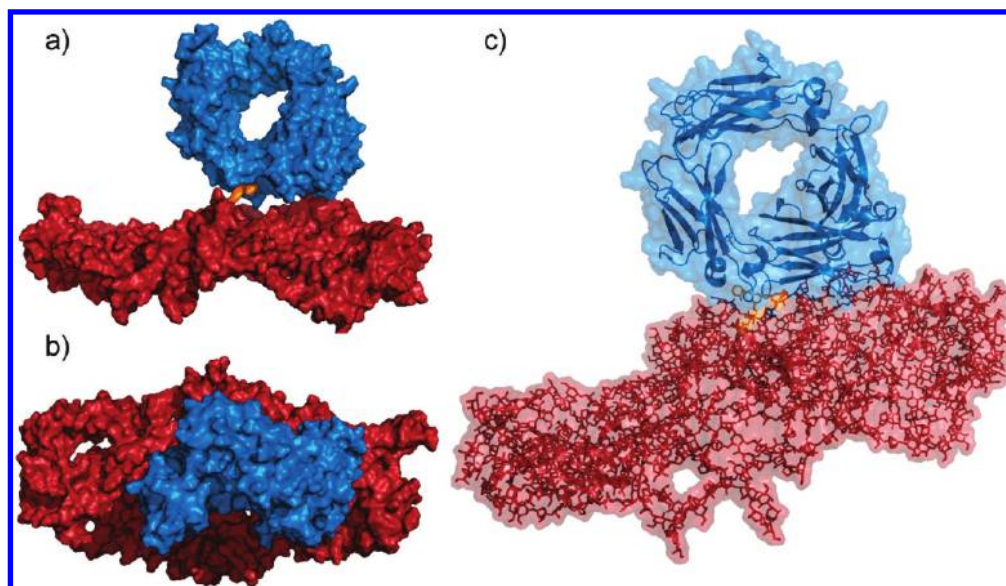


**Figure 8.** Structure reached by the A2P-2LP-AG model after 10 ns of simulation: (a) front, (b) top, and (c) three-quarter views.

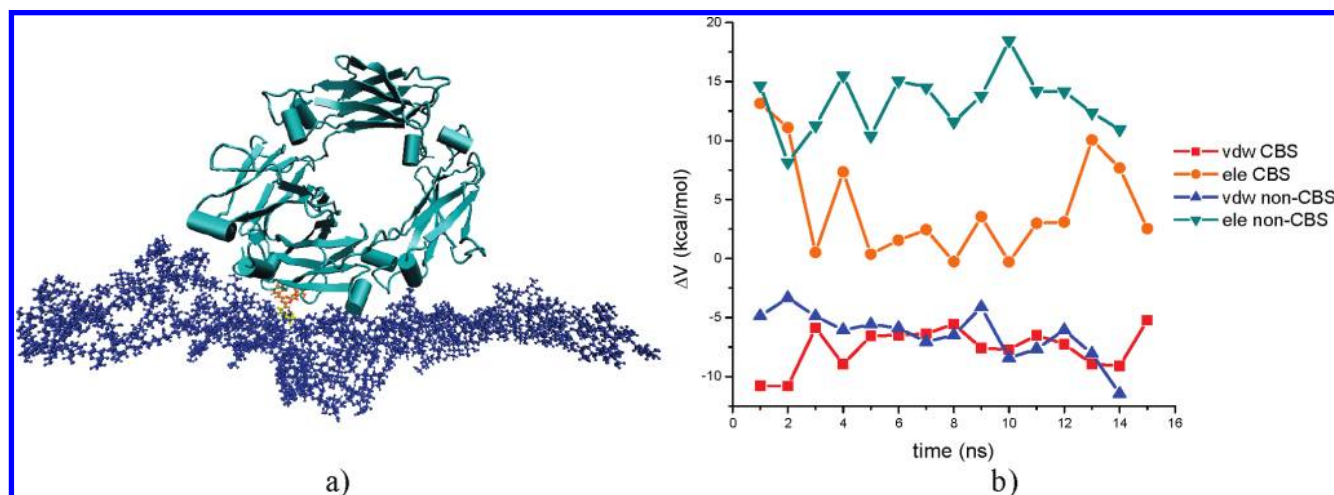


**Figure 9.** A2P-2LP pair in the non CBS pose: (a) structure after 15 ns of simulation and (b) van der Waals (vdw) and electrostatic (ele) interaction energies of A2P and 2LP with the surrounding environment between free and bound state for CBS and non CBS systems.

**TABLE 3: Electrostatic (ele) and van der Waals (vdw) Interaction Energies of A2P and 2LP with the Fc Domain and the Solvent Evaluated after 10 ns of MD Simulation: Comparison between CBS and Non CBS Complexes**

	Fc				H <sub>2</sub> O			
	2LP		A2P		2LP		A2P	
	vdw	ele	vdw	ele	vdw	ele	vdw	ele
free system					-4.94	-25.92	-19.00	-52.92
CBS pose	-2.79	-0.21	-31.22	-9.63	-5.23	-33.62	-7.31	-44.13
non CBS pose	-4.67	-9.69	-22.09	-11.94	-4.96	-26.37	-13.06	-31.51
Δ (CBS-non CBS)	1.88	9.48	-9.13	2.31	-0.27	-7.25	5.75	-12.62

domains. However, the energetic analysis of the MD simulations indicates significant differences in the interactions established by the A2P-2LP pair with IgG, when located in these two binding sites. Since the energetics of the system in the absence of the Fc domain is the same as for the CBS system, the comparison can be based on the interactions developed in the bound system, which is shown in Figure 9b. It can thus be observed that while the van der Waals interaction energy established by the A2P-2LP pair with the surrounding environment (support, solvent and antibody) is similar for both binding sites, electrostatic interactions are significantly less favorable for the non CBS structure. This is mainly due to the loss of interactions of the A2P-2LP pair with the solvent+antibody

environment (about 7.2 kcal/mol) rather than with the support (about 3.3 kcal/mol).

A detailed analysis was performed on the 10th nanosecond of both simulations to break down the interaction energy contribution given by the Fc domain from that of water (Table 3). It is interesting to note that the van der Waals interactions present significant differences in the two cases, which however cancel out when considered together. In particular, van der Waals interactions of A2P with the Fc domain are prevailing in the CBS complex, as expected, but are counterbalanced by the weaker electrostatic interactions established by 2LP. It is also interesting to observe the effect that the solvent has on the stability of the complex: in the CBS pose the electrostatic

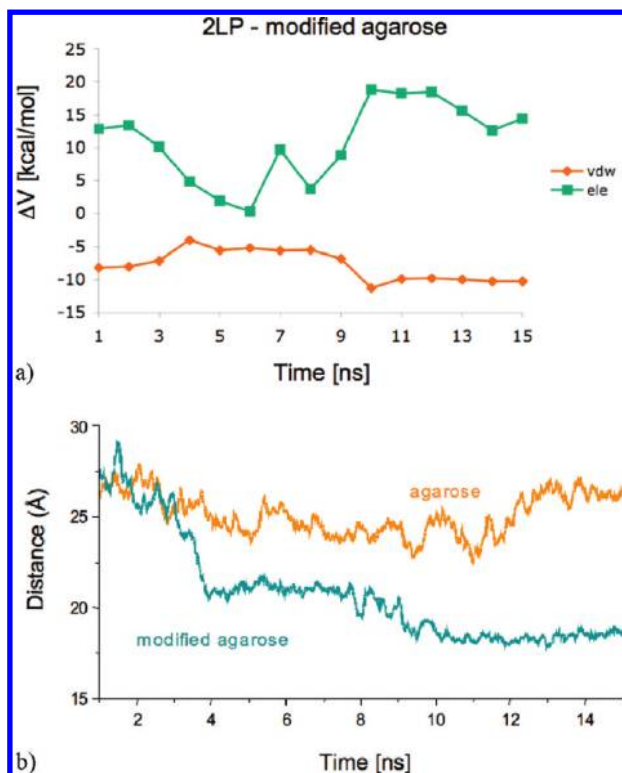


**Figure 10.** (a) Energies of the complex supported on AG modified with 6-*O*-methyl-galactose residues. (b) Distance between a support key residue and the center of mass of one of the CH<sub>3</sub> chains of the Fc domain: AG (green) and AG modified with 6-*O*-methyl-galactose units (orange).

interactions with both ligand and spacer are considerably stronger than in the non CBS pose, which can be mostly ascribed to the fact that in the CBS complex the accessibility to water is significantly larger than in the non CBS pose, in which ligand and spacer are sandwiched between protein and support, which leads thus to a partial desolvation of this area.

**Analysis of the Interaction between IgG and A2P Supported on Modified AG.** To fully understand the performances of a chromatographic system, it is necessary to investigate the influence of the chemical nature of the support material on the binding process. Thus the AG surface was modified by substituting part of the galactose residues with 6-*O*-methyl-galactose units in order to obtain a more hydrophobic support, as previously described in the Methods section. The chosen spacer was also in this case 2LP and the initial structure of the complex was identical to the one adopted for A2P-2LP. The analysis of the evolution of the free binding energy with the simulation time is shown in Figure 10a. In the first 9 ns of simulation the energy of the complex seems to stabilize and to follow a trend similar to that observed for the AG support, though the average interaction energy in this first time span is slightly higher (see Figure 7). However, in the following 5 ns, the complex undergoes a conformational change, as the Fc domain further approaches the support. The average value of the interaction energy in this final time span is positive by about 6 kcal/mol, thus significantly larger than that calculated for the AG surface (about -3 kcal/mol, see Table 3).

In order to quantify the extent of this interaction, the mean distance between one of the residues of the support that plays a key role in the interaction with the antibody and the center of mass of one of the CH<sub>3</sub> chains of the Fc domain was calculated and plotted in Figure 10b. As it can be observed, while the initial

mean distance is similar for both simulations (about 27 Å) in the first 3 ns, which is determined by the similar molecular conformation from which the simulations are started, the situation changes significantly as the system evolves. In fact, while in the case of AG this distance stabilizes at a mean value of about 25 Å, in the case of the modified support it decreases in two steps first to about 21 Å (3–9 ns) and then to 18.4 Å in the last 5 ns.

The energetic and structural evidence can be rationalized in terms of the establishment of interactions between ligand and hydrophobic surface that are competitive with those formed by the affinity ligand in the CBS, which final result is the destruction of the interaction between support and affinity ligand. Though this is clearly a limiting case, this result however indicates that the molecular properties of the surface surrounding the affinity ligand can influence greatly the binding process, up to the point of leading to the loss of affinity, and thus selectivity, of the material.

**Analysis of the Interaction between Pluronic F68 and A2P Spacers.** The experimental data reported and discussed in the experimental section clearly showed that the presence of Pluronic acid in solution affects considerably the performances of the A2P-2LP couple, decreasing its capability to interact with IgG, while its effect is almost negligible for other spacers, such as SS3 or TRZ. To investigate this aspect in detail, some additional simulations focused on the individuation of interactions between Pluronic F68 and the 2LP, SS3, and TRZ spacers were performed. Considering the difficulty of building a reliable molecular model of Pluronic F68 and the relatively small size of the chosen spacers, it was decided to model the interaction between the two molecules using representative molecular fragments for each of them. In particular, it was decided to model Pluronic F68 as ethylene dimethyl ether (EDME), the spacers using the full structure sketched in Figure 1, and A2P only through its triazine core. The rationale for the development of these models lies in the particular nature of the 2LP spacer, where the amino group positioned furthest from the A2P ligand is protonated, and thus charged, in the conditions at which the IgG adsorption process is usually performed. This suggests that a possible explanation for the different behavior of A2P-2LP with respect to other ligand-spacer couples might be the establishment of interactions involving the charged amino group. Following this lead, minimum energy structures of the complexes formed by A2P-2LP/SS3/TRZ and EDME were searched by systematic docking followed by energy minimization protocols performed at the B3LYP/6-31 g(d,p) level considering implicitly the solvent using the IEFPCM model. The calculated minimum energy interaction structures, which XYZ coordinated are reported in the Supporting Information, are reported in Figure 11.

The structures reported in Figure 11 evidence that a hydrogen bond involving directly the spacer arm is formed only for the A2P-2LP - EDME complex and involves directly the ether atom of EDME and the amino group. The interaction energies of the three complexes, computed at the B3LYP/aug-cc-pVTZ level, are -0.87, 0.0, and -0.35 kcal/mol for the complexes involving A2P-2LP, A2P-TRZ, and A2P-SS3, respectively. This supports the initial hypothesis that Pluronic F68 is able to establish significant interactions with the 2LP spacer, which might be responsible for the enhanced sensitivity to Pluronic F68 observed for 2LP materials.

**Comparison between Experiment and Theory.** After having obtained sufficient experimental and theoretical results of ligand, spacer and support interactions as well as information

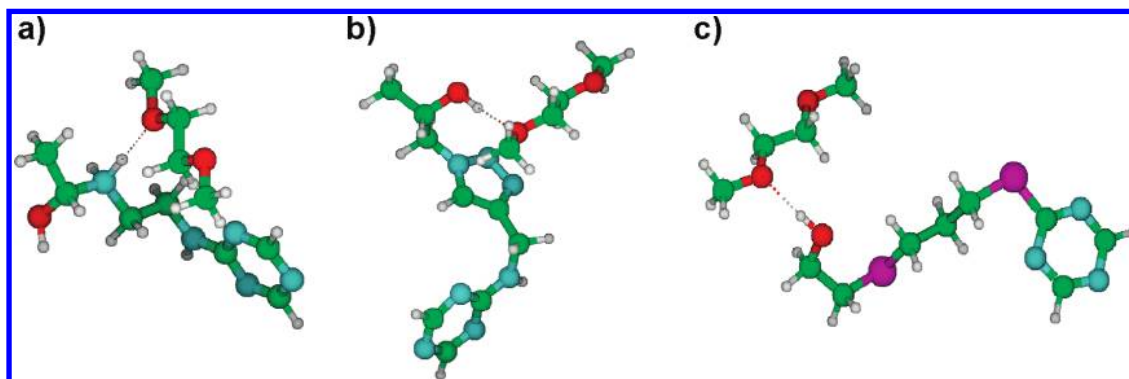


**Figure 11.** Minimum energy structures of the complexes between ethylene dimethyl ether and (a) A2P-2LP, (b) A2P-TRZ, and (c) A2P-SS3.

about the interaction between the ligand-spacer combination and the antifoaming additive Pluronic F68, the computational results can be adopted to interpret the experimental evidence.

**Effect of Spacer Chemistry.** Simulations performed for the reference AG support for the different spacers considered can be directly compared to experimental data measured for the F3 feed (pure IgG) when the support is AG (Figure 3b). It is interesting to observe that, while the calculated interaction energies depend substantially from the adopted spacer, with TRZ based materials predicted to be those with the highest energy of interaction, experimentally no significant differences can be observed. Two concurring effects are most likely responsible for such behavior. The first is that the material has probably reached saturation, which is supported by the fact that the measured DBC for A2P materials are similar to those determined using protein A affinity chromatography. The second is that the differences among the free interaction energies ( $\Delta G$ ) between material and support, that determine the binding constants, are reduced with respect to those calculated among the interaction energies ( $\Delta H$ ) by an entropy–enthalpy compensation effect. This is directly confirmed by free interaction energies calculated adopting the linear interaction energy (LIE) protocol,<sup>52</sup> following the procedure outlined in our previous publications<sup>24,35</sup> and using the van der Waals and electrostatic interaction energies reported in Table 3, scaled using standard LIE parameters.<sup>53</sup> LIE interaction energies calculated for the four spacers differ in fact by no more than 1 kcal/mol for the TRZ, 2LP, and DES spacer, while calculations predict that materials exploiting the SS3 spacer should perform worse than the others. Interestingly, this is confirmed by experiments (Figure 3).

For the F2 feed, TRZ on AG performs better than SS3 and 2LP. With the F1 feed on Fractogel, in the presence of Pluronic F68, TRZ performs significantly better than SS3 and DES. From a theoretical standpoint, the high performances of the TRZ spacer, which DBC is comparable to that of Rmp protein A Sepharose FF, can be related to the finding that this is the only spacer which, when not bound to IgG, has no significant interaction with the support. Also, this is the spacer for which we computed the highest interaction energy with IgG. This can indeed be considered as one of the main findings of this investigation, which supports the hypothesis advanced in our previous study<sup>24</sup> that the interaction of the ligand with the support can have a major impact on the performances of the separation process. In addition, the present work indicates that the best separation performances are obtained when the spacer–ligand pair is not interacting with the surface and is thus highly mobile. This is the motivation for the high interaction energies calculated for the A2P–TRZ system, which, though probably reduced by a significant entropy compensation effect (an indirect measure of the mobility of the ligand–spacer pair, that is directly

related to conformational entropy), is responsible for the high performances obtained when using this specific spacer.

**Effect of Support Chemistry.** Both experiments and theory confirm that not only the ligand headgroup, A2P, but also the spacer and the support chemistry contribute significantly to the capture of IgG. Simulations predict that a more hydrophobic surface reduces the affinity of the ligand for the antibody. This might explain the decrease of IgG capture capability observed experimentally, which is highest for the AG-based matrixes, decreases for Fractoprep and reaches a minimum for Fractogel. In particular, the binding capacity for IgG increases by a factor of 3 (for F1) when changing the support from Fractogel to Fractoprep. This is reasonable as it can be expected that AG is more hydrophilic than Fractoprep, which is a hydrophilic synthetic polyvinylether cross-linked with acrylamide molecules, and Fractogel, a polymethacrylate based support.

Calculations show that a modification of the support structure, consisting in the insertion of  $\text{OCH}_3$  groups, leads to a significant decrease of the energy of interaction between ligand and protein. The origin of this effect is 2-fold, since a change of support shows an impact on both the energy of interaction of the ligand with the support, which must be overcome to let the ligand bind the protein, and on the direct interaction between protein and support.

**Effect of Surface Chemistry.** It is obvious that besides the bare support chemistry, any modification of the support surface can induce a change of the overall properties of an adsorbent. While the thioether based spacers as well as the mercaptoethanol end-capping are noncharged, but rather hydrophobic in nature, the incorporated amino functionality of 2LP and the ethanol-amine end-capping exhibit weak anion exchange properties. An extreme case is the introduction of azido groups, which are rather hydrophilic in nature and bind IgG due to electron donor/acceptor interactions as well as due to the fact that IgG possesses hydrophobic patches on its surface. This additional interaction between surface-bound azide and IgG molecules leads most probably to an increased IgG binding performance of the TRZ-type adsorbents.

**Effect of Ligand Density.** Since this study evidenced the importance of the surface structure, it is important to point out that the density of A2P ligands on the surface influences the IgG capture rate by establishing multiple interactions or, more simply, by modifying the surface properties. Theoretical calculations support the latter interpretation, since docking and successive MD simulations clearly indicated that the dominating binding site of IgG is the CBS. Moreover, the simulations clearly show that a modification of the surface properties can have a significant impact on the materials performances, since, as shown above and confirmed by experiments, a surface that is



able to establish significant van der Waals interaction with the protein may even disrupt the CBS interaction.

**Effect of Pluronic F68 in the Feed.** Experiments with the F1 feed show that materials with the 2LP spacer perform in general better than those with the other spacers. However, when Pluronic acid is added, the introduction of the SS3 or TRZ spacer arm results in an increased binding of IgG compared to adsorbents with 2LP spacers. A similar trend is seen with F2 where the SS3 and TRZ containing adsorbents bind more IgG than AG-2LP-A2P. In particular in the case of AG-TRZ-A2P the binding capacity is even comparable to that achieved for the bench mark adsorbent Rmp protein A Sepharose FF. This is different than what was observed for the pure feed F3, and confirmed by calculations, according to which 2LP should perform similarly to DES and TRZ. The main reason for the deviation of experimental results for the three different spacers is the fact that the composition of the test solutes is very different in their complexity. The main difference between F1 and F3 is the presence of other proteins in the feed and Pluronic acid. It can therefore be reasonably concluded that the different performances can be attributed to competitive interactions of the affinity matrix with other macromolecules present in solution besides the target protein IgG. On the basis of the experimental and theoretical calculations performed to investigate this aspect, two interpretations are possible. The first is that, if Pluronic acid is interacting with the AG surface, then the presence of the TRZ and SS3 spacer arms appear to push the ligand far enough away from the AG surface to enable the ligand to capture IgG. The second is that it is the spacer itself that contributes to increase the interaction energy between Pluronic acid and the support surface functionalized with A2P ligands. The latter interpretation is supported by computational evidence, indicating that the charged amino group of the 2LP spacer can establish some binding electrostatic interaction with the etheric oxygen atoms of Pluronic acid. The competitive adsorption of Pluronic acid on a surface functionalized with 2LP-A2P provides a reasonable explanation of the reason why the 2LP-A2P pair observes a reduction of binding capacity for IgG, when Pluronic acid is present in solution.

#### 4. Summary and Conclusions

As a final remark, it can be concluded that a combined approach exploiting experiments and MD simulations appears as a useful tool for the design of new materials. The simulation results indicate that it is important, when screening ligand libraries, to account for the interaction of the ligand with the support. This is valid both, when designing a new ligand in silico as well as when searching experimentally with a combinatorial library approach, since a viable ligand candidate that was originally tested on one support might behave quite differently on another (more hydrophilic/hydrophobic) and might at the end even perform much better than with the former. The influence of ligand–support interaction on the protein binding process can in actual fact be quite significant, especially if it is competitive to the ligand–protein interaction.

Since the accuracy of the prediction of MD simulations is also satisfactory with more complex sample matrices it can be overall stated that with increasing knowledge of the interaction properties of the participating moieties of ligand, spacer, support and target analyte during the capture of the latter, the more reliable the corresponding predictions obtained by computer simulation studies will be. MD simulations are surely an excellent tool, both, for the prediction of binding capacities in simple feed matrices as well as for the interpretation of experimental results.

**Acknowledgment.** The authors acknowledge the European Commission (EU) for funding this research work, performed under the integrated project AIMs (Advanced Interactive Materials by Design; Contract No. NMP3-CT2004-500160), which was part of the 6th Framework Program of the EU. ProMetic BioSciences is a trademark of ProMetic BioSciences Ltd; PuraBead is registered with the U.S. Patent & Trademark Office; MAbsorbent is registered with the U.S. Patent & Trademark Office; Chemical Combinatorial Library is registered with the U.K. Patent & Trademark Office.

**Supporting Information Available:** The protocols for the preparation of all here-investigated ligands and materials as well as their experimental evaluation. This material is available free of charge via the Internet at <http://pubs.acs.org>.

#### References and Notes

- (1) Waldmann, T. A.; Levy, R.; Collier, B. S. *Hematology* **2000**, 2000, 394.
- (2) Saphire, E. O.; Parren, P.; Pantophlet, R.; Zwick, M. B.; Morris, G. M.; Rudd, P. M.; Dwek, R. A.; Stanfield, R. L.; Burton, D. R.; Wilson, I. A. *Science* **2001**, 293, 1155.
- (3) Scallion, B. J.; Snyder, L. A.; Anderson, G. M.; Chen, Q. M.; Yan, L.; Weiner, L. M.; Nakada, M. T. *J. Immunother.* **2006**, 29, 351.
- (4) MacConnachie, A. M. *Intensive Crit. Care Nurs.* **2000**, 16, 123.
- (5) Keller, K.; Friedmann, T.; Boxman, A. *Trends Biotechnol.* **2001**, 19, 438.
- (6) Roque, A. C. A.; Lowe, C. R.; Taipa, M. A. *Biotechnol. Prog.* **2004**, 20, 639.
- (7) Lowe, C. R. *Curr. Opin. Chem. Biol.* **2001**, 5, 248.
- (8) Labrou, N. E. *J. Chromatogr. B* **2003**, 790, 67.
- (9) Clonis, Y. D. *J. Chromatogr. A* **2006**, 1101, 1.
- (10) Hahn, R.; Shimahara, K.; Steindl, F.; Jungbauer, A. *J. Chromatogr. A* **2006**, 1102, 224.
- (11) Hahn, R.; Bauerhansl, P.; Shimahara, K.; Wizniewski, C.; Tsche-liessnig, A.; Jungbauer, A. *J. Chromatogr. A* **2005**, 1093, 98.
- (12) Roque, A. C. A.; Silva, C. S. O.; Taipa, M. A. *J. Chromatogr. A* **2007**, 1160, 44.
- (13) Hober, S.; Nord, K.; Linhult, M. *J. Chromatogr. B* **2007**, 848, 40.
- (14) Fassina, G.; Ruvo, M.; Palombo, G.; Verdoliva, A.; Marino, M. *J. Biochem. Biophys. Methods* **2001**, 49, 481.
- (15) Fassina, G.; Verdoliva, A.; Odierna, M. R.; Ruvo, M.; Cassini, G. *J. Mol. Recognit.* **1996**, 9, 564.
- (16) Braisted, A. C.; Wells, J. A. *Proc. Natl. Acad. Sci. U.S.A* **1996**, 93, 5688.
- (17) Dias, R. L. A.; Fasan, R.; Moehle, K.; Renard, A.; Obrecht, D.; Robinson, J. A. *J. Am. Chem. Soc.* **2006**, 128, 2726.
- (18) Yang, H. G. P. V.; Carbonell, R. G. *J. Pept. Res.* **2005**, 66, 120.
- (19) Li, R. X.; Dowd, V.; Stewart, D. J.; Burton, S. J.; Lowe, C. R. *Nat. Biotechnol.* **1998**, 16, 190.
- (20) Roque, S. F.; Sproule, K.; Hussain, A.; Lowe, C. R. *J. Mol. Recognit.* **1999**, 12, 67.
- (21) Teng, S. F.; Sproule, K.; Husain, A.; Lowe, C. R. *J. Chromatogr. B* **2000**, 740, 1.
- (22) Newcombe, A. R.; Cresswell, C.; Davies, S.; Watson, K.; Harris, G.; O'Donovan, K.; Francis, R. *J. Chromatogr. B* **2005**, 814, 209.
- (23) Feng, H. L. J.; Li, H.; Wang, X. *Biomed. Chromatogr.* **2006**, 20, 1109.
- (24) Busini, V.; Moiani, D.; Moscatelli, D.; Zamolo, L.; Cavallotti, C. *J. Phys. Chem. B* **2006**, 110, 23564.
- (25) DeLano, W. L.; Ultsch, M. H.; de Vos, A. M.; Wells, J. A. *Science* **2000**, 287, 1279.
- (26) Mateo, C.; Abian, O.; Ernedo, M. B.; Cuenca, E.; Fuentes, M.; Fernandez-Lorente, G.; Palomo, J. M.; Graza, V.; Pessela, B. C. C.; Giacomini, C.; Irazoqui, G.; Villarino, A.; Ovsejevi, K.; Batista-Viera, F.; Fernandez-Lafuente, R.; Guisan, J. M. *Enzyme Microb. Technol.* **2005**, 37, 456.
- (27) Guisan, J. M. *Enzyme Microb. Technol.* **1988**, 10, 375.
- (28) Fernandez-Lafuente, R.; Rosell, C. M.; Rodriguez, V.; Santana, C.; Soler, G.; Bastida, A.; Guisán, J. M. *Enzyme Microb. Technol.* **1993**, 15, 546.
- (29) Fuentes, M.; Mateo, C.; Fernandez-Lafuente, R.; Guisan, J. M. *Biomacromolecules* **2006**, 7, 540.
- (30) Moses, J. E.; Moorhouse, A. D. *Chem. Soc. Rev.* **2007**, 36, 1249.
- (31) Binder, W. H.; Sachsenhofer, R. *Macromol. Rapid Commun.* **2007**, 28, 15.
- (32) Tornøe, C. W.; Christensen, C.; Meldal, M. *J. Org. Chem.* **2002**, 67, 3057.

- (33) Cuatrecasas, P.; Wilchek, M.; Anfinsen, C. B. *Proc. Natl. Acad. Sci. U.S.A.* **1968**, *61*, 636.
- (34) Wilchek, M.; Miron, T. *React. Funct. Polym.* **1999**, *41*, 263.
- (35) Zamolo, L.; Busini, V.; Moiani, D.; Moscatelli, D.; Cavallotti, C. *Biotechnol. Prog.* **2008**, *24*, 527.
- (36) Arnott, S.; Fulmer, A.; Scott, W. E.; Dea, I. C. M.; Moorhouse, R.; Rees, D. A. *J. Mol. Biol.* **1974**, *90*, 269.
- (37) Kirschner, K. N.; Woods, R. J. *Proc. Natl. Acad. Sci. U.S.A.* **2001**, *98*, 10541.
- (38) Kirschner, K. N.; Woods, R. J. *J. Phys. Chem. A* **2001**, *105*, 4150.
- (39) Basma, M.; Sundara, S.; Calgan, D.; Vernali, T.; Woods, R. J. *J. Comput. Chem.* **2001**, *22*, 1125.
- (40) Kirschner, K. N.; Tschampel, S.; Woods, R. GLYCAM04 force field, 2004.
- (41) Cornell, W. D.; Cieplak, P.; Bayly, C. I.; Gould, I. R.; Merz, Jr., K. M.; Ferguson, D. M.; Spellmeyer, D. C.; Fox, T.; Caldwell, J. W.; Kollman, P. A. *J. Am. Chem. Soc.* **1995**, *117*, 5179.
- (42) Case, D. A.; Darden, T. A.; Cheatham, III, T. E.; Simmerling, C. L.; Wang, J.; Duke, R. E.; Luo, R.; Merz, K. M.; Wang, B.; Pearlman, D. A.; Crowley, M.; Brozell, S.; Tsui, H.; Gohlke, H.; Mongan, J.; Hornak, V.; Cui, G.; Beroza, P.; Schafmeister, C.; Caldwell, J. W.; Ross, W. S.; Kollman, P. A. *AMBER 8*; University of California: San Francisco, 2004.
- (43) Case, D. A.; Cheatham, T. E.; Darden, T.; Gohlke, H.; Luo, R.; Merz, K. M.; Onufriev, A.; Simmerling, C.; Wang, B.; Woods, R. J. *J. Comput. Chem.* **2005**, *26*, 1668.
- (44) Morris, G. M.; Goodsell, D. S.; Halliday, R. S.; Huey, R.; Hart, W. E.; Belew, R. K.; Olson, A. J. *J. Comput. Chem.* **1998**, *19*, 1639.
- (45) Frisch, M. J.; Trucks, G. W.; Schlegel, H. B.; Scuseria, G. E.; Robb, M. A.; Cheeseman, J. R.; Montgomery, J. A., Jr.; Vreven, T.; Kudin, K. N.; Burant, J. C.; Millam, J. M.; Iyengar, S. S.; Tomasi, J.; Barone, V.; Mennucci, B.; Cossi, M.; Scalmani, G.; Rega, N.; Petersson, G. A.; Nakatsuji, H.; Hada, M.; Ehara, M.; Toyota, K.; Fukuda, R.; Hasegawa, J.; Ishida, M.; Nakajima, T.; Honda, Y.; Kitao, O.; Nakai, H.; Klene, M.; Li, X.; Knox, J. E.; Hratchian, H. P.; Cross, J. B.; Bakken, V.; Adamo, C.; Jaramillo, J.; Gomperts, R.; Stratmann, R. E.; Yazyev, O.; Austin, A. J.; Cammi, R.; Pomelli, C.; Ochterski, J. W.; Ayala, P. Y.; Morokuma, K.; Voth, G. A.; Salvador, P.; Dannenberg, J. J.; Zakrzewski, V. G.; Dapprich, S.; Daniels, A. D.; Strain, M. C.; Farkas, O.; Malick, D. K.; Rabuck, A. D.; Raghavachari, K.; Foresman, J. B.; Ortiz, J. V.; Cui, Q.; Baboul, A. G.; Clifford, S.; Cioslowski, J.; Stefanov, B. B.; Liu, G.; Liashenko, A.; Piskorz, P.; Komaromi, I.; Martin, R. L.; Fox, D. J.; Keith, T.; Al-Laham, M. A.; Peng, C. Y.; Nanayakkara, A.; Challacombe, M.; Gill, P. M. W.; Johnson, B.; Chen, W.; Wong, M. W.; Gonzalez, C.; Pople, J. A. *Gaussian 03*, revision C.01; Gaussian, Inc.: Wallingford, CT, 2004.
- (46) Schaftenaar, G.; Noordik, J. H. *J. Comput.-Aided Mol. Des.* **2000**, *14*, 123.
- (47) Humphrey, W.; Dalke, A.; Schulten, K. *J. Mol. Graph.* **1996**, *14*, 33.
- (48) DeLano, W. L. The PyMOL Molecular Graphics System, on world wide web <http://www.pymol.org> 2002.
- (49) Chhatre, S.; Titchener-Hooker, N. J.; Newcombe, A. R.; Keshavarz-Moore, E. *Nat. Protoc.* **2007**, *2*, 1763.
- (50) Yang, H.; Gurgel, P. V.; Carbonell, R. G. *J. Chromatogr., A* **2009**, *1216*, 910.
- (51) Horak, J.; Hofer, S.; Lindner, W. *J. Chromatogr. B*, **2010**, to be submitted.
- (52) Carlsson, J.; Ander, M.; Nervall, M.; Aqvist, J. *J. Phys. Chem. B* **2006**, *110*, 12034.
- (53) Aqvist, J.; Hansson, T. *J. Phys. Chem.* **1996**, *100*, 9512.

JP1017168



**Supporting Information file for**

**Experimental and theoretical investigation of effect of spacer  
arm and support matrix of synthetic affinity chromatographic  
materials for the Purification of Monoclonal Antibodies**

Laura Zamolo<sup>a</sup>, Matteo Salvalaglio<sup>a</sup>, Carlo Cavallotti<sup>a\*</sup>, Benedict Galarza<sup>b</sup>, Chris Sadler<sup>b</sup>,  
Sharon Williams<sup>b\*</sup>, Stefan Hofer<sup>c</sup>, Jeannie Horak<sup>c\*</sup>, Wolfgang Lindner<sup>c</sup>,

<sup>a</sup> Dept. di Chimica, Materiali e Ingegneria Chimica “G. Natta”, Politecnico di Milano, Via Mancinelli 7, 20131 Milano, Italy

<sup>b</sup> ProMetic Biosciences Ltd., 211 Cambridge Science Park, Milton Road, Cambridge CB4 0ZA, UK

<sup>c</sup> Department of Analytical Chemistry and Food Chemistry, University of Vienna, Waehringer Strasse 38, 1090 Vienna, Austria

## **Experimental Section**

### **1. Reagents and Materials**

#### **1.1. Chemicals**

#### **1.2. Support materials**

#### **1.3. Equipment**

### **2. Synthesis of ligands and preparation of affinity adsorbents**

#### **2.1. Preparation of A2P-2LP-materials:**

*Preparation of an A2P-amino-dipropyl-amino support (A2P-2LP) ... (1)*

#### **2.2. Preparation of A2P-SS3 and A2P-DES materials**

*Synthesis of A2P-thio-propyl-thiol (A2P-SS3) ... (2)*

*Synthesis of A2P-thio-(3,6-dioxo-octane)-thiol (A2P-DES) ... (3)*

*Preparation of A2P-SS3 and A2P-DES materials ... (2a and 3a)*

*Endcapping with 2-mercaptoethanol ... (2b and 3b)*

#### **2.3. Preparation of A2P-TRZ materials**

*Synthesis of A2P-amino-propyne (A2P-TRZ) ... (4)*

*Azido activation of Fractogel EMD and PuraBead ... (4a)*

*Coupling A2P-amino-propyne onto azido-modified supports ... (4b)*

### **3. Affinity Chromatography**

### **4. Protein Quantification**

#### **4.1. Photometric quantification of proteins at 280 nm**

#### **4.2. The Bradford Assay – total protein determination**

#### **4.3. Protein A HPLC**

#### **4.4. Nephelometry**

#### **4.5. SDS-PAGE Gel electrophoresis**

## Experimental Section

### 1. Reagents and Materials

#### 1.1. Chemicals

A2P-monochloride was kindly provided by ProMetic Biosciences Ltd (PBL).

Copper(I)iodide, 3,6-dioxa-octanedithiol, 2-mercaptoethanol, 3-propargylamine, sodium azide were purchased from Sigma Aldrich (Vienna, Austria). 2-Ethanolamine, N,N-dimethylformamide (DMF), N,N-diisopropylethylamine (DIPEA), ethylenediaminetetraacetic acid, 1,3-propanedithiol, sodium hydroxide, triethylamine (TEA) and 37 % hydrochloric acid were from Fluka (Vienna, Austria). Citric acid was purchased from Sigma Aldrich (Poole, UK). Sodium hydroxide, sodium di-hydrogen orthophosphate, di sodium hydrogen orthophosphate, sodium chloride, hydrochloric acid and HPLC-grade methanol were purchased from Fisher Scientific (Loughborough, UK).

HPLC grade methanol (for synthesis) and acetonitrile were from Merck-VWR (Vienna, Austria). Dichloromethane and methanol for column chromatography were of technical grade.

Phosphate buffered saline (PBS) was prepared by PBL in-house containing 10 mM  $\text{Na}_2\text{HPO}_4$ , 2 mM  $\text{KH}_2\text{PO}_4$ , 137 mM NaCl and 2.7 mM KCl and set to pH 7.4. All buffers were prepared using reverse osmosis water.

NuPAGE LDS sample buffer, NuPAGE Sample Reducing Agent, NuPAGE MOPS (20X, 3-N-morpholino propanesulfonic acid) SDS Running Buffer, NuPAGE Novex 4-12% Bis – Tris pre-cast 10 or 17 well gels, 1.0mm Mark 12 unstained standard and Simply Blue SafeStain are all supplied by Invitrogen (Paisley, UK).

## 1.2. Support materials

Both support-media, the polymethacrylate-based Fractogel® EMD Epoxy (M) as well as the polyacrylamide-type Fractoprep® EMD Epoxy gel are tentacle graphed spherical beads which were provided by Merck KGaA (Darmstadt, Germany). The commercially available Fractogel® EMD (M) comes with particle sizes of 40-90 µm, a pore size of about 80 nm and an epoxide coverage of 1000 µmol/g dry gel. Epoxy activated Fractoprep® EMD per se is a non-commercial support, which was especially prepared by Merck KGaA for the EU-Project AIMs. It has an average particle size of 80 µm, a pore size of 50 nm and an epoxy density of 256 µmol/g dry gel. The conversion factors for vacuum dried (dry gel) to suction dried (wet gel) and in 1 M sodium chloride settled gel (mL) are listed in **Table 1**.

**Table S1. Correlation Factors**

<b>Support</b>	<b>dry gel [g]</b>	<b>wet gel [g]</b>	<b>wet gel [mL]</b>
Agarose	1	10.2	15.7
Fractogel	1	2.3	4.23
Fractoprep	1	3.6	5.59

Fractosil® EMD on the contrary is a silica-based support comprising of epoxy activated irregular silica particles provided by Merck KGaA (Darmstadt, Germany). It has a particle size of 40-90 µm, an epoxide loading of approximately 40 µmol/g (dry) and is stable at pH values ranging from 2 to 9.

PuraBead® is an in-house product from ProMetic Biosciences Ltd. (PBL), (Cambridge, UK). PuraBead® consists of spherical, macro-porous, near-monodisperse 6%-crosslinked Agarose beads with particle sizes of  $90 \pm 10$  µm. The hydrophilic surface of PuraBead combined with its high sanitation stability, which includes 0.5 M sodium hydroxide and

autoclavation at 121°C and its applicability for high flow-rates at low column back pressure makes it an ideal support for bioprocess applications.

In order to avoid misunderstandings we want to state that, the term “A2P-ligand” refers strictly to the ligand head group A2P and not to the A2P-spacer combination per se, which will be separately addressed as A2P-2LP, A2P-SS3, A2P-DES and A2P-TRZ, of which 2LP stands for 1,3-diaminoethane, SS3 for 1,3-propanedithiol and DES for 3,6-dioxo-1,8-octanedithiol.

In all cases, the affinity materials were packed in C10/20 columns (10 mm ID x 20 cm length) with AC 10 adapters from GE Healthcare (Buckinghamshire, UK) for testing.

### **1.3. Equipment**

Affinity chromatography was conducted using an ÄKTA Explorer HPLC system from GE Healthcare (Buckinghamshire, UK).

For high performance liquid chromatography (HPLC) a Waters system (Separation module 2695 and detector 996) with Empower software from Waters Ltd, (Hertfordshire, UK) was used. For the quantification of IgG a 0.8 mL pre-packed Protein-A ImmunoDetection® sensor cartridge with metal guard column from Applied Biosystems (Cheshire, UK) was chosen. This sensor cartridge contains rigid polymeric POROS beads with an average particle size of 20 µm and large flow-through pores and smaller diffusion pores with pore sizes ranging from 5000 to 10000 Å, which provide an overall accessible surface area of 1 m<sup>2</sup>/cartridge.

For SDS-PAGE, an XCell II Mini-Cell set up was used with a PowerEase 500 Power Supply all supplied by Invitrogen (Paisley, UK). Nephelometric measurements were performed on a Dade Behring BNII Nephelometer from Siemens Healthcare (Surrey, UK). Photometrical measurements were done on a spectrophotometer from Perkin Elmer

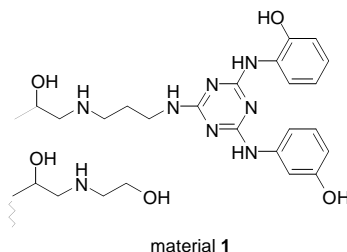
(Beaconsfield, UK) and a Spectofluor microplate reader with a 590 nm filter gfrom Tecan (Theale, Reading UK).

$^1\text{H}$ -NMR spectra were made with a Bruker DRX 400MHz spectrometer. A PEsCiex API 365 triple quadrupole mass spectrometer from Applied Biosystems/MDS Sciex (Concord, Canada) equipped with an ESI ion source was used to generate the MS data. The ion source was an electrospray device and, depending on the analyte, either positive or negative spectra or both were measured.

The elemental analysis of sulfur and nitrogen containing materials were performed with an EA 1108 CHNS-O from Carlo Erba, the determination of CHN was done with a “2400 Elemental Analyzer” from Perkin Elmer.

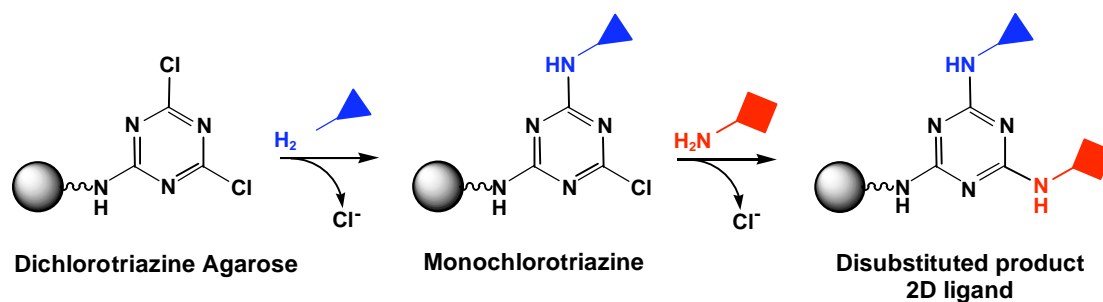
## 2. Synthesis of Ligands and Preparation of affinity adsorbents

### 2.1. Preparation of A2P-2LP-Materials



#### *Preparation of an A2P-amino-support (A2P-2LP) ... (1)*

A2P-2LP was prepared by immobilizing dichloro-triazine with the diamino spacer (2LP) onto the support, creating a dichlorotriazine support in the first instance. The second and the third amino-functional ligand-groups are then subsequently attached to the dichloro triazine core.

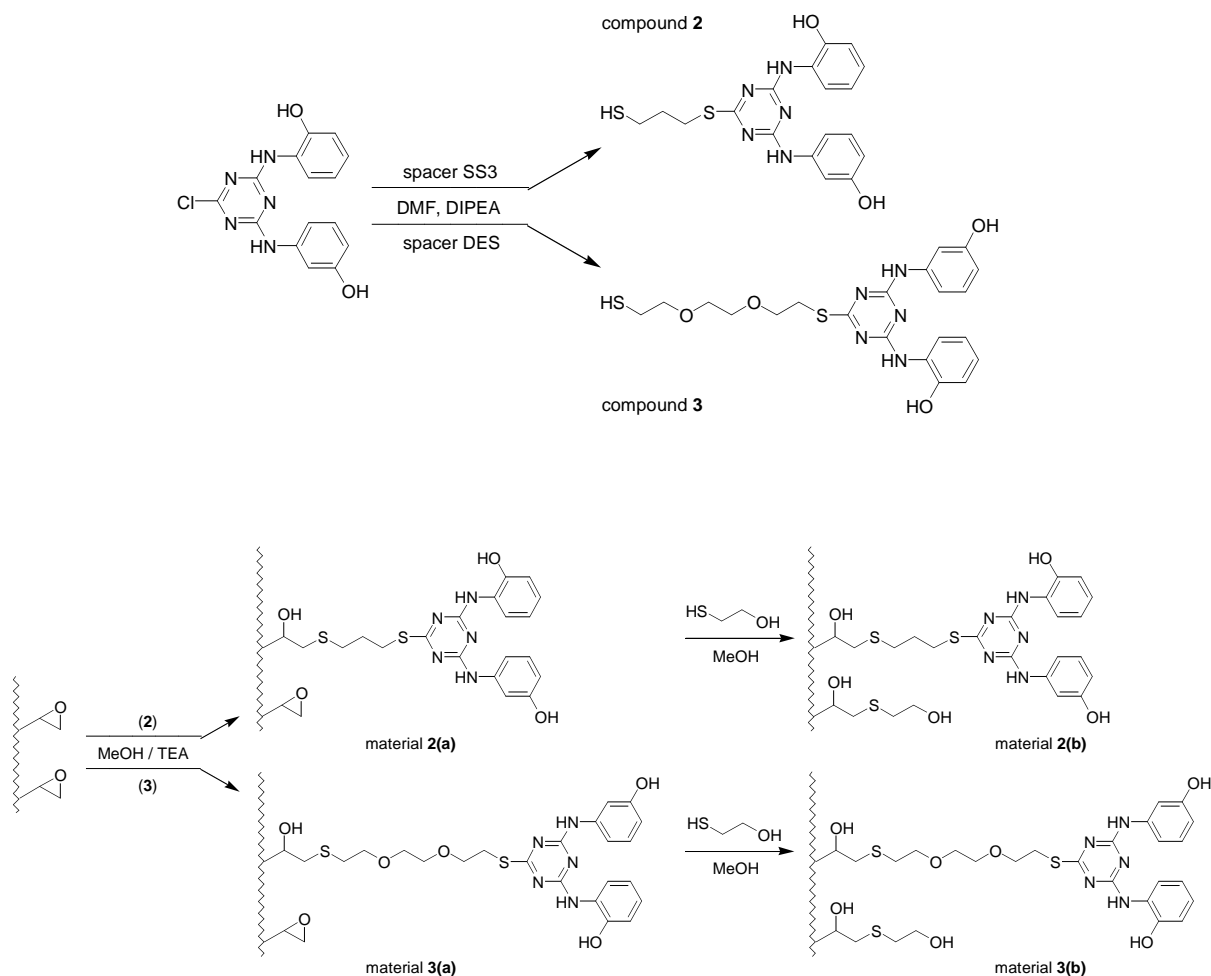


Reaction scheme for the preparation of A2P-2LP-type affinity materials

Since the reactivity of the two available Cl-positions are very different, it is possible to precisely control that in the second instance only amine-2 is being immobilized while the Cl-position three is still free for the final amine to be linked to the ligand. Furthermore as the amine is coupled the chloride from the triazine ring is being released and measure. Thereby it is possible to determine how much of the required amine has been substituted onto the ring. This is done for both amine substitutions. This way it is known how much of each amine is on the triazine core. Note that residual epoxy groups were deactivated through an end-capping reaction with 2-ethanolamine.

The actual ligand densities were determined via residual epoxide assay, where the initial epoxide concentration is being determined, the affinity ligand is being coupled and the remaining epoxide groups are then measured. The actual coverage of affinity ligands is determined by subtraction of the residual epoxide concentration from the initial epoxide concentration.

## 2.2. Preparation of A2P-SS3- and A2P-DES-Materials



### *Synthesis of A2P-thio-propyl-thiol (A2P-SS3) ... (2)*

4 g A2P-monochloride (12.1 mmol) was solved in 12 mL DMF. Subsequently, an equimolar amount of DIPEA (12.1 mmol) and 12 mL 1,3-propanedithiol (120 mmol) were added. The reaction mixture was heated up to 80°C under nitrogen. After a reaction time of 18 h the solvent as well as residual 1,3-propanedithiol were removed via vacuum distillation. The product was purified via column chromatography using a dichloromethane and methanol.



Yield: 50%; MS (ESI, positive) 402.4 [M+H]<sup>+</sup>, 424.3 [M+Na]<sup>+</sup>; <sup>1</sup>H NMR (400 MHz, CD<sub>3</sub>OD): δ = 7.99 (s, 1H), 7.19 (s, 1H), 7.12 – 7.00 (m, 2H), 6.94 – 6.86 (m, 1H), 6.86 – 6.77 (m, 2H), 6.51 (d, 1H) 3.15 (t, 2H), 2.76 (t, 2H), 2.13-2.02 (m, 2H)

### ***Synthesis of A2P-thio-(3,6-dioxo-octane)-thiol (A2P-DES) ... (3)***

The preparation of A2P-DES was performed as previously described for A2P-SS3. Due to the high boiling point of 3,6-dioxo-1,8-octanedithiol (DES), only DMF could be removed via rotary evaporation. The residual DES was removed via column chromatography. In order to obtain a high-purity product a second chromatographic run was indispensable.

Yield: 60%; MS (ESI, positive) 476.4 [M+H]<sup>+</sup>, 498.3 [M+Na]<sup>+</sup>; <sup>1</sup>H- NMR (400 MHz, CD<sub>3</sub>OD): δ = 8.02 (s, 1H), 7.19 (s, 1H), 7.13 – 7.03 (m, 2H), 6.95 – 6.88 (m, 1H), 6.88 – 6.78 (m, 2H), 6.51 (d, 1H), 3.73 (t, 2H), 3.67 (t, 2H), 3.61 – 3.55 (m, 4H), 3.33 – 2.29 (m, 2H), 2.84 (t, 2H)

### ***Preparation of A2P-SS3 and A2P-DES materials ... (2a and 3a)***

The dry Fractogel EMD and Fractoprep EMD were swollen in HPLC-grade methanol and rinsed thoroughly with methanol to remove fines prior to use. For the immobilization of the thiophilic ligands A2P-SS3 (**2a**) and A2P-DES (**3a**), a 1.5 fold excess of ligand (referring to the epoxy density) was added to the methanolic Fractogel EMD slurry, while in case of the Fractoprep EMD material a 2.5 fold excess of ligand was chosen. 4mmol of triethylamine per gram support material was added to catalyse the epoxy-ring opening reaction. The reaction slurry was refluxed for 18 h under nitrogen using a mechanical stirrer to minimize the crushing of the fragile polymeric beads. The final material was excessively washed with HPLC grade methanol.

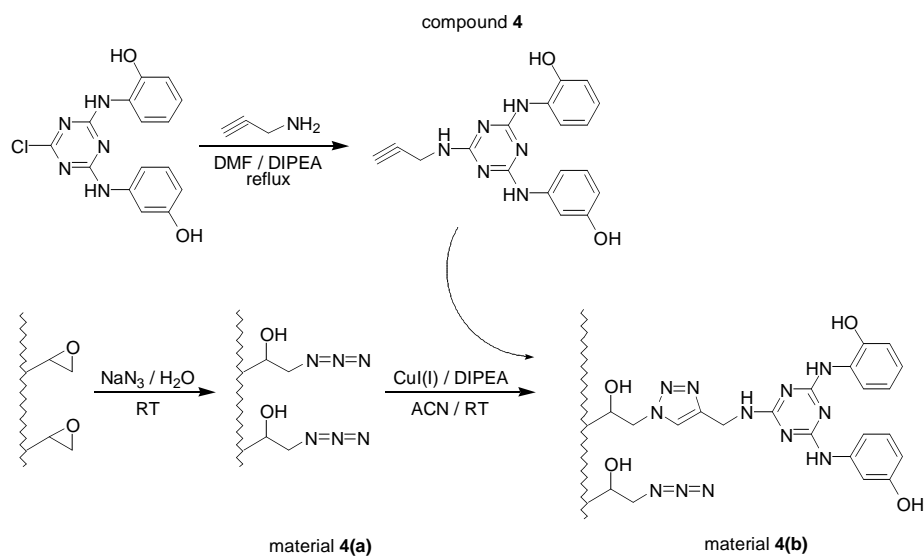
For the determination of the ligand densities, an aliquote of gel was taken before and after endcapping of the material and dried at 60°C under vacuum. The ligand densities were calculated via the sulphur and nitrogen content of the affinity materials. Note that in case of Fractoprep, which is a polyacrylamide-type support, only calculations via the sulphur content lead to reliable results.

### ***Endcapping with 2-mercaptoethanol ... (2b and 3b)***

To a slurry of 10 mL gel in 15 mL HPLC-grade methanol, a tenfold excess of 2-mercaptoethanol and tenfold excess of TEA, referring to the original amount of epoxy groups were added. The reaction was performed as previously described for the immobilization of thiophilic A2P-ligands and stored in bi-distilled water containing 20% methanol.

*Elemental analysis:* FG1-SS3-A2P: A2P-SS3 coverage: 371  $\mu\text{mol/g}$  (C, 53.94%; H, 7.43%; N, 3.43%; S, 2.38%), 2-ME coverage: 73  $\mu\text{mol/g}$  (C, 53.96%; H, 7.65%; N, 3.23%; S, 2.61%); FP1-SS3-A2P: A2P-SS3 coverage: 330  $\mu\text{mol/g}$  (C, 50.69%; H, 7.37%; N, 13.61%; S, 2.14%), 2-ME coverage: 237  $\mu\text{mol/g}$  (C, 50.36%; H, 7.33%; N, 13.18%; S, 2.87%); FG1-DES-A2P: A2P-DES coverage: 325  $\mu\text{mol/g}$  (C, 54.27%; H, 7.34%; N, 3.2%; S, 2.25%), 2-ME coverage: 175  $\mu\text{mol/g}$  (C, 54.19%; H, 7.5%; N, 3.02%; S, 2.81%); FP1-DES-A2P: A2P-DES coverage: 351  $\mu\text{mol/g}$  (C, 52.66%; H, 6.55%; N, 13.7%; S, 2.08%), 2-ME coverage: 156  $\mu\text{mol/g}$  (C, 52.29%; H, 6.78%; N, 13.51%; S, 2.58%); AG-SS3-A2P: A2P-SS3 coverage: 231  $\mu\text{mol/g}$  (C, 47.42%; H, 6.13%; N, 1.83%; S, 1.48%), 2-ME coverage: 0  $\mu\text{mol/g}$  (C, 46.74%; H, 6.46%; N, 1.67%; S, 1.43%).

### 2.3. Preparation of A2P-TRZ-Materials ... (4, 4a and 4b)



#### *Synthesis of A2P-amino-propyne (A2P-TRZ) ... (4)*

1 g A2P-monochloride (3 mmol) was dissolved in 10 mL DMF, followed by the addition of 520  $\mu\text{L}$  DIPEA (3 mmol) and 300  $\mu\text{L}$  3-propargylamine (4.8 mmol). This mixture was refluxed for 18 h under nitrogen. After removal of solvents under reduced pressure, the remaining crude product was purified via column chromatography using dichloromethane and methanol.

Yield 92%; MS (ESI, positive): 349.4  $[\text{M}+\text{H}]^+$ , 697.5  $[2\text{M}+\text{H}]^+$ ;  $^1\text{H}$  NMR (400 MHz,  $\text{CD}_3\text{OD}$ ):  $\delta$  = 7.88 (s, 1H), 7.21 (s, 1H), 7.08 (t, 2H), 6.95 – 6.88 (m, 1H), 6.88 – 6.78 (m, 2H), 6.48 (d, 1H), 4.18 (s, 2H), 2.55 (t, 1H)

#### *Azido activation of Fractogel EMD and PuraBead ... (4a)*

The epoxy-activated support materials were shaken at room temperature in a mixture of water and a tenfold excess of  $\text{NaN}_3$  referring to the amount of epoxy groups on the corresponding support. After 7 days the reaction was terminated and the gel was washed

excessively with water. The amount of bound azido groups was determined via elemental analysis.

*Elemental analysis:* FG1-N<sub>3</sub>: C, 52.67 %; H, 7.16 %; N, 4.73 %; AG-N<sub>3</sub>: C, 45.13 %; H, 6.27 %; N, 1.47 %.

#### ***Coupling A2P-amino-propyne onto azido-modified supports ... (4b)***

1) Azido-Fractogel: 900 mg of A2P-amino-propyne was dissolved in 20 mL HPLC grade acetonitrile and added together with 306  $\mu$ L DIPEA (1.8 mmol) to 3 mL azido-activated Fractogel support. A solution containing 831 mg copper(I) iodide in 40 mL acetonitrile was poured to the slurry, which was then shaken at room temperature for 48 h. Note that all the solvents and solutions were ultrasonicated in order to remove traces of oxygen that might disturb the click reaction. The reaction slurry was washed several times with 0.1 M HCl, 0.5 M NaOH and 0.1 M EDTA. After complete removal of ligands, reagents and copper, the final A2P-TRZ material (**4b**) was rinsed several times with bi-distilled water and HPLC grade methanol before storage in 20% methanol in bi-distilled water. The ligand density was determined via the nitrogen value after subtraction of the nitrogen increment of the underlying azido-modification. *Elemental analysis:* FG-TRZ-A2P coverage: 335  $\mu$ mol/g (C, 52.9 %; H, 7.47 %; N, 7.47 %).

2) Azido-Purabead: Because of the lower azide density of Azido-Purabead this reaction procedure, although basically the same, will be described separately. 832 mg of A2P-amino-propyne and 226  $\mu$ L DIPEA were dissolved in 50 mL acetonitrile and were added to 15 mL of azido-activated PuraBead. 61 mL of a 10 mg/mL copper(I) iodide solution in acetonitrile was poured to the slurry and shaken at room temperature for 48 h. The

washing procedure was equivalent to that described for Fractogel-TRZ-A2P. *Elemental analysis*: AG-TRZ-A2P-coverage: 225  $\mu\text{mol/g}$  (C, 47.03 %; H, 6.42 %; N, 3.49 %)

Note that none of these materials possessing a TRZ-group in their spacer arm, are azido endcapped, meaning that they possess residual azide-groups, after immobilization of the alkyne terminal ligand head-groups. The effect such residual azido groups may have on material performance will be discussed elsewhere in more detail [1].

### **3. Affinity Chromatography**

Three different antibody containing feed solutions were prepared. The first feed solution F1, is a mock feed of well defined chemical composition, that was designed to mimic a “real” Mab supernatant. It contains 1 g/L polyclonal IgG, 1 g/L horse skeletal myoglobin, and 5 g/L human serum albumin in PBS with pH 7.4. Alternatively 1 g/L of the anti-foaming agent Pluronic F-68 was added to F1. The second feed solution F2, is a real CHO cell culture supernatant with human monoclonal IgG1. The third feed solution F3, contains only 1 g/L of pure polyclonal IgG in PBS, pH 7.4. All feed solutions were filtered prior to use.

For the feed solutions F1 and F3, an affinity gel volume of 4.3 mL was packed in C10/20 columns and adjusted to 5.5 cm bed height. Chromatography was performed with a linear flow rate of 300 cm/h and a volumetric flow rate of 3.93 mL/min, which corresponded to an overall residence time of 1.1 minutes.

After packing the adsorbent was equilibrated for 5 column volumes (CV) using PBS, pH 7.4 (equilibration buffer). The adsorbent was loaded with 20 g of IgG per L of adsorbent. The loosely bound or non-bound feed impurities e.g. proteins and DNA were removed with 10 CV of equilibration buffer followed by 5 CV of 50 mM citric acid,

pH 3.5 (pH adjusted with NaOH). The clean in place (CIP) was completed with 5 CV of 0.5 M NaOH.

For feed solution F2 an affinity gel volume of 2.0 mL and a bed height of 2.5 cm were chosen. Chromatography was performed with a linear flow rate of 160 cm/h, a volumetric flow rate of 1.68 mL/min, and a residence time of 1.1 minutes. All process conditions were the same as for feed solutions F1 and F3.

*Summary of experimental data:*

Concerning the sensitivity of the materials towards HSA, it is noteworthy to mention that the results stated in **Table S2** provide only information about the HSA amount that was eluted from the materials during the elution step with citric acid (pH 3.5) and may therefore not necessarily correlate with the actual amount of HSA that was bound to the material. The application fractions as well as the wash and sanitation solutions were not tested for HSA. Generally it can be concluded that Agarose-based A2P materials bind and elute HSA independently from the spacer-arm chosen. Besides that, HSA was also found in the elution fractions of FG1-TRZ-A2P and FP1-DES-A2P.

**Table S2.** Binding and elution data for A2P coupled adsorbents for the mock feedstock F1, containing IgG, MYO and HSA in PBS (pH 7.4) with and without addition of Pluronic F68.

		<b>F1 (no Pluronic) <sup>2)</sup></b>			<b>F1 (with Pluronic) <sup>2)</sup></b>		
<b>Adsorbent <sup>1)</sup></b>	<b>Ligand density [μmol/g dry]</b>	<b>BC-IgG [g/L]</b>	<b>EC-IgG [g/L]</b>	<b>EC-HSA [g/L]</b>	<b>BC-IgG [g/L]</b>	<b>EC-IgG [g/L]</b>	<b>EC-HSA [g/L]</b>
<b>AG-2LP-A2P</b>	497	12.6	9.4	0.32	0.98	0.34	0.21
<b>AG-SS3-A2P</b>	231	5.2	3.7	1.1	7.4	1.0	< 0.2
<b>AG-TRZ-A2P</b>	225	5.2	4.8	0.33	3.4	1.8	0.33
<b>FG2-2LP-A2P</b>	100	1.8	0.0	< 0.2	1.7	0.1	< 0.2
<b>FG1-2LP-A2P</b>	350	3.6	1.9	< 0.2	0.0	0.0	< 0.2
<b>FG1-SS3-A2P</b>	371	1.9	0.9	< 0.2	0.95	0.0	< 0.2
<b>FG1-DES-A2P</b>	351	3.4	1.7	< 0.2	1.7	2.2	< 0.2
<b>FG1-TRZ-A2P</b>	335	3.5	1.1	0.42	7.3	0.6	< 0.2
<b>FP3-2LP-A2P</b>	40	0.0	0.0	< 0.2	4.9	4.6	< 0.2
<b>FP2-2LP-A2P</b>	75	1.8	0.0	< 0.2	1.7	0.1	< 0.2
<b>FP1-2LP-A2P</b>	248	10.2	6.4	< 0.2	16.6	8.1	< 0.2
<b>FP1-SS3-A2P</b>	330	7.5	1.9	< 0.2	0.95	0.98	< 0.2
<b>FP1-DES-A2P</b>	325	10.5	2.4	0.9	2.0	0.0	0.9
<b>FS-2LP-A2P</b>	40	6.5	4.3	< 0.2	5.9	3.7	< 0.2
<b>Rmp Protein A Sephacrose FF</b>	n.a.	16.7	15.6	< 0.2	15.9	15.3	< 0.2

<sup>1)</sup> the following denominations are used for the adsorbents:

support: Agarose PuraBead (AG), Fractogel (FG), Fractoprep (FP) and Fractosil (FS)

spacer: diaminoethyl (2LP), 1,3-propanedithiol (SS3), 3,6-dioxo-1,8-octanedithiol (DES) and [1,2,3]-triazole (TRZ).

ligand density: not available (n.a.)

<sup>2)</sup> binding capacity (BC), elution capacity (EC), immunoglobulin (IgG), human serum albumin (HSA); BC-IgG and EC-IgG determined via Protein A HPLC and EC-HSA via nephelometry

**Table S3.** IgG Binding and elution data for A2P coupled adsorbents tested with cell culture media, pH 7.4 (F2) and IgG in PBS, pH 7.4 (F3)

		F2 (with Pluronic) <sup>2)</sup>			F3 (no Pluronic)	
Adsorbent <sup>1)</sup>	Ligand density [μmol/g dry]	BC-IgG [g/L]	EC-IgG [g/L]	EC-Imp. [g/L]	BC-IgG [g/L]	EC-IgG [g/L]
<b>FP1-2LP-A2P</b>	248	2.1	1.3	3.5	n.a.	n.a.
<b>FS-2LP-A2P</b>	40	1.9	1.3	2.6	n.a.	n.a.
<b>AG-2LP-A2P</b>	497	0.0	0.0	0.4	17.7	13.6
<b>AG-SS3-A2P</b>	231	2.3	0.6	1.2	14.8	7.2
<b>AG-TRZ-A2P</b>	225	3.5	0.6	0.4	16.3	6.1
<b>FG1-TRZ-A2P</b>	335	1.1	0.8	1.7	14.0	8.1
<b>Rmp Protein A Sephacrose FF</b>	n.a.	3.6	4.7	0.1	18.6	19.2

<sup>1)</sup> the following denominations are used for the adsorbents:

support: Agarose PuraBead (AG), Fractogel (FG), Fractoprep (FP) and, Fractosil (FS)

spacer: diaminoethyl (2LP), 1,3-propanedithiol (SS3) and [1,2,3]-triazole (TRZ).

ligand density: not available (n.a.)

<sup>2)</sup> binding capacity (BC), elution capacity (EC), immunoglobulin (IgG), feed impurities (Imp.); BC-IgG and EC-IgG determined via Protein A HPLC and EC-Imp. via Bradford minus the IgG-content determined via Protein A HPLC

## 4. Protein Quantification

### 4.1. Photometric quantification of proteins at 280 nm

The IgG concentration for all chromatography fractions using F3 was determined photometrically measuring the protein absorption at 280 nm. Measurements were performed at a light path of 1cm, using an extinction coefficient of 1.4 for a 1 mg/mL solution of IgG (Gammonorm). PBS buffer at pH 7.4 was used as a blank and samples were tested using quartz cuvettes.



#### **4.2. The Bradford Assay – total protein determination**

The Bradford method used is an adaptation of the classical Bradford Coomassie Blue-binding colourimetric method for total protein quantitation. The “Coomassie (Bradford) Protein Assay Kit” from Pierce (Surrey, UK) [2] contains coomassie G-250 dye and bovine gamma globuline (2 mg/mL) in a solution of 0.9 % saline and 0.05 % sodium azide. This kit is used in a microplate format, with a Bovine Gamma Globulin (BGG) standard curve (from 25-300 µg/mL) in order to determine the total protein concentration present in IgG feed solutions (F1 and F2) as well as the chromatographic samples thereof. For the assay 20 µL from each standard and sample (in duplicates) were transferred into designated wells of a 96-well microplate, and then 180 µL of the Coomassie-Bradford reagent added to each well. The standards, samples and coomassie reagent were mixed and incubated at room temperature on a microplate shaker for 10 minutes. The microplate was read at 590 nm. All samples from F1 and F2 were analysed using the Bradford assay to determine purity and mass balance, however, data will not be shown here.

#### **4.3. Protein A HPLC**

This method used a Protein A (PA ID sensor cartridge column, Applied Biosystems) under specific conditions to determine the concentration of IgG present in samples [3]. Samples were adsorbed with 10 mM sodium phosphate buffer containing 150 mM NaCl at pH 7.2 (adsorption buffer) onto the Protein A column. IgG was eluted using 12 mM HCl containing 150 mM NaCl, pH 2.0 (elution buffer) and was detected at 280 nm. The standard curve established for IgG quantification ranged from 25 µg/mL to 1000 µg/mL with all standards prepared in the adsorption buffer.

#### **4.4. Nephelometry**

The Dade-Behring BNII Nephelometer uses an immunological light scattering technique to determine the formation of immune complexes between the protein of interest (in this case IgG) and an antibody specific for that protein. The technique is based on 'cloudiness' of the solution as the insoluble immune complexes are formed. The measurement is kinetically dependant, as the turbidity of the solution falls as aggregates begin to precipitate out of solution. This assay specifically measured the human polyclonal IgG concentration of the chromatography samples.

The standard curve for human IgG was prepared using N-antiserum to human IgG and N protein standard PY reagent (supplied by Seimens). The standard curve range was between 3.6 µg/mL and 114 µg/mL. The Nephelometer automatically dilutes the samples to be within the standard curve range. This technique was used to measure the IgG content of F1 in the presence and absence of Pluronic F-68. This method is used in preference to the Protein A method as it has been specifically developed to quantify monoclonal and not polyclonal IgG.

#### **4.5. SDS-PAGE Gel electrophoresis**

Samples were prepared by adding 10 µL of the sample to 35 µL of sample buffer and 55 µL of reverse osmosis (RO) water. 5 µL of the prepared sample was loaded into each well of the gel and a molecular weight marker was added to one lane of the gel. The running buffer used was MOPS (1x). After running the gel was removed from the cassette and placed into a dish with ~ 100 mL of RO water and microwaved for 1.5 minutes (high setting on a 650 W microwave). The gel was then agitated for 1 minute and then the water was discarded. This repeated twice then 20 mL of Simply Blue Safestain is added and

microwaved for 60 seconds. The gel is agitated in the stain for 5 minutes after which the stain is discarded and the gel is washed in RO water for 10 minutes by agitation.

## **5. Reference**

- [1] J. Horak, S. Hofer, W. Lindner, to be submitted shortly to J.Chromatogr.A (2009).
- [2] P. Instructions to the Coomassie (Bradford) Protein Assay Kit (23200), Surrey, UK, <http://www.piercenet.com/files/0129as4.pdf>.
- [3] A.B. Operation Instructions for PA ImmunoDetection Sensor Cartridge for Perfusion Immunoassay Technology (8-0038-40-1193 Rev. B), Foster City, USA, <http://docs.appliedbiosystems.com/pebi docs/80038401.pdf> (2002) 1.

## Theoretical Section

### 1. Methodology

#### *IgG molecular model details*

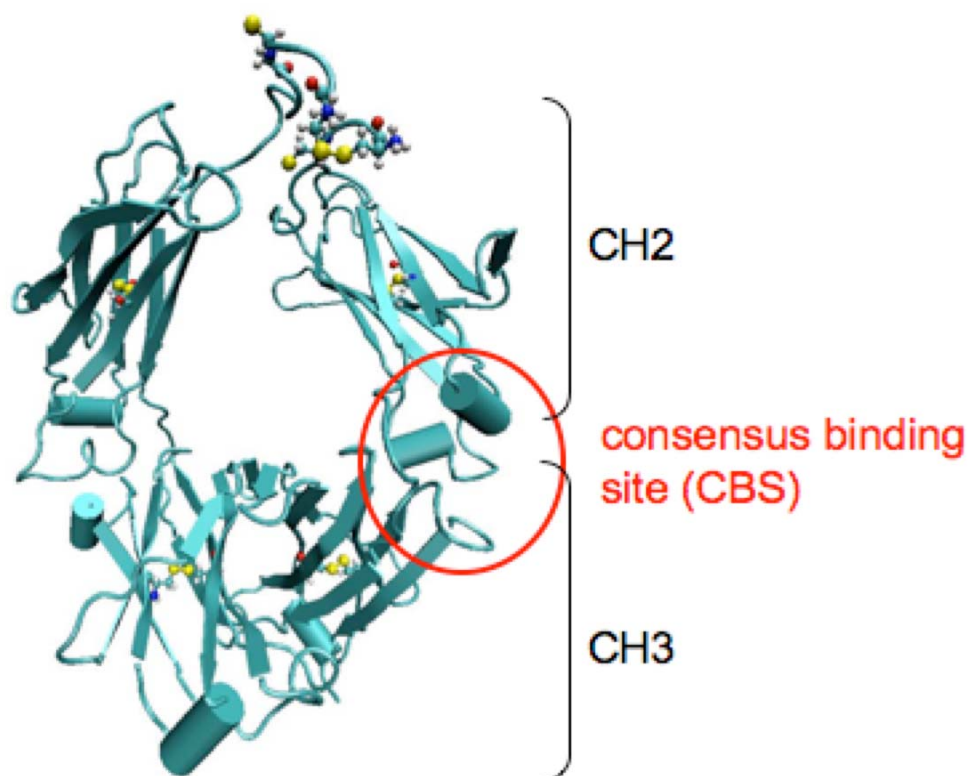


**Figure S1.** Model of the Fc domain of IgG:  $\alpha$ -helixes are represented as cylinders,  $\beta$ -sheets as arrows; cysteine residues are fully displayed to highlight disulfide bridges.

The Fc fragment consists of two identical domains, each formed by two sub-domains, namely the CH2 and CH3 chains; the CH3 domains are kept together at the base by hydrophobic interactions, while the two CH2 chains are connected at the top by a cysteine bond. The amino acid sequence of the PDB file was cut in correspondence of these cysteine residues, as the disulfide bond is necessary to guarantee the stability of the structure of the Fc domain during the MD simulations. Hydrogen atoms were added

considering HIS residues not protonated, as this is the active form of histidines at the pH at which chromatographic separations of IgG is usually performed (pH = 7.6 for A2P<sup>22</sup>); subsequently a MD simulation of 2 ns was performed in explicit water to allow the Fc structure to relax from its crystallographic pose. Residues of the Fc sequence are referred to in the following according to Deisenhofer's numeration of the IgG – protein A complex (PDB id 1FC2<sup>57</sup>).

#### *Agarose molecular model details*

In this work, Agarose was represented by two intertwined double helices; this structure was previously obtained through a 30 ns MD simulation of two parallel Agarose double helices containing 108 Agarose residues each, solvated using explicit TIP3P water molecules and a solvent shell of 12 Å. After 15 ns the system converged to the structure reported in **Figure S2**, which was maintained for the successive 15 ns.<sup>24</sup> This model has the advantage of being more stable and subject to fewer deformations than the structure formed by only one double helix: this is an important requirement as it corresponds to the observed lack of reactivity of Agarose when proteins are present. The size of this system is comparable to that of the protein that we intend to simulate and significantly smaller than that of the Agarose pores (typical diameters of 50-500 nm), thus the curvature of the surface of an Agarose pore due to its pseudo-cylindrical shape can not be observed at the length scales here investigated and can thus safely be neglected.

The third model adopted for the Agarose surface (**Figure 2**), consisting of three intertwined double helices, was developed following a similar procedure using as starting block the stabilized molecular model of **Figure S2**.

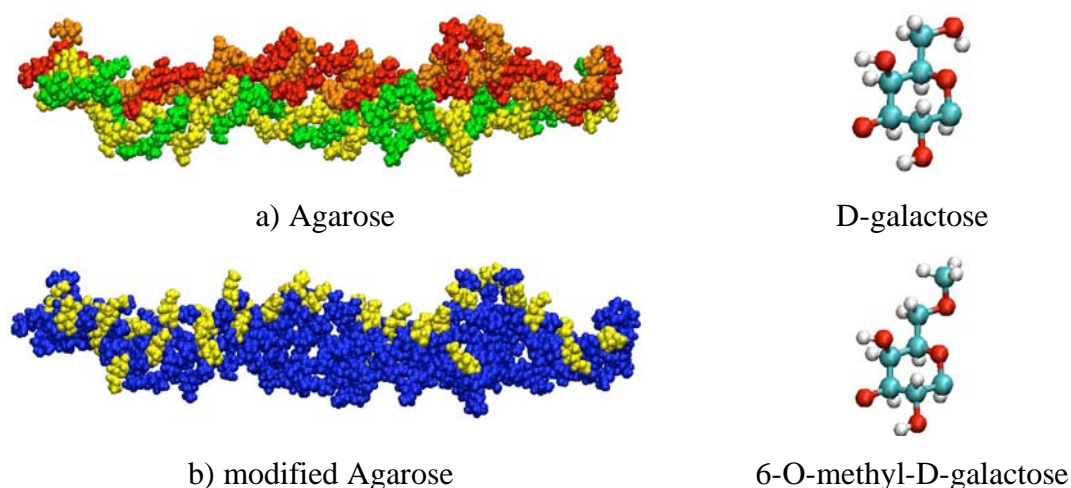


**Figure S2.** Structures of the molecular models of the two supports: a) Agarose and b) Agarose modified with 6-O-methyl-galactose units (in yellow).

#### *Spacers and ligand molecular model details*

New parameters were evaluated for A2P and for the spacers, consistently with Parm94: their geometry was first optimized using density functional theory at the B3LYP/6-31g(d,p) level;<sup>58-60</sup> partial atomic charges were subsequently determined using the RESP formalism on the electrostatic field computed through DFT.<sup>61</sup> The Parm94 force field was then used for the MD simulations using the electrostatic charges determined through quantum chemistry. Solvation free energies of the spacers were determined using the IEFPCM implicit solvation model<sup>62</sup> at the B3LYP/6-31g(d,p) level.

#### *Molecular dynamics simulation details*

The computational protocol adopted for the MD simulations comprised an initial 2000 cycles minimization, in which the complex was restrained with a harmonic potential of the form  $k(\Delta x)^2$ , where  $\Delta x$  is the displacement and  $k$  the force constant ( $k = 500 \text{ kcal/mol/\AA}^2$ ): this first step allowed to remove the unfavourable contacts made by the solvent. Subsequently a second 1500 cycle minimization was performed without restraints. The

temperature was then raised from 0 to 300 K by a simulated annealing of 20 ps at constant volume; during this phase, a weak restraint was imposed on the solute (harmonic potential of the form  $k(\Delta x)^2$ ,  $k = 10 \text{ kcal/mol/\AA}^2$ ) in order to avoid wild fluctuations of its structure. After heating the system, a 100 ps run (equilibration run) was performed at constant pressure to allow the water density to relax. Finally MD simulations were performed for a standard period of 15 ns. Both in the equilibration step and in the standard MD run the terminal residues of the support were restrained ( $k = 10 \text{ kcal/mol/\AA}^2$ ) to correctly reproduce its rigidity; the simulations were performed at 300 K and constant atmospheric pressure. The SHAKE algorithm was used for all the covalent bonds involving hydrogen, which allowed the use of a time step of 2.0 fs.<sup>63</sup> The non-bonded cut off was set to 10 Å.

**Table S4.** Interaction free energies calculated using the Autodock<sup>44</sup> scoring function for the best 15 poses for each A2P-spacer pair; the pose selected for MD simulations is the one in bold (energies in kcal/mol).

	<b><math>\Delta G</math> score (kcal/mol)</b>				
	<b>DES</b>	<b>SS3</b>	<b>TRZ</b>	<b>2LP (CBS)</b>	<b>2LP (non CBS)</b>
<b>1</b>	<b>-7.90</b>	<b>-5.43</b>	<b>-9.09</b>	-9.67	-9.98
<b>2</b>	-7.74	-4.84	-7.97	-9.63	-9.61
<b>3</b>	-6.58	-4.38	-7.75	-9.53	-9.54
<b>4</b>	-6.48	-3.60	-7.57	-9.44	-9.54
<b>5</b>	-6.44	-3.40	-7.39	-9.39	-9.52
<b>6</b>	-6.40	-3.37	-7.34	-9.38	<b>-8.65</b>
<b>7</b>	-6.40	-3.09	-7.27	-9.35	-8.23
<b>8</b>	-6.30	-2.97	-7.09	-9.34	-8.21
<b>9</b>	-6.04	-2.90	-7.06	-9.17	-8.11
<b>10</b>	-6.04	-2.79	-6.91	-9.10	-7.77
<b>11</b>	-5.87	-2.76	-6.91	-9.07	-7.74
<b>12</b>	-5.73	-2.54	-6.88	<b>-8.98</b>	-7.62
<b>13</b>	-5.72	-2.52	-6.76	-8.97	-7.59
<b>14</b>	-5.55	-2.49	-6.62	-8.91	-7.59
<b>15</b>	-5.20	-2.48	-6.54	-8.73	-7.58

To make sure that the initial pose would not affect the analysis of the system and that the results would have a general validity, a second pose was chosen as starting structure for the system with the 2LP spacer, in which the ligand is still placed in the CBS, but in a slightly different pose from the reference structure. Comparing the two poses, it can be noted that one of the two hydroxyphenyl groups of A2P almost occupies the same position, while the second one is oriented in the opposite direction (**Figure S3a**). MD simulations performed for 15 ns revealed that the system converges to interactions of the same extent (15 ns), as is clearly shown in **Figure S3b**, that reports van der Waals and electrostatic interactions of the A2P-2LP pair with the surrounding environment in the two cases. However, when the second pose is considered, a longer time is needed to reach a stable configuration.

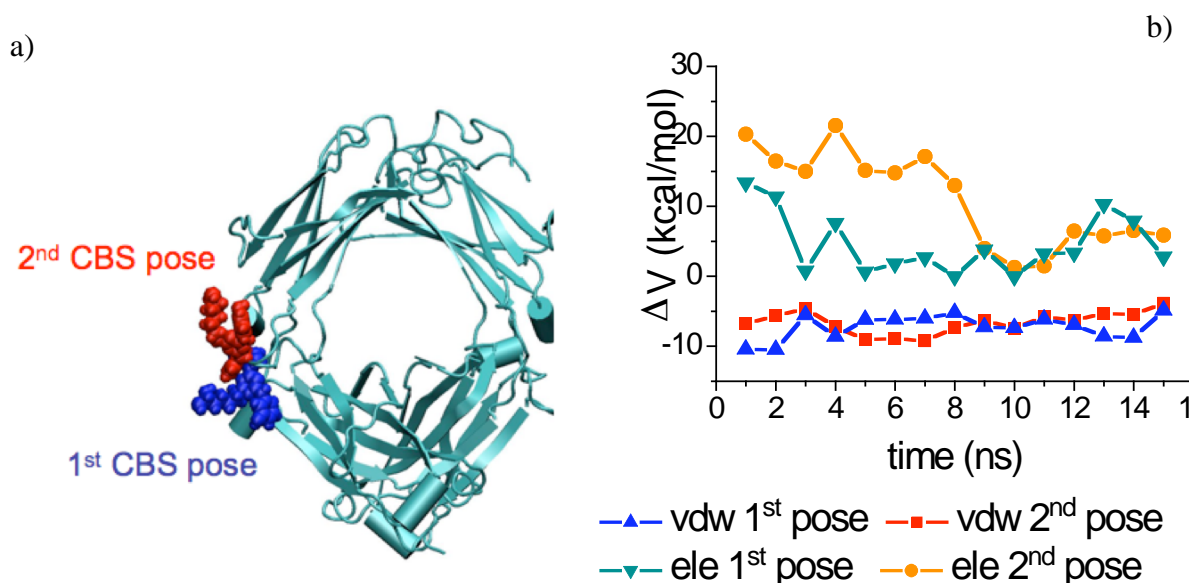


**Figure S3.** Comparison between the two poses of the 2LP-A2P pair in the CBS (the first one is the optimal pose): a) initial structure; b)  $\Delta V_{free \rightarrow bound}^{vdw,ele}$  of the spacer-ligand pair with the surrounding environment (support, solvent and Fc domain).



**Table S5.** Length and solvation free energy of the investigated spacers computed at the B3LYP level using the IEFPCM implicit solvation model for water.

	Spacer	$\Delta G_{\text{solvation}}$ [kcal/mol]	Length [Å]
<b>2LP</b>	-CH <sub>2</sub> -CHOH-CH <sub>2</sub> -NH <sub>2</sub> -(CH <sub>2</sub> ) <sub>2</sub> -NH-	-17.34	6.46
<b>TRZ</b>	-CH <sub>2</sub> -CHOH-CH <sub>2</sub> -(C <sub>2</sub> HN <sub>3</sub> )-CH <sub>2</sub> -NH-	-0.49	7.87
<b>SS3</b>	-CH <sub>2</sub> -CHOH-CH <sub>2</sub> -S-(CH <sub>2</sub> ) <sub>3</sub> -S-	1.03	8.98
<b>DES</b>	-CH <sub>2</sub> -CHOH-CH <sub>2</sub> -S-(CH <sub>2</sub> ) <sub>2</sub> -O-(CH <sub>2</sub> ) <sub>2</sub> -O-(CH <sub>2</sub> ) <sub>2</sub> -S-	2.72	15.05

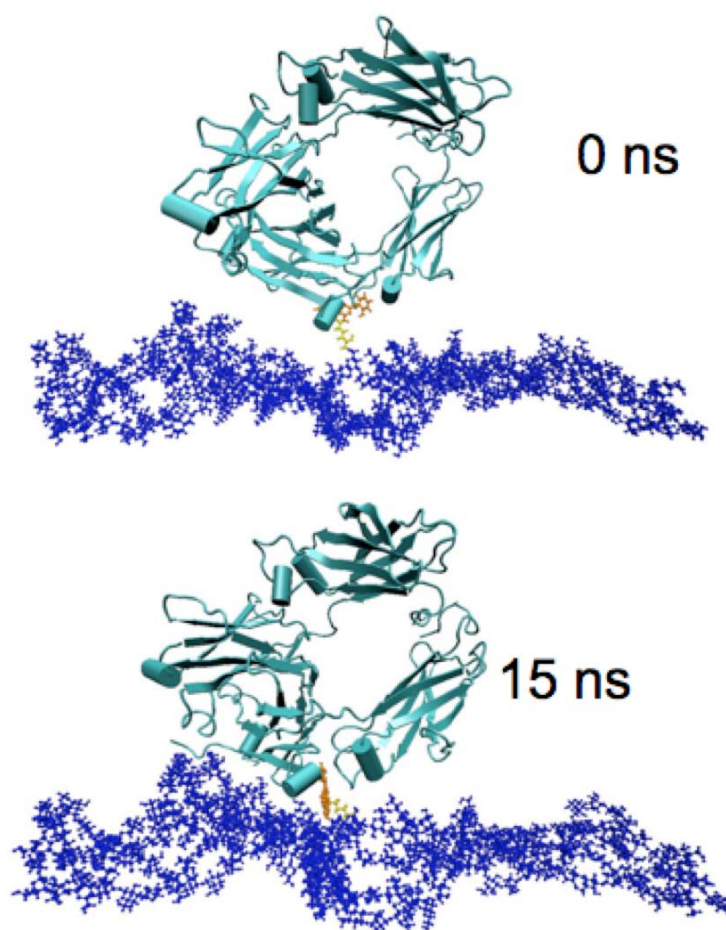


**Figure S4.** Initial (CBS pose, on the left) and final structure (after 15 ns, on the right) of the MD simulation of the complex between IgG and A2P supported on Agarose through the 2LP spacer.

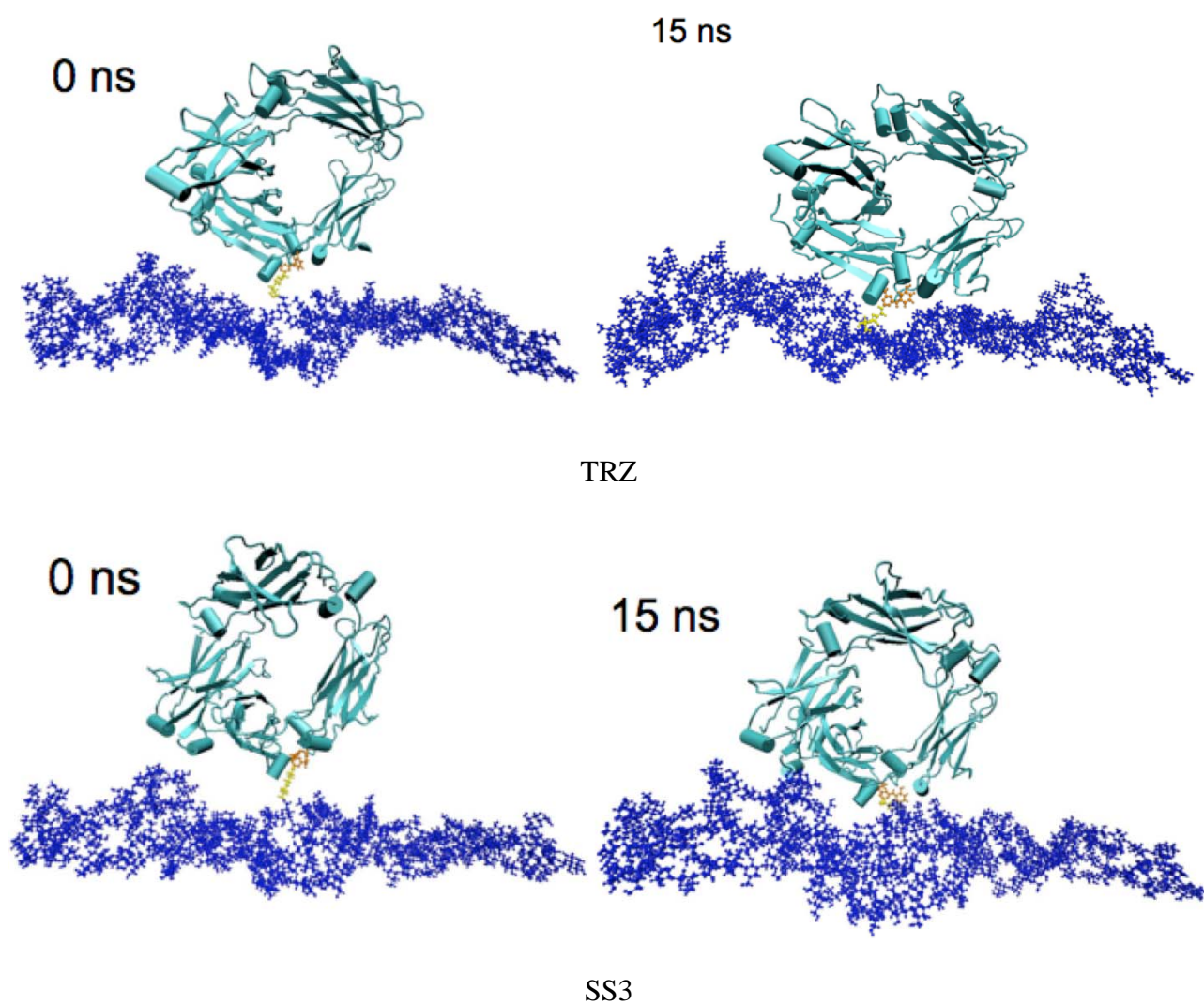


**Figure S5.** Initial (CBS pose, on the left) and final structure (after 15 ns, on the right) of the MD simulation of the complex between the Fc domain of IgG and A2P supported on Agarose through the TRZ and SS3 spacers.

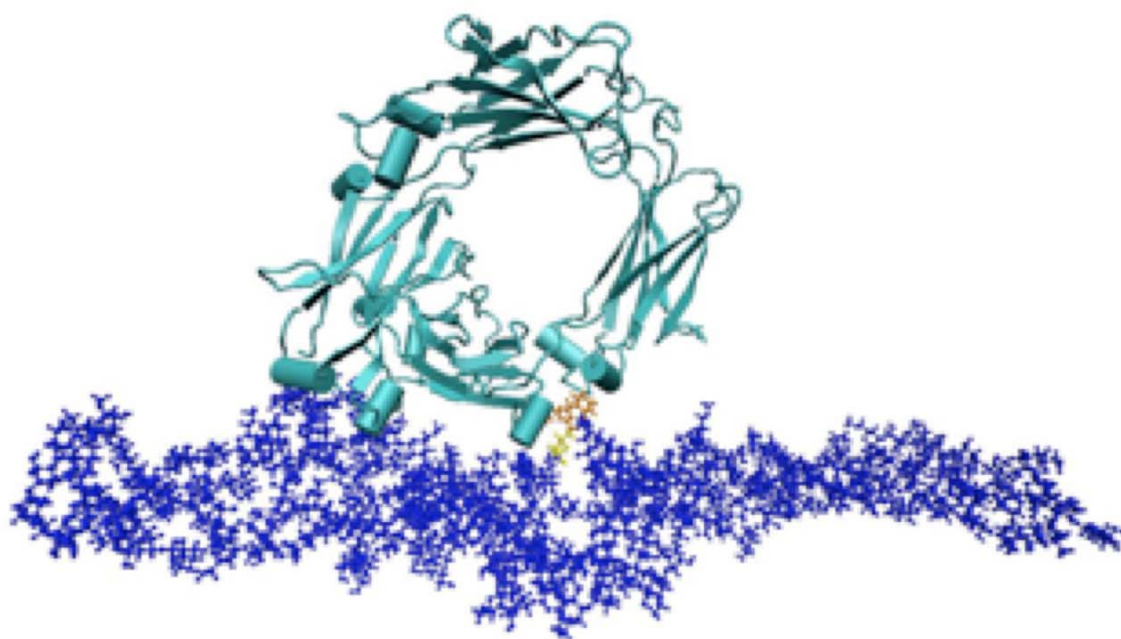


**Figure S6.** Structure of the A2P ligand immobilized with the 2LP spacer on the extended Agarose surface and IgG after 15 ns of simulation.

**Table S6.** Electrostatic (ele) and van der Waals (vdw) interaction energies evaluated for A2P-2LP for the non CBS pose and for the Agarose structure modified inserting 6-O-methyl-galactose units.

		2LP – non CBS - Agarose <sup>a</sup>			2LP – CBS - modified Agarose		
		<i>spacer</i>	<i>Ligand</i>	<i>total</i>	<i>spacer</i>	<i>ligand</i>	<i>total</i>
<b>Free system(support-2LP-A2P)</b>							
H <sub>2</sub> O <sup>b</sup>	vdw	-4.94	-19.00	-23.94	-5.55	-16.77	-22.32
	ele	-25.92	-52.74	-78.66	-24.48	-53.35	-77.83
Support	vdw	-6.80	-10.87	-17.67	-3.79	-14.68	-18.47
	ele	-14.43	-2.28	-16.71	-18.43	-0.52	-18.95
<b>Bound system (support-2LP-A2P-FC)</b>							
H <sub>2</sub> O+FC	vdw	-8.89	-37.11	-46.00	-8.40	-36.97	-45.37
	ele	-37.70	-40.90	-78.60	-34.41	-43.02	-77.43
Support	vdw	-1.34	-1.03	-2.36	-1.33	-4.36	-5.69
	ele	-2.84	-0.14	-2.98	-1.86	-1.12	-2.98
<b><math>\Delta V</math> (bound – free)</b>							
H <sub>2</sub> O+FC	vdw	-3.94	-18.11	-22.06	-2.85	-20.20	-23.05
	Ele	-11.77	11.84	0.06	-9.93	10.33	0.4
Support	vdw	5.46	9.84	15.31	2.46	10.32	12.78
	ele	11.60	2.14	13.73	16.56	-0.60	15.96
<b>Total <math>\Delta V</math> of</b>	vdw	1.52	-8.27	-6.75	-0.39	-9.89	-10.28
H <sub>2</sub> O+FC+support	ele	-0.18	13.98	13.79	6.63	9.73	16.36

a) Average values were evaluated in the 5–15 ns time span for system supported on Agarose (non CBS pose) and in the 10–15 ns time span in the case of modified Agarose.

b) The first column reports the contribution of surrounding environment (H<sub>2</sub>O, Fc, support) considered when evaluating the interaction of the A2P-2LP pair.

## XYZ coordinates

### 2LP-TRN EDME

7	0	-4.035702	-1.513519	0.085317
6	0	-2.764163	-1.100974	0.321240
7	0	-2.347886	0.184759	0.236810
6	0	-3.305613	1.051351	-0.080208
7	0	-4.590489	0.769267	-0.332006
6	0	-4.877553	-0.540510	-0.234187
7	0	-1.873012	-2.049927	0.671026
6	0	-0.479167	-1.791175	0.968867
6	0	0.377378	-1.841193	-0.304655
7	0	1.814045	-1.558741	0.014111
6	0	2.759760	-1.600081	-1.204371
8	0	2.828047	-2.911419	-1.650146
6	0	4.129040	-1.120472	-0.759031
8	0	2.032833	0.900069	1.409114
6	0	2.654843	0.797310	2.692288
6	0	1.691656	2.248039	1.070649
6	0	1.011516	2.252295	-0.290142
8	0	0.731239	3.603606	-0.603765
6	0	0.139996	3.755188	-1.884503
1	0	-2.219008	-3.012969	0.703443
1	0	-3.014243	2.101027	-0.139205
1	0	-5.910031	-0.833808	-0.437091
1	0	-0.391597	-0.809831	1.441913
1	0	-0.137424	-2.549927	1.681087
1	0	0.330281	-2.828101	-0.770736
1	0	0.044968	-1.087297	-1.023532
1	0	1.892933	-0.626445	0.476607
1	0	2.158173	-2.270400	0.689203
1	0	2.305536	-0.924717	-1.943063
1	0	2.209351	-3.048154	-2.405004
1	0	4.787487	-1.088119	-1.629725
1	0	4.077938	-0.120179	-0.320717
1	0	4.555982	-1.814867	-0.028138
1	0	-0.818859	3.220603	-1.954042
1	0	0.802646	3.385401	-2.680746
1	0	-0.036751	4.822644	-2.034216
1	0	0.087457	1.652852	-0.254928
1	0	1.680155	1.807872	-1.047299
1	0	2.599867	2.865772	1.036940
1	0	1.016325	2.664091	1.830952
1	0	2.884641	-0.256952	2.861759
1	0	3.583534	1.380380	2.722385
1	0	1.978827	1.151543	3.480064

# SS3-TRN EDME

7	0	-5.781083	1.300602	0.125911
6	0	-4.645526	0.681646	-0.242684
7	0	-4.522486	-0.629494	-0.481960
6	0	-5.652631	-1.326007	-0.329203
7	0	-6.840979	-0.831512	0.029508
6	0	-6.833258	0.492359	0.241785
16	0	-3.258140	1.759172	-0.409619
6	0	-1.905105	0.603080	-0.866538
6	0	-1.295731	-0.139420	0.326673
6	0	-0.155752	-1.054058	-0.130688
16	0	0.530482	-1.966362	1.316797
6	0	1.755445	-3.072287	0.507454
1	0	-5.595205	-2.399374	-0.516382
1	0	-7.776524	0.953267	0.538502
1	0	-2.302681	-0.092229	-1.609543
1	0	-1.167400	1.246880	-1.356845
1	0	-0.926086	0.587167	1.059857
1	0	-2.073906	-0.733085	0.817441
1	0	-0.522978	-1.793617	-0.851212
1	0	0.654359	-0.490652	-0.598966
6	0	3.100659	-2.445085	0.177730
1	0	1.905573	-3.897134	1.211737
1	0	1.297332	-3.485081	-0.397681
1	0	3.771443	-3.259553	-0.149052
8	0	2.941302	-1.473901	-0.845403
1	0	3.536628	-2.005897	1.087398
1	0	3.798881	-1.018262	-0.945325
6	0	6.613662	-0.775706	-0.985865
1	0	6.874750	-1.213047	-0.012456
1	0	7.434978	-0.125097	-1.314317
1	0	6.472988	-1.575584	-1.715555
8	0	5.390463	-0.049979	-0.916659
6	0	5.436546	1.024574	0.018320
6	0	4.119559	1.778951	-0.077733
1	0	5.580822	0.644834	1.040832
1	0	6.274690	1.696641	-0.216969
8	0	4.166928	2.826180	0.874630
1	0	3.990028	2.175148	-1.097726
1	0	3.282664	1.091605	0.122904
6	0	2.984169	3.606246	0.878212
1	0	3.110054	4.381132	1.637811
1	0	2.812078	4.084813	-0.097465
1	0	2.100106	3.000831	1.128619

## TRZ-TRN EDME

7	0	0.372841	1.190194	-1.043613
7	0	0.841899	0.172439	-1.795223
7	0	0.198139	-0.911386	-1.435040
6	0	-0.686918	-0.599742	-0.444590
6	0	-0.581597	0.753261	-0.187432
6	0	-1.592181	-1.632844	0.165021
7	0	-2.905932	-1.718244	-0.470699
6	0	-3.965285	-0.963138	-0.134350
7	0	-5.094866	-1.122953	-0.876219
6	0	-6.116993	-0.373860	-0.488945
7	0	-6.134727	0.497343	0.535745
6	0	-4.965265	0.570163	1.187373
7	0	-3.856703	-0.109780	0.914096
6	0	0.921903	2.535857	-1.196199
6	0	1.824131	2.956639	-0.020128
8	0	2.944968	2.095853	0.103249
6	0	2.340290	4.374775	-0.246040
8	0	2.331894	-0.247958	1.536585
6	0	3.305709	-1.284957	1.465268
6	0	3.717197	-1.453333	0.009770
8	0	4.718602	-2.456828	-0.022862
6	0	5.200437	-2.699113	-1.333637
6	0	1.853291	-0.034224	2.859238
1	0	-3.008272	-2.293560	-1.310510
1	0	-4.914301	1.263776	2.029999
1	0	-7.041025	-0.474422	-1.063144
1	0	-1.740911	-1.426446	1.226422
1	0	-1.119784	-2.614123	0.067972
1	0	1.502732	2.523572	-2.121919
1	0	0.087595	3.235967	-1.308566
1	0	2.669890	1.270926	0.550397
1	0	2.968336	4.677802	0.595685
1	0	2.945820	4.418852	-1.157762
1	0	1.515610	5.087827	-0.340138
1	0	1.218526	2.939246	0.901855
1	0	-1.097330	1.409092	0.502554
1	0	2.668458	0.248354	3.539747
1	0	1.364218	-0.937364	3.248096
1	0	1.123342	0.776354	2.813082
1	0	4.184735	-1.033403	2.078290
1	0	2.883629	-2.226163	1.847378
1	0	2.844675	-1.736285	-0.597345
1	0	4.101717	-0.499686	-0.386119
1	0	5.963833	-3.477492	-1.260643
1	0	4.398830	-3.046050	-2.002723
1	0	5.650964	-1.796120	-1.772222





## **Appendix 4**

### **Publication 4**





# Optimization of a ligand immobilization and azide group endcapping concept via “Click-Chemistry” for the preparation of adsorbents for antibody purification

Jeannie Horak\*, Stefan Hofer, Wolfgang Lindner

*Institute of Analytical Chemistry, University of Vienna, Währingerstrasse 38, 1090-Vienna, Austria*

## ARTICLE INFO

### Article history:

Received 11 August 2010

Accepted 23 October 2010

Available online 30 October 2010

### Keywords:

Epoxide  
Azide  
Click reaction  
Protein A  
Size exclusion  
Antibody purification  
Protein aggregation  
B14-ligand  
Cell culture

## ABSTRACT

This report describes and compares different strategies to deactivate (endcap) epoxide groups and azide groups on bio-chromatographic support surfaces, before and after ligand attachment. Adsorbents possessing epoxide groups were deactivated using acidic hydrolysis or were endcapped with 2-mercaptoethanol or 2-ethanolamine. The influence of surface-bound 2-ethanolamine was demonstrated for the triazine-type affinity adsorbent B14-2LP-FractoAIMs-1, which was tested in combination with the weak anion exchange material 3-aminoquinuclidine-FractoAIMs-3 (AQ-FA3). Azide groups were modified with 2-propargylalcohol using Click-Chemistry. Besides the conventional one-pot Click reaction, an alternative approach was introduced. This optimized Click protocol was employed (i) for the preparation of the weak anion exchange material AdQ-triazole-FractoAIMs-3 (AdQ-TRZ-FG) and (ii) for the endcapping of residual azide groups with 3-propargyl alcohol. Using the new Click reaction protocol the ligand immobilization rate was doubled from 250 to 500  $\mu\text{mol/g}$  dry adsorbent. Furthermore, the modified support surface was proven to be inert towards the binding of immunoglobulin G (IgG) as well as feed impurities. A thorough evaluation of modified surfaces and adsorbents was performed with dynamic binding experiments using cell culture supernatant containing monoclonal human immunoglobulin G (h-IgG-1). Besides SDS-Page, a recently introduced Protein A – size exclusion HPLC method (PSEC-HPLC) [1] was used to visualize the feed impurity composition and the IgG content of all collected sample fractions in simple PSEC-Plots. A surprising outcome of this study was the irreversible binding of IgG to azide modified surfaces. It was found that organic azide compounds, e.g. 1-azide-3-(2-propen-1-yloxy)-2-propanol (AGE-N3) promote antibody aggregation to a slightly higher extent than the inorganic sodium azide. The possibility that the Hofmeister Series of salt anions may be applicable to predict the properties of the corresponding organic compounds is discussed.

© 2010 Elsevier B.V. All rights reserved.

## 1. Introduction

In recent years, monoclonal antibodies, in particular human or humanized immunoglobulin G (IgGs) have emerged as one of the key products in biopharmaceutical industry. Monoclonal antibodies (Mabs) are expected to not only maintain their position in the market, but to even further expand and dominate the biopharmaceutical landscape in the years to come. The production of Mabs is indisputably a billion dollar business. There is a constant need to improve the process design for both, the use of improved cell lines with increased growth rates using optimized cell media compositions [2] or the possibility to introduce more efficient purification technologies in downstream processing. In turn, every new process developed must be critically analyzed to ensure financial viability of the process change.

In this context, inter alia, a problem remains, the loss of therapeutic activity caused by an association of proteins in their unfolded or partially unfolded state, which is especially critical if non-target proteins are incorporated [3]. The overall therapeutic activity of such conglomerates (complexes) is highly unpredictable and need-less to say, their formation must be prevented. Another difficulty is that large aggregates are present in very small quantities of 0.3% or less. This makes their trace analytical detection rather difficult [4]. SDS-Page gel electrophoresis [5], field flow fractionation [5], turbidity [6] and size exclusion chromatography (SEC) combined with UV-detection, static light scattering detection (SLS) [7], dynamic light scattering detection (DLS) [4] and multi-angle laser light scattering (MALLS) detection [8,9] are frequently used techniques. The main factors for aggregate formation are the lowering of pH [10], heat [11,12] agitation [13], the addition or presence of certain preservatives or contaminants [14,13] and freezing as well as freeze-drying [15]. The lowering of the ion strength during ultra-/diafiltration in the last production steps seem to have a stronger effect on aggregate formation than sheer forces or a high

\* Corresponding author. Tel.: +43 1 4277 52373; fax: +43 1 4277 9523.  
E-mail address: [Jeannie.Horak@univie.ac.at](mailto:Jeannie.Horak@univie.ac.at) (J. Horak).

local protein concentration [16]. With the increased productivity in upstream processing and a certain concentration dependency of aggregate formation, general interests are now shifted towards the production of tailor-made, aggregate-resistant antibodies to enable even higher production rates for Mabs [17].

Alternatively, it is possible to further improve the purification media to enable milder elution conditions, e.g. as it is the case for optimized Protein A media [18] or to modify the elution conditions, e.g. through addition of sodium chloride, ethylene glycol or urea [19].

Overall, the production costs for MABs as therapeutics become a key factor in downstream processing, resulting in the high demand to reduce these constraints. As a consequence the replacement of Protein A affinity materials with non-proteinaceous, tailor-made affinity media for a specific drug or a group of drugs seem a promising alternative. Ligand library search based on “trial and error”, and computer modeling studies are often used for small synthetic, bio-mimetic and peptide-mimetic affinity ligands [20–22]. Besides that, genetic engineering has proven to be a potential tool for the design of large protein-type ligands with pre-defined properties [23].

Although affinity ligands can be very selective in the capture of their target protein, the effect the underlying support media, the spacer chemistry and other support surface modifications may have on the overall material performance should not be neglected and should be reviewed critically. Extensive studies on the influence of spacer length and spacer chemistry have shown that a simple change in spacer-chemistry can come with a very profound change in the antibody capture properties of the A2P-ligand head group (a synthetic ligand designed for the capture of antibodies) [24–27]. Besides thiophilic and amino-spacer chains also a new immobilization concept, suitable for biological and bio-active affinity ligands [28,29] was employed, the so-called “Click-Chemistry”. This copper (I) mediated 1,3-dipolar Huisgen cycloaddition reaction involves the coupling of an alkyne and an azide moiety, terminal on the ligand or the support surface. The result is the formation of a [1,2,3]-triazole linkage within the spacer chain [30]. Although advertised as easy going and straight-forward, still little is known about the precise mechanism of the coupling reaction [31–33]. A reaction scheme of a proposed mechanism is shown in Fig. 1. Recent studies show that Click-Chemistry is strongly dependant on the chemical properties of the reagents and the reactants used [34]. In case of solid phase reactions, the local environment surrounding the reacting groups, which includes the ligand itself may influence the yield of the Click-reaction strongly. Note that this immobilization concept was already applied for a variety of different chromatographic supports such as agarose [35,36], polymeric beads [37] and silica gel [38]. However, little to no information was provided concerning the possible reasons for the low immobilization rates.

The purpose of the presented study was to provide a better understanding about how and how strong the underlying surface modification can influence the performance of the final affinity adsorbent for the capture of h-IgG1. In order to unfold the contribution of a chosen endcapping strategy, it was necessary to investigate the modified support surfaces in the absence of the actual ligand. Only in the second step, an affinity-type ligand was introduced. It is important to mention that all modified support surfaces were tested with the same batch of cell culture feed to mimic near-real process conditions. This approach allowed a precise comparison of material performance. All test samples were measured with the in-house developed Protein A – size exclusion high performance liquid chromatographic (PSEC-HPLC) method [1] as well as SDS-Page gel electrophoresis using silver staining. In the final stage, possible reasons will be provided why azide-modified support surfaces bind IgG and how this problem was overcome using an improved Click Chemistry approach. The applicability of our optimized Click pro-

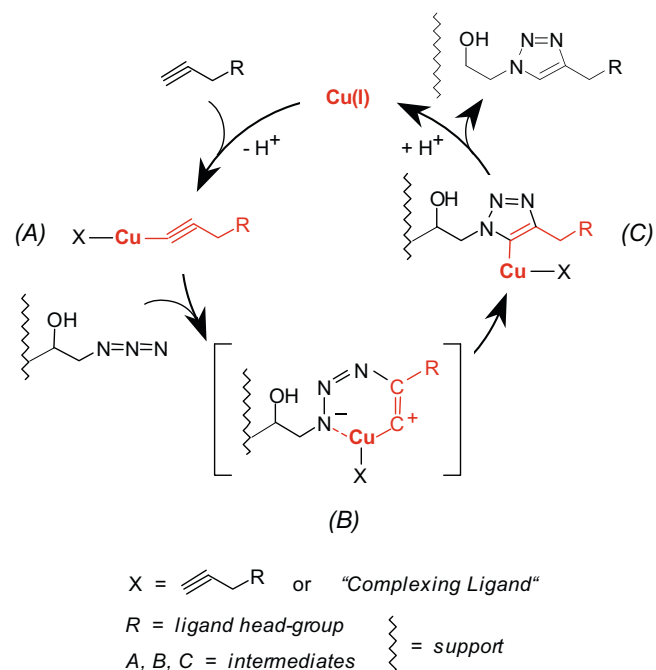


Fig. 1. Proposed mechanism for the Cu(I)-mediated 1,3-dipolar Huisgen cycloaddition reaction.

tolol was demonstrated for azide-group endcapping on support surfaces as well as affinity-ligand attachment.

## 2. Experimental

### 2.1. Chemicals and materials

The chemicals 1-(2-propenyloxy)-2,3-epoxy propane (AGE), 1-azabicyclo [2.2.2] octan-3-amine dihydrochloride (AQ  $\times$  2 HCl), dicyclohexylcarbo diimide (DCC), ethylenediaminetetraacetic acid (EDTA), 4-pentynoic acid, 2-ethanolamine, 2-mercaptoethanol, 3-propargylalcohol, potassium dihydrogen phosphate, di-sodium hydrogen phosphate, sodium azide, sodium chloride (NaCl), sodium hydroxide, N-ethyl-diisopropylamine (DIPEA), triethylamine (TEA), citric acid (CA), hydrochloric acid and Amberlite IRA-402 were purchased from Sigma-Aldrich (Vienna, Austria).

Throughout this study only in-house bi-distilled water was used. Water, buffer solutions and cell culture feed were filtered through a 0.22  $\mu\text{m}$  cellulose acetate membrane filter from Sartorius, purchased through Wagner&Munz (Vienna, Austria). Note that 10 mM phosphate buffer saline (PBS) solutions with increasing NaCl content of 0 mM, 75 mM, 150 mM and 300 mM will be denominated as PBS-0, PBS-75, PBS-150 and PBS-300 throughout this article.

Polyclonal human immunoglobulin G, Gammanorm (h-IgG, 165 mg/mL) was from Octapharma (Germany). Cell culture supernatant containing approximately 50 mg/L human monoclonal IgG1 (h-IgG1) from CHO-expression systems with a pH of 7.5 and a conductivity of 17 mS/cm at 33 °C was obtained from ExcellGene (Monthey, Valais, Switzerland). Isoelectric focusing (IEF) of Protein A purified monoclonal antibodies (MAB) from clarified cell culture broth was done in collaboration with Merck KGaA (Darmstadt, Germany). The IEF showed that the MAB consisted of an undeterminable number of variants with pIs between 7.5 and 9.3. Sample dialysis was performed with Spectra/Pore® CE Float-A-Lyzer® G2 with 10 mL volume size and a molecular-weight-cut-off (MWCO) of 3.5–5 kDa from Spectrum Europe B.V. (Breda, Netherlands) For further information see Fig. S2 [39].

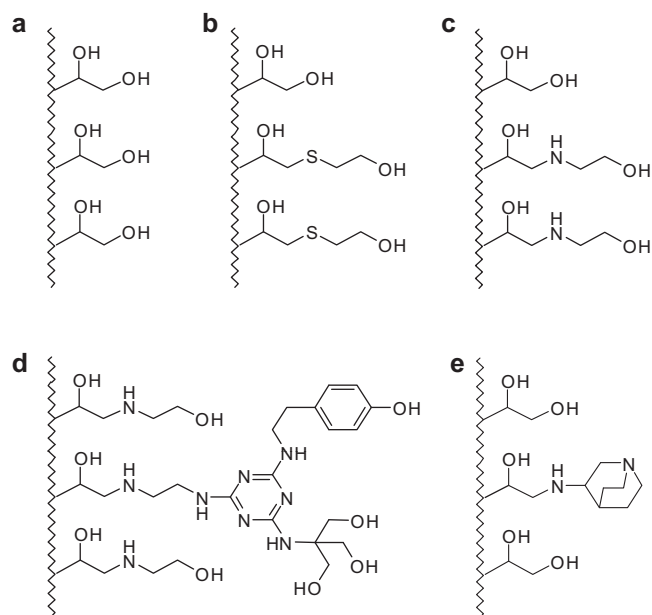


**Fig. 2.** Endcapping strategies for epoxide-activated Fractogel supports via (a) acid catalysed epoxide ring opening, (b) with 2-mercaptoethanol and (c) with 2-ethanolamine; (d) the IgG capture material B14-2LP-FA1, which comprises a triazine-core B14-ligand with a 1,3-diaminoethane spacer (2LP) bound to the non-commercial FractoAIMs-1 (FA1) support from Merck KGaA and is endcapped with 2-ethanolamine; (e) the weak anion exchanger 2-aminoquinuclidine-FractoAIMs-3 (AQ-FA3).

The Protein A HPLC Cartridge (PA ID Sensor Cartridge) from Applied Biosystems (Brunn am Gebirge, Austria) contained 0.8 mL of rigid polymeric POROS beads with an average particle size of 20  $\mu\text{m}$ . It also possessed large flow-through pores and smaller diffusion pores with pore sizes ranging from 5000 to 10,000  $\text{\AA}$ . The overall accessible surface area was stated as 1  $\text{m}^2/\text{cartridge}$  by the manufacturer. The silica-based TSKgel G3000SWXL column with 7.8 mm ID  $\times$  30.0 cm length (particle size: 5  $\mu\text{m}$ ) and the TSKgel SWXL guard column with 6.0 mm ID  $\times$  4.0 cm length were from Tosoh Bioscience (Stuttgart, Germany).

FractoAIMs<sup>®</sup>-1 (FA1) and FractoAIMs<sup>®</sup>-3 (FA3) were epoxy activated ( $\sim 0.93$  and 1.38 mmol/g (dry) gel), polymethacrylate-based, tentacle-grafted support media, designed by Merck KGaA (Darmstadt, Germany) for the EU-Project AIMS (Advanced Interactive Materials by Design). The spherical beads had a mean particle size of 40  $\mu\text{m}$  with tuned pore-size and pore-size distribution. Note that FractoAIMs<sup>®</sup>-3 was obtained as a slurry in 2-propanol. The commercially available support, Fractogel<sup>®</sup> EMD Epoxy (M) from Merck KGaA (Darmstadt, Germany) had particle sizes of 40–90  $\mu\text{m}$ , a pore size of about 80 nm and epoxide coverage of 1000  $\mu\text{mol/g}$  dry gel.

The affinity sorbent B14-2LP-FA1 was equipped with a novel triazine-type B14-ligand that was linked with a 1,2-diaminoethane spacer to FractoAIMs-1 and was surface-endcapped with 2-ethanolamine. Note that B14-2LP-FA1 (Fig. 2d) is a non-commercial adsorbent that was provided by ProMetic BioSciences Ltd.<sup>TM</sup> (Cambridge, UK). Due to propriety rights owned by ProMetic BioSciences Ltd.<sup>TM</sup> the exact protocol for the preparation of B14-2LP-FA1 cannot be disclosed. The preparation of adsorbents with similar structure was described elsewhere [27].

## 2.2. Equipment and method description

### 2.2.1. Bio-chromatography

For dynamic binding experiments an L-6200A Intelligent Pump with a D-6000A Interface from Merck-Hitachi (Darmstadt, Germany) and a single wavelength UV-975 Intelligent UV/VIS

detector from Jasco, Biolab (Vienna, Austria) were used. All measurements were performed at 280 nm. Column switching was performed manually using a 2-position/6-port switching valve from Rheodyne. The application of biological sample was performed with a Minipuls 3 peristaltic pump and polyvinylchloride (PVC) calibrated peristaltic tubing with 1.02 mm ID, both from Gilson (Villiers-le-Bel, France).

For preparative bio-chromatography, XK 16/20 columns with two AK 16 adapters and C10/20 columns with two AC 10 adapters from GE-Healthcare (Vienna, Austria) were used. The former was used for anion-exchange type adsorbents, while affinity-type adsorbents were packed in the latter. Both column-types were employed in combination with Superformance Filter F with 16 mm ID or 10 mm ID from Götec-Labortechnik GmbH (Mühlthal, Germany).

Further details concerning the experimental set-up and column packing can be found in our recently published article [1].

### 2.2.2. Online Protein A and size exclusion high performance liquid chromatography (PSEC-HPLC)

Following the previously described analytical method [1], all collected sample fractions were analyzed on an Agilent 1100 series LC system equipped with a binary pump, a multi-wavelength detector and a 2-position/6-port switching valve from Agilent (Vienna, Austria). The isolation and quantification of IgG was performed on a Protein A column, which was coupled in series with the SEC column in order to distribute the feed impurities by their molecular weight (MW) using 10 mM phosphate buffer with 150 mM NaCl, pH 7.20 (application buffer; PBS-150). The 2-position/6-port switching valve allowed the separate elution of IgG from the Protein A column using 12 mM HCl with 150 mM NaCl, pH 2–3 (elution buffer). If not otherwise stated, 100  $\mu\text{L}$  sample volumes were applied and measurements were performed at 280 nm. The sample tray thermostat was set to 10  $^{\circ}\text{C}$  and the column thermostat was adjusted to 25  $^{\circ}\text{C}$ .

**Establishment of PSEC-diagrams.** In order to visualize and compare the experimental results of several PSEC-HPLC runs, the size-exclusion chromatograms of cell culture feed samples were sliced into molecular weight areas of interest; area sections A (660–150 kDa;  $\blacktriangle$ ), B (150–17 kDa;  $\bullet$ ), C (17–0.15 kDa;  $\Delta$ ), D (<0.15 kDa;  $\circ$ ) and E (<0.1 kDa plus adsorbed impurities (ads. imp.);  $\times$ ). The Protein A section of the PSEC chromatogram provides the amount of bound or eluted h-IgG1 (150 kDa;  $\blacksquare$ ). The percent peak area ratios of these sample chromatogram sections are calculated relative to the corresponding peak area sections of the application feed and plotted against subsequently collected material test fractions (10 mL). The amount of IgG and feed impurities in the application feed is thereby stated as 100% for each section. Since the SEC area sections are normalized by the amount of adsorbent used (1 mL for affinity adsorbents and 2.5 mL for anion exchange adsorbents), the feed-flow through a bio-chromatographic column is described as [mL feed per mL gel].

### 2.2.3. SDS-Page gel electrophoresis

The Mini-PROTEAN<sup>®</sup> 3 Cell with a Mini-PROTEAN 3 Cell/PowerPac 300 System (220/240 V) and all required chemicals including a Precision Plus Protein Standard (unstained) were obtained from Bio-Rad Laboratories Inc. (Vienna, Austria). All hand cast slab gels were prepared according to the general procedure for SDS-Page Laemmli buffer systems provided by Bio-Rad [40]. If not otherwise stated, 10%-Tris-HCl gels with 10 sample wells and 0.75 mm thickness were prepared. Samples were mixed in a 1:1 ratio with Laemmli buffer (10% 2-mercaptoethanol) and incubated for 5 min at 90  $^{\circ}\text{C}$ . In general, 15  $\mu\text{L}$  sample and 3  $\mu\text{L}$  molecular weight marker were applied. Protein staining was performed with the ProteoSilver<sup>TM</sup> Plus Silver Stain Kit (PROT-SIL2) from Sigma (Vienna, Austria) [1,41].

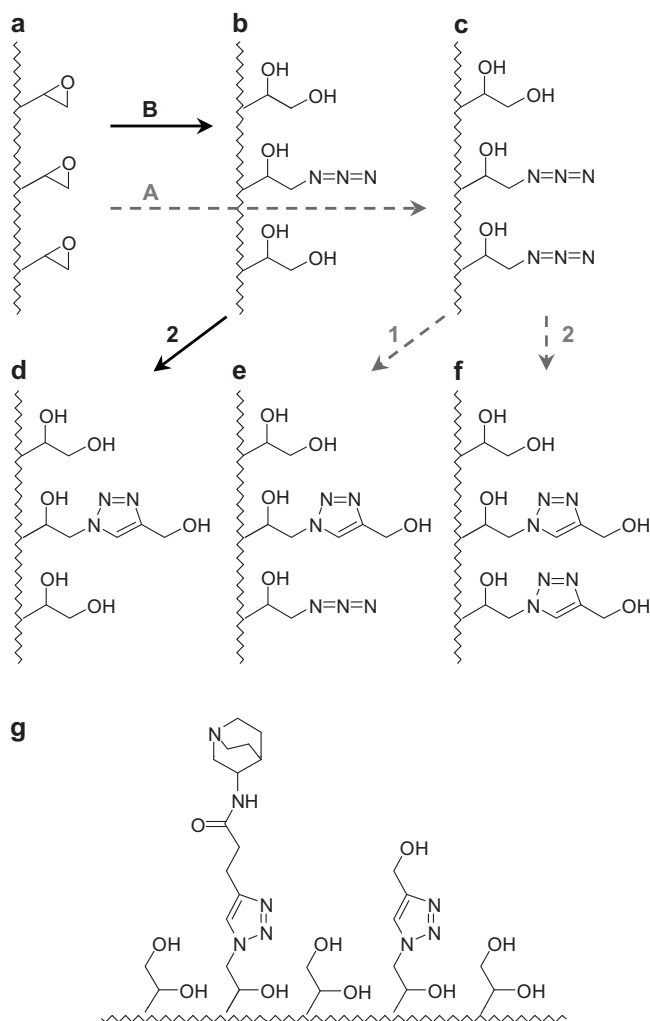


**Fig. 3.** Modification of (a) Epoxy-FractoAIMs-3 (FA3) with varying amount of sodium azide (A and B) leading to (b) FA3-N<sub>3</sub> (B, 750  $\mu\text{mol/g}$ ) and (c) FA3-N<sub>3</sub> (A, 1.38 mmol/g) and the endcapping of azide-groups with 3-propargylalcohol employing 2 different Click-reaction protocols (1 and 2), leading to the materials (d) FA3-TRZ-CH<sub>2</sub>-OH (B2), (e) FA3-TRZ-CH<sub>2</sub>-OH (A1) and (f) FA3-TRZ-CH<sub>2</sub>-OH (A2). Material (g) AdQ-TRZ-Fractogel (B2; AdQ-TRZ: 500  $\mu\text{mol/g}$ ) was prepared on Azide-Fractogel (B, 676  $\mu\text{mol/g}$ ) employing Click protocol 2.

### 2.3. Preparation of materials

The synthesis of ligands, surface modifications of adsorbents and the preparation of affinity-type adsorbents (Figs. 2 and 3) are described in the [electronic supplementary materials](#).

#### 2.3.1. Click-protocol-1

To a suspension of 3 mL of FA3-N<sub>3</sub> (A) material (1 mol-equiv. azide groups: 1.38 mmol/g dry gel) in methanol, 4 mol-equiv. of 3-propargyl alcohol was added together with 3 mol-equiv. DIPEA and followed by the addition of 5–7 mol-equiv. Cu(I) in acetonitrile. The suspension was shaken on an orbital shaker for 3 days at room temperature. The final gel was washed successively with water, 10 mM HCl, 0.5 M NaOH, 0.1 M EDTA and methanol until the final material was completely white. FA3-triazole-CH<sub>2</sub>-OH (A-1) was stored in 20% (v/v) aqueous methanolic solution until use (Fig. 3e).

Note that all solvents and solutions were ultrasonicated for several minutes before use and that the Click-reaction was performed under nitrogen to prevent an early oxidation of Cu(I) to Cu(II).

#### 2.3.2. Click-protocol-2

Copper (I) was prepared through addition of sodium L-ascorbate (2 mol-equiv.) to an aqueous CuSO<sub>4</sub> solution (2 mol-equiv.), under streaming nitrogen. After addition of 3-propargyl alcohol (3 mol-equiv.) at room temperature, the bright yellow Cu(I)-propyne complex was mixed to the azide-modified support (azide groups: 1 mol-equiv.). The reaction slurry was covered with nitrogen and shaken for 3 days at room temperature on an orbital shaker. The addition of methanol and a few mL of brine enhanced the solubility of the alkyne-Cu(I) complex. Note that the Cu(I)-propyne alcohol complex precipitates, but will eventually dissolve as the Click reaction proceeds. The azide modified gel was washed with 10 mM HCl, 0.1 M EDTA, water and methanol until white in color (Fig. 3d and f).

### 2.4. Evaluation of material performance

#### 2.4.1. Dynamic break-through experiments

For all dynamic binding capacity (DBC) experiments, the adsorbents were suspended in 1 M sodium chloride and left to settle in a graduated 5 mL volumetric cylinder. In general, 2.5 mL of test media were packed into 16 mm ID columns using Superformance filter discs to separate the gel from the column adapter. Only for the affinity material B14-2LP-FA1 a smaller gel amount of 1 mL adsorbent were used in combination with the 10 mm ID columns. After settling of the adsorbent by gravity, a bed height of 1 cm was adjusted employing a compression factor of 20%. The affinity adsorbent was equilibrated with application buffer (PBS-75, pH 7.20), while the anion exchange materials were rinsed with 0.1 M HCl prior to equilibration with the application buffer. In general, 10 mL sample volumes were collected. All citric acid (CA), hydrochloric acid (HCl) and cleaning-in-place (CIP) fractions were immediately neutralized with 5 M NaOH or 1 M CA solutions.

#### 2.4.2. DBC for the endcapped epoxide and azide-activated adsorbents

After the dead volume (T<sub>0</sub>) of the column has elapsed, 10  $\times$  10 mL fractions of flow-through feed were collected. All columns were rinsed with 3  $\times$  10 mL of salt free PBS-0 buffer, followed by 1  $\times$  10 mL of PBS-75, PBS-150 and PBS-300, all at pH 7.2. IgG elution was performed with 2  $\times$  10 mL of 50 mM citric acid (CA, pH 3.50) and 1  $\times$  10 mL 0.1 M HCl solution. Before sanitation of the adsorbent (cleaning-in-place, CIP) with 2  $\times$  10 mL 0.5 M sodium hydroxide solution, the column was rinsed with PBS-0 until a neutral pH was reached.

#### 2.4.3. DBC for B14-2LP-FA1/AQ-FA3 combination

After collecting 25  $\times$  10 mL cell culture flow-through fractions, B14-2LP-FA1 was rinsed with PBS-0 until base line. IgG was eluted with 50 mM citric acid, pH 3.50. Before sanitation of the adsorbent with 0.5 M NaOH the column was thoroughly rinsed with PBS-0. The elution fractions were dialyzed for 24 h using CE Float-A-Lyzer® G2 membrane tubes and PBS-75 as dialysis buffer [39]. The pooled dialysis samples were applied onto the anion exchange adsorbent AQ-FA3 in flow-through mode without fraction collection. Bound feed impurities were eluted with PBS-300 from AQ-FA3.

#### 2.4.4. DBC for AQ-FA3/B14-2LP-FA1 combination

The 200 mL cell culture feed were dialyzed twice for 24 h using PBS-75. The dialyzed feed was applied onto the anion exchange adsorbent AQ-FA3 in flow-through mode, before application onto B14-2LP-FA1. Fraction collection, IgG elution and column sanitation were performed as earlier mentioned.



#### 2.4.5. Investigations on azide group promoted protein aggregation

The protein stock solutions A to G contained each 5 mg/mL IgG in PBS-75, pH 7.20. They were spiked with an increasing amount (1, 5, 10, 25, 50, 75 and 100 mg/mL) of the azide compounds, sodium azide or 1-azido-3-(2-propen-7-yloxy)-2-propanol (AGE-N<sub>3</sub>). Note that the same molar quantities of sodium azide as well as AGE-N<sub>3</sub> were employed. All samples were shaken on a Thermomixer compact from Eppendorf (Vienna, Austria) at 25 °C and 1400 rpm for 3 h and 24 h, centrifuged and their supernatants measured with Protein A HPLC (injection volume: 10 µL).

Since shear forces as well as heat were reported to promote protein aggregation, three control samples without the addition of azide compounds, each containing only 5 mg/mL IgG were tested. One was stored motionless at 25 °C (control sample) and the two other samples were shaken at 25 °C (sample S) and 60 °C (sample H).

### 3. Results and discussion

#### 3.1. Epoxide-activated support materials

In order to allow a fast and effective immobilization of affinity ligands, the adsorbent surface had to be sufficiently activated and hydrophilized. The polymethacrylate type support matrices used in this study have tentacle grafted surfaces. These tentacles increase the overall surface area and function as an extension of the actual spacer-chain. Since the epoxide groups on the tentacles as well as within the surface pores of the adsorbent are highly reactive, they have to be deactivated or endcapped after ligand immobilization. An example for the deactivation of reactive groups is shown in Fig. 2a for the acidic hydrolysis of epoxide groups. The endcapping of the epoxide group with 2-mercaptoethanol and 2-ethanolamine is visualized in Fig. 2b and c. Both concepts, the coupling of thiophilic ligands as well as amino-functional ligands onto solid supports are state of the art and therefore well discussed in literature [42–44]. A comprehensive study dealing with the influence of spacer-chain chemistry and support chemistry on the IgG capture performance of the bio-mimetic ligand A2P from a chromatographic as well as a theoretical thermodynamic viewpoint was recently published [27].

In order to unfold the contribution of these surface modifications to the overall performance of affinity adsorbents, it was necessary to investigate these surface modifications unimpaird by the affinity ligand. Only after that the affinity ligand B14 was introduced. The B14-2LP-FA1 adsorbent (Fig. 2d) with its 1,2-diaminoethane spacer arm plus a surface endcapping with 2-ethanolamine is admittedly an extreme example to demonstrate how strongly spacer-chemistry and surface-chemistry can influence material performance, but it also shows how such difficulties can be overcome during down-stream processing.

##### 3.1.1. Endcapping strategies for epoxy-activated supports

For the control experiments Fig. 3 visualizes and compares the performance of the three most common end-capping strategies for epoxy activated support media, namely acidic hydrolysis (FA3-OH), the addition of 2-mercaptoethanol (FA3-S-(CH<sub>2</sub>)<sub>2</sub>-OH) and the addition of 2-ethanolamine (FA3-NH-(CH<sub>2</sub>)<sub>2</sub>-OH). The binding of IgG and feed impurities to the surface modified adsorbents during feed application (Fig. 4a) as well as their elution from the adsorbents during a number of wash, elution and sanitation steps (Fig. 4b) are displayed in Protein-A-Size-Exclusion-Chromatographic plots (PSEC-plots) [1].

These PSEC-plots show clearly that the simple incorporation of hydroxyl groups through acidic hydrolysis (FA3-OH) lead to a sup-

port surface, which is practically inert towards the binding of feed impurities as well as h-IgG1. Only a small negligible amount of feed impurity E binds to FA3-OH. Note that these SEC area section E impurities consist partially of low-MW-impurities below 0.1 kDa and partially of large MW-impurities that retain on the surface of the silica-based SEC-column (E: <0.1 kDa + ads. imp.). The corresponding SDS-Page slab gel for FA3-OH in Fig. 4c shows that this support modification elute feed impurities with 25 kDa under salt-free condition (lane 2; W2) as well as when 75 mM NaCl (PBS-75; lane 3) is added. PBS buffer containing 150 mM NaCl (PBS-150; lane 4) removes the major part of the feed impurities with MW above 50 kDa. The elution of bound IgG (bands 25 kDa and 50 kDa) is seen in lane 4 and lane 5. The latter resembles the wash step with PBS-buffer containing 300 mM NaCl (PBS-300). The actual elution fractions CA1 and CA2 are completely clear. Only a slight smear of feed impurities and a small amount of IgG can be seen in the cleaning in place fraction S1 in lane 8.

The PSEC-plot for material FA3-S-(CH<sub>2</sub>)<sub>2</sub>-OH in Fig. 4 shows that this type of surface modification captures approximately 20% of feed impurities in the range of 150–17 kDa (area section B) during feed application. The corresponding elution diagram provide the information that also a small amount of feed impurity E has bound to the adsorbent and can easily be removed under salt-free condition (PBS-0; W1, W2 and W3) as well as with PBS-75 and PBS-150. The absence of impurity B in the elution diagram may indicate that it binds strongly to the adsorbent and cannot easily be eluted. Another possibility is that it has decomposed under the acidic elution condition, which would explain the protein smear over the entire lane 6 (C1) on the corresponding slab gel. It is also visible that FA3-S-(CH<sub>2</sub>)<sub>2</sub>-OH binds a small amount of IgG (lane 6). The elution of IgG is promoted by salt as well as by lowering of the pH (lane 6). IgG is found in the sample fractions PBS-75, PBS-150, PBS-300 and C1, with distinct bands for fractions PBS-150 and CA1.

Undoubtedly, adsorbent FA3-NH-(CH<sub>2</sub>)<sub>2</sub>-OH exhibits the strongest capture performance for feed impurities as well as for IgG. This surface modification binds about 80–90% of the high-MW feed impurities A (≥150 kDa), 40% of B (150–17 kDa) and 10% of E (<0.1 kDa plus ads. imp.), but also 10% of IgG (Fig. 4a). Taking a look at the protein composition of the elution fractions, it is clear from Fig. 4b that the few amino groups on the material surface can actually capture feed impurity A from 6 flow-through fractions (>600 area%) and feed impurity B from about 1.5 flow-through fractions. In accordance with the slab gel results, it is apparent that the largest portion of the bound feed impurities can only be removed from this adsorbent during sanitation (S1 and S2). It is also evident that a large amount of feed impurities elute together with IgG into the C1 fraction. The elution diagram shows that the salt wash steps PBS-75 and PBS-150 lead mainly to the elution of IgG and feed impurity E. The high MW impurities A and B start to elute with PBS-300. Since most IgG is found in fraction PBS-150 and CA1, but only little in PBS-300, it is most likely that IgG was bound by two different mechanisms to the adsorbents. The underlying hydroxyl groups, present due to acidic hydrolysis of residual epoxy groups after immobilization of 2-ethanolamine resemble the first discussed FA3-OH support. As previously stated, this surface modification tends to bind a small amount of IgG. This weakly bound IgG elutes as soon as salt is added to the wash solution. The 2-ethanolamine modification, on the other hand, binds IgG strongly and needs a pH switch towards lower pH (C1) or higher pH (S1 and S2) values in order to release IgG as well as feed impurities from its embrace.

Obviously adsorbent FA3-NH-(CH<sub>2</sub>)<sub>2</sub>-OH functions as an anion exchanger (AIE), which makes any affinity-type adsorbent, that was endcapped with 2-ethanolamine or which possessed a spacer chain with embedded amino groups, a mixed-mode material with partial AIEX-properties. The most suitable endcapping strategy for

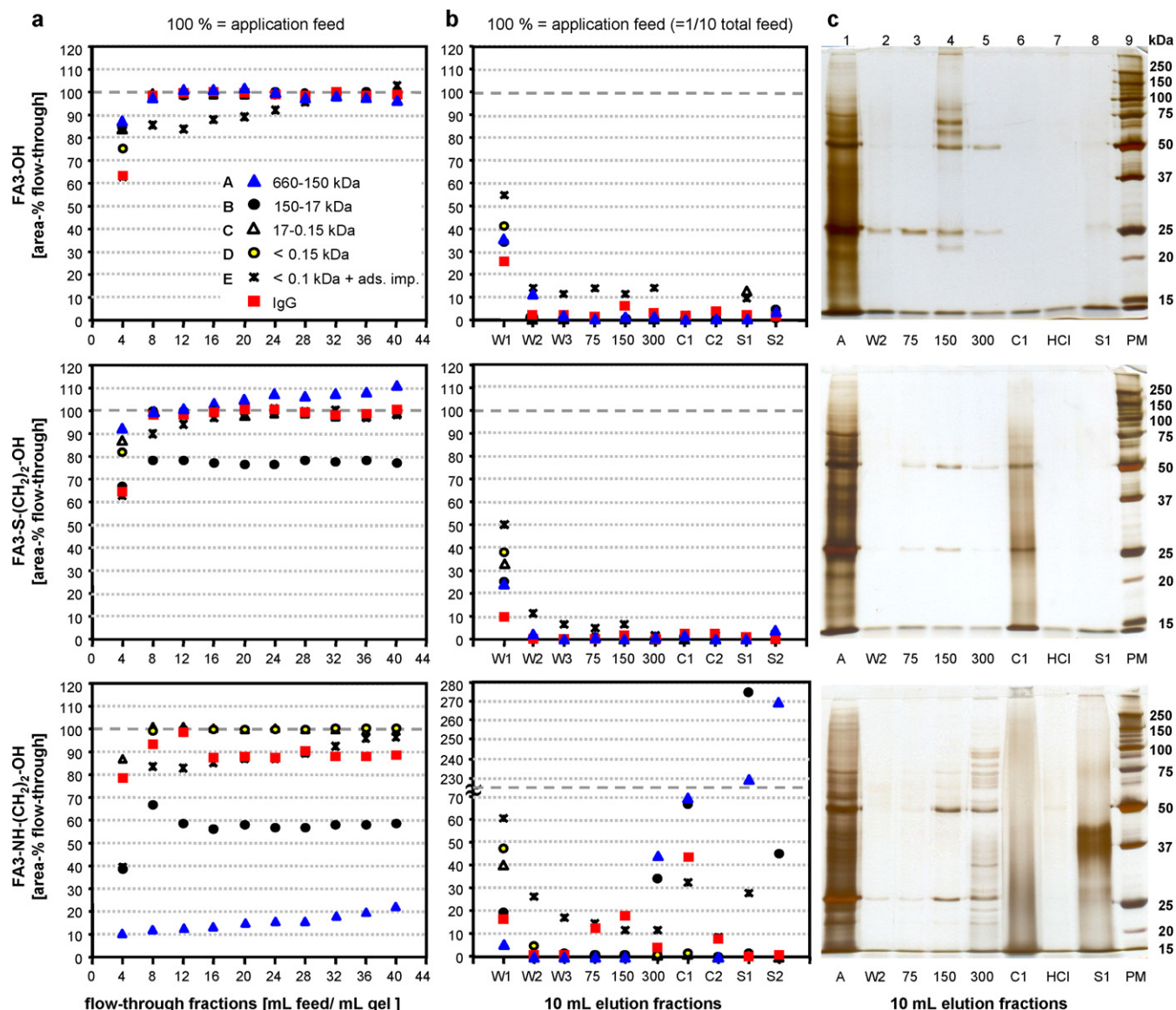


**Fig. 4.** Performance evaluation of FractoAIMs-3 Epoxy materials after acidic hydrolysis (FA3-OH) and after endcapping of epoxide groups with 2-mercaptoethanol (FA3-S-(CH<sub>2</sub>)<sub>2</sub>-OH) and 2-ethanolamine (FA3-NH-(CH<sub>2</sub>)<sub>2</sub>-OH), employing cell culture supernatant at pH 7.4 for testing. Sample composition were visualized with (a) PSEC-diagram for collected flow-through fractions, (b) PSEC-diagram for wash and elution fractions and (c) SDS-PAGE slab gels under reduced conditions; A: application feed, W2: wash solution (salt-free), 75: PBS with 75 mM NaCl, 150: PBS with 150 mM NaCl, 300: PBS with 300 mM NaCl, C1: 50 mM citric acid, pH 3.50, HCl: 0.1 M HCl, S1: 0.5 M NaOH; IgG light chain: 25 kDa, IgG heavy chain: 50 kDa.

epoxy-activated support materials was clearly the epoxy ring opening under acidic condition.

The reason for the sometimes observed deviation between chromatographically established PSEC-diagrams and SDS-Page results may lie on one hand on the large background signal of the neutralized citric acid (C) and sanitation (S) solutions (Fig. 4b), which were subtracted from the actual sample signal of the SEC run. On the other hand, silver staining is a very effective and sensitive staining technique, with which traces of proteins down to the lower nano-gram level can be visualized. Nonetheless, the color intensities of the silver-stained protein bands do not necessarily correlate with the actual concentration of proteins in solution. Therefore, the actual quantity of protein impurities in some of the slab gel lanes may just as well be too small to be chromatographically detectable.

### 3.1.2. Performance evaluation of B14-2LP-FA1

The following chapter describes two antibody purification strategies from cell culture supernatant. Both protocols include the

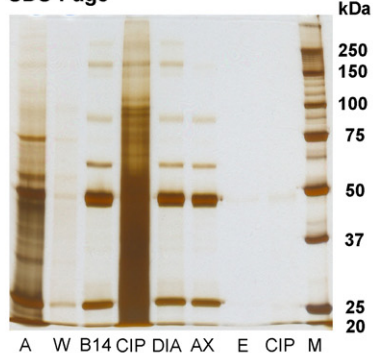
affinity-type IgG-capture media B14-2LP-FA1 (Fig. 2d), the anion exchanger adsorbent AQ-FA3 (Fig. 2e) and a dialysis step prior to the AQ-FA3 clean-up. The main difference between the two protocols is the reversed order in which the two adsorbents are employed in the purification scheme.

Fig. 5a shows the SDS-Page gel and SEC results for the purification sequence using B14-2LP-FA1 in the first step, which is the IgG capture step. Lane 3 on the SDS-Page gel shows that the elution fraction (B14) contains predominantly IgG (short chain 25 kDa and heavy chain 50 kDa) with only a slight smear of feed impurities across the lane. Distinct bands of feed impurities can be seen at 60, 90, 200 and 300 kDa, of which the 60 kDa band is the most pronounced one. The highly intense CIP lane of B14-2LP-FA1 in Fig. 5a proves that the underlying anion exchanger lattice of B14-2LP-FA1 leads to a very strong binding of feed impurities. It also proves that feed impurities that bind to B14-2LP-FA1, remain on the adsorbent and do not elute with IgG into the citric acid elution fraction (pH 3.50). Furthermore, Lane 6 (AX) shows that the

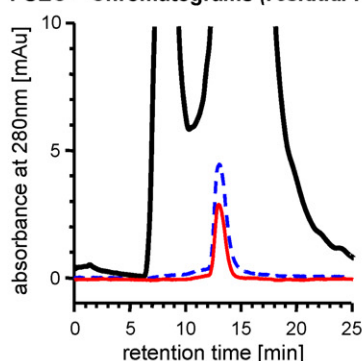


## a Purification cascade: B14-2LP-FA1 / AQ-FA3

## SDS-Page



## PSEC – Chromatograms (residual feed impurities without IgG)

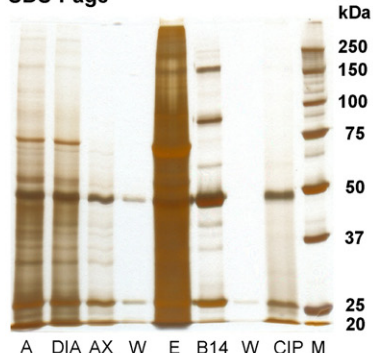


- A Application (cell culture feed)  
W Wash (PBS-0)  
B14 B14-2LP-FA1 - Elution (50 mM citric acid, pH 3.5)  
CIP Cleaning in place (0.5 M NaOH)  
DIA Dialysis with 3-5kDa Float-a-Lyzers  
AX Anion-exchanger (AQ-FA3), flow-through fraction  
E AX - Elution (PBS-300)  
M Protein marker

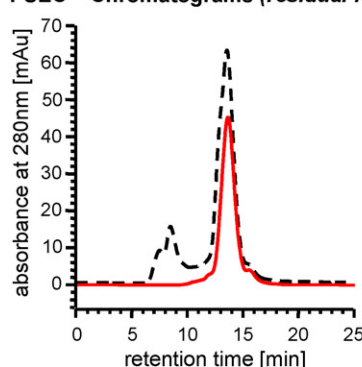
— cell culture feed (A)  
- - B14-2LP-FA1 + dialysis (DIA)  
— AQ-FA3 flow-through fraction (AX)

## b Purification cascade: AQ-FA3 / B14-2LP-FA1

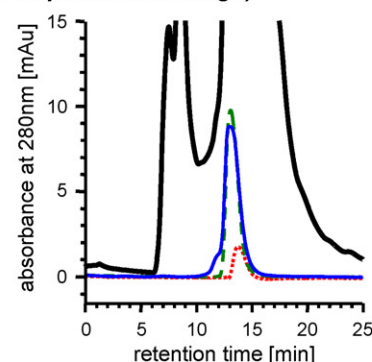
## SDS-Page



## PSEC – Chromatograms (residual feed impurities without IgG)



- - dialysed cell culture feed (DIA)  
— AQ-FA3 flow-through fraction (AX)



— cell culture feed (A)  
— B14-2LP-FA1 (B14)  
- - 50 mM citric acid (neutralized with 1M NaOH)  
..... 1 g/L NaN<sub>3</sub>

**Fig. 5.** Material performance evaluation via SDS-Page and PSEC-HPLC employing two different purification strategies for the isolation of monoclonal h-IgG1 from cell culture feed using the weak anion exchange adsorbent AQ-FA3 and the IgG capture media B14-2LP-FA1 in the order (a) B14-2LP-FA1/AQ-FA3 and in the reversed order (b) AQ-FA3/B14-2LP-FA1.

use of an anion exchange media in the final polishing step does not markedly improve the purity of the final IgG solution. Only the feed impurity band at 300 kDa and the slight smear across the lane can be removed. The impurity band 200 kDa is slightly reduced. How-

ever, although the impurities at 60 kDa and 90 kDa still remain in solution, the AQ-FA3 media could remove 19% of the feed impurities that have eluted from B14-2LP-FA1. The PSEC chromatogram of the elution fraction of B14-2LP-FA1 provides evidence that B14-

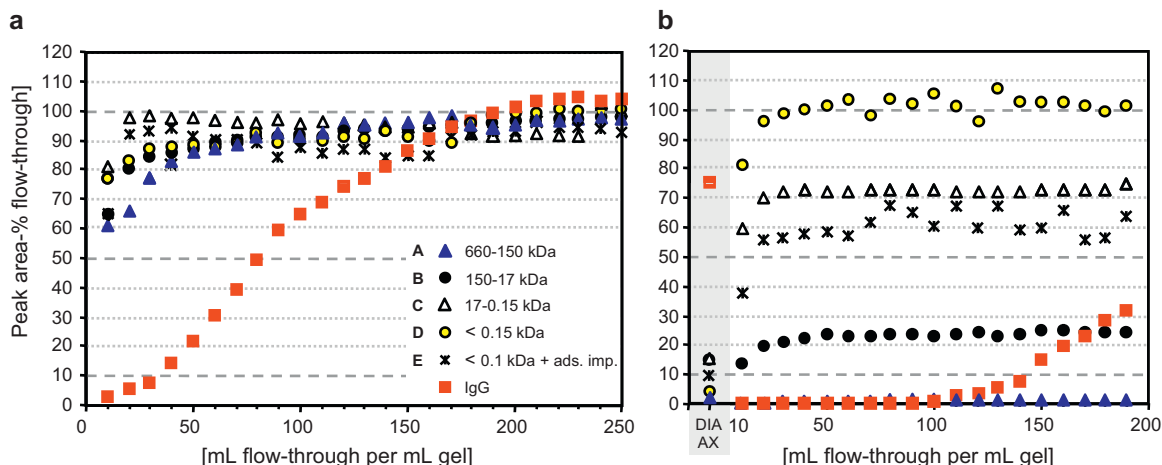


**Fig. 6.** PSEC-diagrams showing the dynamic break-through performance of B14-2LP-FA1 in the purification schemes (a) B14-2LP-FA1/AQ-FA3 and (b) AQ-FA3/B14-2LP-FA1, where DIA stands for dialysis (MWCO: 3–5 kDa) and AX for the pre-purification step using AQ-FA3.

2LP-FA1 can capture only 14% of the total amount of applied IgG, but can remove 99.88% of applied feed impurities.

It can be assumed that with the progressing capture of feed impurities, the binding capacity of B14-2LP-FA1 for IgG is gradually decreasing, due to the sterical hindrance exhibited by the large amount of impurities competing with the low concentration of IgG in the feed. In order to verify this hypothesis, B14-2LP-FA1 was tested with a “pre-purified” feed that was dialyzed and purified with AQ-FA3.

A comparison of the two SDS-Page gels in Fig. 5a and b shows that the two experiments lead to reciprocal results. As intended, the intense elution lane of AQ-FA3 (E) in Fig. 5b proves that AQ-FA3 can remove most of the feed impurities, before the feed enters the B14-2LP-FA1 column. The elution lane of B14-2LP-FA1 (B14) shows a slight smear across the lane with additional impurity bands at 30 kDa and 40 kDa. There are impurity bands at 60, 90 and 200 kDa, of which the latter two are most distinct. The presence of IgG (25 kDa and 50 kDa) in the CIP-fraction of B14-2LP-FA1 is most likely caused by a too short elution time due to a slight peak tailing. An evaluation of the PSEC-chromatograms for the AQ-FA3/B14-2LP-FA1 scheme lead to a total removal of 99.98% of feed impurities and a 5-fold increase in IgG-binding for the B14-2LP-FA1 adsorbent compared to the inverse purification scheme.

Fig. 6 shows the dynamic binding performance of B14-2LP-FA1, when employed in the first (Fig. 6a) and when applied in the second clean-up step (Fig. 6b). The left column in the PSEC-diagram in Fig. 6b visualizes the feed composition after dialysis and after clean-up with AQ-FA3. This feed composition was used as a reference for the corresponding PSEC-plot. Due to the lack of available pre-purified feed and the unexpected performance of B14-2LP-FA1, the feed application had to be terminated at 30%-DBC. A dynamic binding capacity of 3.7 g/L IgG at 30% column break-through was obtained. These two PSEC-plots show clearly that B14-2LP-FA1 has suffered the loss of IgG capture performance due to a seemingly unsuitable spacer chemistry and endcapping chemistry. But on the other hand the SDS-Page gels have shown that although B14-2LP-FA1 binds a large amount of feed impurities, which reduce its IgG binding capacity, these impurities do not elute with IgG. B14-2LP-FA1 can be classified as a mixed-mode adsorbent which isolates IgG and removes feed impurities in a single purification step.

### 3.2. Click-reaction for ligand immobilization on solid supports

#### 3.2.1. Modified Click-reaction protocol

The so-called Click reaction is a cycloaddition reaction between azide and alkyne functional groups, leading to a [1,2,3]-triazole ring as the connecting link [30,45]. This reaction is known to be fast and straight forward; needing only a small catalytic amount of 1–5 mol% of copper (I) salt to promote the coupling reaction. Cu(I) can be directly employed using copper (I) iodide or using a CuSO<sub>4</sub>/sodium ascorbate system, where Cu(I) is fashioned in aqueous solutions shortly before the coupling reaction is initiated [46].

The proposed mechanism for the Cu(I) mediated Click reaction is shown in Fig. 1. The formation of the intermediate A, the copper (I)–acetylide complex [33] and the intermediate C, the copper (I)–triazolide [32] are proven and documented. By this scheme Cu(I) exits this reaction cascade untempered and can enter the next reaction cycle as soon as the first intermediate has formed. However, the presence of oxygen in the solution may transform Cu(I) to its inactive Cu(II) counterpart, preventing its participation in the next cycle. Therefore, even for reactions employing CuI, the reducing agent sodium ascorbate has to be added to ensure that Cu(I) remains at all times in its reactive form.

Another difficulty that may occur is a possible complexation of the Cu(I) or Cu(II) ions by one of the reacting partners which includes the ligand head group and the solid support. The latter

has occurred for the polymethacrylate-based supports FractoAIMs-3 and Fractogel. A possible remedy may be the addition of an “auxiliary or complexing ligand”, which per se binds to Cu(I) but leaves one or more free sites to partake in the Click reaction. Such “complexing ligands” contain two or more sulfur or amino groups [47–49,32,50,37,51] that complexate with Cu(I) or Cu(II) [52]. Unfortunately, experiments with the “complexing ligand” bathophenanthroline disulfonate [49] had to be terminated due to irreversible binding of the reagent as well as the bathophenanthroline–Cu(I) complex to the Fractogel surface.

Another possibility to drive the cycloaddition reaction forward is to add more and more Cu(I) as the Click-reaction proceeds. However, this method leaves us with a large amount of surface-bound copper that has to be removed from the adsorbent after ligand immobilization. Plus, the surface bound copper provide a sterical hindrance, leading to much reduced immobilization rates.

The way out of this dilemma evolved in the implementation of a new procedure, which proved to be an applicable and simple alternative to the one-pot approach. Hereby, the alkyne modified ligand is combined and stirred with an equimolar amount of Cu(II) and sodium ascorbate until only the alkyne–copper complex, the so-called copper–acetylide is present in solution. This highly reactive intermediate is then added to the azide-modified polymethacrylate-type support under oxygen-free condition. With this new Click-procedure it is possible to double the ligand immobilization yield for AdQ-TRZ-Fractogel (B2) as well as produce fully azide group endcapped support surfaces after ligand immobilization (Fig. 3g).

Note that the complementary assembly, using alkyne-modified supports in combination with azide-terminal affinity ligands was not investigated, although literature had predicted that this reversed approach could provide much higher immobilization rates [37]. The choice to endow the ligand with the alkyne functionality was made deliberately. Cu(I) activated alkyne groups are very reactive and reportedly prone to unspecific binding of feed proteins [35]. Of course it may be possible to deactivate residual alkyne groups with azide-terminal endcapping reagents, but the reaction yield might not be sufficient and any remaining alkyne–Cu(I) complex is by far more reactive than idle azide-groups.

#### 3.2.2. Endcapping strategies for azide group activated support surfaces

Fig. 7 shows the corresponding PSEC-diagrams and SDS-Page slab gels for the azide-modified FractoAIMs-3 support material (FA3-N<sub>3</sub>) before and after azide-endcapping with 3-propargyl alcohol using two different endcapping protocols (Fig. 3; 1 and 2) for two different FA3-N<sub>3</sub> support materials (Fig. 3A and B). The two azide functional supports FA3-N<sub>3</sub> (A) and FA3-N<sub>3</sub> (B) possess azide-group densities of 1.38 mmol/g (A) and 750  $\mu$ mol/g (B) dry gel. Note that the residual epoxide groups have been deactivated through acidic hydrolysis prior to any surface modification via Click-Chemistry. A description of the preparation of azide-group modified support media with tuned azide group density (Fig. S1) can be found in the electronic supplementary material.

Material FA3-N<sub>3</sub> (A) in Fig. 7a shows clearly that an azide-modified adsorbent without affinity ligand attached to its surface is on its own capable to capture a large amount of IgG. It binds about 86% of the applied h-IgG1 from the cell culture supernatant after 20% dynamic break through of IgG. Besides that FA3-N<sub>3</sub> (A) also binds mainly the feed impurities A (>150 kDa) and E (<0.1 kDa plus ads. imp.). Unexpectedly, the elution diagram in Fig. 7b and the SDS-gel in Fig. 7c of FA3-N<sub>3</sub> (A) show that only a small amount of “intact” IgG elute from the column. On the other hand, wash solutions W2, PBS-75 and PBS-150 (lanes 2–4) show an idle 25 kDa band, which may be light-chain IgG. This would indicate a degradation of IgG during clean-up. However, only the presence of both IgG polypep-

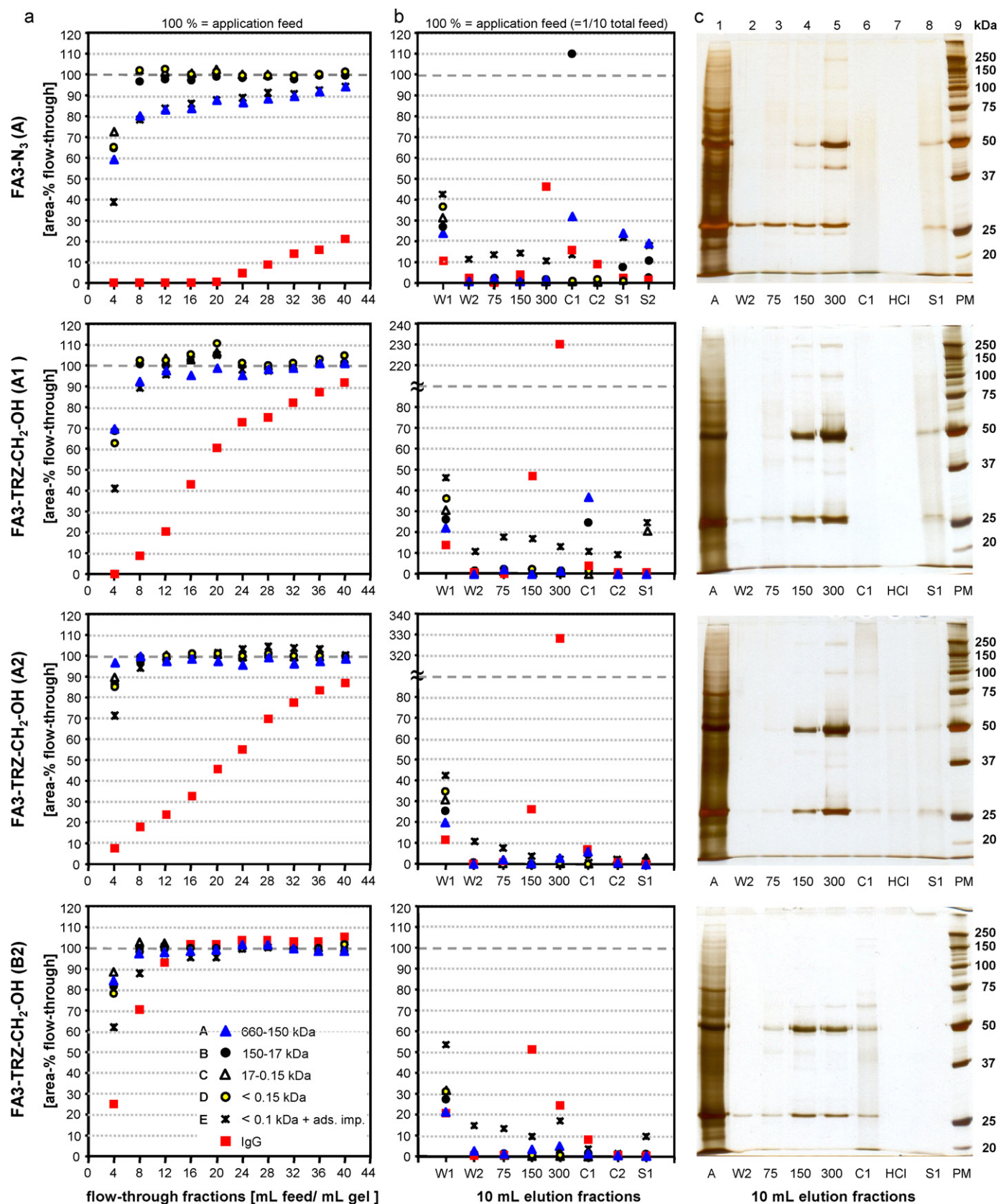


**Fig. 7.** Performance evaluation of Azido-FractoAIMs-3 support materials with and without azide group endcapping using 3-propargylalcohol, employing cell culture supernatant at pH 7.4 for testing. Sample composition were visualized with (a) PSEC-diagram for collected flow-through fractions, (b) PSEC-diagram for wash and elution fractions and (c) SDS-PAGE slab gel under reduced conditions; (A) application feed, W2: wash solution (salt-free), 75: PBS with 75 mM NaCl, 150: PBS with 150 mM NaCl, 300: PBS with 300 mM NaCl, C1: 50 mM citric acid, pH 3.50, HCl: 0.1 M HCl, S1: 0.5 M NaOH; IgG light chain: 25 kDa, IgG heavy chain: 50 kDa.



tide chains, the 25 kDa and the 50 kDa fragments within the same lane is a clear indicator for the presence of IgG. In the case that only one of the two characteristic peptide chains is present, this peptide may be a non-IgG related feed impurity or a degradation product of IgG. In the latter case, this IgG fragment may have been already present in the application feed or created during purification. In the latter case the “other” IgG fragment ought to possess other binding and elution properties.

To verify if an azide-modified support can actively break IgG molecules into their heavy and light chain, the former DBC-experiment was repeated with a standard IgG solution (100 mg/L human polyclonal IgG in PBS-75) in the absence of feed impurities. The absence of a lone 25 kDa lane in wash solution W2 plus the presence of both IgG fragments in the other wash and elution fractions prove that material FA3-N<sub>3</sub> (A) does not induce the fragmentation of IgG molecules (Fig. S3) [39]. Furthermore, it proves that the 25 kDa feed impurity was already present in the application feed.

The elution diagram of FA3-N<sub>3</sub> (A) in Fig. 7b shows that the elution of IgG is strongly salt dependant. IgG emerges strongest with PBS-300, while the low salt buffers PBS-75 or PBS-150 have almost no effect on IgG elution. A decreasing amount of IgG elutes with 50 mM citric acid, pH 3.50 (C1 and C2) and during sanitation (S1 and S2). On the SDS-Page gel, however only one distinct feed impurity band at about 40 kDa (lane 5) and a weak band at about 24 kDa are seen in the PBS-300 wash fraction. A slight smear of impurities over the entire lane is seen in the lanes PBS-75, PBS-150, PBS-300, C1 and S1. Possible reasons for the obviously low recovery of IgG will be discussed separately and in more detail in Section 3.2.4.

A comparison of the PSEC break-through diagrams for the two endcapped materials FA3-TRZ-CH<sub>2</sub>-OH (A1) and FA3-TRZ-CH<sub>2</sub>-OH (A2) in Fig. 7a show that both adsorbents are still endowed with the ability to capture IgG, but to a much smaller extent. The second endcapping strategy (B2) provides a support surface that binds little IgG and little to no feed impurities. Also in the PSEC elution diagrams in Fig. 7b the same tendency can be observed. While for FA3-TRZ-CH<sub>2</sub>-OH (A1), feed impurity E can be found at about 10–20% in all collected fractions, impurity A and B are found with 37% and 25% only in the C1 elution fraction and impurity C only in S1. For material FA3-TRZ-CH<sub>2</sub>-OH (A2) the elution PSEC diagram (Fig. 7b) shows only a slight elution of impurity E of about 3–12% in fraction W2 as well as in the three NaCl containing fractions. Only about 5% of feed impurity A is present in fraction C1. Concerning the elution behavior for IgG, both materials show the same tendency. With PBS-150 some of the bound IgG elute from the column, while the major amount elute with PBS-300. A comparison of SDS-gels show that FA3-TRZ-CH<sub>2</sub>-OH (A2) does not bind feed impurities strongly, since the sanitation lane of the latter is clearer than that of FA3-TRZ-CH<sub>2</sub>-OH (A1).

The main difference between the two surface modifications, FA3-TRZ-CH<sub>2</sub>-OH (A2) and FA3-TRZ-CH<sub>2</sub>-OH (B2) is the reduced azide group density of the latter. FA3-N<sub>3</sub> (B) possesses only 750  $\mu\text{mol/g}$  azide groups, which is half the number of FA3-N<sub>3</sub> (A). Both adsorbents are endcapped with Click reaction protocol-2. The resulting endcapped support FA3-TRZ-CH<sub>2</sub>-OH (B2) binds only little IgG, which mostly elutes with the salt wash step PBS-150, followed by PBS-300. Traces of IgG are found in the elution fraction C1. The sanitation solution is free of IgG and free of feed impurities. Overall it can be stated that a tuned number of azide groups, sufficient to achieve the desired ligand density, but not too densely set as to induce sterical hindrance during endcapping provides the best results, concerning IgG recovery and purity of the elution fractions.

### 3.2.3. Recovery of IgG for different endcapping strategies

A summary of bound and eluted IgG in Fig. 8, shows that 9% of applied IgG binds to FA3-NH-(CH<sub>2</sub>)<sub>2</sub>-OH during feed application,

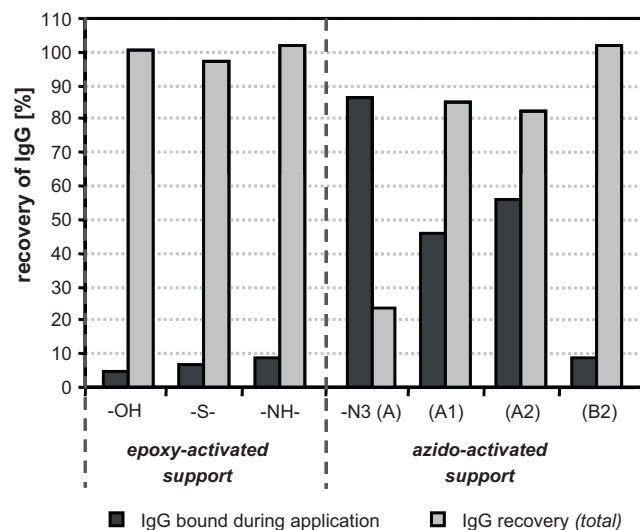


**Fig. 8.** Percentage of IgG, bound during application of cell culture supernatant containing h-IgG1 and the total recovery of IgG, which includes the wash, elution and sanitation steps for the epoxide-activated adsorbents FA3-OH (OH), FA3-S-(CH<sub>2</sub>)<sub>2</sub>-OH (-S-), FA3-NH-(CH<sub>2</sub>)<sub>2</sub>-OH (-NH-) and FA3-N<sub>3</sub> (-N<sub>3</sub>) and the azide functionalized adsorbents FA3-TRZ-(CH<sub>2</sub>)<sub>2</sub>-OH (A1, A2 and B2).

while the simple surface modification FA3-OH captures only 5% IgG. For all three investigated surface modifications a total recovery of approximately 100% IgG can be obtained.

In case of the azide group activated supports and their endcapped versions, only material FA3-TRZ-CH<sub>2</sub>-OH (B2) with the low azide group density using the Click protocol 2 provide comparable results, with 9% for the binding and 100% for the recovery of IgG. The non-endcapped support FA3-N<sub>3</sub> (A) with the high azide group density captures 86% of the applied IgG, but releases only 24% thereof. Comparing the two endcapped versions of FA3-N<sub>3</sub> (A), it is clear that FA3-TRZ-CH<sub>2</sub>-OH (A1) binds approximately 10% less IgG, but only releases 3% more intact IgG compared to its counterpart. Nonetheless, Click protocol 2 is superior, because the resulting adsorbent FA3-TRZ-CH<sub>2</sub>-OH (A2) binds less feed impurities, while capturing more IgG. Furthermore, it provides purer elution fractions as previously demonstrated in the PSEC diagrams and the SDS-Page gels in Fig. 7.

### 3.2.4. Azide group promoted aggregation of IgG

The big question that remains is what had happened to the IgG fraction, which was bound to FA3-N<sub>3</sub> (A), but was not even found in the final sanitation fractions? Is it still bound on the adsorbent or was it decomposed into smaller fragments?

In order to solve this dilemma, we will first take a look at the chemical properties of inorganic azide groups and then discuss how organic surface bound azide groups may have interacted with IgG. In general, terminal azide groups are linear, polarized and possess an extended  $\pi$ -electron system that endows them with electron donor/acceptor properties with resonance structures quite similar to thiocyanate. From the smaller representative, the cyanate, we know that they adsorb antibodies via dipole-dipole interactions and can specifically interact with the sugar moieties within antibodies. But since this interaction is mostly used to immobilize antibodies onto surfaces for structural investigations such as scanning electron microscopy (SEM), little is unknown if these antibodies actually maintain their bioactivity after detachment [53,54].

The Hofmeister Series was created to describe the propensity of common salt anions and cations to increase the surface tension of a protein in solution and thus cause their precipitation. Nonetheless, we will suppose that surface bound anions

behave in a similar manner as their ionic analog. Consider that the position an anion partakes within the Hofmeister series corresponds to its degree of hydration in the following order:  $\text{SO}_4^{2-} > \text{HPO}_4^{2-} > \text{OH}^- > \text{F}^- > \text{HCOO}^- > \text{CH}_3\text{COO}^- > \text{Cl}^- > \text{Br}^- > \text{NO}_3^- > \text{I}^- > \text{SCN}^- > \text{ClO}_4^-$  [55–57].

Furthermore, azide-anions possess similar free energy of hydration values [ $-\Delta G_{\text{hydr}}$ ] and water absorbance properties [ $A_{\text{W}}$ ] [58] as observed for SCN. Also an investigation on the electron-transfer properties of nucleophilic anions to 1-pyrenesulfonic acid radical cation ( $\text{Py}^+\text{SA}^-$ ) in Nafion membranes provide similar attenuation factors [AF] for both, SCN and N3 for the difference in quenching within the membranes and in bulk solution [57].

[ $-\Delta G_{\text{hydr}}$ ]:  $\text{SO}_4 > \text{Cl} > \text{Br} > \text{N}_3 > \text{SCN}$  [58]

[ $A_{\text{W}}$ ]:  $\text{SO}_4 \gg \text{Cl} > \text{Br} > \text{NO}_2 > \text{I} > \text{ClO}_4 > \text{SCN} > \text{N}_3 > \text{PO}_4 > \text{CrO}_4$  [58]

[Cloud Point]:  $\text{H}_2\text{O} > \text{F} > \text{CH}_3\text{COO} > \text{Cl} > \text{Br} > \text{N}_3 > \text{NO}_3$  [59]

[AF]:  $\text{SCN} > \text{N}_3 > \text{I} > \text{Cl}$  [57]

Taking these reported properties of azide anions into account, it seems possible that they belong to the Group C of the Hofmeister Series, which comprises the non-hydrated anions [55]. It is also reported that chaotropic agents promote protein unfolding. They can promote conformational changes in the protein structure, which may induce the reduction or even complete loss of protein activity [60–62].

Considering that azide groups are poorly hydrated and rather hydrophobic in nature, it seems possible that they can alter or disrupt the water structure of proteins and enhance their own attraction for protein binding. This may explain the high binding capacity of IgG on azide-modified support media. If the surface bound azide groups incite protein unfolding and can actually promote the exposure of certain areas on the protein that are sensitive to inter-protein interactions then an excess of closely aligned azide groups may lead to a surface-induced aggregate formation of IgG. Such an aggregation would lead to high molecular weight (MW) entities of low concentration. Note that due to conformational changes of the antibody molecule, induced by a partial un-folding or association to higher MW conglomerates, a recognition and binding to Protein A may be hindered.

In order to verify this hypothesis, polyclonal h-IgG was incubated with sodium azide and with the organic azide compound, 1-azide-3-(2-propen-1-yloxy)-2-propanol (AGE-N<sub>3</sub>) under various conditions.

Fig. 9a, shows clearly that IgG molecules are least sensitive to shear forces (S) provided by agitation than to heat (H), which is obviously the strongest aggregation inducer. Since all samples were agitated in the same manner, the value for sample (S) is practically the baseline value for all other test samples. It is also apparent that an increasing amount of sodium azide has no effect on IgG recovery as long as the incubation time is below 3 h. Once the contact time for IgG and sodium azide was increased to 24 h, the recovery rate for IgG decreases with increasing amount of sodium azide added to the solution. Surprisingly, this effect is more pronounced for the organic azide compound AGE-N<sub>3</sub> (Fig. 9b) than for sodium azide. Note that for AGE-N<sub>3</sub> the incubation time dependency is much reduced and differs only by 3–5%, with higher values for the long incubation times. Also less AGE-N<sub>3</sub> is needed to induce the same reduction of traceable IgG compared to sodium azide. While 100 g/L sodium azide (sample G) is necessary to provoke a 30% reduction of detectable IgG, only 25% of AGE-N<sub>3</sub> (sample D) is needed to obtain the same result. Another interesting feature is the visible appearance of the protein aggregates per se. The supernatants of the AGE-N<sub>3</sub> containing samples C and D are slightly milky and pinkish in color and their aggregates are thread-like in nature. In case of samples incubated with sodium azide, their precipitates are flocculent with a colorless clear to milky supernatant.

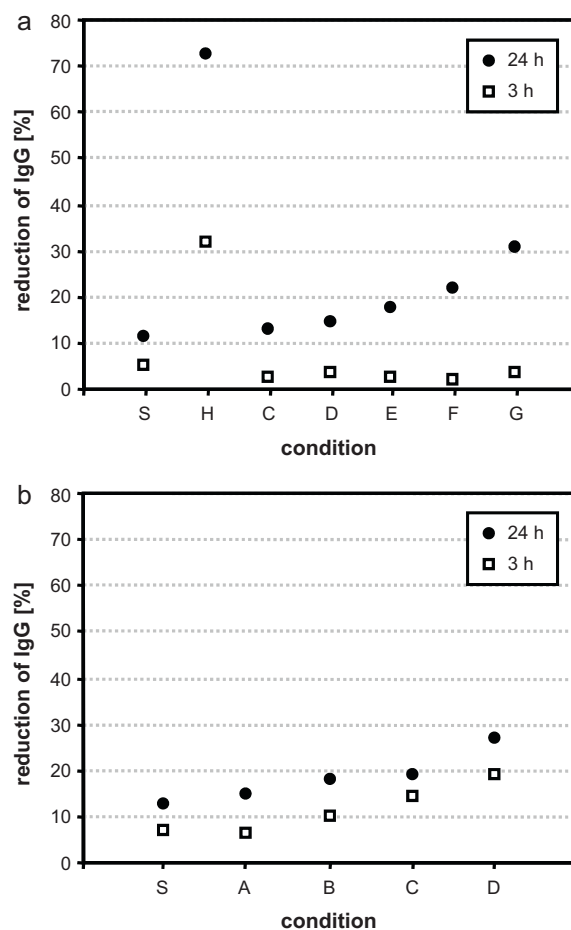


**Fig. 9.** Reduction of detectable IgG in solution after incubation of polyclonal h-IgG for 3 h and 24 h with solutions containing (a) NaN<sub>3</sub> and (b) AGE-N<sub>3</sub> and other aggregate-forming conditions: S (azide-free, shear stress at 1400 rpm, 25 °C), H (azide-free, heat stress, 60 °C), and A to G resemble samples with addition of varying amount of NaN<sub>3</sub> or mol-equivalents of AGE-N<sub>3</sub> (1, 5, 10, 25, 50, 75, 100 g/L NaN<sub>3</sub>) tested under otherwise same conditions at 25 °C and 1400 rpm. All samples were tested with Protein A HPLC.

The reason for the more pronounced protein aggregation effect of AGE-N<sub>3</sub> lies in its strong lipophilic nature, which makes it viable to interact stronger with hydrophobic patches on the surface of IgG molecules than its ionic counterpart. It can be assumed that shear forces as well as the binding of IgG molecules to multiple attachment points on a support surface lead to a partial unfolding of their protein structure. The increased accessibility of hydrophobic areas on the protein will increase the interaction tendency between the IgG molecules as well as between IgG and the organic surface bound azide groups.

### 3.2.5. Performance of AdQ-triazole-Fractogel (AdQ-TRZ-FA3) with and without azide group endcapping

Click protocol 2 was used for the immobilization of the anion exchange ligand N-1-azabicyclo [2.2.2] oct-3-yl-4-pentynamide (AdQ-pentyne) onto an azide group modified Fractogel support as well as for the final endcapping of residual azide groups with 2-propargyl alcohol (Fig. 6g).

The reason for using Fractogel instead of the previously discussed FractoAIMs-3, is simply because the AdQ-pentyne ligand performs better in combination with Fractogel. This indicates that also the physical support properties such as pore size and pore size distribution play an important role in material performance. Since AdQ-TRZ-FA3 is a weak anion exchange material, the larger pore

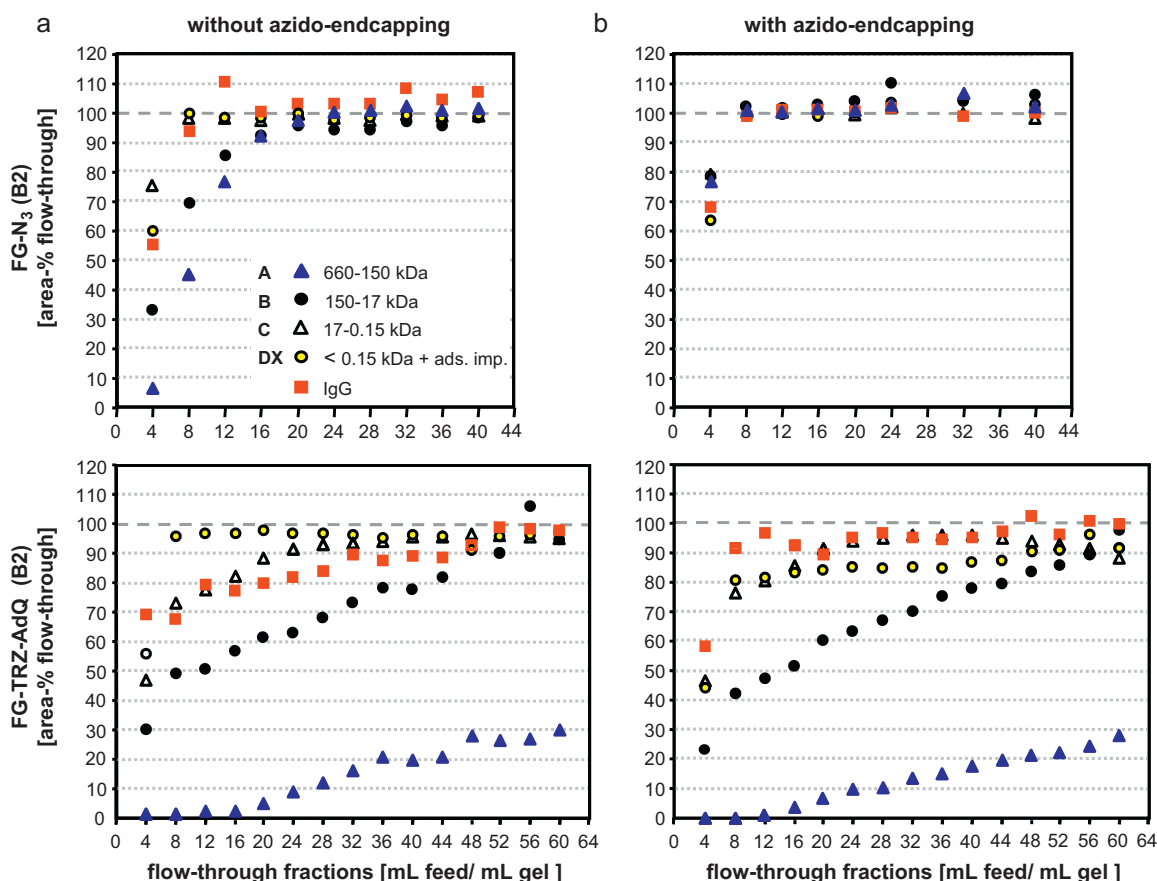


**Fig. 10.** PSEC-diagrams showing the dynamic break-through performance of (a) Azido-Fractogel material FG-N<sub>3</sub> (B2) and the modified adsorbent (b) FG-TRZ-AdQ (B2), both with and without azide group endcapping using the Azido-Fractogel with reduced azide group density (676  $\mu\text{mol/g}$ ) and Click-protocol 2 for the endcapping with 3-propargylalcohol.

size of Fractogel improves the binding performance of the adsorbents for the capture of feed impurities such as host cell proteins and DNA.

It is probable that the larger pore-size of Fractogel combined with the low azide group density of FG-N<sub>3</sub> (B2) facilitates the accessibility of azide groups for the Click-reaction. Note that with the conventional one-pot Click reaction (protocol 1) only a low AdQ-pentyne coverage of 250  $\mu\text{mol/g}$  was obtained, while for protocol 2, 500  $\mu\text{mol/g}$  could be achieved. Furthermore, the immobilization of the AdQ-pentyne ligand is very efficient, leaving only 176  $\mu\text{mol/g}$  residual azide groups to be deactivated with 3-propargyl alcohol. The main difficulty observed during material preparation was the complexation of Cu(I) and Cu(I)-acetylide to the Fractogel support surface, which was significantly reduced with Click protocol 2.

The PSEC diagrams in Fig. 10 visualize the performance of FG-N<sub>3</sub> (B2) and AdQ-TRZ-FG (B2) before and after azide group endcapping using the same batch of cell culture feed as earlier employed for the preliminary investigations. While the non-endcapped Azido-Fractogel binds mainly high MW feed impurities A (660–150 kDa) and B (150–17 kDa) and little IgG, all feed impurities as well as IgG are not retained on the endcapped support. Comparing the two AdQ-TRZ-FG (B2) materials, it is apparent that the non-endcapped adsorbent binds more IgG and less of the low MW feed impurities than its azide group endcapped counterpart.

#### 4. Conclusions

This study has shown that any type of purification media will observe a natural loss in performance, once non-target molecules bind to the adsorbent. It does not appear to make a difference if

they are small and large in number or large in molecular weight but present only in traces. In any case the undesired binding of non-target compounds induces also steric hindrance, blocking otherwise accessible binding sites for the target molecule.

The right choice of reagent or strategy for the endcapping or deactivation of the remaining reactive groups after ligand attachment can be crucial and difficult to make. For epoxide activated support surfaces a simple hydrolysis reaction, which leads to a fast and simple ring-opening seemed best suitable. The hydroxylated support surface is inert towards the capture of feed impurities as well as IgG. However, the introduction of 2-ethanolamine onto the surface for an affinity-type adsorbent such as B14-2LP-FA1 seems at first sight unwise. But at a second glance the so-modified adsorbent resembles a mixed-mode material, which combines the removal of feed impurities with the capture and release of practically pure Mab.

For azide-modified support surfaces, we have learned that even an optimized Click-reaction protocol for ligand attachment and azide group endcapping may not be sufficient to obtain inert support surfaces. Here we could show that a too close alignment of reactive groups can resemble for their neighboring groups a steric hindrance in the final endcapping reaction after ligand immobilization. Another advantage of our modified Click approach, which is based on the off-line preparation of the copper (I)-acetylide complex lies in the tendency of polymethacrylate type support media to capture copper (I). Once bound to the surface, copper (I) is no more part of the reaction cycle and provide a profound hindrance for further immobilization reactions. Furthermore, we have discovered that inorganic as well as organic surface-bound azide groups do not only bind IgG but are also capable to induce aggregate for-

mation. However, with an optimized immobilization strategy for ligand attachment and surface endcapping via Click Chemistry, the modified adsorbent only exhibits the desired properties of the attached ligand without interference from the underlying support chemistry.

## Acknowledgments

This study was performed within the EU-Project AIMs (Advanced Interactive Materials by Design; NMP3-CT-2004-500160), which is part of the 6th Framework Program of the European Union. The authors would like to thank ProMetic BioScience Ltd. for allowing us to evaluate their non-commercial affinity adsorbent, B14-2LP-FA1, Chris Sadler for making the B14 ligand and Sharon Williams for valuable discussions throughout the AIMs Project.

## Appendix A. Supplementary data

Supplementary data associated with this article can be found, in the online version, at [doi:10.1016/j.jchromb.2010.10.025](https://doi.org/10.1016/j.jchromb.2010.10.025).

## References

- [1] J. Horak, A. Ronacher, W. Lindner, J. Chromatogr. A 1217 (2010) 5092.
- [2] P. Decaria, A. Smith, W. Whitford, BioProcess Int. 7 (2009) 44.
- [3] J.P. Lopez-Bote, C. Langa, P. Lastres, C. Rius, A. Marquet, R. Ramos-Ruiz, C. Bernabeu, Scand. J. Immunol. 37 (1993) 593.
- [4] K. Ahrer, A. Buchacher, G. Iberer, D. Josic, A. Jungbauer, J. Chromatogr. A 1009 (2003) 89.
- [5] H.-C. Mahler, W. Friess, U. Grauschopf, S. Kiese, J. Pharm. Sci. 98 (2009) 2909.
- [6] H.-C. Mahler, R. Mueller, W. Friess, A. Delille, S. Matheus, Eur. J. Pharm. Biopharm. 59 (2005) 407.
- [7] K. Ahrer, A. Buchacher, G. Iberer, A. Jungbauer, J. Chromatogr. A 1043 (2004) 41.
- [8] A. Hawe, W. Friess, M. Sutter, W. Jiskoot, Anal. Biochem. 378 (2008) 115.
- [9] T. Wang, J.A. Lucey, J. Dairy Sci. 86 (2003) 3090.
- [10] J.D. Lewis, R.T.C. Ju, A.I. Kim, S.L. Nail, J. Colloid Interface Sci. 196 (1997) 170.
- [11] D.A. McCarthy, A.F. Drake, Mol. Immunol. 26 (1989) 875.
- [12] I. Oreskes, D. Mandel, Anal. Biochem. 134 (1983) 199.
- [13] R. Thirumangalathu, S. Krishnan, M.S. Ricci, D.N. Brems, T.W. Randolph, J.F. Carpenter, J. Pharm. Sci. 98 (2009) 3167.
- [14] M. Garcia, M. Monge, G. Leon, S. Lizano, E. Segura, G. Solano, G. Rojas, J.M. Gutierrez, Biologicals 30 (2002) 143.
- [15] J.-M. Sarciaux, S. Mansour, M.J. Hageman, S.L. Nail, J. Pharm. Sci. 88 (1999) 1354.
- [16] K. Ahrer, A. Buchacher, G. Iberer, A. Jungbauer, J. Membr. Sci. 274 (2006) 108.
- [17] L. Jespers, O. Schon, K. Famm, G. Winter, Nat. Biotechnol. 22 (2004) 1161.
- [18] S. Gulich, M. Uhlen, S. Hober, J. Biotechnol. 76 (2000) 233.
- [19] A.A. Shukla, P.J. Hinckley, P. Gupta, Y. Yigzaw, B. Hubbard, BioProcess Int. 3 (2005) 36.
- [20] S. Kabir, Immunol. Invest. 31 (2002) 263.
- [21] R. Li, V. Dowd, D.J. Stewart, S.J. Burton, C.R. Lowe, Nat. Biotechnol. 16 (1998) 190.
- [22] A.C.A. Roque, M.A. Taipa, C.R. Lowe, J. Chromatogr. A 1064 (2005) 157.
- [23] S. Hober, K. Nord, M. Linhult, J. Chromatogr. B 848 (2007) 40.
- [24] V. Busini, D. Moiani, D. Moscatelli, L. Zamolo, C. Cavallotti, J. Phys. Chem. B 110 (2006) 23564.
- [25] A.R. Newcombe, C. Cresswell, S. Davies, K. Watson, G. Harris, K. O'Donovan, R. Francis, J. Chromatogr. B 814 (2005) 209.
- [26] L. Zamolo, V. Busini, D. Moiani, D. Moscatelli, C. Cavallotti, Biotechnol. Prog. 24 (2008) 527.
- [27] L. Zamolo, M. Salvalaglio, C. Cavallotti, S. Hofer, J. Horak, W. Lindner, B. Galarza, C. Sadler, S. Williams, J. Phys. Chem. B 114 (2010) 9367.
- [28] W.H. Binder, C. Kluger, Curr. Org. Chem. 10 (2006) 1791.
- [29] W.H. Binder, R. Sachsenhofer, Macromol. Rapid Commun. 28 (2007) 15.
- [30] H.C. Kolb, M.G. Finn, K.B. Sharpless, Angew. Chem. Int. Ed. 40 (2001) 2004.
- [31] V. Aucagne, J. Berna, J.D. Crowley, S.M. Goldup, K.D. Haenni, D.A. Leigh, P.J. Lusby, V.E. Ronaldson, A.M.Z. Slawin, A. Viterisi, D.B. Walker, J. Am. Chem. Soc. 129 (2007) 11950.
- [32] C. Nolte, P. Mayer, B.F. Straub, Angew. Chem. Int. Ed. 46 (2007) 2101.
- [33] V.O. Rodionov, V.V. Fokin, M.G. Finn, Angew. Chem. Int. Ed. 44 (2005) 2210.
- [34] Y. Angell, K. Burgess, Angew. Chem. Int. Ed. 46 (2007) 3649.
- [35] B.P. Duckworth, J. Xu, T.A. Taton, A. Guo, M.D. Distefano, Bioconjugate Chem. 17 (2006) 967.
- [36] S. Punna, E. Kaltgrad, M.G. Finn, Bioconjugate Chem. 16 (2005) 1536.
- [37] M. Slater, M. Snauko, F. Svec, J.M.J. Frechet, Anal. Chem. 78 (2006) 4969.
- [38] M. Ortega-Munoz, J. Lopez-Jaramillo, F. Hernandez-Mateo, F. Santoyo-Gonzalez, Adv. Synth. Catal. 348 (2006) 2410.
- [39] Electronic Supplementary Material.
- [40] B.-R.L. Instruction Manual for Mini-PROTEIN® 3 Cell, Inc., Available from: <http://www.plant.uoguelph.ca/research/homepages/raizada/Equipment/RaizadaWeb%20Equipment%20PDFs/9B.%20miniprotein3%20cell%20manual.pdf>.
- [41] S.-A. Technical Bulletin for ProteoSilver™ Plus Silver Stain Kit (PROT-SIL2), Inc., Available from: <http://www.sigmaaldrich.com/etc/medialib/docs/Sigma/Bulletin/protsil2bul.Par.0001.File.tmp/protsil2bul.pdf>.
- [42] J. Hardouin, M. Duchateau, L. Canelle, C. Vlieghe, R. Joubert-Caron, M. Caron, J. Chromatogr. B 845 (2007) 226.
- [43] J. Porath, T.W. Hutchens, Int. J. Quantum Chem. 14 (1987) 297.
- [44] W. Schwartz, D. Judd, M. Wysocki, L. Guerrier, E. Birck-Wilson, E. Boschetti, J. Chromatogr. A 908 (2001) 251.
- [45] W.D. Sharpless, P. Wu, T.V. Hansen, J.G. Lindberg, J. Chem. Educ. 82 (2005) 1833.
- [46] K.M. Kacprzak, N.M. Maier, W. Lindner, Tetrahedron Lett. 47 (2006) 8721.
- [47] T.R. Chan, R. Hilgraf, K.B. Sharpless, V.V. Fokin, Org. Lett. 6 (2004) 2853.
- [48] W.G. Lewis, F.G. Magallon, V.V. Fokin, M.G. Finn, J. Am. Chem. Soc. 126 (2004) 9152.
- [49] J.D. Megiatto Jr., D.I. Schuster, J. Am. Chem. Soc. 130 (2008) 12872.
- [50] V.O. Rodionov, S.I. Presolski, D. Diaz Diaz, V.V. Fokin, M.G. Finn, J. Am. Chem. Soc. 129 (2007) 12705.
- [51] A.E. Speers, G.C. Adam, B.F. Cravatt, J. Am. Chem. Soc. 125 (2003) 4686.
- [52] E.A. Ambundo, Q. Yu, L.A. Ochrymowycz, D.B. Rorabacher, Inorg. Chem. 42 (2003) 5267.
- [53] P.E. Mazeran, J.L. Loubet, C. Martelet, A. Theret, Ultramicroscopy 60 (1995) 33.
- [54] G. Zhou, L. Veron, A. Elaissari, T. Delair, C. Pichot, Polym. Int. 53 (2004) 603.
- [55] E. Leontidis, Curr. Opin. Colloid Interface Sci. 7 (2002) 81.
- [56] L.A. Munishkina, J. Henriques, V.N. Uversky, A.L. Fink, Biochemistry 43 (2004) 3289.
- [57] T. Tachikawa, R. Ramaraj, M. Fujitsuka, T. Majima, J. Phys. Chem. B 109 (2005) 3381.
- [58] P. Lo Nostro, L. Frattini, B.W. Ninham, P. Baglioni, Biomacromolecules 3 (2002) 1217.
- [59] M. Lagi, P. Lo Nostro, E. Frattini, B.W. Ninham, P. Baglioni, J. Phys. Chem. B 111 (2007) 589.
- [60] S.-M. Choi, C.-Y. Ma, J. Agric. Food Chem. 53 (2005) 8046.
- [61] S. Oscarsson, J. Chromatogr. B 666 (1995) 21.
- [62] K.B. Song, S. Damodaran, Han'guk Saenghwa Hakhoechi 25 (1992) 393.





# Supplementary Material

## Optimization of a ligand immobilization and azide group endcapping concept via “Click-Chemistry” for the preparation of adsorbents for antibody purification.

Jeannie Horak, Stefan Hofer, Wolfgang Lindner  
( Contact Email: [Jeannie.Horak@univie.ac.at](mailto:Jeannie.Horak@univie.ac.at) )

### 1. Optimization of azido group immobilization

**Fig. S1** shows the results of two azido group immobilization studies. In the first experiment (**Fig. 1Sa**) aliquots of 0.5 mL FractoAIMs-3 were incubated for 1, 2, 3, 4 and 5 days with 0.5 mL solutions containing 750  $\mu\text{mol}$  sodium azide per gram gel, 10 mol% triethylamine (TEA) and 2 vol% methanol. The second experiment (**Fig. S1b**) was performed similar to the former, but keeping the reaction time constant at 2h and varying the sodium azide concentration (250, 500, 750, 1000, 1500 and 2000  $\mu\text{mol/g}$ ). Both experiments were performed in Eppendorf reaction vessels using a Thermomixer compact from Eppendorf (Vienna, Austria), employing a temperature of 40°C and an agitation speed of 1400 rpm. The azide group immobilization rate was determined with elemental analysis employing the nitrogen content.

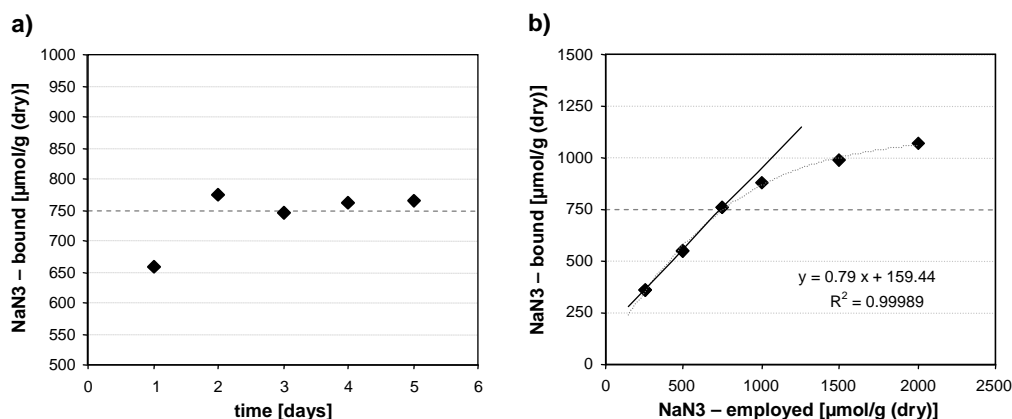


**Figure S1.** Modification of epoxide-activated FractoAIMs-3 support with  $\text{NaN}_3$ .  
a) reaction time dependent azidation (750  $\mu\text{mol/g}$   $\text{NaN}_3$  in bi-distilled water, 40°C)  
b)  $\text{NaN}_3$  concentration dependent azidation (2 days, 40°C)

Correlation factors for FractoAIMs-3: 1 g wet = 0.3001 g dry  
1 g dry = 4.6896 mL wet

Note that the term “g wet” stands for adsorbents, which were rinsed with bi-distilled water and were suction dried gel for 30 sec, while “mL wet” indicates the gel volume after a sedimentation time of 24 h in 1 M aqueous sodium chloride solution. The term “g dry” describes adsorbents, which were dried at 60°C under vacuum (18 mbar).

## **2. Synthesis and material preparation.**

### **2.1. Chemicals and Materials**

Solvents for synthesis such as petrolether (PE), ethylacetate (EA), dichloromethane (DCM) and methanol (MeOH) were of technical grade and purchased from various suppliers (Vienna, Austria). For column chromatographic purification of synthesis products, silica gel 60 from Merck and self-prepared 3-amino-propyl-silica gel 60 (1.2 mmol NH<sub>2</sub>-groups, non-silanol endcapped) were used. The TLC-aluminium sheets, silica gel F<sub>254</sub> and NH<sub>2</sub>F<sub>254s</sub> were from Merck purchased through VWR (Vienna, Austria).

### **2.2. Preparation of 2-Hydroxyethy-sulfanyl-FractoAIMs-3, 2-Hydroxyethyl-amino-FractoAIMs-3 and Hydroxy-FractoAIMs-3**

The modified FractoAIMs-3 (FA3) materials, FA3-S-(CH<sub>2</sub>)<sub>2</sub>-OH and FA3-NH-(CH<sub>2</sub>)<sub>2</sub>-OH were prepared by addition of 5 mol equivalents (referring to mol epoxide groups) of 2-mercaptoopropanol (plus 10 mol% TEA) or 5 mol equivalents of 2-ethanolamine to a slurry of 5 mL FractoAIMs-3 in bi-distilled water (**Fig. 2b and 2c**). The reaction mixtures were stirred under reflux for 24 h under nitrogen using a mechanical stirrer. Both adsorbents were washed thoroughly with water, before the deactivation of remaining epoxide groups via acidic hydrolysis using 100 mL 0.5 M sulfuric acid. The slurry was stirred at 60°C for 12-24 h. The adsorbent FA3-OH was prepared with the above mentioned procedure by acidic hydrolysis of Epoxy-FractoAIMs-3 (**Fig. 2a**). All modified adsorbent were thoroughly washed with water and methanol. The elemental analysis of a dried aliquot of the corresponding adsorbent with exception of the latter, lead to the following ligand densities:

FA3-OH (**Fig.2a**): not available

FA3-S-(CH<sub>2</sub>)<sub>2</sub>-OH (**Fig.2b**): 1.76 mmol/g; (C, 53.52%; H, 7.42%; N, 0.05%; S, 5.65%)

FA3-NH-(CH<sub>2</sub>)<sub>2</sub>-OH (**Fig.2c**): 1.03 mmol/g; (C, 55.16%; H, 7.63%; N, 1.44%; S, 0.02%).

### **2.3. Preparation of Azido-FractoAIMs-3**

a) The FA3-N<sub>3</sub> (A) material (**Fig. 3c**) with an azide group density of 1.38 mmol/g (dry) gel was prepared by the addition of 5 mol equiv. of sodium azide (plus 10 mol% TEA) to an aqueous slurry of FractoAIMs-3. The reaction mixture was stirred at 40°C with a mechanical stirrer for 3 days under nitrogen.

b) The FA3-N<sub>3</sub> (B) material (**Fig. 3b**) with a tuned azide group density of 750 µmol/g (dry) were prepared by addition of the desired loading amount of sodium azide to an aqueous slurry of epoxide activated support. According to the immobilization study in **Fig. S1**, a reaction time of 2 days at 40°C and the addition of 10 mol% TEA as a catalyst for epoxide ring opening were sufficient to obtain the desired azide group density. Note that after azidation, the remaining epoxide groups on FA3-N<sub>3</sub> (A) and FA3-N<sub>3</sub> (B) were opened using the same acidic hydrolysis protocol as earlier described for the FA3-OH material.

FA3-N<sub>3</sub> (A) / (**Fig. 3c**): 1.38 mmol/g; (C, 54.78%; H, 6.91%; N, 5.80%)

FA3-N<sub>3</sub> (B) / (**Fig. 3b**): 0.750 mmol/g; (C, 55.91%; H, 7.24%; N, 3.15%)

The residual azide groups on FA3-N<sub>3</sub> (A) and (B) materials were endcapped with Click reaction protocol 1 and/or Click reaction protocol 2. Both methods are described in the experimental section of the manuscript.

## **2.4. Preparation of AdQ-TRZ-Fractogel (B2)**

### **2.4.1. Synthesis of *N*-1-azabicyclo [2.2.2] oct-3-yl-4-pentynamide (AdQ-pentyne)**

An aliquot of 1-azabicyclo [2.2.2] octan-3-amine dihydrochloride (also known as 3-aminoquiniclidine = AQ) was ground to a fine powder and dried under vacuum at 60°C to remove traces of water. Thereof 2 g (10 mmol) was suspended in 100 mL HPLC-grade dichloromethane (DCM) upon addition of 2 mL (15 mmol) triethylamine (TEA) to obtain the free amine. After stirring for 2h under nitrogen, 1 g (11 mmol) of 4-pentynoic acid and 2.4 g (12 mmol) of 1,3-dicyclohexylcarbodiimide (DCC) dissolved in 30 mL DCM each were subsequently added at 0°C. The reaction solution was stirred for 3h at 0°C under nitrogen, then at room temperature over night and for 1h under reflux (if necessary). Precipitated TEA-HCl and dicyclohexyl urea were filtered and the crude product was purified via column chromatography employing subsequently silica gel 60 and a self-prepared amino-silica gel 60 (3-aminopropyl silane loading: 1.2 mmol/g) with petrolether (PE), ethylacetate (EA) and methanol (MeOH). PE and EA removed the impurities, while product elution starts with the addition of 1% and 7% of MeOH. The product was visualized as orange spots on amino-TLC plates (EA:MeOH (6:1 (v/v)) mix) using subsequently iodine (1 g iodine on 10 g silica gel 60) and sodium dichromate dye solution (5% sodium dichromate in 10% sulfuric acid). The isolated product was filtered through a glass-fiber filter in order to remove traces of silica gel. The clear oil-like product solidifies to a white solid under vacuum with a reaction yield of 65%.

MS (ESI, positive):  $m/z$  207.3 [M+H]<sup>+</sup>, 229.2 [M+Na]<sup>+</sup>; 413.4 [2M+H]<sup>+</sup>, 435.4 [2M+Na]<sup>+</sup>;

<sup>1</sup>H NMR (400 MHz, CDCl<sub>3</sub>):  $\delta$  5.91 (s, 1H), 4.01 - 3.94 (m, 1H), 3.36 – 3.33 (dd, 1H), 2.90 – 2.72 (m, 4H), 2.57 – 2.37 (m, 5H), 2.03 (t, 1H), 1.92 (m, 1H), 1.73 - 1.61 (m, 3H), 1.52 – 1.42 (m, 1H);

<sup>13</sup>C NMR (100 MHz, CDCl<sub>3</sub>):  $\delta$  171.22, 83.45, 69.97, 56.64, 47.86, 47.19, 47.05, 35.82, 26.23, 26.04, 20.63, 15.47

### **2.4.2. Preparation of 1H - 1,2,3 - triazole, 1 - Fractogel, 4 - *N*-[1-azabicyclo [2.2.2] oct-3-yl] propyl amide (AdQ-TRZ-FG)**

The activated, bright orange AdQ-pentyne-Cu(I)-complex was prepared by the addition of AdQ-pentyne (1.5 equiv. relative to the desired ligand density) in water:MeOH at 95:5 (v/v) to the freshly prepared aqueous Cu(I) solution (1.5 equiv. CuSO<sub>4</sub> x 5 H<sub>2</sub>O and 1.5 equiv. L-sodium ascorbate). The AdQ-pentyne-Cu(I) solution was then stirred for 5 min before its addition to the Azido-Fractogel support (FG-N<sub>3</sub> (B2)), which was prepared in the same manner as FA3-N<sub>3</sub> (B2). The slurry was covered with nitrogen and shaken for 4 days at room temperature on an orbital shaker. The modified material (**Fig. 6g**) was washed as previously described.

It was observed that AdQ-TRZ binds Cu(I) strongly and that the introduction of air (or oxygen) into the slurry of the EDTA wash-step can increase the removal rate of copper due to the oxidation of Cu(I) to

Cu(II), which can easily be captured by EDTA. Alternatively the gel can be washed with 0.1 M hydrochloric acid and bi-distilled water before a final rinse with 1 M EDTA.

The residual azide-groups were deactivated with 3-propargyl alcohol using the click-protocol-2. The density of bound AdQ-ligand was determined by elemental analysis using the nitrogen-content of the material.

Azide-group content (**Fig. 3b**): 676  $\mu\text{mol/g}$ ; (C, 46.61%; H, 6.50% and N, 2.84%);

AdQ-TRZ content (**Fig. 3g**): 500  $\mu\text{mol/g}$ ; (C, 53.07%; H, 7.55% and N, 4.24%);

(residual azide-groups: 176  $\mu\text{mol/g}$ )

## 2.5. Preparation of 3-aminoquinuclidine-FractoAIMs-3 (AQ-FA3)

An aliquot of 1.04 g 3-aminoquinuclidine-dihydrochloride (5.2 mmol; AQ) was dissolved in a solution containing 10 mL bi-distilled water, 2 mL methanol and 1 mol-equivalent of TEA (5.2 mmol), relative to the AQ-amount used. This solution was stirred for 5-10 min. before addition to a stirred slurry of 40 mL FractoAIMs-3 in 20 mL of bi-distilled water. The reaction mixture was stirred under nitrogen for 48 h under reflux condition employing a mechanical stirrer. The modified support was rinsed with 3 x 200 mL of bi-distilled water. The residual epoxy-groups were hydrolyzed with 150 mL of 0.5 M sulfuric acid in bi-distilled water at 60°C for 24 h under nitrogen.

AQ-FractoAIMs-3 (**Fig. 2e**): 514  $\mu\text{mol/g}$ ; (C, 55.97%; H, 7.44%; N, 1.44%).

## 2.6. Preparation of 1-azido-3-(2-propen-1-yloxy)-2-propanol (= AGE-N3)

An aliquot of 12 g of Amerlite ion exchange resin was conditioned with 0.1 M hydrochloric acid over night and washed until a neutral pH was reached. To these resins 150 mL bi-distilled water, 2 mL methanol, 10 g (154 mmol) sodium azide and 7.12 mL (60 mmol) 1-(2-propenyloxy)-2,3-epoxypropane (also known as allyl glycidyl ether = AGE) were added. The reaction mixture was shaken on an orbital shaker for 3 days. The methanol in the product containing solution was evaporated under vacuum on a rotary extractor, before addition of sodium chloride in excess and extraction of the product with DCM. After evaporation of the solvent, crude product with a yield of 94% was obtained [1].

Further purification was performed on 3-aminopropyl silica gel, using a step gradient of PE and DCM. First elution of product was observed at 5% DCM and complete elution of product was obtained with 50% DCM. TLC: amino-silica sheets with PE:DCM - 1:5 (v/v) as running buffer and dyed subsequently with iodine-silica and sodium dichromate dye solution. AGE-N<sub>3</sub> was obtained as a viscose, yellow liquid at an overall yield of 70%.

MS (ESI, negative):  $m/z$  141 [ $M+2H^+-H_2O$ ],

<sup>1</sup>HNMR (400 MHz, CDCl<sub>3</sub>):  $\delta$  5.84 – 5.96 (m, 1H), 5.28 (dd, 1H), 5.22 (dd, 1H), 4.00 – 4.07 (m, 2H), 3.90 – 4.00 (m, 1H), 3.44 – 3.58 (m, 2H), 3.30 – 3.44 (m, 2H), 2.45 (d, OH);

<sup>13</sup>CNMR (100 MHz, CDCl<sub>3</sub>):  $\delta$  134.54, 118.04, 72.81, 71.58, 70.08, 53.88.

### **3. Dialysis of cell culture feed solution and related samples**

Dialysis was performed with Spectra/Pore® CE Float-A-Lyzer® G2 with 10 mL volume size and a molecular-weight-cut-off (MWCO) of 3.5-5 kDa from Spectrum Europe B.V. (Breda, Netherlands) in 2 L glass beakers filled with 2 L PBS-75 (10 mM phosphate buffer with 75 mM NaCl, pH 7.20) spiked with 1 g/L sodium azide.

The rim of the beaker was furnished with parafilm to allow the adhesion of the Styrofoam float-ring of the dialysis tube on top of the parafilm rim of the beaker. Thereby the Float-A-Lyzer tubes were forced to remain near the beaker walls and the magnetic stirrer kept the dialysis solution gently in motion, while the dialysis tubes stayed in place (**Fig. S2**). The beaker with the dialysis tube could be covered with a large expanded parafilm or with a glass disc to prevent the contamination of the dialysis solution. Furthermore the beaker was cooled with ice in order to prevent an early feed fouling. In general, the samples were dialysed twice. A change of dialysis solution was performed in a 12h interval. The additional advantage of this experimental set-up was that due to a slight gravity effect (since a small section of the tube is above the buffer surface) the dilution effect due to osmotic forces could be reduced.



**Figure S2.** Spectra/Pore CE Float-A-Lyzer® G2 in a 2L glass beaker rimmed with parafilm and positioned on a magnetic stirrer

### **4. Protein aggregation test**

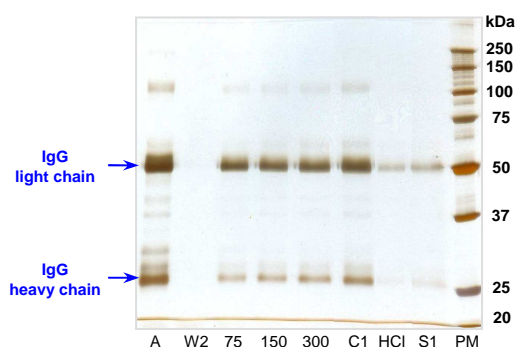


**Figure S3.** SDS-PAGE slab gel (10%-TRIS-HCl; reduced) for FA3-N<sub>3</sub> (A1) tested with a polyclonal h-IgG standard solution containing 100 mg/L h-IgG in PBS-75 buffer (10 mM phosphate, 75 mM NaCl, pH 7.20) and 1 g/L NaN<sub>3</sub>;

**A:** application feed, **W2:** wash solution (PBS-0, salt-free), **75:** PBS with 75 mM NaCl, **150:** PBS with 150 mM NaCl, **300:** PBS with 300 mM NaCl, **C1:** 50 mM citric acid, pH 3.50, **HCl:** 0.1 M HCl, **S1:** 0.5 M NaOH; IgG light chain: 25 kDa, IgG heavy chain: 50 kDa

### **5. Reference:**

[1] B. Tamami, H. Mahdavi, Tetrahedron Letters 42 (2001) 8721.



## **Appendix 5**

### **Publication 5**







Contents lists available at ScienceDirect

Journal of Chromatography A

journal homepage: [www.elsevier.com/locate/chroma](http://www.elsevier.com/locate/chroma)



## Static and dynamic binding capacities of human immunoglobulin G on polymethacrylate based mixed-modal, thiophilic and hydrophobic cation exchangers

Stefan Hofer<sup>a</sup>, Alexander Ronacher<sup>a</sup>, Jeannie Horak<sup>a</sup>, Heiner Graalfs<sup>b</sup>, Wolfgang Lindner<sup>a,\*</sup>

<sup>a</sup> Department of Analytical Chemistry, University of Vienna, Währinger Strasse 38, 1090 Vienna, Austria

<sup>b</sup> Laboratory for Polymer Derivatization, Performance & Life Science Chemicals, Merck KGaA, Frankfurter Strasse 250, 64293 Darmstadt, Germany

### ARTICLE INFO

Article history:  
Available online xxx

Keywords:  
Cation exchange  
Thiophilic adsorption  
Hydrophobic interaction chromatography  
Mixed-modal ligands  
Antibody purification  
Cell culture supernatant

### ABSTRACT

The aim of this study was to investigate functional increments of ion exchange type ligands, which may improve the performance of mixed-modal ligands for antibody capture out of feed solutions with pH above 6.0 and containing sodium chloride concentrations of 150 mM and higher. For this purpose several functional groups such as sulfonyl, sulfanyl, amide, methoxy, short alkyl and aromatic moieties were tested in combination with a strong sulfonic acid and/or a weak carboxylic acid group. Therefore a series of ligands were synthesized and subsequently coupled onto epoxide activated Fractogel<sup>®</sup> EMD. In the first instance, all materials were tested by static binding capacity measurements (SBC) under test conditions, comprising a wide variety of different sodium chloride concentrations and differing pH values ranging from 4.5 to 7.5. From these preliminary experiment it was found that especially the aromatic groups improved the binding of human immunoglobulin G (h-IgG) under isotonic conditions, while other increments, e.g. thiophilic or amide groups, were not able to increase the capacity significantly. Taking the SBC results into account, the most promising materials were investigated under dynamic binding conditions (DBC) with a reduced selection of test conditions (pH 5.5, 6.5 and 7.4 at 75 and 150 mM NaCl). N-benzoyl-homocysteine (material J) and 3,5-dimethoxybenzoyl-homocysteine (material K) showed 100% DBCs of 37 mg/mL and 32 mg/mL in the presence of 75 mM NaCl and pH 6.5. Material L carrying mercaptobenzoic acid as a ligand and tested with the same solution provided a 100% DBC of 68 mg/mL. The influence of Pluronic F68 in a mock feed solution as well as in cell culture supernatant was investigated with the best performing bio-affinity type adsorbent, material L. For the real sample feed subsequent SDS-PAGE was conducted for the collected fractions.

© 2011 Elsevier B.V. All rights reserved.

### 1. Introduction

Although the importance of monoclonal antibodies (mAbs) in biopharmaceutical industry is steadily growing, their large-scale manufacturing is still expensive [1] as downstream processing still accounts for up to 60% of the overall production costs [2]. The most prominent media in the purification of immunoglobulin G (IgG) are up to date Protein A resins, since they allow the direct and most-efficient capture of IgG from a cell culture supernatant [3]. Hence, Protein A media require a reduced number of pre-operational steps such as de-salting, buffer change and pH adjustments, which are not only laborious, but are most of all inconvenient. Their obvious drawbacks are, however, the chemical and enzymatic instability of the protein-type ligand, which could be significantly improved by protein engineering [4]. But although the availability and chemical

stability of Protein A has been improved in recent years, it appears to be by a factor of 10 more expensive than alternative materials for antibody purification. Cleaning in place (CIP) and digestion by enzymes present in the cell culture feed may induce degradation and ligand leakage [5,6]. The reduced number of ligands present on the adsorbent surface leads subsequently to decreased binding capacities for the target protein. Furthermore, decoupled Protein A and degradation products thereof [7,8] have to be removed from the target mAb with additional polishing steps, which is rather counterproductive.

Since cation exchange type IgG capture media (CIEX) provide comparable IgG binding capacities to affinity-based adsorbents, but do not suffer from the same drawbacks, they resemble an interesting alternative to the latter [9–12]. The major advantage of CIEX media are their robustness against CIP and against autoclaving as well as their stability towards enzyme promoted ligand deterioration. Common cation exchangers perform best at buffer concentrations around 25 mM and at pH values of up to 0.5–1 pH units below or above the pI of the target protein [13,14]. The

\* Corresponding author. Tel.: +43 1 4277 52300; fax: +43 1 4277 9523.  
E-mail address: [Wolfgang.Lindner@univie.ac.at](mailto:Wolfgang.Lindner@univie.ac.at) (W. Lindner).

cell culture broth usually provides an isotonic environment with almost neutral pH and a salt concentration of about 150 mM sodium chloride. Under these conditions, the salt ions compete with the target protein for the ionic binding sites on the support material and decrease the binding capacity of the CIEX material. Furthermore, if an inappropriate pH is used, the charge densities on the ion exchange media may be reduced and on the surface of the target molecule the charge may change to an extent where their net polarity is reversed. In the worst case this will lead to a reduced or even no capture of IgG [15]. Consequently, the properties of the buffer system concerning conductivity and pH are of utmost importance in ion exchange chromatography and therefore additional unfavorable intermediate process steps often need to be implemented such as adjustment of pH and/or buffer dilution. The latter also includes an unfavorable increase of buffer volume and overall buffer consumption. Hence, it can be stated that the selectivity of CIEX-type adsorbents depend on the buffer conditions [16,17], which is an additional reason why the industrial application of strong (SCX) and weak (WCX) cation exchangers for mAb purification seem to be less popular although a considerable range of CIEX-type adsorbents are commercially available [18,19].

Examples for alternative process technologies, which are less dependent on buffer pH are thiophilic adsorption chromatography (TAC) and hydrophobic interaction chromatography (HIC) [20]. The IgG capture properties of thiophilic ligands are based on the attraction and interaction of spacer-chain embedded sulfanyl or sulfonyl groups towards antibodies. This was discovered in the year 1985 by Porath et al. [21]. The so-called electron donor–acceptor interaction properties of sulfur atoms within sulfur containing groups [22,23] are recognized as a responsible force for affinity and specificity of TAC adsorbents for antibody capture [24–26]. The major disadvantage of this adsorbent type is their need for high amount of structure forming (chaotropic) salts, without which no binding would take place. Both, sulfanyl and sulfonyl bonds are stated to exhibit thiophilic properties, but differ in their lipophilicity [22,23,27–29]. The beneficial influence of thiophilic spacer arms for IgG capture with the Mimetic Ligand™ A2P has been demonstrated using computational modeling studies as well as chromatographic performance evaluation [30,31].

Another method, often used for purification of antibodies under isotonic conditions, is hydrophobic interaction chromatography (HIC). Similar to thiophilic adsorbents, structure forming salts as, e.g. ammonium sulfate support the binding of antibodies to HIC media, but with a change in selectivity. HIC ligands consist of small aliphatic chains (C1–C6) or of one or more phenyl groups and are mainly used for the polishing of final MAb products [32,33]. Their selectivity towards IgG was found to be dependent on the chemical structure of the HIC ligands, namely whether they are aliphatic or aromatic in nature [24].

A further development along the line of MAb purification media development is the introduction of hydrophobic charge induction chromatographic (HCIC) ligands such as mercapto-ethyl-pyridine (MEP). Although this ligand type bears a basic group, it also contains an aromatic and therefore lipophilic moiety, if the pH is adjusted correctly. By increasing the pH-value, the charge of the aromatic heterocycle decreases and MEP ligands therefore behave similar to a HIC material. With decreasing pH, the ligand becomes positively charged and bound IgG is released [20,34,35].

The idea of combining cation exchange with thiophilic and/or hydrophobic moieties is not entirely new [23], but a more systematic investigation on the influence of structure variation is still missing. Commercially available adsorbents with similar mixed-modal CIEX-properties are, e.g. Capto™ MMC from GE Healthcare with N-benzoyl-homocysteine [36] and MBI-Hypercel™ with 2-mercapto-5-benzimidazolesulfonic acid from Pall Lifescience [37,38], as their interactive groups. Another interesting, but

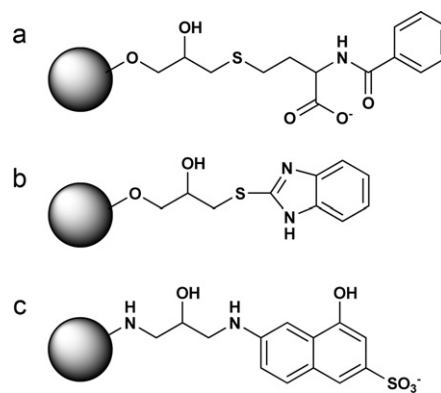


**Fig. 1.** Ligand structures of commercial adsorbents (a) Capto™ MMC, (b) MBI Hypercel™, and (c) 6-amino-4-hydroxy-2-naphthalene sulfonic acid.

non-commercial material is 6-amino-4-hydroxy-2-naphthalene sulfonic acid [39]. These mixed-modal CIEX ligands (Fig. 1) exhibit untypical properties for cation exchangers. They bind IgG at higher pH values or higher salt concentrations compared to any common strong and weak cation exchange adsorbents.

The aim of this contribution lies in the creation of novel cation exchanger adsorbents with the capability to bind antibodies at near isotonic salt conditions and to investigate the influence of specific molecular scaffolds and functional groups on the overall binding properties. First preliminary investigations of their IgG capture performance were performed via static binding capacity (SBC) tests in dependence to the conductivity and pH-value of the test solutions containing standard polyclonal h-IgG. The best performing adsorbent was then characterized under near-real process conditions with a mock feed solution containing Pluronic F-68 in comparison to cell culture supernatant employing dynamic binding capacity (DBC) measurements.

## 2. Experimental

### 2.1. Reagents and chemicals

Pluronic F-68, sodium azide, sodium chloride, sodium hydroxide, sodium dodecyl sulfate, acetic acid, sodium dihydrogenphosphate, disodium hydrogenphosphate, 2-mercaptoethanol as well as the ProteoSilver™ Plus Silver Stain Kit (PROTSIL2) were purchased from Sigma–Aldrich (Vienna, Austria). Sodium acetate, acetic acid and pentyl alcohol was acquired from Merck (Darmstadt, Germany). 30% Acrylamide/bis solution, ammonium persulfate, precision plus protein standard (unstained), Laemmli sample buffer and N,N,N',N'-tetra-methyl-ethylenediamine (TEMED) and 10× tris/glycine/SDS buffer were obtained from BIO-RAD (Vienna, Austria).

Fractogel® EMD Epoxy (M) with an epoxide group density of 1000 µmol/g dry gel, Fractogel® EMD SO3 (M) and Fractogel® EMD COO (M) had particle sizes of 40–90 µm and pore sizes of about 800 Å. All three Fractogel type media are cross-linked polymethacrylate resins modified with the tentacle-grafting technology from Merck KGaA (Darmstadt, Germany). Elemental analysis (sulfur content) was used for ligand density determination of Fractogel® EMD SO3 (440 µmol/g; C: 51.75%; H: 7.78%; N: 0.80%; S: 1.41%) and Fractogel® EMD COO (261 µmol/g; C: 52.34%; H: 7.37%; N: 0.37%; S: 0.069%). By titration with 1 M NaOH, 462 µmol/g and 510 µmol/g of ionic groups were determined for these two materials, respectively. The Capto™ MMC gel (average particle size: 75 µm, ionic capacity according to the manufacturer: 0.07–0.09 mmol/mL) was purchased from GE Healthcare (Vienna, Austria). Titration provided 504 µmol/g ionic acid groups and ele-

mental analysis 509  $\mu\text{mol/g}$  ligands (C: 47.34%; H: 6.6%; N: 0.83%; S: 1.63%).

Bi-distilled water was prepared in house, filtered through 22  $\mu\text{m}$  cellulose acetate filter from Sartorius Stedim Biotech GmbH (Goettingen, Germany) and was ultrasonicated prior to use.

Polyclonal human immunoglobulin G (h-IgG) Gammanorm® (165 mg/mL with a purity of 95%) from Octapharma (Lachen, Switzerland) consisted of the IgG subclasses IgG<sub>1</sub> (59%), IgG<sub>2</sub> (36%), IgG<sub>3</sub> (4.9%) and IgG<sub>4</sub> (0.5%), respectively, and contained also a small amount of IgA (82.5  $\mu\text{g/mL}$ ). Polyclonal human IgG Beriglobin® (160 mg/mL with a purity of 95%) from CSL Behring (Vienna, Austria) comprised of IgG<sub>1</sub> (61%), IgG<sub>2</sub> (28%), IgG<sub>3</sub> (5%), IgG<sub>4</sub> (6%) and 1.7 mg/mL IgA. The cell culture supernatant was purchased from Excellgene (Monthey, Switzerland). It contained 39.6  $\mu\text{g/mL}$  human monoclonal IgG1 (h-IgG1) expressed by a Chinese hamster ovary (CHO) cell line and 2.2  $\mu\text{g/mL}$  DNA. It had a conductivity of 25.9 mS/cm ( $\sim 218$  mM NaCl) and a pH of 7.7 at 33.2 °C. After dialysis, the application feed contained 32.9  $\mu\text{g/mL}$  h-IgG1 and 0.93  $\mu\text{g/mL}$  DNA. It was adjusted to 1 mg/mL IgG using IgG (Beriglobin), 75 mM NaCl, 1 mg/mL Pluronic F-68, 1 mg/mL sodium azide and pH 6.5. The cell culture feed was dialyzed with Spectra/Por® Float-A-Lyzer® tubes (10 mL) from Spectrum Laboratories, Inc. (Eindhoven, Netherlands), which had a Biotech Cellulose Ester Membrane with a molecular weight cut-off (MWCO) of 3–5 kDa. Dialysis was performed twice using 2 L 10 mM PBS with 75 mM NaCl at pH 7.2.

## 2.2. Equipment

The dynamic binding capacity (DBC) measurements were performed using a Gilson® Minipuls 3 peristaltic pump (Villiers-le-Bel, France) for feed loading. This peristaltic pump was equipped with a standard pump head with 10 rollers and 2 channels. The feed flow was adjustable from 0.3 mL/min to 30 mL/min and the pump could withstand a back pressure of 5 bar. A calibrated polyvinylchloride (PVC) tubing with 1.02 mm ID was used. The low-pressure HPLC system consisting of a degasser, binary pump, auto injector (not used), 6-port/2-position switching valve (Agilent 1200 Series) and a multi wavelength detector UV/vis detector of the Agilent 1100 Series was from Agilent (Waldbrunn, Germany). Both pumps were connected over the 6-port 2-position switching valve to the bio-chromatographic column, which was connected to the MWD detector from Agilent, followed by the pH-conductivity device pH/C-900 from GE Healthcare (Vienna, Austria) and the automated sample collector Advantec SF-3120 (Dublin, USA).

For the dynamic binding capacity measurements, a C 10/10 column with two AC10 flow adapters from GE Healthcare (Vienna, Austria) was used. The 1 mL gel sample was packed at a bed-height of 1.3 cm between two Superformance Filter F membranes with 10 mm ID from Götec-Labortechnik GmbH (Mühlthal, Germany).

The IgG content of all feed related samples was determined via Protein A high-performance liquid chromatography (Protein A HPLC) using a pre-packed Protein-A ImmunoDetection® sensor cartridge filled with 0.8 mL of POROS® 20  $\mu\text{m}$  particles possessing pore sizes between 500 and 1000 nm from Applied Biosystems (Vienna, Austria). All other standard IgG samples were quantified photometrically on the UV/vis spectrometer Specord50 from Analytik Jena (Jena, Germany) at a wavelength of 280 nm and a path length of 10 mm. The DNA-content was measured with a Quant-iT PicoGreen dsDNA-kit from Invitrogen GmbH (Lofer, Austria) on the fluorescence spectrometer LS 50 B from PerkinElmer (Vienna, Austria). Hellma 105.251-QS ultra-micro fluorescence cuvettes with 3 mm  $\times$  3 mm light path and 45  $\mu\text{L}$  cell volume were obtained through Wagner & Munz (Vienna, Austria). Data acquisition was performed with FL WinLab software from PerkinElmer (Vienna, Austria).

SDS-PAGE was performed on a Mini-Protein 3 device powered by a Mini-PROTEAN 3 Cell/PowerPac 300 System (220/240 V) of Bio-Rad (Vienna, Austria). The testing of different adsorbents via SBC test protocol 2 was performed fully automated, using the laboratory automation workstation Biomek® FX<sup>P</sup> from Beckman Coulter Inc. (Krefeld, Germany) in combination with Multi Screen HTS filter plates with 0.65  $\mu\text{m}$  for 96 well plates from Millipore (Schwalbach, Germany) and UV-Star Platte 96 K (Greiner Bio-One, Essen, Germany).

## 2.3. Sample analysis

### 2.3.1. Protein A-HPLC

The IgG content of the feed solutions was determined with the Protein A-HPLC method. The binding buffer was 10 mM phosphate buffer with 150 mM NaCl at pH 7.20, while the elution buffer was 12 mM HCl with 150 mM NaCl at a pH of approximately 2.5. The injection volume was 100  $\mu\text{L}$  and the absorbance was measured at 280 nm [40].

### 2.3.2. DNA quantification

The quantification of dsDNA from cell culture supernatant as well as all related sample fractions was performed with the Quant-iT™ PicoGreen® dsDNA assay kit according to the technical instructions provided by Invitrogen (Lofer, Austria) [40,41].

### 2.3.3. SDS-gel electrophoresis

The 8% and 10%-Tris-HCl gels with a thickness of 0.75 mm and 10 sample wells were hand-cast according to the instruction manual provided by BioRad [42]. The protein samples were treated with Laemmli buffer [43] or with Laemmli buffer containing 5% 2-mercaptoethanol at a 1:1 ratio. In later case the samples were heated for 5 min at 90 °C to obtain information of the reduced protein molecules, before application of 5  $\mu\text{L}$  of the sample-Laemmli mix to each sample wells.

Protein bands were stained with silver using the ProteoSilver™ Plus Silver Stain Kit (PROTSIL2) as recommended by the manufacturer [44].

## 2.4. Bio-chromatography

### 2.4.1. Kinetic binding study

For the equilibrium binding study three representative adsorbents (materials **A**, **E** and **L**) of the three adsorbent categories, strong thiophilic, weak aliphatic and weak aromatic cation exchanger were chosen. The test adsorbents were conditioned with 25 mM acetate/phosphate buffer with 75 mM NaCl at pH 5.5 for materials **A** and **E**, and with 75 mM NaCl at pH 6.5 for material **L**. The resins were suction dried via glass fritted funnel (pore size 3) under vacuum and aliquots of 3  $\times$  30 mg for each test adsorbent were transferred into 1.5 mL Eppendorf vials. The h-IgG (Gammanorm) solutions contained 8 mg/mL IgG for materials **A** and **E**, and 5 mg/mL IgG for material **L**. To each vial 1 mL of IgG solution was added and shaken for 5, 30, 60, 120 and 240 min at 25 °C and 1400 rpm on a thermomixer-compact from Eppendorf (Hamburg, Germany). After centrifugation at 10,000 rpm for 1 min with a mini-spin centrifuge from Eppendorf (Hamburg, Germany) the supernatant was removed. Each sample was washed for 5 min with 3  $\times$  1 mL application buffer, before elution of IgG with 3  $\times$  1 mL of application buffer with 1 M NaCl using an agitation time of 5 min. Note that for each wash and elution step, the sample vials were centrifuged at 1400 rpm. The supernatants for feed application and elution were measured at 280 nm. The solutions were diluted 1:4 if necessary. All values are the average of triple measurements. In order to state elution capacities in mg IgG per mL adsorbent, the correlation factors



0.92 mL, 1.44 mL and 1.52 mL per 1 g adsorbent were determined for materials **A**, **E** and **L**.

#### 2.4.2. Static binding capacity (SBC)

**2.4.2.1. SBC test protocol 1.** The SBC measurements were performed with standard polyclonal IgG solutions containing 5 mg/mL h-IgG, Gammanorm® in 25 mM PBS buffer prepared at seven different pH values (4.5, 5, 5.5, 6, 6.5, 7 and 7.5) and with 4 different NaCl concentrations (0, 75, 150 and 300 mM NaCl). To an aliquot of 10  $\mu$ L of settled adsorbent, 200  $\mu$ L of the IgG test solution (5 mg/mL) was added. The test slurry was agitated for 15 min, before the adsorbent was washed 3 times for 5 min with 1 mL binding buffer through shaking. Elution was induced by agitating the adsorbent 3 times for 5 min with elution buffer containing 1 M NaCl at the same pH as the binding buffer. The elution solutions were measured at 280 nm and diluted 1:4 if necessary. This protocol was performed manually.

**2.4.2.2. SBC test protocol 2.** Because of the insufficient buffering at low pH, the PBS buffer from test protocol 1 was exchanged for a 25 mM acetate/phosphate buffer. Also the IgG concentration was doubled and the incubation time of the adsorbent with antibody solution was increased to 2 h. The washing and elution steps were performed as previously described in SBC test protocol 1. This protocol was performed automated by the liquid handler Biomek® FX<sup>P</sup>. Aliquots of 20  $\mu$ L of the corresponding adsorbents (in suspension) were placed into the wells of the Multi Screen HTS filter plate, which was then positioned in the Biomek® FX<sup>P</sup> device. All other steps were performed fully automated by the robotic workstation. After sedimentation of the adsorbent, the supernatant was removed by suction and 200  $\mu$ L of the corresponding IgG test solutions (10 mg/mL buffer of the corresponding pH and sodium chloride concentration) were added. After 120 min of agitation the supernatants were removed by suction, transferred into a UV-Star Platte 96K well plate and diluted by a 1:1 ratio. The IgG concentrations of the SBC-solutions were determined at a wavelength of 280 nm. The washing of the adsorbent was performed by adding 3  $\times$  200  $\mu$ L acetate/phosphate buffer with a similar pH and sodium chloride concentration as the corresponding binding buffer and subsequent shaking for 5 min. The wash solutions were removed by suction. For IgG elution, 200  $\mu$ L elution buffers with 1 M sodium chloride at pH 7.0 were added to the adsorbent. The elution solution was rinsed into a UV-Star Platte 96K and measured at 280 nm. Afterwards the solution was diluted 1:1 and was re-measured.

In order to minimize the error inflicted by unspecific binding of IgG to the walls of the well plates, all “static binding capacities” presented in this study are in fact expressed via the elution capacities and resemble the average values of triple measurements. Their standard deviation was overall between 3% and 9%. Note that the actual binding capacities for the IgG capture steps are not shown.

#### 2.4.3. Dynamic binding capacity (DBC)

All tested CIEX adsorbents were suspended in a 1 M NaCl solution and were allowed to settle in a graduated 5 mL volumetric flask to ensure an accurate determination of 1 mL of gel used for the measurement. The gel was inserted into the C 10/10 column on top of a 10 mm ID filter membrane discs placed on the AC10 flow adapters. The gel was allowed to settle by gravity, before the second filter disc and the second AC10 flow adapter were placed above the settled gel. The column was purged at a flow rate of 5 mL/min and the adapter was positioned to a final bed height of 13 mm.

The DBC measurements were performed with two standard IgG solutions prepared with IgG Gammanorm® and IgG Beriglobin® containing 1 mg/mL IgG in 25 mM phosphate buffer with 75 mM or 150 mM NaCl at pH values of 5.5, 6.5 and for the most promising adsorbent also at pH 7.4. As it is known from other studies that Pluronic can strongly affect the DBC results of MAb selec-

tive sorbents, Pluronic-F68 was included in the screening scheme. Therefore a further test was performed with a mock feed solution containing 1 mg/mL Pluronic F-68 and 150 mM NaCl at pH 6.5. In addition, material **L** was tested with a dialyzed cell culture supernatant, which was adjusted to pH 6.5 and 75 mM NaCl. It was spiked with IgG Beriglobin to increase the IgG concentration to 1 mg/mL, besides 1 mg/mL Pluronic F-68 and 1 mg/mL NaN<sub>3</sub>. For all DBC measurements, if not stated otherwise, the polyclonal IgG, Beriglobin® was used at a concentration of 1 mg/mL in the corresponding application buffer.

After loading of the IgG test solution via peristaltic pump onto the column until 100% breakthrough of IgG was reached, the column was washed with the corresponding application buffer. The flow rate was 0.6 mL/min (57 cm/h), which is equivalent to a residence time of 1.3 min. The elution buffer had the same pH as the binding buffer, but its salt content was increased to 1 M NaCl. In the case of the dialyzed feed experiment, the wash solution consisted of 25 mM phosphate buffer and 0 mM NaCl. The elution of h-IgG was performed by applying firstly a linear salt gradient from 0 mM to 1 M NaCl within an elution volume of 110 mL, which was followed by an isocratic elution with 1 M NaCl for additional 10 mL. If not otherwise stated, all adsorbents were sanitized with 0.5 M NaOH. Note that sample fractions of 10 mL were collected.

### 2.5. Synthesis

Several ligands with different functional groups were synthesized and coupled onto the solid support, subsequently exhibiting different chemical properties. The synthesis of these ligands, their immobilization onto the support material and their physico-chemical characterization are described in detail in [electronic supplementary material](#). Note that ligand densities were determined via elemental analysis (EA) and acid/base titration (T) and are stated as  $\mu$ mol ligand per gram dry gel in [Table 1](#). If not stated otherwise, ligand densities mentioned in this study refer to the results obtained by titration. A summary of the investigated mixed-modal CIEX-ligand structures are depicted in [Fig. 2](#).

## 3. Results and discussion

### 3.1. Kinetic binding study

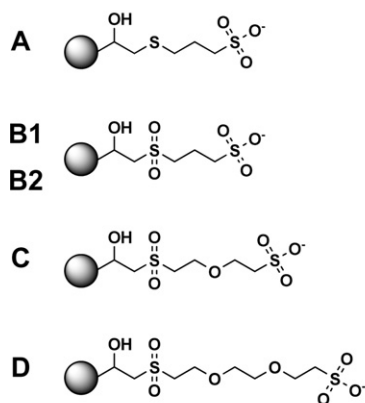
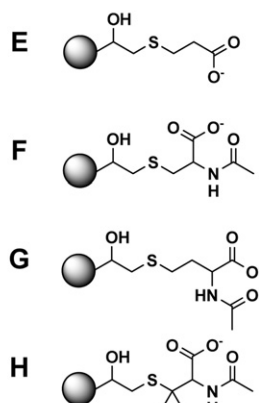
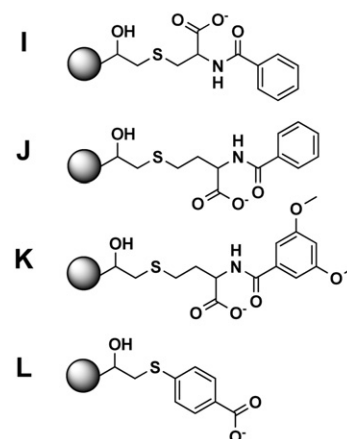
In order to determine the time-dependency of IgG capture for the various adsorbents discussed in this article, one of each of the three types of cation exchangers, strong thiophilic, weak aliphatic and weak aromatic ([Fig. 2](#)), was chosen as a representative for the group. The adsorbents are materials **A**, **E** and **L**. The equilibrium kinetics in [Fig. 3](#) was determined via static binding capacity (SBC) tests, where each data point resembled the averaged elution capacity result of triple measurements with an average standard deviation of 8.3%.

A comparison of the three tested adsorbents reveals a fast IgG capture kinetic for materials **A** and **E**, where after 15 min saturation was accomplished and only minor changes in the elution capacities could be seen. Material **L** on the other hand shows a much slower binding kinetic compared to materials **A** and **E**. Partially, this result may have been caused by the slightly lower IgG concentration of 5 mg/mL used for the testing of material **L** instead of 8 mg/mL used for the former two adsorbents. However, the equilibration curve for material **L** indicates that this adsorbent binds IgG slightly slower, but possesses an overall higher binding capacity for IgG, since saturation was not yet reached after 40 min and even after 3 h the binding curve is still slightly ascending. Nevertheless, the imprecision of SBC measurements terminated after 120 min as it is the case for SBC test protocol 2 is low and can be considered being negli-

**Table 1**

Overview of investigated mixed modal weak and strong cation exchange ligands together with their abbreviations (Abbr.) and ligand densities (LD) determined via elemental analysis (EA) and titration (T).

	Abbr.	Adsorbent	LD (EA) [ $\mu\text{mol/g}$ ]	LD (T) [ $\mu\text{mol/g}$ ]
Thiophilic sulfonic acid	<b>A</b>	3-Mercapto-1-propanesulfonic acid	1207	1023
	<b>B1</b>	3-Sulfonyl-1-propanesulfonic acid	955	637
	<b>B2</b>	3-Sulfonyl-1-propanesulfonic acid	1011	886
	<b>C</b>	2-(2-Sulfonylethoxy)-ethanesulfonic acid	840	564
	<b>D</b>	3,6-Dioxa-8-sulfonyl-1-octanesulfonic acid	790	457
Aliphatic HIC	<b>E</b>	3-Mercaptopropionic acid	1100	1043
	<b>F</b>	N-Acetyl-L-cysteine	1031	941
	<b>G</b>	N-Acetyl-D,L-homocysteine	843	727
	<b>H</b>	N-Acetyl-D,L-penicillamine	759	604
Aromatic HIC	<b>I</b>	N-Benzoyl-L-cysteine	709	641
	<b>J</b>	N-Benzoyl-D,L-homocysteine	887	843
	<b>K</b>	N-(3,5-Dimethoxybenzoyl)-D,L-homocysteine	909	738
	<b>L</b>	4-Mercaptobenzoic acid	950	950
Commercial	–	Fractogel® EMD SO <sub>3</sub>	440	462
	–	Fractogel® EMD COO	261	510
	–	Capto™ MMC	509	504

**Strong cation exchanger****thiophilic****Weak cation exchanger****aliphatic****aromatic**

**Fig. 2.** Overview of investigated strong and weak cation exchanger adsorbents combined with a variety of different functional groups and different lipophilicities. Note that materials **B1** and **B2** are structurally identical, but were prepared with different synthesis protocols.

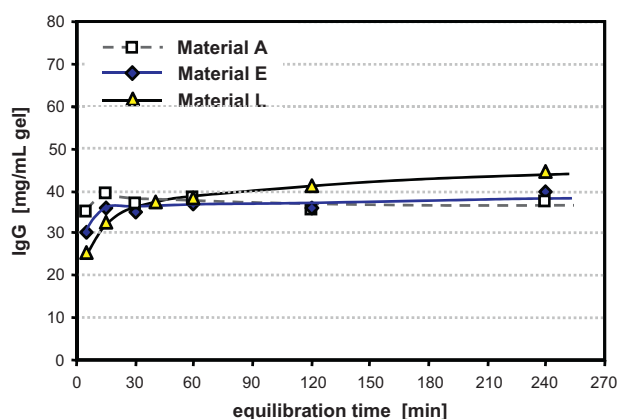


**Fig. 3.** Kinetic binding study for materials **A**, **E** and **L**, using 25 mM acetate/phosphate buffer with 75 mM NaCl adjusted to pH 5.5 for materials **A** and **E**, and adjusted to pH 6.5 for material **L**. 1 mL IgG test solution with 8 mg/mL IgG for materials **A** and **E**, and 5 mg/mL IgG for material **L** were added to 30 mg adsorbent and agitated for 5, 30, 60, 120 and 240 min at 25 °C. The data points are averaged elution capacities determined with triple measurements and calculated to mg IgG per mL adsorbent.

ble. In general, one has to differentiate between the fast primary binding, which exhibits in a strong binding of IgG to the adsorbent and a secondary binding that is rather slow and weak. Therefore, equilibration times above 2 h and static binding results determined by the difference between the IgG content in the supernatant and the original feed should be avoided. All SBC results presented in this article are solely the elution capacities.

### 3.2. Thiophilic cation exchange adsorbents with sulfonic acid group

The immobilization of sulfonic acid bearing ligands onto Fractogel® EMD Epoxy was conducted by coupling the dithiol functional ligands 1,3-propanedithiol, 2,2'-oxydiethanethiol, 3,6-dioxa-1,8-octanedithiol to the epoxide-activated support surface. The subsequent oxidation of the sulfanyl and the sulfhydryl groups to sulfonyl and sulfonic acid groups lead then to materials **B1**, **C** and **D** (Fig. 2 and Table 1). Alternatively, material **A** was prepared through direct immobilization of 3-mercaptopropyl sulfonic acid onto the support. The subsequent oxidation of the sulfanyl group led to material **B2** (see electronic supplementary material, Fig. S2).

These immobilization and oxidation reactions are straightforward and easy to accomplish providing sufficiently high ligand densities of 800–1000  $\mu\text{mol/g}$  dry gel, respectively determined by elemental analysis (Table 1). Comparing the ligand densities obtained by elemental analysis (EA) with the titration results for the sulfhydryl determination using the 2,2'-dipyridyl disulfide (DPDS) method [45] (460–780  $\mu\text{mol/g}$ ) lead to rather strong deviations. However, the acid/base titration (T) results for the sulfonic acid group provided similar but lower values (460–640  $\mu\text{mol/g}$ ) as earlier obtained with the DPDS method. The reason for the strong differences of EA results and results obtained by DPDS method or titration lies in the possible cross-linking of surface bound ligands with epoxide groups in close proximity. This undesired reaction may occur during the preparation process despite the huge excess of dithiol-functional ligand used. The additional formation of disulfide bridges can only partially explain the imbalance between the DPDS results and the EA results, since disulfide bridges ought to break during the oxidation reaction, when the sulfur atoms are oxidized to sulfonic acid groups, and this imbalance still existed after the oxidation process. The slightly higher ligand densities obtained with elemental analysis compared to the acid/base titration results for materials **A** and **B2** as well as the higher ligand density of precursor material **A** compared to its oxidized analog, material **B2**, point clearly towards the formation of a small amount of disulfide bridges during the first reaction step.

Fig. 4 depicts the SBC results of materials **A**, **B1**, **B2**, **C** and **D** under all investigated pH values (pH 4–7.5) and salt conditions (0–300 mM NaCl) established with SBC test protocol 2. A comparison with the commercial strong cation exchanger Fractogel® EMD  $\text{SO}_3^-$  in Fig. 5 shows slightly lower yet comparable binding capacities for materials **A** and **B2**. The materials **B1**, **C** and **D** provide rather low IgG binding under all test conditions.

Note that material **B2** is structurally similar to material **B1**, with the difference that in case of **B1** the ligand was directly immobilized, while **B2** was prepared in a two step immobilization and oxidation protocol with material **A** as a precursor. The improved performance of material **B2** was clearly the result of the different preparation protocol, where no cross-linking of the ligand was possible combined with a slightly higher ligand density.

The main differences between materials **B1**, **C** and **D** are a slight decrease in ligand density, combined with an increase in the length of their spacer chains by one and two ethoxyl groups. Since no significant variation in IgG capture performance of these three adsorbents was observed, it can be assumed that spacer length and slight variations in ligand densities in the range of  $\pm 100 \mu\text{mol/g}$  have little to no influence on the IgG capture performance of thiophilic sulfonic acid type adsorbents.

The difference in material performance observed for the precursor material **A**, which lack a sulfonyl group compared to material **B2**, leads to the conclusion that the incorporation of a sulfonyl group has a somewhat negative effect on IgG capture, when combined with a sulfonic acid head group.

Concerning IgG capture performance, all thiophilic sulfonic acid adsorbents have in common that they were not able to bind sufficient amounts of IgG under high pH values and high salt concentrations. In the absence of sodium chloride, material **A** shows a maximum binding capacity of 86 mg/mL at pH 5.0, while for material **B2** the maximum was of 72 mg/mL at the same pH. Fractogel® EMD  $\text{SO}_3^-$  in Fig. 5 provided the best IgG capture performance with 118 mg/mL IgG at 0 mM NaCl and pH 5.0.

Note that the ligand densities of material **A** and **B2** were about 1023  $\mu\text{mol/g}$  and 886  $\mu\text{mol/g}$ , respectively, which was twice as high as that of the commercial sulfonic acid cation exchanger with a ligand density of around 440  $\mu\text{mol/g}$  dry resin. The SBC results for Fractogel® EMD  $\text{SO}_3^-$  and material **A** decrease strongly with increasing pH and reach 18 mg/mL and 16 mg/mL, respectively at a pH of

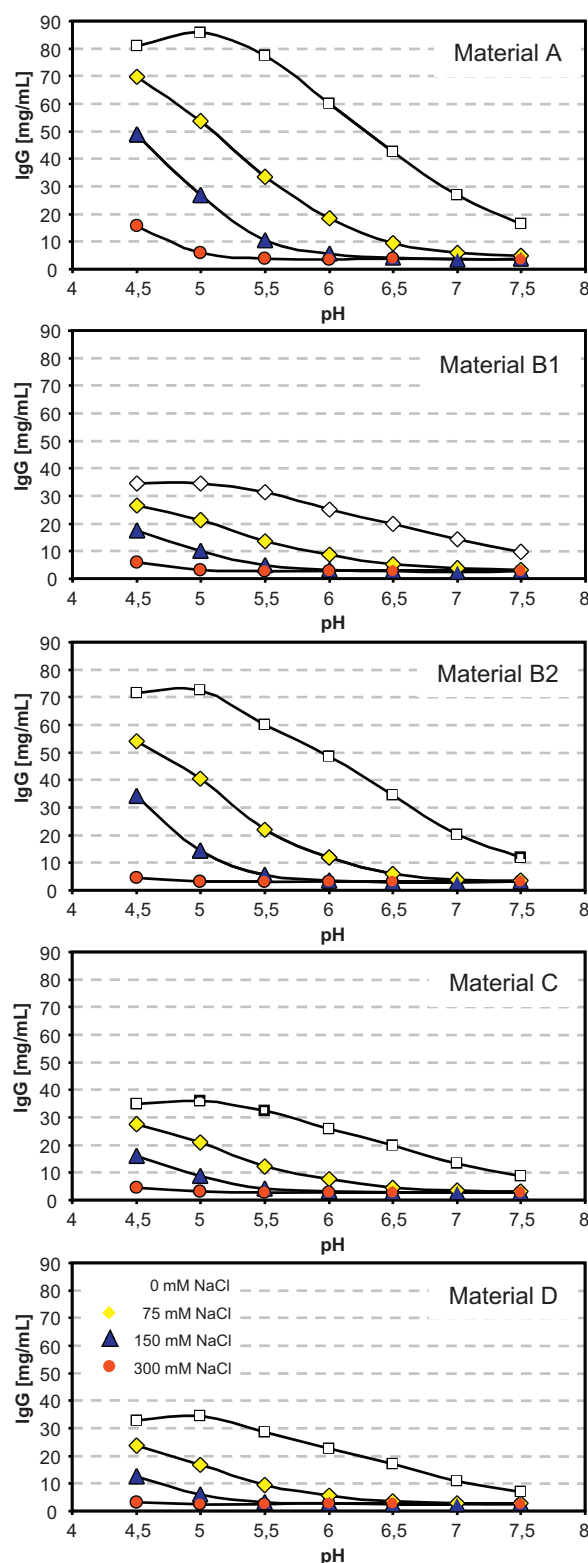


**Fig. 4.** Static binding capacity (SBC) results for materials **A**, **B1**, **B2**, **C** and **D** using polyclonal h-IgG are plotted against the pH-values (from pH 4.5 to 7.5) of test solutions containing varying amount of sodium chloride (0, 75, 150, 300 mM NaCl). SBC-tests were performed according to SBC test protocol 2.

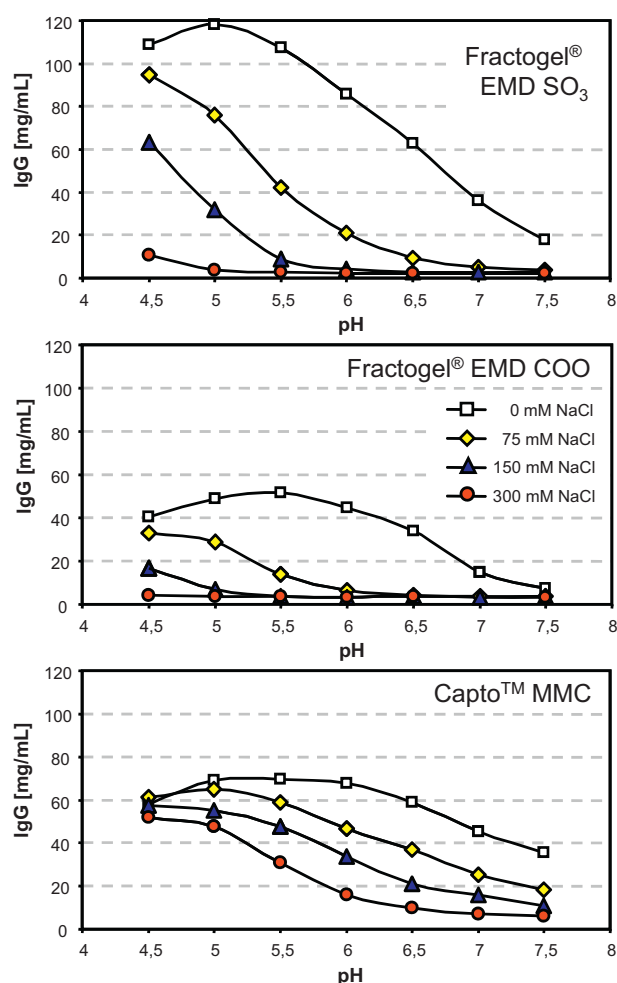


**Fig. 5.** SBC diagrams for the commercial cation exchanger adsorbents Fractogel® EMD SO<sub>3</sub> and COO from Merck KGaA and Capto™ MMC from GE Healthcare tested with polyclonal h-IgG at different pH-values (from pH 4.5 to 7.5) and different sodium chloride concentrations (0, 75, 150 and 300 mM NaCl). SBC-tests were performed according to SBC test protocol 2.

7.5. On the other hand, a decrease of pH down to 4.5 provided only a slight decrease of elution capacities to 109 mg/mL and 81 mg/mL for the two investigated adsorbents at 0 mM NaCl. For sample solutions containing sodium chloride, the peak maximum shifted from 5.0 to 4.5. This led to elution capacities for Fractogel® EMD SO<sub>3</sub> and material **A** at 75 mM NaCl and pH 4.5 of 95 mg/mL and 70 mg/mL, respectively. In the presence of 150 mM NaCl and pH values of 5.5 and lower, both materials perform very similar, but in general, it can be concluded that Fractogel® EMD SO<sub>3</sub> performs slightly better compared to material **A**, independent of the pH value and salt content of the test solution.

Note that the use of thiophilic adsorbents always goes hand in hand with the addition of high amounts of structure forming salts, which follow the Hofmeister series [25]. In the present study no chaotropic additives were used, since they are rather undesired in large-scale downstream processing of mAbs. In case of sodium chloride, its structure forming effect can be considered being negligible.

### 3.3. Weak cation exchange adsorbent

Since the investigated sulfonic acid type adsorbents **A** and **B** did not seem to be much influenced by the change of the sulfanyl linkage to a sulfonyl group, all other adsorbents

(**E** to **L**) were only prepared with a sulfanyl group. In any case, a conversion of the sulfanyl group to the corresponding sulfonyl group would not be possible with the oxidation protocol used in this study, since the carboxylic acid group would be oxidized to a per acid with the additional danger of ligand degradations. Nonetheless, it can be expected that a replacement of the sulfonic acid group by carboxylic acid ought to have a much stronger influence on material performance than a possible oxidation of the sulfanyl group as stated earlier.

In a first attempt, 3-mercaptopropionic acid was bound to the support material with a ligand density of 1043  $\mu\text{mol/g}$  dry gel, which is denominated as material **E** (Fig. 2). As depicted in Figs. 5 and 6a, the static binding capacities of material **E** investigated at 0 mM and 75 mM NaCl using SBC test protocol 1 were all below the results obtained for the bench mark material Fractogel® EMD SO<sub>3</sub>, which were established with SBC test protocol 2. As stated in Section 3.1, an equilibration time of 15 min was sufficient for material **E**. A significant deviation between SBC test protocol 1 and SBC test protocol 2 is not expected. For IgG test solutions with NaCl concentration of 150 mM and above, and with pH values below 6.0, binding capacities of material **E** were higher than those of Fractogel® EMD SO<sub>3</sub>. For example at pH 5.5 and 150 mM NaCl binding capacities of 20 mg/mL for material **E** and 9 mg/mL for the bench mark material were obtained. Under higher pH conditions, both materials were not able to bind significant amounts of h-IgG.

A comparison with the weak cation exchanger Fractogel® EMD COO (ligand density: 509  $\mu\text{mol/g}$  dry gel) measured with SBC test protocol 2 depicted in Fig. 5, exhibited for SBC tests with 0 mM NaCl generally lower elution capacities for material **E** (Fig. 4). Also at pH 4.5 and 75 mM NaCl, the commercial weak cation exchanger showed slightly higher capacities, namely 33 mg/mL compared to 22 mg/mL for material **E**. But for pH values between 4.5 and 5.5 at 150 mM NaCl as well as for pH 4.5 and 5.0 at 300 mM NaCl, material **E** performed much better than Fractogel® EMD COO. Material **E** was able to reach binding capacities of up to 15 mg/mL for test solutions containing 300 mM NaCl at pH 5.0, which was also the optimum pH for 150 mM NaCl solutions with a binding capacity of 26 mg/mL. For test solution containing 75 mM NaCl material **E** showed a maximum binding of 34 mg/mL IgG at pH 5.5. In case of test solutions without sodium chloride addition, a maximum elution capacity of 41 mg/mL at pH 6.0 was obtained. Note that for IgG solutions with pH values below or above the optimum pH value, a drop of binding capacities was observed. It is noticeable to mention that the earlier discussed thiophilic sulfonic acid ion exchangers showed peak maxima for test solutions containing 75 mM or more NaCl at pH 4.5.

Thus a question remains; why is Fractogel® EMD COO an insufficient IgG capture material under isotonic conditions, while another carboxylic acid carrying adsorbent is able to bind substantial amounts of IgG? Note that both adsorbents have the same underlying polymethacrylate support matrix, bearing a similar tentacle structures on their surface. It seems obvious that the different ligand attachment chemistries of the two adsorbents are responsible for their different IgG binding properties. Elemental analysis of the commercial weak cation exchanger provided evidence of the presence of nitrogen and the absence of sulfur, while material **E** possessed a sulfanyl linkage. It can therefore be assumed that the sulfanyl group is responsible for the enhanced binding properties of material **E**, although it is rather difficult to relate the different IgG capture performances decidedly to thiophilic properties or an altered overall lipophilicity.



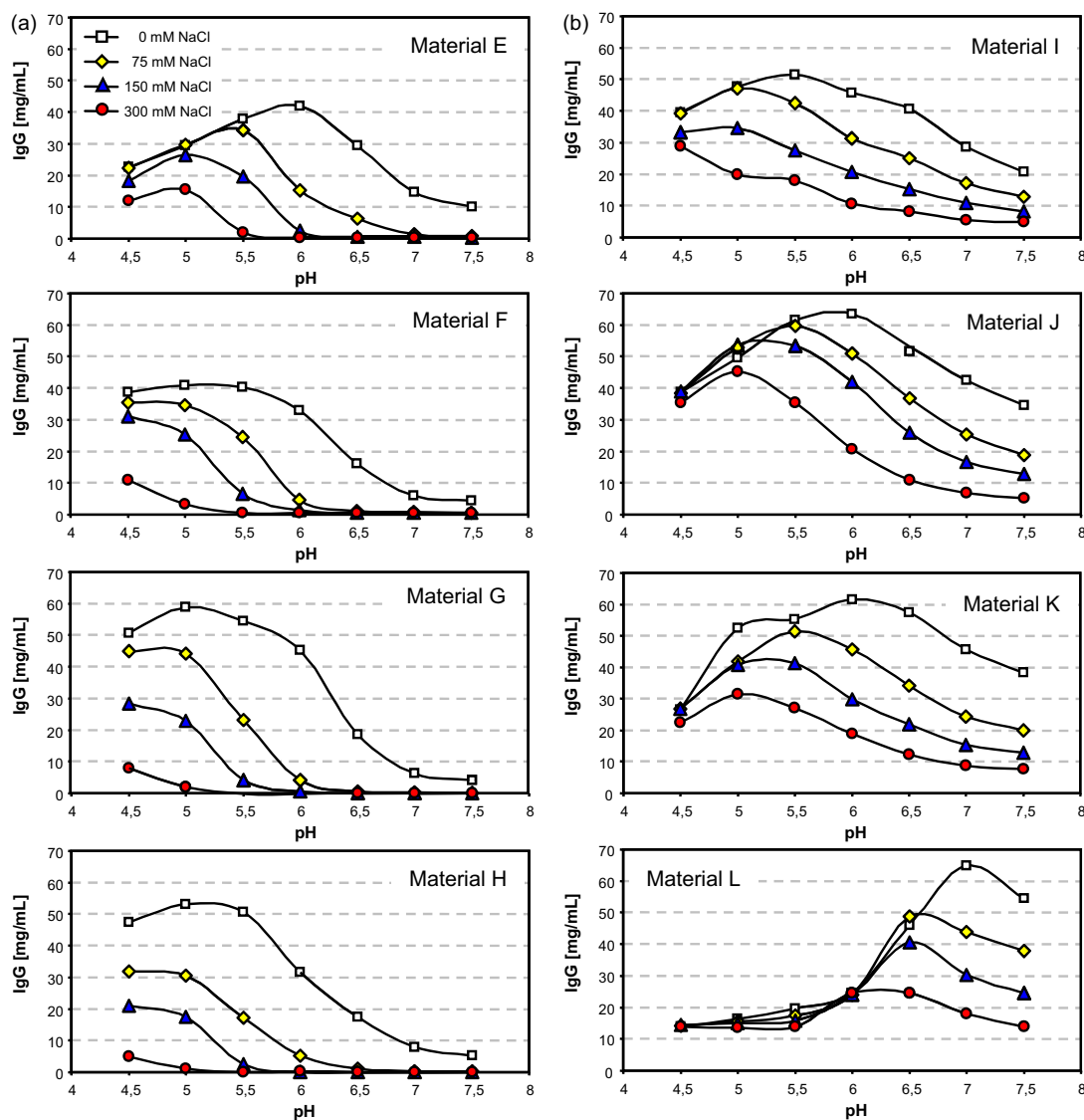


**Fig. 6.** SBC diagrams for the aliphatic HIC materials **E**, **F**, **G** and **H** were established with SBC test protocol 1, the aromatic HIC materials **I**, **J**, **K** and **L** were established with SBC test protocol 2. All adsorbents were tested with polyclonal h-IgG at different pH-values (pH 4.5–7.5) and different sodium chloride concentrations (0, 75, 150 and 300 mM NaCl).

#### 3.4. Aliphatic hydrophobic interaction adsorbents

Based on the results obtained for 3-mercaptopropionic acid, further carboxylic acid bearing adsorbents with additional amide and aliphatic or aromatic moieties were prepared (Fig. 2).

All adsorbents were so-called “endcapped” with 2-mercaptoethanol to deactivate any residual epoxide groups. Note that the yields of the “endcapping” reactions judged by elemental analysis were for all adsorbents negligible. It can be expected that any residual epoxide groups present after ligand immobilization, ought to be unstable under the harsh immobilization conditions of pH >12 and may have reacted already to vicinal diol groups as a side reaction.

Cysteine and derivatives thereof were chosen as suitable ligands, because they exhibit a sulfhydryl group for ligand attachment and a carboxylic acid group accessible for capturing mAbs (see electronic supplementary material, Fig. S1). Furthermore several amino acids were already reported as potential antibody capture materials, especially histidine [46–48], but also tryptophane and phenylalanine [49]. An even further advanced material was the PAM (Protein A mimic) ligand [50], a tetrameric polypeptide with

affinity for antibody capture at binding conditions of neutral pH and isotonic salt concentrations.

The first candidate N-acetyl-L-cysteine gained a maximum ligand density of 941  $\mu\text{mol/g}$  and was abbreviated as material **F**. In comparison material **G**, carrying N-acetyl-D,L-homocysteine as a ligand, comes with an additional methylene group in the spacer chain. Material **H** carries N-acetyl-D,L-penicillamine as a ligand, which is similar to material **F** except for the two methyl groups attached to the carbon chain between the sulfanyl group and the carboxylic acid group.

Note that materials **F**, **G** and **H** were tested in batch experiments with SBC test protocol 1. Their results are depicted in Fig. 6a. While material **E** showed for measurements with decreasing salt content, a significant shift as well as increase of the binding capacity maximum with increasing pH for pH values above 4.5, e.g. pH 6 for 0 mM NaCl, this tendency was amiss or barely noticeable for material **F**, **G** and **H**. Only the curves obtained with test solutions containing 0 mM salt showed a similar, but much weaker trend. Another difference was the higher binding capacities for material **F**, **G** and **H** at low pH and 0, 75 and 150 mM NaCl compared to material **E**. With increasing pH, this behavior changes and material **E** exceeds the



n-acetylated materials. Only for the measurement with feed solutions containing 300 mM employing SBC test protocol 1, the IgG binding capacity of material **E** exceeds those of materials **F**, **G** and **H**. Above pH 5.5 none of these materials were able to capture substantial amounts of IgG in the presence of 300 mM NaCl.

Summing up these observations, the introduction of an amide group did not improve the IgG capture performance of investigated adsorbents under test conditions with pH values higher than 6.0 at 150 mM NaCl or higher. As can be seen in Table 2, the binding capacities for the materials discussed in this chapter were under the stated test condition within the range of strong cation exchangers as well as the investigated commercial ion exchangers Fractogel® EMD SO3 and Fractogel® EMD COO.

A comparison of the three cysteine related materials **F**, **G** and **H** exhibits only minor differences in performance. One of these deviations is the considerably higher capacity of material **G** compared to material **F** and **H**, although material **F** possess a higher ligand density. This effect is possibly based on the elongated spacer and the resulting increased lipophilicity of the ligand. The binding capacity curve for material **H** at 0 mM NaCl exceeds that of material **F** in Fig. 6a. For solutions with increased salt concentration, material **H** shows comparable or lower binding capacities compared to material **F**.

### 3.5. Aromatic hydrophobic interaction adsorbents

#### 3.5.1. Static binding capacity study

The coupling of benzoyl-cysteine and benzoyl-homocysteine onto Fractogel led to the materials **I** and **J**. Furthermore 3,5-dimethoxybenzoyl-homocysteine was immobilized, which resulted in material **K** (Fig. 2 and Table 1). Fig. 6b shows the results of the SBC studies made by SBC test protocol 2. Besides a few exceptions, material **I** showed the lowest binding capacities of this series of aromatic cation exchangers, what can partially be assigned to the fact that it possesses the lowest ligand density of these 3 materials. The binding maximum for material **I** during the absence of sodium chloride was reached at pH 5.5 and was 52 mg/mL. Materials **J** and **K** exposed their maxima at pH 6.0 and showed binding capacities of 64 mg/mL and 61 mg/mL, respectively. The peak maximum of material **I** obtained by testing with test solution containing 75 mM sodium chloride was found again at a lower pH compared to materials **J** and **K**. Also the binding capacities measured were lower than those of materials **J** and **K**. In average, material **J** exhibits the highest capacities, followed closely by material **K** and material **I**. The source of these differences is the beneficial effect of a higher ligand density, since a higher number of ionic groups are able to bind more IgG due to an increased number of ionic interaction sites on the sorbent. The additional methoxy groups of material **K** did not significantly improve the performance of that material. For the desired binding condition at pH 6.5 and 150 mM NaCl, considerably high SBC values were found for materials **I**, **J** and **K**, namely 15.2, 26.0 and 21.8 mg/mL respectively (Table 2). Under this condition, material **E**, measured with SBC test protocol 1 exposed a binding capacity of only 0.53 mg/mL.

The commercial adsorbent Capto™ MMC gel from GE Healthcare has a very similar ligand structure compared to material **J** and provided therefore similar SBC results (Fig. 5), although the ligand density of Capto™ MMC is just about 500  $\mu\text{mol/g}$  dry gel. Capto™ MMC is also a N-benzoyl-homocysteine based material, but with a different binding chemistry [51] carrying therefore a different spacer arm. The support material is Sepharose. During tests with feed solutions containing 0 mM NaCl and pH below 5.5, the binding capacities exceeded those of material **J**, but with increasing salt concentrations and increasing pH, material **J** performs better than Capto™ MMC by up to 8 mg/mL (Table 2).

The conclusion of these experiments is the positive influence of an aromatic moiety in close proximity to the carboxylic acid group, which favors IgG capture out of feed solutions containing more than 75 mM NaCl and possessing pH values above 5.5. Note that a close proximity relates to approximately 4 bonds between the aromatic and the carboxylic acid group. The subsequent next step was therefore, the coupling of 4-mercaptobenzoic acid onto epoxide activated Fractogel, which produces a sulfanyl bridge in the spacer chain. The resulting adsorbent was named material **L**.

Several ligands comparable to 4-mercaptobenzoic acid such as 4-aminobenzoic acid [52] and 2-mercaptopyridine-3-carboxylic acid [53] have already been reported. They both possess a carboxylic acid group connected directly to an aromatic ring. The spacer chain of the nicotinic acid ligand contained a sulfanyl linkage at the same position as in material **L**. The aminobenzoic acid bearing material was coupled onto divinyl sulfone activated agarose and was tested only in the presence of 0.7 M  $(\text{NH}_4)_2\text{SO}_4$ , while the 2-mercaptopyridine-3-carboxylic acid, which was also bound onto divinyl sulfone activated sepharose, was able to capture IgG out of human serum without the addition of lyotropic salts. Interestingly this ligand was not able to capture IgG in the absence of lyotropic salts, when it was connected via epichlorohydrin to the support material.

The ligand density of material **L** was about 950  $\mu\text{mol/g}$  and the SBC-curves were surprisingly different compared to all the other investigated adsorbents (Fig. 6b). The ideal pH of the test solutions containing 75 mM and 150 mM NaCl was pH 6.5, and provided binding capacities of 49 mg/mL and 41 mg/mL, respectively, which represent a significant improvement compared to before mentioned ligands. Under these conditions material **J** showed binding capacities of 36.7 mg/mL and 26.0 mg/mL, respectively (Table 2). Interestingly, the binding capacities of material **L** at low pH dropped down to 14.2 and 14.4 mg/mL under above conditions. Note that under these conditions the benzoic acid is partly or even totally protonated and therefore possesses no ionic but very lipophilic character. On the other side, the target protein is highly (positively) charged and therefore the interactions are weak, and the affinity of the protein towards the ligand is low. As an outcome of all the SBC tests the three most promising materials **J**, **K** and **L** were chosen to be characterized in terms of their dynamic binding performance.

#### 3.5.2. Dynamic binding capacity studies

For economic reasons and in order to save time, the previous SBC measurements served primarily for the elimination of the less promising ligands. The materials tested under dynamic conditions were the material **J**, **K**, **L** and the commercial adsorbent Capto™ MMC from GE Healthcare. For all dynamic binding capacity tests (DBC), adsorbent volumes of 1 mL at a bed height of 1.3 cm were used. In an additional measurement with material **L** using 2.5 mL adsorbent packed in the same column at a bed height of 3.2 cm, it was shown that both experimental settings provided comparable results for 100%-DBC and elution capacity (EC) (chapter 4 in supplementary information). The PBS buffer used, contained 75 or 150 mM sodium chloride with a pH of 5.5 or 6.5. In the case of material **L**, measurements at pH 5.5 were not performed. Instead DBC tests were conducted at pH 7.4 and 75 mM NaCl, which resemble conditions comparable to cell culture feed. The DBC results are summarized in Table 3. Material **J** and **K** provided very similar values for 100%-DBC and for the elution capacities (EC). These DBC results stood in good accordance with SBC results, although the latter were slightly higher than the dynamic test results. Material **J** showed an elution capacity of 31 mg/mL at pH 6.5 and 75 mM NaCl and material **K** showed an EC of 34 mg/mL. SBC measurements exhibited under similar conditions IgG binding capacities of 36.7 mg/mL and 34.3 mg/mL. This consistence between SBC and DBC measurements was found throughout all tests for material **J** and **K**. For SBC as well as DBC tests polyclonal h-IgG Beriglobin was used. A com-

**Table 2**  
Elution capacity (EC) results from static binding capacities (SBCs) tests for mixed modal cation exchanger adsorbents.

Thiophilic sulfonic acid <sup>b</sup>		Aliphatic HIC <sup>a</sup>		Aromatic HIC <sup>b</sup>	
Adsorbent	EC [mg/mL]	Adsorbent	EC [mg/mL]	Adsorbent	EC [mg/mL]
Fractogel EMD SO <sub>3</sub> <sup>−</sup>	2.98	Merck EMD COO <sup>−b</sup>	3.52	Material <b>I</b>	15.2
Material <b>A</b>	4.12	Material <b>E</b>	0.53	Material <b>J</b>	26.0
Material <b>B1</b>	2.74	Material <b>F</b>	0.49	Material <b>K</b>	21.8
Material <b>B2</b>	2.95	Material <b>G</b>	0.00	Material <b>L</b>	40.7
Material <b>C</b>	2.78	Material <b>H</b>	0.06	Capto MMC	20.9
Material <b>D</b>	2.49				

<sup>a</sup> SBC test protocol 1 (manual) using PBS buffer at pH 6.5 and 150 mM NaCl.  
<sup>b</sup> SBC test protocol 2 (automated) using PBS/acetate buffer at pH 6.5 and 150 mM NaCl.

**Table 3**  
Summary of dynamic binding capacities at 10% and 100% breakthrough of IgG (DBC<sub>10%</sub> and DBC<sub>100%</sub>) and elution capacities at DBC<sub>100%</sub> (EC<sub>100%</sub>) for different feed solutions.

Application conditions			Material <b>J</b> (Benzoyl-homocysteine)		Material <b>K</b> (3,5-Dimethoxybenzoyl-homocysteine)		Material <b>L</b> (Mercaptobenzoic acid)	
pH	NaCl [mM]	Feed <sup>a</sup>	DBC <sub>100%</sub> [mg/mL]	EC <sub>100%</sub> [mg/mL]	DBC <sub>100%</sub> [mg/mL]	EC <sub>100%</sub> [mg/mL]	DBC <sub>100%</sub> [mg/mL]	EC <sub>100%</sub> [mg/mL]
5.5	75	A	55	53	46	47	—	—
		B	53	55	—	—	—	—
5.5	150	A	—	—	41	36	—	—
		B	—	—	—	—	—	—
6.5	75	A	37	31	32	34	68	57
		B	—	—	—	—	68	57
		C	—	—	—	—	42	31
6.5	150	A	23	19	23	18	52	39
		B	15	18	—	—	—	—
		D	—	—	—	—	43	35
7.4	150	A	—	—	—	—	34	28

<sup>a</sup> Feed solutions: (A) IgG Beriglobin (1 mg/mL) in 25 mM PBS buffer. (B) IgG Gammanorm (1 mg/mL) in 25 mM PBS buffer. (C) Dialyzed cell culture feed with 10 mM PBS buffer with 75 mM NaCl, spiked with IgG Beriglobin to 1 mg/mL, Pluronic F-68 (1 mg/mL) and NaN<sub>3</sub> (1 mg/mL). (D) IgG Beriglobin in 150 mM NaCl spiked with Pluronic F-68 (1 mg/mL). Test conditions: 1 mL adsorbent at a flow rate of 0.6 mL/min and detection at 280 nm.

parison between two different types of polyclonal h-IgG, namely Beriglobin (feed A) and Gammanorm (feed B) was also done for the materials **J** and **L**. Table 3 summarizes the 100%-DBC and EC results investigated with four different test solutions, including a dialyzed cell culture feed (feed C) and a mock feed solution spiked with Pluronic-F68 (feed D).

Fig. 7 shows the IgG concentration plotted against the volume of applied feed. Material **L** exhibits practically same dynamic capture performance for feed A and feed B, which demonstrates that material **L** is not sensitive to slight variations in the composition of polyclonal h-IgG.

The dynamic test results for material **L** using feed A and B showed surprisingly high DBC values of about 68 mg/mL for 100% break-through of IgG and elution capacities of 57 mg/mL for test solutions containing pH 6.5 and 75 mM NaCl. In this case the dynamic measurements exceeded the results of the SBC measurements, which exhibited an elution capacity of 48.8 mg/mL.

In order to investigate the influence of the foam reducing agent Pluronic-F68 on the IgG capture performance of material **L**, a further DBC test with an IgG standard solution containing Pluronic F-68 (feed D) was conducted. The addition of Pluronic F-68 to the test solution led to a decrease of the elution capacity at 150 mM sodium chloride and pH 6.5 from 39 to 35 mg/mL. Additionally a DBC test was performed under isotonic conditions (pH: 7.4, NaCl: 150 mM) leading to an EC of 28 mg/mL and showed that substantial amounts of IgG could be captured also under such conditions. A final test of material **L** was done with a dialyzed cell culture supernatant containing typical impurities of a fermentation broth such as host cell proteins and DNA. Feed C was additionally spiked with Pluronic F-68 (1 mg/mL) and sodium azide (1 mg/mL), and was adjusted to pH 6.5 and 75 mM NaCl. The salt concentration resembles a 1:1 dilution of a feed solution with 150 mM NaCl and is in fact the ideal compo-

sition for antibody capture for material **L**. The elution of captured IgG was conducted with a sodium chloride gradient from 0 mM to 1 M NaCl.

For the entire DBC run, 10 mL fractions were collected and their antibody content was determined with the Protein A-HPLC method. For the application feed and a representative elution fraction also

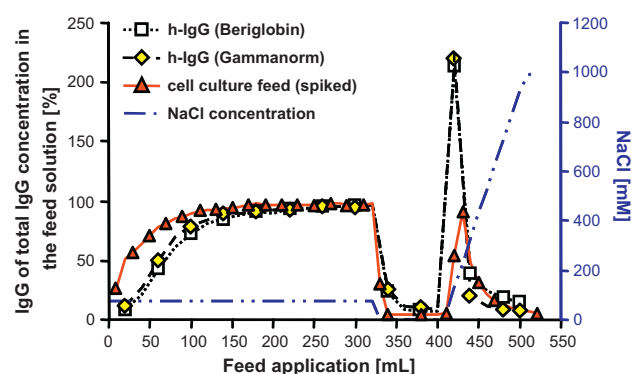


**Fig. 7.** Dynamic break-through curves of the aromatic HIC material **L** using polyclonal h-IgG Beriglobin (feed A: 1 mg/mL h-IgG in PBS with 75 mM NaCl at pH 6.5), polyclonal h-IgG Gammanorm (feed B: 1 mg/mL h-IgG in PBS with 75 mM NaCl at pH 6.5) and a dialyzed cell culture supernatant with monoclonal h-IgG1 (32 µg/mL) spiked with polyclonal IgG Gammanorm (feed C: 1 mg/mL h-IgG in PBS with 75 mM NaCl, 1 mg/mL Pluronic F-68 and 1 mg/mL NaN<sub>3</sub> at pH 6.5). DBC-tests were performed at room temperature and at a flow-rate of 0.6 mL/min. For feed A and B the wash solutions had the composition of the binding buffer and the elution buffer contained 1 M NaCl at pH 6.5. The wash solution for the cell culture supernatant experiment consisted of a 25 mM phosphate buffer without salt and pH 6.5. The elution was performed by applying a linear salt gradient starting at 0 mM NaCl and ending at 1 M NaCl. Cleaning in place was conducted with 0.5 M NaOH solution for all 3 experiments.

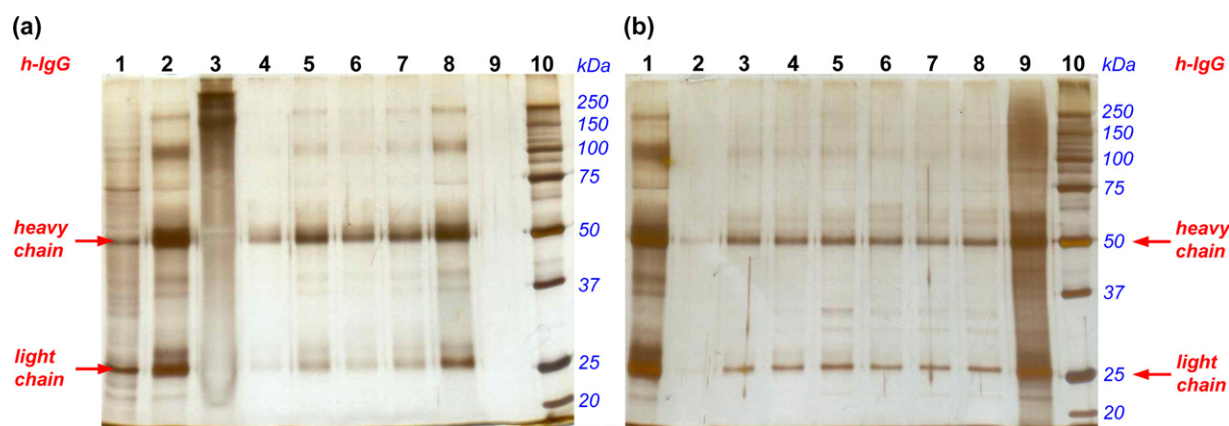


**Fig. 8.** Reduced and silver stained SDS-PAGE slab gels for collected DBC fractions (10 mL each) of material **L** tested with dialyzed cell culture supernatant (feed C). 10% Tris-HCl gel and 3  $\mu$ L sample loads were used. (a) Lane 1: original dialyzed feed (32  $\mu$ g h-IgG/mL); lane 2: dialyzed feed spiked with polyclonal h-IgG (feed C: 1 mg/mL h-IgG); lane 3: non-reduced feed C (spiked); lanes 4–7: loading fraction 1–4; lane 8: final loading fraction 17; lane 9: final wash fraction; lane 10: molecular weight marker. (b) Lane 1: feed C; lanes 2–8: elution fractions 1–7; lane 9: CIP (0.5 M NaOH); lane 10: molecular weight marker.

DNA-analysis was performed. These DNA tests exhibited that the removal of DNA was successful, which means that the aromatic ring did not interact with their purine or pyrimidine scaffolds. The amount of DNA dropped from 0.93  $\mu$ g/mL to <0.15  $\mu$ g/mL, which is below the limit of detection. Furthermore, the composition of some of the collected flow-through, wash and elution fractions was also visualized with SDS-PAGE using silver staining in Fig. 8.

### 3.5.3. SDS-PAGE

The SDS-PAGE gel in Fig. 8a shows in the lanes 1 and 2, the dialyzed feed before and after spiking with polyclonal IgG to a concentration of 1 mg/mL. Although the same sample volume was applied, the feed impurity composition of the spiked feed sample had shifted towards more distinct bands at approximately 28, 37, 40, 100 and 250 kDa. The non-reduced spiked feed in lane 3 suggests that most feed impurities were of high molecular weight of 75 kDa and higher. Furthermore, all three lanes were over-laid with a protein smear, which was absent in the flow-through fractions 1–4 (lanes 4–7). The first break-through of h-IgG was found in load fraction 1, while a slight break-through of the impurities 28, 37, 40, 100 and 250 kDa was observed for the following load samples. The final loading fraction 17 (lane 8) exhibited a significant break-through of h-IgG and all feed impurities. The elution fractions 1 to 7 (lanes 2–8) in Fig. 8b showed no enrichment of h-IgG, which mirrors the results of the DBC diagram established by the quantification of h-IgG via the Protein A-HPLC method (Fig. 7). The most intensive bands of reduced h-IgG at 25 and 50 kDa occurred in the elution fraction 3 (lane 4). The h-IgG content in this fraction was about 90% of what was present in the application feed. The elution fractions 2 and 4 (lane 3 and 5) contained only 54% and 48% h-IgG, respectively. The last elution fraction contained still 5% h-IgG, which indicates an insufficient elution. Only a small purification factor was obtained, since some impurities were co-eluted with h-IgG.

The absence of the protein smear and other feed impurities in the flow-through fractions 1–4 (lanes 4–7), their reduced presence in the elution fraction suggests and their most distinct presence in the cleaning-in-place (CIP) fraction in lane 9 suggests that material **L** is a mixed-modal adsorbent, which binds h-IgG and removes feed-impurities in a single purification step. The presence of the 25 and 50 kDa bands indicates that h-IgG could not be effectively eluted with a shallow linear sodium chloride gradient. An elongated elution with 1 M sodium chloride would probably solve this problem, also an increased pH would be an option for improved elution conditions.

The elution peak maximum was reached after 30 mL of elution buffer had passed through the column, and the NaCl concentration at this point was around 200 mM. The shape of the IgG elution peak exhibited a tailing, which is not uncommon for polyclonal IgG, since it is rather complex and diverse in its composition. Cell culture supernatant with a higher concentration of mAb was unfortunately not available. The resulting elution capacity of 43 mg/mL was satisfying and further investigations on the field of aromatic acids will be conducted in the near future. In comparison to the cysteine and homocysteine based benzamido materials, the DBC results of material **L** were outstanding. At pH 6.5 and 150 mM sodium chloride the binding capacity of benzoyl homocysteine could be doubled. Also the commercial adsorbent Capto<sup>TM</sup> MMC, which possessed with 20 mg/mL 100% DBC almost the same binding capacity for feed A as material **J**, could be outperformed. A further advantage of 4-mercaptobenzoic acid is its simple structure and immobilization chemistry, which allows an easy large-scale production of the corresponding adsorbent. However, the question remains whether or not there is a thiophilic influence of the sulfur atom or not? Only a reference material where the sulfanyl linkage is exchanged (preferably by an oxo group) can answer this question. But what can be stated here is the fact, that the 4-mercaptobenzoic acid is able to bind IgG under physiological condition without the addition of structure forming salts.

## 4. Conclusion

During the creation, synthesis and characterization via SBC tests several findings crystallized out. First of all ligands based on dithiols coupled onto Fractogel turned out to provide unsatisfactory h-IgG capture results compared to the investigated commercial cation exchangers adsorbents. This seems to be the result of the bifunctionality of the CIE-X-ligands in combination with the tentacle grafting of the support surface and their general tendency for disulfide cross-linking on this particular support. On the other hand, the direct coupling of 3-mercaptopropylsulfonic acid, which lack the possibility of disulfide bridge formation, provided comparable results to commercially available strong cation exchangers, e.g. Fractogel<sup>®</sup> EMD SO<sub>3</sub>. However, their capture performance for h-IgG from solutions containing considerably high amount of sodium chloride was still insufficient. An improvement of the binding capacity could be observed, after replacement of the strong sulfonic acid group by a carboxylic acid group. Good results gave material **E**, the tentacle based gel bearing the mercaptopropionic acid ligand. The subsequent introduction of N-acetyl-cysteine and



N-acetyl-homocysteine derivatives was not able to compete with this simple carboxylic acid compound, only the introduction of aromatic moieties brought an improvement of the IgG binding performance. Subsequently, these benzamido bearing carboxylic acid groups coupled onto Fractogel were able to bind antibodies with decent capacities at pH values higher than 6.0 and sodium chloride concentrations of 75 mM and higher, but there was still potential for improvement. Consequently a new ligand in the form of 4-mercaptobenzoic acid was introduced. It exhibited outstanding binding properties under conditions very near to neutral pH and at high sodium chloride concentrations. During DBC tests this material was able to bind up to 68 mg IgG per mL resin in the presence of 75 mM sodium chloride and a pH of 6.5, which is significantly higher than previous generations of mixed-modal materials, bearing, e.g. N-benzoyl-homocysteine based ligands. This high binding capacity makes this simple mixed-modal ion exchange based bioaffinity type material highly competitive to commercially available mixed-modal ligands for the capture of h-IgG from cell culture feed.

### Acknowledgements

This research study was performed within the Christian-Doppler-Laboratory for Molecular Recognition Materials, which was funded by the Austrian Government and the industrial partners (Merck, AstraZeneca, piChem, Fresenius Kabi and Sandoz) via the Austrian Christian Doppler Society.

### Appendix A. Supplementary data

Supplementary data associated with this article can be found, in the online version, at [doi:10.1016/j.chroma.2011.06.012](https://doi.org/10.1016/j.chroma.2011.06.012).

### References

- [1] S.S. Farid, J. Chromatogr. B: Anal. Technol. Biomed. Life Sci. 848 (2007) 8.
- [2] K. Keller, T. Friedmann, A. Boxman, Trends Biotechnol. 19 (2001) 438.
- [3] B. Kelley, Biotechnol. Prog. 23 (2007) 995.
- [4] S. Hober, K. Nord, M. Linholt, J. Chromatogr. B 848 (2007) 40.
- [5] R. Hahn, K. Shimahara, F. Steindl, A. Jungbauer, J. Chromatogr. A 1102 (2006) 224.
- [6] J.N. Carter-Franklin, C. Victa, P. McDonald, R. Fahrner, J. Chromatogr. A 1163 (2007) 105.
- [7] M.I. Gomez, A. Lee, B. Reddy, A. Muir, G. Soong, A. Pitt, A. Cheung, A. Prince, Nat. Med. (N.Y., NY, U.S.) 10 (2004) 842.
- [8] F. Steindl, C. Armbruster, R. Hahn, C. Armbruster, H.W.D. Katinger, J. Immunol. Methods 235 (2000) 61.
- [9] A. Stein, A. Kiesewetter, J. Chromatogr. B: Anal. Technol. Biomed. Life Sci. 848 (2007) 151.
- [10] B. Lain, M.A. Cacciuto, G. Zarbis-Papastois, Bioprocess Int. 7 (2009) 26.
- [11] D.K. Follman, R.L. Fahrner, J. Chromatogr. A 1024 (2004) 79.
- [12] A. Ljungloef, K.M. Lacki, J. Mueller, C. Harinarayan, R. van Reis, R. Fahrner, J.M. Van Alstine, Biotechnol. Bioeng. 96 (2006) 515.
- [13] J.X. Zhou, S. Dermawan, F. Solamo, G. Flynn, R. Stenson, T. Tressel, S. Guhan, J. Chromatogr. A 1175 (2007) 69.
- [14] T. Ishihara, T. Kadoya, N. Endo, S. Yamamoto, J. Chromatogr. A 1114 (2006) 97.
- [15] W. Kopaciewicz, M.A. Rounds, J. Fausnaugh, F.E. Regnier, J. Chromatogr. 266 (1983) 3.
- [16] C. Harinarayan, J. Mueller, A. Ljungloef, R. Fahrner, J. Van Alstine, R. van Reis, Biotechnol. Bioeng. 95 (2006) 775.
- [17] N. Forrer, A. Butte, M. Morbidelli, J. Chromatogr. A 1214 (2008) 71.
- [18] A. Staby, H. Jacobsen Jan, G. Hansen Ronni, K. Bruus Ulla, H. Jensen Inge, J. Chromatogr. A 1118 (2006) 168.
- [19] A. Franke, N. Forrer, A. Butte, B. Cvijetic, M. Morbidelli, M. Johnck, M. Schulte, J. Chromatogr. A 1217 (2010) 2216.
- [20] J. Chen, J. Tetrault, Y. Zhang, A. Wasserman, G. Conley, M. Di Leo, E. Haimes, A.E. Nixon, A. Ley, J. Chromatogr. A 1217 (2010) 216.
- [21] J. Porath, F. Maisano, M. Belew, FEBS Lett. 185 (1985) 306.
- [22] J. Horak, W. Lindner, J. Chromatogr. A 1043 (2004) 177.
- [23] J. Horak, W. Lindner, J. Chromatogr. A 1191 (2008) 141.
- [24] P.P. Berna, N. Berna, J. Porath, S. Oscarsson, J. Chromatogr. A 800 (1998) 151.
- [25] E. Boschetti, J. Biochem. Biophys. Methods 49 (2001) 361.
- [26] A. Schwarz, J. Kohen, M. Wilchek, React. Polym. 22 (1994) 259.
- [27] M. Numata, Y. Aoyagi, Y. Tsuda, T. Yaita, A. Takatsu, Anal. Chem. 79 (2007) 9211.
- [28] J.T. Andersson, G. Kaiser, Anal. Chem. 69 (1997) 636.
- [29] U.B. Finger, W. Brummer, E. Knieps, J. Thommes, M.R. Kula, J. Chromatogr. B 675 (1996) 197.
- [30] V. Busini, D. Moiani, D. Moscatelli, L. Zamolo, C. Cavallotti, J. Phys. Chem. B 110 (2006) 23564.
- [31] L. Zamolo, M. Salvalaglio, C. Cavallotti, S. Hofer, J. Horak, W. Lindner, B. Galarza, C. Sadler, S. Williams, J. Phys. Chem. B 114 (2010) 9367.
- [32] R. Hahn, K. Deinhofer, C. Machold, A. Jungbauer, J. Chromatogr. B 790 (2003) 99.
- [33] C. Machold, K. Deinhofer, R. Hahn, A. Jungbauer, J. Chromatogr. A 972 (2002) 3.
- [34] E. Boschetti, L. Guerrier, Int. J. Bio-Chromatogr. 6 (2001) 269.
- [35] J. Chen, J. Tetrault, A. Ley, J. Chromatogr. A 1177 (2008) 272.
- [36] K.A. Kaleas, C.H. Schmelzer, S.A. Pizarro, J. Chromatogr. A 1217 (2010) 235.
- [37] P. Girot, E. Averty, I. Flayeux, E. Boschetti, J. Chromatogr. B 808 (2004) 25.
- [38] W. Mueller, J. Chromatogr. 510 (1990) 133.
- [39] A. Heeboll-Nielsen, M. Dalkiaer, J.J. Hubbuch, O.R.T. Thomas, Biotechnol. Bioeng. 87 (2004) 311.
- [40] J. Horak, R. Alexander, W. Lindner, J. Chromatogr. A 1217 (2010) 5092.
- [41] <http://probes.invitrogen.com/media/pis/mp07581.pdf>.
- [42] I. B.-R.L. Instruction Manual for Mini-PROTEAN® 3 Cell, <http://www.plant.uoguelph.ca/research/homepages/raizada/Equipment/RaizadaWeb%20Equipment%20PDFs/9B.%20miniprotean3%20cell%20manual.pdf>.
- [43] U.K. Laemmli, Nature 227 (1970) 680.
- [44] I.S.-A. Technical Bulletin for ProteoSilver™ Plus Silver Stain Kit (PROT-SIL2), <http://www.sigmaaldrich.com/etc/medialib/docs/Sigma/Bulletin/protosil2bul.Par.0001.File.tmp/protosil2bul.pdf>.
- [45] B. Preinerstorfer, W. Bicker, W. Lindner, M. Lammerhofer, J. Chromatogr. A 1044 (2004) 187.
- [46] Q. Luo, H. Zou, Q. Zhang, X. Xiao, J. Ni, Biotechnol. Bioeng. 80 (2002) 481.
- [47] A. El-Kak, S. Manjini, M.A. Vijayalakshmi, J. Chromatogr. 604 (1992) 29.
- [48] E. Nedonchele, O. Pitiot, M.A. Vijayalakshmi, Appl. Biochem. Biotechnol. 83 (2000) 287.
- [49] R.C.A. Ventura, R. De Lima Zollner, C. Legallais, M. Vijayalakshmi, S.M.A. Bueno, Biomol. Eng. 17 (2001) 71.
- [50] A.C.A. Roque, C.S.O. Silva, M.A. Taipa, J. Chromatogr. A 1160 (2007) 44.
- [51] J.-L. Maloisel, N. Thevenin, WO Patent 2003024588 (2003).
- [52] G.H. Scholz, P. Wippich, S. Leistner, K. Huse, J. Chromatogr. B 709 (1998) 189.
- [53] K.L. Knudsen, M.B. Hansen, L.R. Henriksen, B.K. Andersen, A. Lihme, Anal. Biochem. 201 (1992) 170.

# **Supplementary Material**

## **Performance evaluation of mixed-modal, thiophilic and hydrophobic cation exchanger adsorbents for the purification of human immunoglobulin G**

Stefan Hofer, Alexander Ronacher, Jeannie Horak, Heiner Graalfs, Wolfgang Lindner

(Contact Email: [Wolfgang.Lindner@univie.ac.at](mailto:Wolfgang.Lindner@univie.ac.at))

### **1. Reagents and equipment**

L-Cystine, 1,3-propanedithiol, 2,2'-oxydiethanethiol, 3,6-dioxa-1,8-octane-dithiol, hydrogen peroxide (30%), 3-mercapto-1-propanesulfonic acid sodium salt, sodium hydroxide, N,N-diisopropylethylamine (DIPEA), triethylamine (TEA), 2,2'-dipyridyl disulfide (DPDS), hydrochloric acid (37% v/v), 3-mercaptopropionic acid, 4-mercaptobenzoic acid, 3,5-dimethoxybenzoyl chloride, N-acetyl-L-cysteine, N-acetyl-D,L-homocysteine thiolactone and D,L-homocysteine thiolactone hydrochloride were purchased from Sigma Aldrich (Vienna, Austria). benzoyl chloride was acquired from Merck (Darmstadt, Germany) and N-acetyl-D,L-penicillamine hemihydrate from Alfa Aesar (Karlsruhe, Germany). Tris (2-cyanoethyl) phosphine was a kind donation of CYTEC (New Jersey, USA).

If not otherwise stated, all solvents used for ligand synthesis were supplied by Sigma Aldrich (Vienna, Austria) and were of purest grade available, with exception of dichloromethane and methanol for flash chromatography, which were of technical grade. For flash chromatography silica gel 60 (0.040-0.063 mm particle size) from Merck (Darmstadt, Germany) was used.

Fractogel® EMD Epoxy (M), a cross-linked polymethacrylate resin modified with the tentacle-grafting technology and an epoxy group density of 1000 µmol/g dry gel, was provided by Merck KGaA (Darmstadt, Germany).

<sup>1</sup>H NMR spectra were made with a Bruker DRX 400MHz spectrometer. The units for the chemical shift (δ) are given in parts per million (ppm). The massspectrometric data were acquired on a PEsSciex API 365 triple quadrupole mass spectrometer from Applied Biosystems/MDS Sciex (Concord, Canada). The ion source was an electrospray device and, depending on the analyte, either positive or negative spectra or both were measured. The elemental analysis of sulfur containing materials were performed with an EA 1108 CHNS-O from Carlo Erba (Rodano, Italy), the determination of CHN was done with a "2400 Elemental Analyzer" from Perkin Elmer (Vienna, Austria). The titration of the ionic groups was performed on a Mettler Toledo autotitrator DL676 (single burette drive, 10 mL), equipped with an Ag/AgCl pH-electrode (DG-111-SC) (Giessen, Germany) with 0.1 M sodium hydroxide.

## 2. Synthesis of HIC-based cation exchange ligands

### 2.1 N-Benzoyl-D,L-homocysteine-thiolactone and N-(3,5-Dimethoxybenzoyl)-D,L-homocysteine-thiolactone

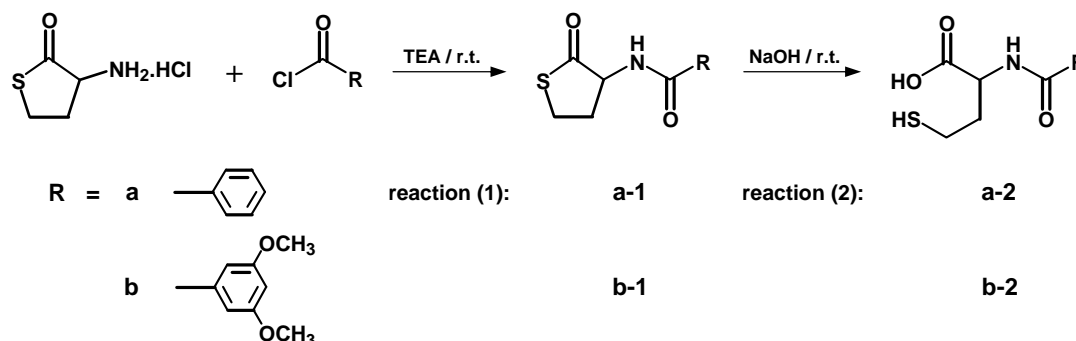


**Figure S1: Reaction scheme for N-Benzoyl-D,L-homocysteine-thiolactone and N-(3,5-Dimethoxybenzoyl)-D,L-homocysteine-thiolactone**

1.5 g D,L-Homocysteine-thiolactone hydrochloride (10 mmol) was dissolved in 16 mL dry dichloromethane with a two-fold excess of diisopropylethylamine (DIPEA) and cooled at 0°C in an ice bath. An equimolar amount of benzoyl chloride (a) or 3,5-dimethoxybenzoyl chloride (b) dissolved in dry dichloromethane was added dropwise to the reaction flask under constant stirring. The solution was kept under these conditions for 30 minutes and was then brought to room temperature, where it was allowed to stay another 18 hours until completion of the reaction was observed via TLC (**Fig. S1**). After evaporation of the solvent, the solid residue was re-dissolved in ethyl acetate and washed with an aqueous solution of citric acid (10% w/v). The organic phase was collected, the solvent evaporated and the solid white product was purified via flash-chromatography using silica gel 60 and dichloromethane/methanol (10:0.5).

#### (a-1) N-Benzoyl-D,L-homocysteine-thiolactone (J)

Reaction yield: 2g (90%)

MS (ESI, positive): 222.4 [M+H]<sup>+</sup>, 104.7 [M-116]<sup>+</sup>, 443.2 [2M+H]<sup>+</sup>

<sup>1</sup>H-NMR [400 MHz, CD<sub>3</sub>OD]: δ = 7.86 (d, 2H), 7.57 (t, 1H), 7.48 (t, 2H), 4.93 - 4.87 (m, 1H), 3.53 - 3.45 (m, 1H), 3.38-3.33, (m, 1H), 2.70 - 2.62 (m, 1H), 2.41-2.29 (m, 1H)

#### (b-1) N-(3,5-Dimethoxybenzoyl)-D,L-homocysteine-thiolactone (K)

Reaction yield: 2.47 g (88%).

MS (ESI, positive): 282.2 [M+H]<sup>+</sup>, 165.1 [M-116]<sup>+</sup>, 304.4 [M+Na]<sup>+</sup>

<sup>1</sup>H-NMR [400 MHz, CD<sub>3</sub>OD]: δ = 7.02 (d, 2H), 6.67 (t, 1H), 4.90-4.83 (m, 1H), 3.84 (s, 6H), 3.53-3.43 (m, 1H), 3.38-3.29 (m, 1H), 2.69-2.61 (m, 1H), 2.41-2.29 (m, 1H)

## 2.2. N-Benzoyl-D,L-homocysteine and N-(3,5-Dimethoxybenzoyl)-D,L-homocysteine

The opening of the thiolactone ring was performed under basic conditions. 10 mmol of N-benzoyl-D,L-homocysteine thiolactone (a-1) or N-(3,5-dimethoxybenzoyl)-D,L-homocysteine thiolactone (b-1) were dissolved in 6 mL of 5 M sodium hydroxide. In order to increase the solubility, 10 mL methanol was added (**Fig S1**). After 18 h of stirring under nitrogen, the reaction was stopped and the solvent was evaporated under reduced pressure. The remaining solid was dissolved in ethyl acetate and washed with 0.01 M HCl, providing a yield of 2.4 g (~99%).

### (a-2) N-Benzoyl-D,L-homocysteine (J)

Reaction yield: 2.37 g (99%)

MS (ESI, positive): 240.2 [M+H]<sup>+</sup>, 222.3 [M-H<sub>2</sub>O+H]<sup>+</sup>, 105.1 [M-134]<sup>+</sup>

<sup>1</sup>H-NMR [CD<sub>3</sub>OD]: δ = 7.88 (d, 2H), 7.56 (t, 1H), 4.86 – 4.80 (m, 1H), 2.72 – 2.58 (m, 2H), 2.28 – 2.13 (m, 2H)

### (b-2) N-(3,5-Dimethoxybenzoyl)-D,L-homocysteine (K)

Reaction yield: 2.49 g (99%)

MS (ESI, positive): 300.4 [M+H]<sup>+</sup>, 282.2 [M-H<sub>2</sub>O+H]<sup>+</sup>, 322.4 [M+Na]<sup>+</sup>,

<sup>1</sup>H-NMR [400 MHz, CD<sub>3</sub>OD]: δ = 7.04 (d, 2H), 6.62 (t, 1H), 4.84 – 4.78 (m, 1H), 3.86 (s, 6H), 2.73 – 2.55 (m, 2H), 2.28 – 2.11 (m, 2H)

## 2.3. N,N-Dibenzoyl-L-cystine

5 g L-Cystine (20.8 mmol) were solved in 50 mL 2 M sodium hydroxide and cooled down to 4°C. 45.7 mmol benzoyl chloride were added dropwise under stirring to the reaction mixture. After addition of benzoyl chloride, the solution was stirred for 2 h at room temperature, before adding hydrochloric acid (35% v/v) until the mixture reached a pH of 1. The reaction solution was then extracted 3 times with ethyl acetate. The organic phase were collected and evaporated under reduced pressure. Further purification via flash chromatography was performed with methanol/dichloromethane (50:1) on silica gel 60.

Reaction yield: 2.97 g (82%).

MS (ESI, positive): 449.2 [M+H]<sup>+</sup>, 897.2 [2M+H]<sup>+</sup>, 431 [M-H<sub>2</sub>O+H]<sup>+</sup>

MS (ESI, negative): 447 [M-H]<sup>-</sup>, 895.3 [2M-H]<sup>-</sup>

<sup>1</sup>H-NMR [400 MHz, CD<sub>3</sub>OD]: δ = 7.83 (d, 4H), 7.52 (t, 2H), 7.43 (t, 4H), 4.99 – 4.92 (m, 2H), 3.46 – 3.40 (m, 2H), 3.22 – 3.13 (q, 2H)

## 2.4. N-Benzoyl-L-cysteine (I)

N,N-Dibenzoyl-L-cystine (7.5 g, 17 mmol) was reduced according to Burns et al. [1] with tris (2-carboxyethyl) phosphine (TCEP) at pH 4.5. TCEP was prepared by refluxing tris (2-cyanoethyl) phosphine in concentrated HCl under nitrogen atmosphere for 2 h. The resulting solution was evaporated under reduced pressure. Afterwards N-benzoyl-L-cystine was mixed with a two fold excess of TCEP in 400 mL of an ultra-sonicated ammonium acetate buffer system (25 mM) in methanol/water (1:1) at pH 4.5. Although the reduction was almost complete within one hour, the reaction was allowed to run

overnight under nitrogen atmosphere. The solvent was evaporated under reduced pressure and the remaining crude white solid was dissolved in 50 mM hydrochloric acid and extracted three times with ethyl acetate. After solvent removal using rotary evaporation, clean product were obtained. No further purification steps were necessary.

Reaction yield: 7.5 g (99%).

MS (ESI, positive): 226.3  $[M+H]^+$ , 208.1  $[M-H_2O+H]^+$ , 248.4  $[M+Na]^+$

$^1H$ -NMR [400 MHz,  $CD_3OD$ ]:  $\delta$  = 7.87 (d, 2H), 7.55 (t, 1H), 7.47 (t, 2H), 4.81 – 4.75 (m, 1H), 3.15 – 3.09 (m, 1H), 3.04 – 2.96 (m, 1H)

### 3. Immobilization and modification of the ligands

Note that all ligands were immobilized onto Fractogel EMD Epoxy support material. The below listed ligands are abbreviated by letters A to L. The chemical structures of the corresponding adsorbents are listed in **Fig. 2** following the same abbreviations A to L as employed for the ligands.

The immobilization rate (ligand density) was determined via elemental analysis (EA) employing the sulfur and nitrogen content of the surface attached ligands. Alternatively, the sulfonic acid content and carboxylic acid content were determined via titration using 0.1 M NaOH (T). Throughout the article the ligand density based on the titration values are used as the effective ligand density. Alternatively the thiol content of the adsorbents were determined photometrically using the 2,2'-dipyridyl disulfide (DPDS) method [2].

#### 3.1. Cation exchanger adsorbents with sulfanyl and sulfonyl-linkage

##### a) General procedure for ligand immobilization (sulfanyl-linkage):

To 20 mmol of the ligand (1,3-propanedithiol (2 mL), 2,2'-oxydiethanethiol (2.5 mL) or 3,6-dioxa-1,8-octane-dithiol (3.27 mL)) and 10 mmol of TEA (1.4 mL) were added to 1 g epoxy-activated support material (epoxide group density: 1 mmol/g) and heated to 70°C under nitrogen atmosphere for 18 h. The modified adsorbent was thoroughly washed with methanol.

##### **Immobilization of 1,3-propanedithiol**

Ligand density (EA): 1015  $\mu\text{mol/g}$  dry gel; (C: 51.99%; H: 7.76%; N: 0.12%; S: 6.49%)

Thiol group density (DPDS): 783  $\mu\text{mol/g}$  dry gel

##### **Immobilization of 2,2'-oxydiethanethiol**

Ligand density (EA): 953  $\mu\text{mol/g}$  dry gel; (C: 51.55%; H: 7.75%; N: 0.10%; S: 6.1%)

Thiol group density (DPDS): 660  $\mu\text{mol/g}$  dry gel

##### **Immobilization of 3,6-dioxa-1,8-octanedithiol**

Ligand density (EA): 872  $\mu\text{mol/g}$  dry gel; (C: 51.67%; H: 7.84%; N: 0.11%; S: 5.58%)

Thiol group density: 460  $\mu\text{mol/g}$  dry gel



b) Oxidation of sulfanyl groups to sulfonyl groups (sulfonyl-linkage):

The oxidation of sulfanyl groups was performed with a freshly prepared performic acid solution, containing 28.5 mL formic acid with 5 mL H<sub>2</sub>O<sub>2</sub> (30%). The performic acid solution was stirred for 2 h at room temperature. 3 g modified adsorbent were suspended in 20 mL methanol and 10 mL formic acid. The performic acid solution was added drop wise under gentle stirring and cooling with ice. Afterwards the solution was stirred for additional 4 hours at room temperature. The oxidized adsorbent was then extensively washed with distilled water and methanol [3,4].

c) Alternative procedure:

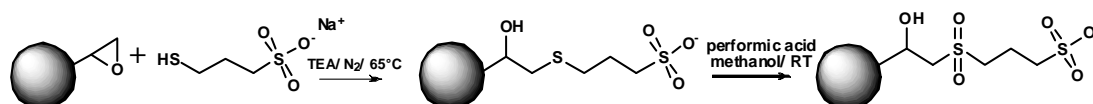


**Figure S2: Coupling and oxidation of 3-mercaptopropylsulfonic acid**

Material A (another production batch with a slightly lower ligand density) was oxidized according to the above mentioned general procedure leading to material B2, which possesses the same chemical structure as material B1.

**3-Sulfonyl-1-propanesulfonic acid (B1)**

Ligand density (EA): 955 μmol/g dry gel; (C: 48.16%; H: 7.23%; N: 0.16%; S: 6.12%)

Sulfonic acid density (T): 637 μmol/g dry gel);

**3-Sulfonyl-1-propanesulfonic acid (B2)**

Ligand density (EA): 1011 μmol/g dry gel; (C: 46.71%; H: 7.28%; N: 0.131%; S: 6.47%)

Sulfonic acid density (T): 886 μmol/g dry gel).

**2-(2-Sulfonylethoxy)-ethanesulfonic acid (C)**

Ligand density (EA): 840 μmol/g dry gel; (C: 46.29%; H: 6.95%; N: 0.511%; S: 5.38%)

Sulfonic acid density (T): 564 μmol/g dry gel

**3,6-Dioxa-8-sulfonyl-1-octanesulfonic acid (D)**

Ligand density (EA): 790 μmol/g dry gel, C: 48.72%; H: 7.36%; N: 0.36%; S: 5.06%)

Sulfonic acid density (T): 457 μmol/g dry gel

### 3.2. Cation exchange adsorbents with sulfanyl-linkage

Coupling of the carboxylic acid and sulfonic acid as well as cysteine and homocysteine based ligands.

#### a) General procedure for ligand immobilization:

A solution containing 10 mmol of 3-mercapto-1-propanesulfonic acid (A) in 15 mL methanol-water mixture (10:1), an equimolar amount of 5 M sodium hydroxide solution (10 mmol) and 10 mol-equivalents (relative to mol epoxide groups) of triethylamine (TEA) were mixed. This reaction solution was added to 1 g epoxy-activated support material (1000  $\mu\text{mol}$  epoxy groups/dry g) and heated for 18 h at 65°C under nitrogen using a mechanical stirrer. The modified adsorbent was then washed with methanol, followed by subsequent wash-steps employing aqueous solutions of 50 mM citric acid, 0.5 M sodium hydroxide and distilled water until neutral pH was reached.

#### b) Deactivation of residual epoxide groups on the adsorbents:

Per gram adsorbent suspended in 15 mL methanol, 0.5 mL 2-mercaptoethanol was added. The reaction mixture was refluxed under nitrogen over night employing a mechanical stirrer. The adsorbent was washed with methanol until odorless.

Ligand density determination and acid content measurements were performed as previously described. The coverage of 2-mercaptoethanol was determined via elemental analysis. Note that if the reagent was not bound in stoichiometrical quantities to the epoxide groups, the residual epoxy groups were endcapped by a ring-opening reaction using 2-mercaptoethanol. Note that this epoxide group endcapping was only performed on adsorbents with ligand densities below 950  $\mu\text{mol/g}$ .

#### **3-Mercapto-1-propanesulfonic acid (A)**

In the case of 3-mercapto-1-propanesulfonic acid, which was purchased as a sodium salt, the free acid (A) was obtained through addition of the 5 M sodium hydroxide solution.

Ligand density (EA): 1207  $\mu\text{mol/g}$  dry gel; (C: 49.27%; H: 7.27%; N: 0.13%; S: 7.73%)

Sulfonic acid density (T): 1023  $\mu\text{mol/g}$  dry gel

#### **3-Mercaptopropionic acid (E)**

Ligand density (EA): 1100  $\mu\text{mol/g}$  dry gel; (C: 52.22%; H: 7.7%; N: 0.15%; S: 3.34%)

Sulfonic acid density (T): 1043  $\mu\text{mol/g}$  dry gel

#### **N-Acetyl-L-cysteine (F)**

Ligand density (EA): 1031  $\mu\text{mol/g}$  dry gel; (C: 50.11%; H: 7.17%; N: 1.51%; S: 3.3%)

Carboxylic acid density (T): 941  $\mu\text{mol/g}$  dry gel

#### **N-Acetyl-D,L-homocysteine (G)**

Ligand density (EA): 921  $\mu\text{mol/g}$  dry gel; (C: 51.01%; H: 7.12%; N: 1.48%; S: 2.95%)

Carboxylic acid density (T): 835  $\mu\text{mol/g}$  dry gel

#### After endcapping with 2-mercaptoethanol:

Ligand density (EA): 843  $\mu\text{mol/g}$  dry gel; (C: 51.01%; H: 7.58%; N: 1.402%; S: 2.7%)

Carboxylic acid density (T): 727  $\mu\text{mol/g}$  dry gel

2-mercaptoethanol coverage: 0  $\mu\text{mol/g}$  dry gel

#### **N-Acetyl-D,L-penicillamine (H)**

Ligand density (EA): 775  $\mu\text{mol/g}$  dry gel; (C: 52.8%; H: 7.8%; N: 1.42%; S: 2.48%)

Carboxylic acid density (T): 703  $\mu\text{mol/g}$  dry gel

After endcapping with 2-mercaptoethanol:

Ligand density (EA): 759  $\mu\text{mol/g}$  dry gel; (C: 51.11%; H: 7.52%; N: 1.33%; S: 2.43%)

Carboxylic acid density (T): 604  $\mu\text{mol/g}$  dry gel

2-Mercaptoethanol coverage: 0  $\mu\text{mol/g}$

#### **N-Benzoyl-L-cysteine (I)**

Ligand density (EA): 715  $\mu\text{mol/g}$  dry gel; (C: 54.44%; H: 7.28%; N: 1.38%; S: 2.29%)

Carboxylic acid Density (T): 634  $\mu\text{mol/g}$

After endcapping with 2-mercaptoethanol:

Ligand density (EA): 709  $\mu\text{mol/g}$  dry gel; (C: 53.73%; H: 7.2%; N: 1.38%; S: 2.27%)

Carboxylic acid density (T): 641  $\mu\text{mol/g}$

2-Mercaptoethanol coverage: 0  $\mu\text{mol/g}$  dry gel

#### **N-Benzoyl-D,L-homocysteine (J)**

Ligand density (EA): 828  $\mu\text{mol/g}$  dry gel; (C: 54.62%; H: 8.22%; N: 1.5%; S: 2.65%)

Carboxylic acid density (T): 820  $\mu\text{mol/g}$

After endcapping with 2-mercaptoethanol:

Ligand density (EA): 887  $\mu\text{mol/g}$  dry gel; (C: 54.27%; H: 7.63%; N: 1.4%; S: 2.84%)

Carboxylic acid density (T): 843  $\mu\text{mol/g}$

2-Mercaptoethanol coverage: 50  $\mu\text{mol/g}$  dry gel

#### **N-(3,5-Dimethoxybenzoyl)-D,L-homocysteine (K)**

Ligand density (EA): 930  $\mu\text{mol/g}$  dry gel; (C: 54.22%; H: 7.34%; N: 1.47%; S: 2.99%)

Carboxylic acid density (T): 841  $\mu\text{mol/g}$

After endcapping with 2-mercaptoethanol:

Ligand density (EA): 909  $\mu\text{mol/g}$  dry gel; (C: 54.23%; H: 7.33%; N: 1.43%; S: 2.91%)

Carboxylic acid density (T): 738  $\mu\text{mol/g}$

2-mercaptoethanol coverage: 0  $\mu\text{mol/g}$  dry gel

#### **4-Mercaptobenzoic acid (L)**

Ligand density (EA): 950  $\mu\text{mol/g}$  dry gel; (C: 51.62%; H: 7.11; N: <0.05%; S: 3.04%)

Carboxylic acid density (T): 950  $\mu\text{mol/g}$

### **4. Dynamic binding capacity test at increased bed height**

An additional DBC test was performed with 2.5 mL of material **L** to determine its performance at an increased bed height compared to 1 mL as stated in the article resulting in a bed height of 3.2 cm. A test solution (feed B) containing 1mg/mL polyclonal h-IgG Gammanorm<sup>®</sup> in 25 mM phosphate buffer with 75 mM NaCl at pH 6.5 was applied onto the column until 100% breakthrough was reached. After washing with application buffer, the elution was performed with 25mM PBS-buffer with 1 M NaCl at pH 6.5 and a

flow rate of 0.6 mL/min, which equals a residence time of 3.25 min. Cleaning in place was conducted with 0.5 M NaOH solution. Other parameters were equivalent to those described in the original article.

The result of this experiment was an elution capacity of 55 mg/mL. For 100% DBC a value of 68 mg/mL and for 10% DBC a value of 21 mg/mL were determined. These values stand in good accordance to the results obtained for the first experiment performed with an adsorbent volume of 1 mL, which exhibited an elution capacity of 57 mg/mL and 68 mg/mL for 100% DBC. Only the 10% DBC value differed with 11 mg/mL from the earlier experiment. The increase in 10% DBC is the result of the overall higher residence time of IgG molecules in the column and a shorter relative distribution area at the head of the column (Fig. S3).

For a better comparison of the two DBC curves established for the same adsorbent at different bed heights, these curves were normalized to the amount of applied feed. Due to the strongly differing application time for feed, wash and elution solution between the two experiments at different bed heights also their x-axis were displayed in two different scales to give credit to the 2.5 times higher bed height.

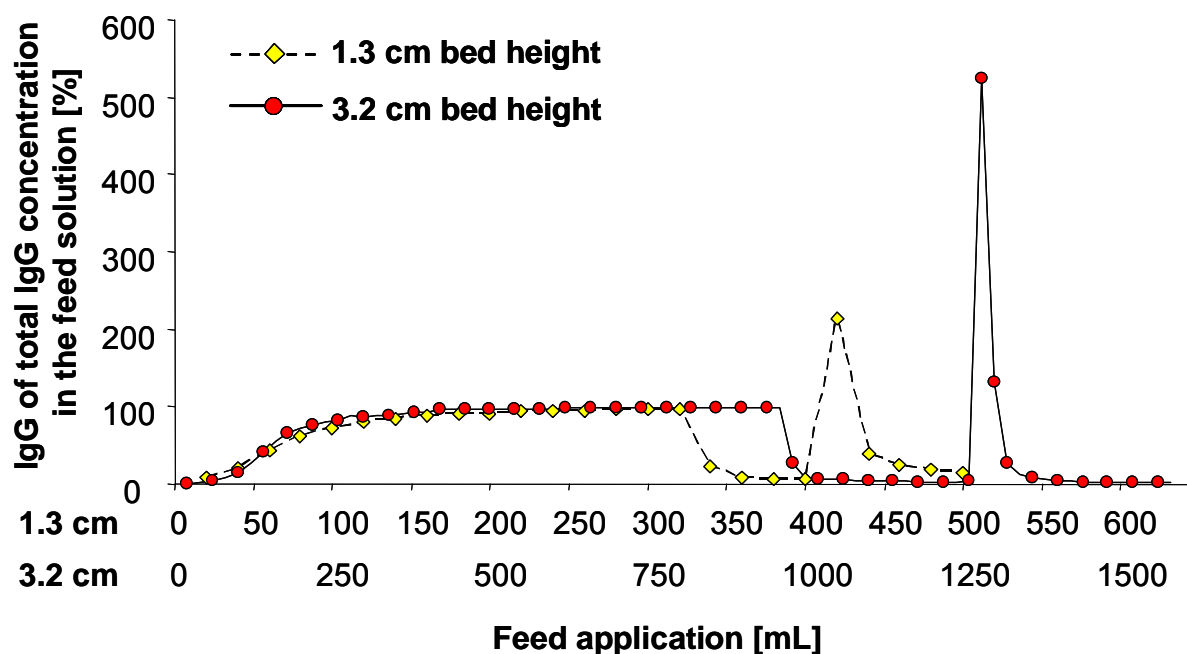


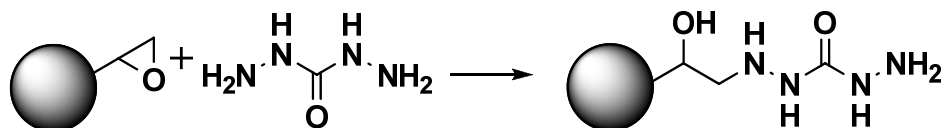
**Figure S3:** Dynamic break-through curves for the aromatic HIC material **L** using polyclonal h-IgG (feed B) tested at 2 different bed heights (1.3 cm and 3.2 cm). For better comparison two different scales for the x axis were used in order to give credit to the different adsorbent volumes and therefore different amounts of application feed solutions applied. Nonetheless, the application time for feed, wash and elution solution was comparatively longer for the 3.2 cm bed height experiment compared to the DBC test at 1.3 cm bed height

## References

- [1] J.A. Burns, J.C. Butler, J. Moran, G.M. Whitesides, J. Org. Chem. 56 (1991) 2648.
- [2] B. Preinerstorfer, W. Bicker, W. Lindner, M. Lammerhofer, J. Chromatogr. A 1044 (2004) 187.
- [3] J. Horak, W. Lindner, J. Chromatogr. A 1191 (2008) 141.
- [4] C.H. Hirs, J. Biol. Chem. 219 (1956) 611.

## 6.2. Additional experimental data

### 1) Coupling of carbodihydrazide on Fractogel EMD Epoxy



- 1 g Fractogel ( = 1mol Epoxy groups)
- 20 mol carbodihydrazide (1.8 g)
- 15 mL H<sub>2</sub>O

Reaction took place overnight at 70°C, severe washing with hot water and methanol (no acetone!)

Elemental analysis:

Sample	Anal.Nr.	w-% C	w-% H	w-% N	w-% S
SH020	050920/29	51.35	7.46	3.39	<0.02
mmol/g		42.79	74.6	2.42	

Ligand density: 605  $\mu$ mol/g, Yield: 60.5 %; Batch code: SH020

This material will be referred to as material 1, and the subsequent endcapping is described in the following reaction 2

### 2) Acidic hydrolysis of material 1

- 100 mg of material 1
- 100  $\mu$ L 2 M H<sub>2</sub>SO<sub>4</sub>
- 900  $\mu$ L H<sub>2</sub>O
- 1 mL MeOH

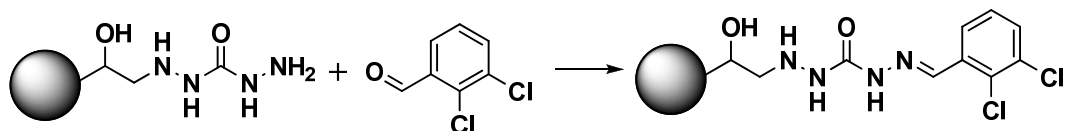
Reaction took place overnight at 45°C. Washing with H<sub>2</sub>O and MeOH

Elemental analysis:

Sample	Anal.Nr.	w-% C	w-% H	w-% N	w-% S
SH024	050920/30	51	7.67	3.32	0.52
mmol/g		42.5	76.7	2.37	0.1625

Yield: n/A, Batch Code: SH024; This material will be referred to as material 2. As a functional test, it was coupled to dichlorobenzaldehyde, see reaction 3

### 3) Coupling of 2,3-dichlorobenzaldehyde onto material 2



Solution A: 158 mg 2,3-dichlorobenzaldehyde dissolved in 1 mL MeOH

Solution B: 7.5  $\mu$ L formic acid dissolved in 1 mL water

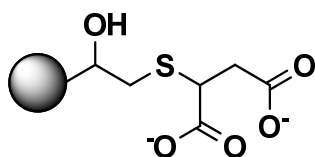
- 10,3 mg Gel (material 2)
- 50 $\mu$ L solution A
- 50 $\mu$ L MeOH
- 50 $\mu$ L water
- 50 $\mu$ L solution B

Shaking for 2 h, washing with MeOH and water, drying under vacuum at 60°C

Sample	Anal. Nr.	w-% C	w-% H	w-% N	w-% S	w-% Cl
SH036	051011/18	51.96	7.4	3.18	0.931	2.73
mmol/g	X78/043	43.3	74	2.27	0.29	0.77

Bound 2,3-dichlorobenzaldehyde: 385  $\mu$ mol/g. Batch code: SH036

### 4) Coupling of mercaptosuccinic acid onto Fractogel EMD Epoxy



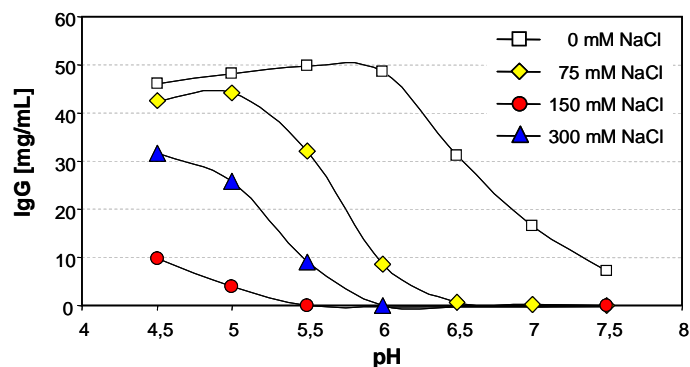
- Fractogel: 3 g
- mercaptosuccinic acid: 4.5 g
- 2.4 g NaOH
- triethylamine: 4.2 mL
- MeOH: 45 mL
- H<sub>2</sub>O: 4.5 mL

The mixture was refluxed over night under nitrogen atmosphere, afterwards severely washed with MeOH and water. Elemental analysis:

Sample	Anal-Nr.	w-% C	w-%H	w-% N	w-% S
SH070	060130/16	51.36	7.24	<0.05	3.62
mmol/g		42.8	72.4		1.131

Ligand density: 1.131 mmol/g; Batch code: SH070

SBC: (measured with SBC 1):



##### 5) Coupling of A2P-DES onto SartoAIMs Epoxy 1

- 21 sheets SartoAIMs Epoxy 1 à 9 cm<sup>2</sup>
- 0.9 g A2P-DES (2 mmol)
- 52 mL MeOH
- 0.5 mL triethylamine

The mixture was refluxed overnight under nitrogen atmosphere. Afterwards the sheets were washed severely with MeOH. Elemental analysis:

Sample	Analnr.	w-% C	w-% H	w-% N	w-% S
SH123	060530/35	61.47	10.42	0.245	0.065
mmol/g		51.225	104.2	0.175	0.02

Ligand density: 0.06  $\mu\text{mol}/\text{cm}^2$ ; Batch code: SH123. This material will be referred to as material 5.

##### 6) Endcapping of material 5

- 21 sheets of material 5
- 0.75 mL mercaptoethanol
- 0.5 mL triethylamine
- 60 mL MeOH

The mixture was refluxed overnight under nitrogen atmosphere. Afterwards the sheets were washed severely with MeOH. Elemental analysis:

Sample	Analnr.	w-% C	w-% H	w-% N	w-% S
SH125	060530/39	60.43	10.13	0.3	0.072
mmol/g		50.358	101.3	0.2143	0.0225

Batch code: SH125

#### 7) Reaction of Fractogel raw material with sodium azide

- 1 mL Fractogel (raw material), formerly transferred from i-propanol to MeOH
- 130 mg NaN<sub>3</sub>
- 278 µL TEA
- 5 mL water

The mixture was shaken at room temperature for 4 days, afterwards the gel was washed with distilled water. Elemental analysis:

Sample	Analnr.	w-% C	w-% H	w-% N
SH205	22.12/18	53.41	7.43	0.19
mmol/g		44.508	74.3	0.136

Ligand density: 45 µmol/g. Batch code: SH205

#### 8) Reaction of Fractogel raw material with aminoethanol

- 1 mL Fractogel (raw material), formerly transferred from i-propanol to MeOH
- 120 µL aminoethanol (2 mmol)
- 278 µL TEA
- 0.7 mL MeOH
- 2 mL water

The mixture was refluxed overnight, afterwards severely washed with MeOH. Elemental analysis:

Sample	Analnr.	w-% C	w-% H	w-% N	w-% S
SH206	061206/22	53.63	7.57	0.221	0.048
mmol/g		44.69	75.7	0.158	0.015

Ligand density: 157 µmol/g. Batch code: SH206

#### 9) Reaction of Fractogel raw material with mercaptoethanol

- 1 mL Fractogel (raw material), formerly transferred from i-propanol to MeOH
- 140 µL mercaptoethanol
- 278 µL TEA
- 0.7 mL MeOH
- 1.5 mL water

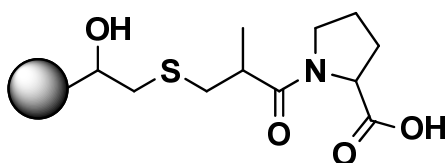


The mixture was heated up to 60°C under nitrogen atmosphere for 18 h. Afterwards the gel was washed with MeOH. Elemental analysis:

Sample	Analnr.	w-% C	w-% H	w-% N	w-% S
SH207	061206/23	53.56	7.79	0.071	0.457
mmol/g		44.63	77.9	0.051	0.143

Ligand density: 142 µmol/g. Batch code: SH207

#### 10) Coupling of captopril onto Fractogel EMD



- 6.51 g captopril (30 mmol)
- 30 mmol NaOH
- 3 g Fractogel
- 45 mL MeOH
- 6.5 mL H<sub>2</sub>O
- 4.2 mL TEA

The mixture was refluxed overnight under nitrogen atmosphere. Afterwards it was washed with MeOH and H<sub>2</sub>O. Titration: 859.5 µmol/g; Elemental analysis:

Sample	Analnr.	w-% C	w-% H	w-% N	w-% S
SH227	070206/08	53.23	7.44	1.42	2.76
mmol/g		44.358	74.4	1.014	0.863

Batch code: SH227. This material will be referred to as material 10.

#### 11) Endcapping of material 10 with mercaptoethanol

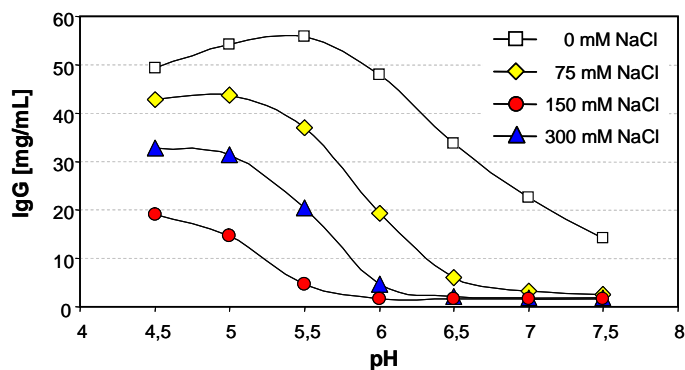
- 3 g material 10
- 1 mL mercaptoethanol
- 50 mL MeOH
- 4 mL TEA

The mixture was refluxed overnight under nitrogen atmosphere. Afterwards it was washed with MeOH. Titration: 766 µmol/g; Elemental analysis:

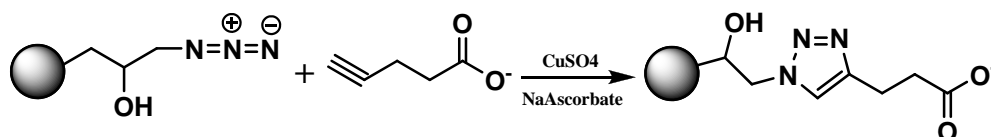
Sample	Analnr.	w-% C	w-% H	w-% N	w-% S
SH228	070206/09	53.2	7.67	1.42	2.6
mmol/g		44.33	76.7	1.0143	0.8125

Batch code: SH228

SBC (measured with SBC protocol 2):



### 12) Coupling of 4-pentynoic acid onto azide activated Fractogel

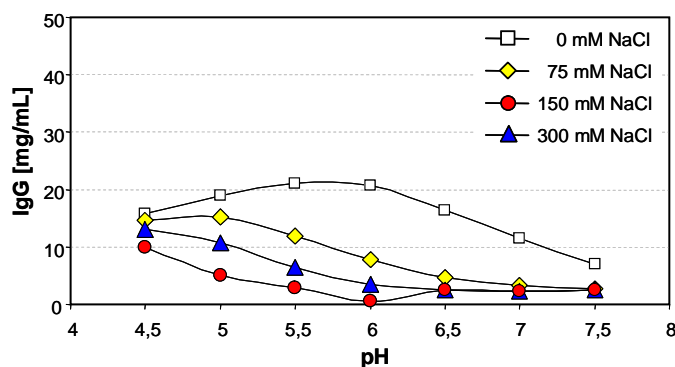


- 1 g FG-N<sub>3</sub> (azide density: 1.03 mmol/g)
- 490 mg 4-pentynoic acid (4mmol)
- 1 mL 1M CuSO<sub>4</sub> solution in H<sub>2</sub>O
- 306 mg sodium ascorbate (2 mmol)
- 10 mL H<sub>2</sub>O:t-BuOH solution (2:1)

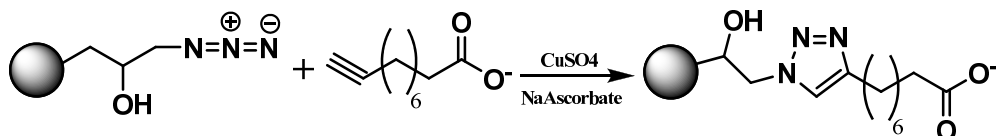
The reaction took place overnight under room temperature. It was washed severely with 0.1 M HCl, 0.1 M NaOH, water and MeOH. Elemental analysis: N/A;

Titration: 569.7  $\mu$ mol/g; Batch code: SH238

SBC (measured with SBC protocol 2):



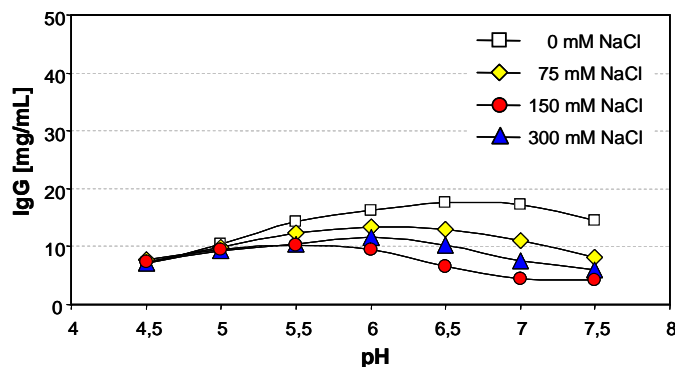
### 13) Coupling of 10-undecynoic acid onto azide activated Fractogel



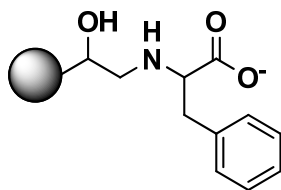
- 1 g FG-N<sub>3</sub> (azide density: 1.03 mmol/g)
- 911 mg 10-undecynoic acid (5mmol) solved in 3 mL acetonitril
- 190 mg CuI (1 mmol) solved 19 mL acetonitril (ultrasonicated)
- 512 µL diisopropylethylamine (3 mmol)

The mixture was shaken for 48 h at room temperature. It was washed with MeOH, H<sub>2</sub>O, 0.05 M 8H-Chinolin solution in MeOH: H<sub>2</sub>O = 3:2, 0.2 M HCl solution in MeOH: H<sub>2</sub>O = 3:2, H<sub>2</sub>O. Note: alternation washing with NaOH and HCl should also be sufficient, and no contamination of 8H-chinolin can occur. Titration: 299 µmol/g; Elemental analysis: not available. Batch code: SH245.

SBC (measured with SBC protocol 2):



### 14) Coupling of phenylalanine onto epoxy activated Fractogel



- 1 g Fractogel
- 1.65 g phenylalanine
- 9.7 mL 1 M NaOH

- 30 mL MeOH
- 1.4 mL TEA

The reaction took place at ~62°C for 18 h. Afterwards the gel was severely washed with water, MeOH and 1 M HCl. Titration: N/A; Elemental analysis:

Probenn.	Analnr.	w-% C	w-% H	w-% N	w-% S
SH248	070312/17	55.08	7.92	0.33	<0.02
mmol/g		45.9	79.2	0.236	

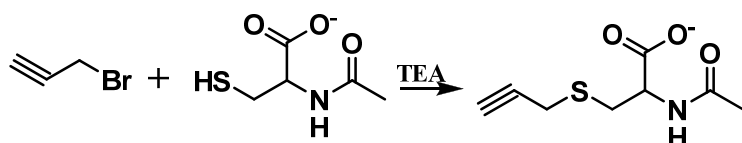
Ligand density: 236 µmol/g. Batch code: SH248

#### 15) Esterification of cystin with thionyl chloride

- 400 mL MeH (HPLC grade, cooled with ice)
- 40 mL thionyl chloride added dropwise

This mixture was stirred for 30 minutes. Afterwards 9.6 g cystine (40 mmol) were added portionwise. The mixture was stirred for additional 18 h at room temperature. The solvent and thionyl chloride was removed via rotary evaporator. Yield: 10.7 g (~100%), MS [ESI, positive]: 269.4 [M+H]<sup>+</sup>, 291.2 [M+Na]<sup>+</sup>, 537.4 [2M+H]<sup>+</sup>, 166 [M-102]<sup>+</sup>, 134.3 [M-134]<sup>+</sup>; Batch code: SH295.

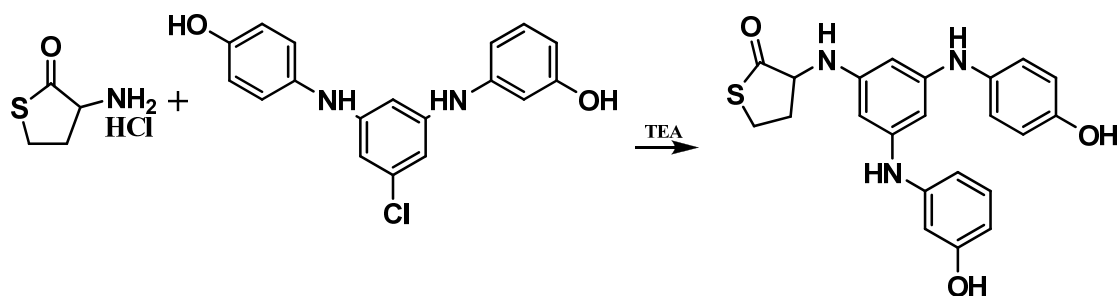
#### 16) Reaction of propargyl bromide with N-acetyl-L-cysteine



- 5 g N-acetyl-L-cysteine (30.6 mmol)
- 100 mL DMF
- 4.5 mL TEA
- 4 mL propargyl bromide solution

Mixture was stirred for 18 at 58 °C and subsequent purification with flash chromatography. Yield: N/A, MS [ESI, negative]: 199.9 [M-H]<sup>-</sup>, 401.2 [2M-H]<sup>-</sup>, 423.2 [2M+Na-2H]<sup>-</sup>; Batch code: SH289.

17) Reaction of A2P-Cl with homocysteinethiolactone hydrochloride



- 7g A2P-Cl (21 mmol)
- 8.79 mL diisopropylethylamine (52.5 mmol)
- 110 mL DMF
- 4.8 g homocysteinethiolactone hydrochloride (31.5 mmol)

The mixture was refluxed for 18 h. Afterwards the product was purified via flash chromatography using silica gel and a dichloromethane-MeOH = 50:1 solution.

The product is an orange solid. Yield: 8.6 g (~ 100%). MS [ESI, positive]: 411.3 [M+H]<sup>+</sup>, 821.3 [2M+H]<sup>+</sup>, 433.3 [M-Na]<sup>+</sup>, 339.3 [M-71]<sup>+</sup>, Batch code: SH505.



## 7. Summary

The rapid growth of biotechnological and pharmaceutical industry clearly shows that the impact of the purification of vaccines, especially those of recombinant monoclonal antibodies, is tremendous on the production costs. Therefore the aim of this work was the creation of cost effective, robust biocompatible stationary phases with high protein binding capacities and high selectivity important for the future development of this industry.

To achieve this aim two different approaches were used: On the one hand mixed modal cation exchanger materials, able to bind hIgG under isotonic conditions should be created and evaluated, and on the other hand low molecular weight, biomimetic ligands should be coupled with different spacer chemistries onto solid supports and again tested for their antibody binding properties. Latter approach was used in combination with beads and with membranes.

In the case of mixed modal cation exchangers, several different approaches were tested e.g. the combination of thiophilic moieties with a sulfonic acid. Extensive SBC tests exhibited good binding capacities for pure IgG solutions under binding conditions typical for common cation exchangers, i.e. pH of ~ 5 and 0 - 75 mM sodium chloride, but not for a more isotonic environment. Further investigations lead to the conclusion that weak cation exchangers, in this particular case carboxylic acids, are more suitable for antibody capture under more isotonic like conditions. For example 3-mercaptopropionic acid showed very interesting binding properties. This material was able to capture 20 mg IgG/mL gel out of a pure hIgG solution containing 150 mM NaCl and pH 5.0, out of which Merck's SO<sub>3</sub> ion exchanger bound only 9 mg/mL.

Further improvement was made by the combination of cysteine and homocysteine scaffolds with aromatic groups, which led to significant binding of up to 26 mg/mL IgG at pH 6.5 and the presence of 150 mM sodium chloride during SBC tests.

The best performing material of this study was a mercaptobenzoic acid bearing material, which was able to capture 41 mg/mL out of a 150 mM sodium chloride solution and pH 6.5.

The most promising materials were subject of more intense investigations under dynamic binding conditions (DBC) with a reduced selection of test conditions (pH

5.5, 6.5 and 7.4 at 75 and 150 mM NaCl). For example N-benzoyl-homocysteine showed 100% DBCs of 37 mg/mL in the presence of 75 mM NaCl and pH 6.5 and mercaptobenzoic acid captured 68 mg/mL. After additional DBC tests with Pluronic F68 containing mock feed solution and cell culture supernatant, the characterization of these materials was accomplished.

The studies based on affinity ligands were accomplished using 2 different ligands, A2P and B14 coupled onto two different kinds of chromatographic support media. The investigations dealing with membranes exhibited several interesting findings: A2P in combination with 3,6-dioxa-1,8-octanedithiol as a spacer results in good binding capacities, but comes with low recovery (~30%). The replacement of this spacer by an 1,2,3-triazole group was able to improve the recoveries by up to 20%. Therefore all subsequent experiments were performed using this particular binding strategy. This triazole-A2P combination was tested using different membranes, differing from each other by different thickness, pore size, etc. The same ligand strategy was used for B14, and again a set of different membranes was used to find the ideal combination. For both A2P and B14 the so called SartoAIMs Epoxy 2 membranes turned out to provide best capacities as well as the best recovery. During tests using cell culture feed stocks, A2P showed low recovery and therefore the yield dropped down to practically zero.

Similar tests were performed using soft gels instead of membranes. Again the biomimetic ligand A2P was coupled via a set of different spacers onto soft, compressible gels with subsequent chemical and functional characterisation (DBC). 3,6-dioxa-1,8-octanedithiol, 1,3-propanedithiol and the 1,2,3-triazole spacer were used to couple A2P onto Fractogel, Fractoprep and Purabead. Outcome was the low tolerance against the antifoaming agent Pluronic F68 of the combination of A2P and thiophilic spacer. The combination of A2P with the triazole spacer was able to improve this situation and almost no loss of capacity could be observed after addition of Pluronic to the IgG solution. The binding capacity of A2P-triazole in combination with Purabead was even able to compete with commercial rmp-Protein A Sepharose FF. Explanations of the different behaviour of the different spacer chemistries were given with molecular dynamic (MD) calculations. As computational calculations predicted, the TRZ spacer showed on



the one hand no tendency to interact strongly with Pluronic, and on the other hand this spacer turned out to be comparatively rigid and does not interact significantly with the surface of the support material.

After successful implementation of the triazole spacer for antibody absorbents the ligand B14 was also bound via triazole spacer onto a series of different non commercial absorbents provided by Merck KGaA. These epoxy activated polymethylmethacrylate tentacle materials differ from each other by differences in pore size as well as in epoxy group densities and are labelled as FractoAIMs 1, 2 and 3. This ligand in combination these support materials exhibited astonishing dynamic binding capacities, even superior to commercial Protein A materials in terms of their 30% DBC results. During these studies the tremendous importance of the endcapping was highlighted. Note that as part of the coupling via triazole spacer, the support material has to be activated by azide groups. It was shown that azide groups are able to interact with impurities as well as with h-IgG. By suppression of the interaction of impurities and h-IgG with remaining azide groups the purity of the elution fractions as well as the binding capacity could be improved.

## **8. Zusammenfassung**

Das rasante Wachstum der (bio-)pharmazeutischen Industrie erfordert immer bessere und kosteneffizientere Herstellungsmethoden für deren Produkte, allen voran rekombinant hergestellte monoklonale Antikörper. Ein Großteil der Herstellungskosten rührt von der Aufreinigung, welche daher ein Ansatzpunkt für verbesserte Methoden darstellt.

Ziel dieser Studie war es, Materialien herzustellen und auch zu testen, welche eine einfachere und kostengünstigere Aufreinigung von Antikörpern ermöglichen sollten. Hierfür wurden 2 verschiedene Ansätze gewählt: Zum einen sollte ein Säurefunktion tragendes Mixed-Mode Material hergestellt werden, welches fähig ist, unter isotonen Bedingungen Antikörper zu binden. In einem anderen Zugang wurde versucht, mit Hilfe eines niedermolekularen, biomimetischen Affinitätsliganden ein Material zu kreieren, welches in Bezug auf Kosteneffizienz mit dem momentanen Protein A konkurrieren kann. Diese Liganden wurden mit

verschiedenen Kopplungsstrategien an zweierlei Arten von Supportmaterialien gebunden: an Fractogel und Fractogel verwandte Gele sowie an Membranen hergestellt aus Cellulose.

Im ersten Teil wurde versucht, einen Kationenaustauscher mit salztoleranten Gruppen zu kombinieren. Hierfür wurden Sulfonsäuren mit thiophilen Funktionen gekoppelt. Letztere sind bekannt, unter Zusatz von großen Mengen an strukturbildender Salzen (z.B. Ammoniumsulfat) Antikörper unter isotonen Bedingungen verhältnismäßig selektiv zu binden. Im präparativen Maßstab ist der Zusatz an so großen Mengen strukturbildender Salze naturgemäß unerwünscht, und dementsprechend blieb die Bindungskapazität in Anwesenheit von hohen Konzentrationen an Natriumchlorid und neutralem pH unter den Erwartungen, wie umfangreiche statische Bindungskapazitätstests (SBC) unter unterschiedlichen Bedingungen (pH: 4,5 - 7,5; NaCl-Konzentration: 0, 75, 150 und 300 mM) bewiesen. Eine Verbesserung brachte der Wechsel von Sulfonsäuren zu Carbonsäuren, im einfachsten Fall der 3-Mercaptopropionsäure. Dieses Material war in der Lage 20 mg IgG/mL Gel aus polyklonalen IgG Lösungen in Gegenwart von 150 mM Natriumchlorid und pH 5 zu binden. Das Referenzmaterial von Merck KGaA, Fractogel<sup>®</sup> EMD SO<sub>3</sub><sup>-</sup>, band unter denselben Bedingen nur 9 mg IgG.

Weitere Verbesserungen wurden erzielt durch eine Kombination von Cystein und Homocystein mit diversen aromatischen Verbindungen. Auch in diesem Fall wurden umfangreiche SBC Tests durchgeführt, und das erfolgreichste Material aus dieser Serie konnte bei Anwesenheit von 150 mM NaCl und einem pH von 6,5 26 mg IgG/mL Gel binden. Da eine der Carbonsäuregruppe benachbarte aromatische Einheit das Bindungsverhalten des Mixed-Mode Materials positiv zu beeinflussen schien, wurde die 4-Mercaptobenzoessäure an Fractogel gebunden. Überraschendes Ergebnis waren 41 mg gebundenes IgG/mL Gel bei Anwesenheit von 150 mM NaCl und einem pH von 6,5.

Die vielversprechendsten Materialien wurden ebenfalls unter verschiedenen dynamischen Bedingungen getestet (pH 5,5, 6,5 und 7,4; NaCl Konzentration 75 und 150 mM). Das N-Benzoyl-Homocystein tragende Material war fähig bei Anwesenheit von 75 mM NaCl und einem pH von 6,5 37 mg/mL bis zum vollständigen Durchbruch des IgG zu binden, die Mercaptobenzoessäure band sogar 68 mg/mL. Weitere Tests mit letzterem Material wurden durchgeführt, um den Einfluss von Pluronic F68, einem Antischaummittel, zu testen. Ebenfalls

wurde ein Test mit einem Zellkulturüberstand in Gegenwart von 75 mmol/L Natriumchlorid und pH 6,5 durchgeführt, aus welchem 42 mg/mL gebunden werden konnten.

Die Studien zu den Affinitätsliganden wurden mit 2 verschiedenen Liganden durchgeführt: A2P und B14, beide von Prometic BioSciences entwickelt. Zum einen wurden diese Liganden auf Membranen gebunden. Diese Versuche zeigten einige interessante Ergebnisse: Der A2P-Ligand gebunden mit 3,6-Dioxa-1,8-oktandithiol zeigte in statischen Bindungstests gute Kapazitäten, gab aber den gebundenen Analyten unter milden Bedingungen nur schwer wieder frei. Dies resultierte in Wiederfindungsraten von ~30%. Der Ersatz des thiophilen Spacers gegen eine auf dem Gebiet der Biochromatographie neuartigen Kopplungsstrategie, der so genannten Click-Chemie, resultierte in der Bildung eines 1,2,3-Triazolringes. Durch den Wechsel der Spacer Strategie konnte die Wiederfindungsrate in SBC-Tests um bis 20% erhöht werden. Alle folgenden Experimente wurden daher mittels Click-Chemie gekoppelt. Unter Benutzung letztgenanntem Spacers wurden eine Reihe verschiedener Membran getestet (Sartobind und nicht kommerzielle SartoAIMs 1, 2 und 3 Membranen), welche sich in Membrandicke, Porengröße, etc. ... unterschieden. Dieselbe auf der Click-Chemie basierenden Versuchsreihe wurde auf diesen Membranen auch mit dem B14 Liganden durchgeführt, und die Resultate der SBC-Tests mit reinen IgG Lösungen führte für beide Liganden zu dem Schluss, dass die als SartoAIMs 2 bezeichnete Membran als diejenige mit den besten Kapazitäten als auch besten Wiederfindungsraten identifiziert werden konnte. Dynamische Bindungskapazitätstests (DBC) mit Zellkulturüberständen zeigten, dass die mit B14 bestückten SartoAIMs 2 Membranen die höheren Kapazitäten und besseren Wiederfindungsraten besaßen.

Ähnliche Versuchsreihen wurden auch auf Gelen durchgeführt. Der A2P-Ligand wurde mit 3,6-Dioxa-1,8-oktandithiol, 1,3-Propandithiol und mittels Click-Chemie auf die Trägermaterialien (Fractogel<sup>®</sup> EMD Epoxy, nicht kommerziell erhältliches Fractoprep und PuraBead<sup>®</sup> P6HF) gebunden. Resultat der DBC-Tests war die Intoleranz des A2P Liganden in Kombination zu thiophilen Spacern gegenüber Pluronic F-68. Der Wechsel zur Click-Chemie führte zu einer beinahe konstant

bleibenden Bindungskapazität im Vergleich zwischen reiner IgG Lösung und einer IgG Lösung, der Pluronic F-68 zugesetzt wurde (1 g/L). Der A2P-Triazole Ligand war in Kombination mit PuraBead<sup>®</sup> sogar in der Lage, ähnliche Mengen an h-IgG aus einer Zellkulturlösung zu binden wie kommerziell erhältliches rmp-Protein A Sepharose FF Material. Die verbesserte Bindungskapazität des A2P-Triazole Liganden wurde mittels Computational Chemistry näher durchleuchtet und folgende Erklärungen wurden gefunden. Der 1,2,3-Triazole Spacer zeigt laut Berechnungen keine starke Tendenz, mit Pluronic F68 zu interagieren, wodurch der Ligand für den Analyten besser zugänglich ist. Eine weitere Erklärung besagt, dass der Triazole Ring weniger Beweglichkeit besitzt, wodurch ein Umklappen und somit das Interagieren des A2P Liganden mit der Oberfläche des Trägermaterials minimiert wird, welches ebenfalls in höheren Bindungskapazitäten resultiert. Beides wurde für A2P in Kombination mit 3,6-Dioxa-1,8-oktandithiol als Spacer nicht gefunden.

Nach den erfolgreichen Versuchen A2P mittels Click-Chemie an verschiedene Gelmaterialien zu binden, wurden die Tests mit B14 fortgesetzt. In diesem Fall wurde der Ligand an nicht kommerziell erhältliche Gele von Merck KGaA gebunden. Diese dem Fractogel verwandten epoxidaktivierten Materialien unterschieden sich durch ihre Porengröße als auch Epoxygruppendichte und wurden als FractoAIMs 1, 2 und 3 bezeichnet. Diese zeigten in Kombination mit dem B14-Triazole Liganden ausgezeichnete dynamische Bindungskapazitäten. Der 30%-DBC Wert des vielversprechendsten Materials B14-Triazole-FractoAIMs 3 (11,3 mg/mL) überstieg sogar den des kommerziellen Protein A Gels (8,8 mg/mL). Während dieser Studien kristallisierte sich weiters die enorme Wichtigkeit der richtigen Endcapping Strategie heraus. Da die Epoxidgruppen des Trägermaterials vor Durchführung der Click-Chemie in Azidgruppen umgewandelt werden musste, die Click-Chemie aber Ausbeuten von im Schnitt etwa 30% aufwies, waren große Mengen nicht umgesetzter Azidgruppen auf der Oberfläche vorhanden. Unglücklicherweise sind diese nicht inert und interagieren mit IgG als auch mit Verunreinigungen der Zellkulturüberstände. Dies resultierte in negativen Auswirkungen auf die Selektivität als auch den dynamischen Bindungskapazitäten. Mit Hilfe verbesserter Endcapping Strategien konnten diese negativen Interaktionen soweit verbessert werden, dass dem kommerziellen

Protein A Materialien (MabSelect) ähnliche Elutionskapazitäten erreicht werden konnten, nämlich 20,4 mg/mL für MabSelect und 15.9 mg/mL für B14-Triazole-FractoAIMs 3.



## 9. Curriculum Vitae



### *Personal Data*

<b>Name:</b>	Mag. Stefan Hofer
<b>Address:</b>	Stumpergasse 51/12 1060 Vienna Austria
<b>Telephone:</b>	0676/7978282
<b>E-mail:</b>	Stefan.Hofer@univie.ac.at
<b>Date of Birth:</b>	07.08.1978
<b>Place of Birth:</b>	Amstetten/Austria
<b>Family Status:</b>	Single
<b>Citizenship:</b>	Austria

### *Education*

03/2005 - 2011      PhD studies at the Department of Analytical Chemistry and Food Chemistry, University of Vienna, under the supervision of Prof. Dr. Lindner. The PhD thesis is/was performed in collaboration with the “CDL-Labors for Molecular Recognition” and the AIMS project (Advanced Interactive Materials by design, <http://www.aims-eu.de/>)

Title of the PhD thesis: “*Development of novel artificial ligands for antibody purification/enrichment based on affinity principles and cation exchangers combined with hydrophobic interaction*” (in progress)

03/1997 - 12/2004      Chemistry studies at the University of Vienna, completed with the Magister degree under the supervision of Prof. Dr. Mag. Allmaier in cooperation with Biutec, an environmental analysis company

Title of the diploma thesis: „*Detection of pesticides via LC-ESI-Quadrupol-mass spectrometry*“ (written in German)

## ***Jobs***

06/2010 until now	Lab manager at Oekolab - Gesellschaft für Umweltanalytik GmbH / A member of JTI Group of companies
03/2005 - 12/2009	Scientific coworker at the University of Vienna including teaching duties (tutor for labs)
05/2003 - 07/2004	Paid diploma thesis at Biutec GmbH

## ***Publications***

*Influence of different spacer arms on Mimetic Ligand A2P and B14 membranes for human IgG purification*

Cristiana Boi, Simone Dimartino, Stefan Hofer, Jeannie Horak, Sharon Williams, Giulio C. Sarti, Wolfgang Lindner

**Journal of Chromatography B** (2011), 879 (19), 1633 - 1640

*Performance evaluation of Mimetic Ligand B14-triazole-FractoAIMs adsorbents for the capture of human monoclonal immunoglobulin G from cell culture feed*

Jeannie Horak, Stefan Hofer, Chris Sadler, Sharon Williams, Wolfgang Lindner:

**Analytical and Bioanalytical Chemistry** (2011), 400 (8), 2349 - 2359

*Experimental and Theoretical Investigation of Effect of Spacer Arm and Support Matrix of Synthetic Affinity Chromatographic Materials for the Purification of Monoclonal Antibodies*

Laura Zamolo, Matteo Salvalaglio, Carlo Cavalotti, Benedict Galarza, Chris Sadler, Sharon Williams, Stefan Hofer, Jeanie Horak, Wolfgang Lindner:

**Journal of Physical Chemistry B** (2010), 114 (29), 9367 - 9380

*Optimization of a ligand immobilization and azide group endcapping concept via Click-Chemistry for the preparation of adsorbents for antibody purification*

Jeannie Horak, Stefan Hofer, Wolfgang Lindner:

**Journal of Chromatography B** (2010), 878 (32), 3382 - 3394



*Static and dynamic binding capacities of human immunoglobulin G on mixed-modal, thiophilic and hydrophobic poly(methacrylate) cation exchangers*

Stefan Hofer, Alexander Ronacher, Heiner Graalfs, Jeannie Horak, Wolfgang Lindner:

**Journal of Chromatography A**, article in press (DOI: 10.1016/j.chroma.2011.06.012)

## ***Poster Presentations***

### **SPICA 2008**

**Symposium on  
Preparative and  
Industrial  
Chromatography and  
Allied Techniques**

Zurich, Switzerland,  
September 28 - October  
01, 2008

Development of novel mixed-mode cation exchange materials  
for antibody purification

*Stefan Hofer<sup>1</sup>, Heiner Graalfs<sup>2</sup>, Wolfgang Lindner<sup>1</sup>*

<sup>1</sup>*Christian Doppler Laboratory for Molecular Recognition  
Materials, Department of Analytical Chemistry & Food  
Chemistry, University of Vienna*

<sup>2</sup>*Merck KGaA, Darmstadt, Germany*

Influence of Different Spacer Arms on A2P Affinity  
Membranes for Human IgG Capture

*C. Boi, S. Dimartino<sup>1</sup>, G. C. Sarti<sup>1</sup>, S. Hofer<sup>2</sup> and W. Lindner<sup>2</sup>,*

<sup>1</sup>*Università di Bologna, Italy*

<sup>2</sup>*University of Vienna, Austria*

### **Affinity 2011**

**19th Biennial Meeting  
of the International  
Society of  
Molecular Recognition**

Tavira, Portugal, 16.06-  
19.06.2011

Contribution of Surface Modification Strategies for Affinity-  
type Adsorbents prepared via Click Chemistry for the  
Purification of Monoclonal Antibodies

*J.Horak<sup>1</sup>, S.Hofer<sup>1</sup>, S.Williams<sup>2</sup>, W.Lindner<sup>1</sup>*

<sup>1</sup>*University of Vienna, Austria*

<sup>2</sup>*ProMetic BioSciences Ltd., UK*